# NOTE TO USERS

**This reproduction is the best copy available.**

uOttawa

L'Université canadienne
Canada's university

**FACULTÉ DES ÉTUDES SUPÉRIEURES ET POSTOCTORALES**

uOttawa

L'Université canadienne
Canada's university

**FACULTY OF GRADUATE AND POSDOCTORAL STUDIES**

Jennifer Lento

AUTEUR DE LA THÈSE / AUTHOR OF THESIS

Ph.D. (Biology)

GRADE / DEGREE

Department of Biology

FACULTÉ, ÉCOLE, DÉPARTEMENT / FACULTY, SCHOOL, DEPARTMENT

Habitat Space and Energy Availability as Determinants of Size Distributions of Lotic Assemblages

TITRE DE LA THÈSE / TITLE OF THESIS

Antoine Morin

DIRECTEUR (DIRECTRICE) DE LA THÈSE / THESIS SUPERVISOR

CO-DIRECTEUR (CO-DIRECTRICE) DE LA THÈSE / THESIS CO-SUPERVISOR

David Currie

Mark Forbes

Rees Kassen

Frances Pick

Gary Sprules (University of Toronto at Mississauga)

Gary W. Slater

Le Doyen de la Faculté des études supérieures et postdoctorales / Dean of the Faculty of Graduate and Postdoctoral Studies

# Habitat space and energy availability as determinants of size distributions of lotic assemblages

**Jennifer Lento**

Thesis submitted to the
Faculty of Graduate and Postdoctoral Studies
In partial fulfillment of the requirements
For the PhD in Biology

Department of Biology
Faculty of Science
University of Ottawa

*Your file Votre référence*
*ISBN:* 978-0-494-69132-8
*Our file Notre référence*
*ISBN:* 978-0-494-69132-8

# Table of Contents

# List of Tables

# List of Figures

# Abstract

Size spectra in aquatic systems have shown a strong consistency of shape across a range of environmental conditions and among different groups of organisms, with higher normalized biomass of small organisms than large. Two main hypotheses have been proposed to explain this consistency in patterns. The energy hypothesis states that because of the inefficient transfer of energy between trophic levels, large organisms (as predators) have less energy available to them per unit habitat than small organisms. The habitat hypothesis states that space availability in the habitat shapes size spectra because small organisms perceive greater habitat space due to the presence of crevices and interstitial spaces that large organisms cannot access. My research examined body size spectra of organisms in 17 stream sites, testing both the energetic and habitat hypotheses for macroinvertebrates, crayfish, and fish. Body size research in lotic systems has rarely included all three groups of organisms, despite the potential importance of large organisms to ecosystem function. I developed a sampling method (electrobugging) to improve collection of large mobile macroinvertebrates; this method collected additional taxa and size classes not sampled by traditional methods. Slopes of size spectra including macroinvertebrates, crayfish, and fish were similar among sites. Large macroinvertebrates, crayfish, and fish contributed approximately half or more of the biomass in each site, while the contribution of small macroinvertebrates was negligible. To examine the habitat hypothesis, I developed a method to estimate habitat space from digital photographs of stream substrates by fitting organisms of different sizes to profiles extracted from the photos. Stable nitrogen isotopes were used to estimate trophic position and test the energetic hypothesis. The results of the test of both hypotheses suggested that

both energy availability and space availability affected the normalized biomass of organisms in our study sites, although energy availability explained more of the variation in normalized biomass. The strong relationship between normalized biomass and $\delta^{15}N$ suggested that energy availability contributed to primary structuring of size spectra, controlling the negative linear relationship of normalized biomass with size. Space availability had a weaker effect on normalized biomass, and may have contributed to secondary structuring of size spectra, controlling deviations from linearity in the normalized biomass-body size relationship.


## Résumé

Les spectres de taille dans les systèmes aquatiques ont typiquement la même forme avec une densité de biomasse (biomasse normalisée) des petits organismes supérieure à celle des gros organismes peu importe les conditions environnementales et les groupes taxonomiques. Deux hypothèses principales ont été proposées pour expliquer la stabilité des spectres de taille. L'hypothèse énergétique stipule qu'à cause de l'inefficacité des transferts d'énergie entre les niveaux trophiques, les gros organismes (en tant que prédateurs) ont accès à moins d'énergie par unité de surface d'habitat que les petits organismes. L'hypothèse de l'habitat stipule que la disponibilité d'espace façonne les spectres de taille et que les petits organismes perçoivent plus d'espace utilisable parce qu'ils peuvent occuper les crevasses et l'espace interstitiel inaccessible aux gros organismes. Les spectres de taille des organismes de 17 ruisseaux ont été examinés pour éprouver les hypothèses énergétique et de l'habitat pour les macroinvertébrés, écrevisses et poissons. Les travaux préalables ont rarement traité de ces trois groupes malgré l'importance fonctionnelle potentielle des gros organismes pour les écosystèmes. J'ai

développé une méthode d'échantillonnage utilisant un engin de pêche électrique pour améliorer la capture des gros macroinvertébrés mobiles ; cette méthode permet de capturer des taxa et des classes de taille d'organismes qui ne sont pas récoltés par les méthodes traditionnelles. Les pentes des spectres de taille incluant les macroinvertébrés, les écrevisses et les poissons étaient similaires entre les sites. Les gros macroinvertébrés, les écrevisses et les poissons formaient environ la moitié ou plus de la biomasse dans chaque site alors que la biomasse des petits organismes était négligeable. Pour éprouver l'hypothèse de l'habitat, J'ai développé une méthode pour estimer l'espace disponible à partir de photographies numériques des substrats des ruisseaux en ajustant des organismes de taille variable aux profils extraits à partir des photos. Les isotopes stables d'azote ont été utilisés pour estimer la position trophique et éprouver l'hypothèse énergétique. Les résultats suggèrent que la densité de biomasse est affectée par la disponibilité d'énergie et d'espace, et que la disponibilité d'énergie explique une portion plus grande de la variabilité de la densité de biomasse que la disponibilité d'espace. La forte relation entre la densité de biomasse et $\delta^{15}N$ suggère que la disponibilité d'énergie est la force structurante primaire des spectres de taille et contrôle la relation négative entre la densité de biomasse et la taille. La disponibilité d'espace a un effet moindre sur la densité de biomasse et pourrait être la force structurante secondaire responsable des déviations de linéarité des spectres de taille de la densité de biomasse .

# Acknowledgements

I would like to thank my supervisor, Antoine Morin, for his support, guidance, and encouragement (including some much-needed pep talks!) throughout my PhD research. I have learned so much from you during these past 5 years, and you have helped me to develop into a better scientist. So much of this research would not have been possible without your strong dedication to my project. For all the time spent wandering the adhesives aisle in Reno Depot, trying to attach targets to rocks in your kitchen sink, visiting the stream sites to photograph and re-photograph the substrates, and of course sealing and resealing the edges of the viewing box (thank you Magic Cloth!), I am forever grateful. It was a long and often painful process, but I hope that you are as proud of the final product as I am!

My committee members David Currie, Mark Forbes, and Rees Kassen constantly challenged me to think about the theoretical basis for my research as well as the implications of my results, and for that I am grateful. The unique insights that each of you provided helped to strengthen my research. I would also like to thank the additional members of my examining committee: Frances Pick and Gary Sprules. Your comments and suggestions greatly helped to improve the quality of this thesis.

There are numerous people who provided invaluable assistance to me in the field or in the lab at some point during the 5 years of my PhD research. Thank you to Cathy Sun, Julie Scott, Rakesh Rajput, Isabelle Lavoie, Alana Plummer, Mark Kelly, and Rebecca D'Onofrio for your help. Special thanks to Ben Basu for showing me the ropes in my first sampling season, and for carrying the heavy electrofisher when we had a long hike to get to a sampling site! Special thanks as well to Sandra Noble, without whose

strong organizational skills, work ethic, and constant enthusiasm I might not have made it through my intense sampling season in 2006. Even when our sampling days turned into 12 or 14 hour marathons (as they usually did), you never lost your enthusiasm or your drive, and that was more of a help to me than you realize. Whether we were talking about icebergs and snowstorms to distract ourselves from the intense heat, or waiting out a thunderstorm in the truck (it's ok to electrofish as long as there's no lightning, right?), I was always grateful for your help!

To all of the members of the Morin lab past and present, thank you for your endless support and for being a sounding board when I needed it the most. In particular, I would like to thank Jaynie Stephenson for helping me get started, giving me invaluable sampling advice, and teaching me the methods used in the lab. I would have been so lost without your help! I would also like to say a special thank you to my "work husband," Liza Hamilton. I looked forward to our Morning Chat every day, and always knew I could rely on you to help me get through any issues and make me laugh! I couldn't have asked for a better labmate or friend for this journey.

I would also like to thank the "unofficial lab members" who have encouraged me and helped me throughout my research. Thank you to Alana Plummer, who provided much-needed support and encouragement at a time when I had no labmates to turn to. Thank you for taking up the role of sounding board even though our research fields were so different; you helped me get through some very stressful periods and became a close friend in the process. I would also like to thank my good friend and conference buddy, Isabelle Lavoie. You have always been there for me, ready to discuss my ideas and even branch into the world of body size research yourself! I am in constant awe of everything

that you've accomplished, and have been motivated (as have many other members of the lab) to succeed because of witnessing your drive and genuine interest in science. Your nerdiness has inspired me to become the geek that I am today!

As always, my family has been the support base that has helped me get through the stressful times and succeed when I felt sure that I could not. I would not have made it this far without my family's love and encouragement, and I am so grateful to all of you for believing in me. My deepest thanks to my parents Peter and Patricia, who have helped me so much throughout all the seemingly endless schooling. Part of my success is due to your constant faith in me.

Last but certainly not least, I wish to thank my amazing husband Rakesh. I could not have come this far without your continual love and encouragement. This has been a difficult journey for both of us, but you have been incredibly patient, selfless, and understanding throughout, particularly during the final year when you barely got to see me. You always had to deal with the fallout if some part of my research wasn't working, pick up my slack when I had no time to even cook a meal, and be ready to head out into the field when I desperately needed to fit in another sampling day. All this was done without a complaint, and with an understanding that it would all be worth it in the end, and you'd eventually get your wife back. Well, I'm finally done – want to go see a movie?

# Statement of Thesis Contributions

The following thesis is presented as a series of manuscripts that will be submitted to journals for publication. To that end, there is repetition between chapters, particularly in terms of methods, to allow each chapter to stand alone as an individual manuscript. Please note that the same set of data is used (all though not always in full) for all chapters, but is re-described in each methods section. Further, the pronoun we is used throughout the thesis, as manuscripts will be submitted with myself and my supervisor listed as authors. However, I completed the work and wrote the thesis.

# Chapter 1 – General Introduction

Body size is ecologically important because it is related to numerous aspects of organism function, and it is easier to measure than most physiological or functional parameters (Kozlowski and Gawelczyk 2002). Relationships with body size have been described for several parameters, such as home range area (Haskell et al. 2002; Jetz et al. 2004), energy use, growth rate, and food web interactions (Peters 1983; Woodward et al. 2005). Analysis of an organism's body size can therefore reveal a great deal about its interactions with other individuals and with the environment (Allen et al. 2006). The rate at which functional parameters scale with body size and the shape of body size distributions among species show predictable patterns (Kozlowski and Gawelczyk 2002; Woodward et al. 2005). Though attempts have been made to explain these patterns, their cause is still a subject of debate (Kozlowski and Gawelczyk 2002; Allen 2006; van der Meer 2006).

**Body Size Scaling Relationships**

The relationship between the rates of biological processes and body size is allometric, meaning that with a change in body size, there is a disproportionate change in rate (Schmidt-Nielsen 1984; Woodward et al. 2005). This relationship generally takes the form $y = a * x^b$, where y is the dependent variable (the rate or process), $a$ is a constant, x is body mass, and $b$ is the scaling coefficient (Damuth 1981; Peters 1983; Schmidt-Nielsen 1984). In an allometric relationship, the scaling coefficient ($b$) is not equal to 1 (Woodward et al. 2005). With log-transformation, the slope of the relationship will therefore be greater than one if y increases at a faster rate than body size, and less than one if y increases at a slower rate than body size (Schmidt-Nielsen 1984). One benefit of the observed relationships of biological function with body size is that rates that might normally be difficult to measure may instead be estimated by an organism's body size (Peters 1983; Blackburn and Gaston 1994). Because

of its association with such parameters as food intake, growth, and production, body size may be used as a summary measure of all these functional processes (Woodward et al. 2005; Allen et al. 2006), and a useful way to make comparisons between populations, independent of taxonomy (Allen et al. 2006).

There has been extensive documentation of allometric relationships between metabolic rates and body size (Peters 1983). The overwhelming pattern in these studies is a scaling of metabolic rate with body mass raised to 3/4 power (Peters 1983; Schmidt-Nielsen 1984; Damuth 1987; West and Brown 2005). This pattern is evident across a wide range of organisms, from insects to mammals, and is thus one of the most pervasive patterns observed in biology (Peters 1983). Kleiber was the first to recognize this pattern; his observation was in contrast to the previously accepted assumption that metabolic rate scaled as mass to the 2/3 power as a result of surface to volume ratios (Peters 1983; West and Brown 2005). However, the reason why body size scaling is not attributed to organisms' surface area is still unclear.

Quarter-power scaling predominates in the scaling relationships of several other parameters with body size, including growth rate, blood circulation time, lifespan, lengths of aortas, and RNA concentrations (Brown et al. 2000; West and Brown 2005). Quarter-power scaling is evident among all the taxonomic classes that have been considered of both plants and animals, indicating that there must be a common functional explanation for all organisms. Several hypotheses have been proposed, but most have been too specific to apply to the full range of organisms for which these scaling patterns are visible (Brown et al. 2000). West et al. (1997) suggest that fractal branching networks within plants, mammals, and insects lead to quarter power scaling. The 2/3 scaling that was previously described was

based on the limitation of heat exchange across the surface area of the body (Brown et al. 2000), while the 3/4 scaling of West et al. (1997) is based on the limitations of the transport networks within the body. West et al. (1997) hypothesize that the self-similar design of such networks supports fractal geometry (which deals in fourths) rather than Euclidean geometry (which deal in thirds). However, this hypothesis does not make suggestions for organisms that lack fractal branching networks, but that follow the same scaling patterns, suggesting that it cannot act as an overall explanation of the patterns in body size. Although there is strong evidence that body size displays predictable relationships with various biological parameters, the mechanism behind these observed scaling patterns is still a source of debate (van der Meer 2006).

**Body Size Distributions**

Consistent patterns have also been visible in body size distributions (Damuth 1981, 1987; Lawton 1990; Schmid et al. 2000). Body size distributions plot the relationship between density, biomass, or normalized biomass and body size. Because metabolism scales with size, the density of organisms within size classes can be used to estimate variables such as community respiration and production (Bourassa and Morin 1995). However, despite a great deal of research on the topic, it is still unclear which forces shape the size distributions of organisms (Kerr and Dickie 2001; Kozlowski and Gawelczyk 2002; Allen 2006).

The majority of terrestrial studies have investigated species size distributions, which generally plot the relationship between density and body size, by using average, maximum, or predefined optimal body sizes for species (Blackburn and Gaston 1997; Cyr et al. 1997; Ackerman et al. 2004). However, while individuals within a species may have similar mechanisms for utilizing energy, the size range of a species during its lifetime can be very

large, affecting its energy requirements and usage through time. In addition, the use of an optimal size for a species has been criticized because it is unclear whether the majority of individuals actually reach their optimum size (Kozlowski and Gawelczyk 2002; Allen et al. 2006). Aquatic studies have generally used individual-based size distributions (Cyr et al. 1997; Leaper et al. 2001; White et al. 2007), perhaps because in the case of benthic macroinvertebrates in particular, most species are represented by juveniles, experiencing a wide range of body size during their time within the aquatic habitat, and only maturing (and reproducing) outside that habitat. While both types of size distributions are closely related (Cyr et al. 1997), using plots of individuals rather than species removes the bias towards adult life stages, and allows the consideration of all ontogenetic stages. Examining body size distributions at the individual level may provide a more accurate relationship with actual energy use (Ackerman et al. 2004) and prediction of biological rates. The use of individuals also allows us to draw conclusions about functional interactions based only on body size, and potentially apply our findings to other groups of organisms in other environments. Individual size distributions in aquatic systems originally described the relationship between biomass and body size, plotting the sum of the biomass in each of a range of logarithmically-defined size classes (Sheldon et al. 1972). However, normalized biomass size spectra have become more commonly used to examine aquatic communities (Kerr and Dickie 2001). Normalized biomass is calculated by dividing the biomass concentration in a size class by the width of that size class (i.e., for a size class that ranges from 2 to 4 μg, the width of the size class is 2). This method of representing size distributions was developed by Platt and Denman (1975) as a way to account for differences in the size of log-based size classes. Whereas a biomass

distribution would display a slope of 0 if the biomass in all size classes was equal, a normalized biomass distribution would display a slope of -1 (Kerr and Dickie 2001).

When considered on a large scale, the body size distributions of terrestrial species have been shown to be right-skewed in a large number of studies (Kozlowski and Gawelczyk 2002; Allen et al. 2006), with higher densities of small organisms than large (Cyr et al. 1997). Body size distributions of aquatic individuals have also been shown to be right-skewed (Morin et al. 1995; Solimini et al. 2001), with log-linear negative relationships evident when several taxonomic classes are included (Morin and Nadon 1991; Cattaneo 1993; Cyr et al. 1997; Kerr and Dickie 2001). Allen et al. (2006) outline the main hypotheses that have been proposed to explain the predominantly right-skewed size distribution of species. The five hypotheses are based on theories about evolutionary processes, dispersal, community interactions, habitat complexity, and energetic constraints. Allen et al. (2006) suggest that all the proposed mechanisms act on body size distributions, though they operate at different temporal and spatial scales. The best way to investigate their influence is therefore not to determine which act on species size distributions (as they all do in some way), but to determine which provides the best explanation for the particular patterns we observe in any one community. However, of these five hypotheses, only two apply to individual-based size distributions. The effects of evolution, species dispersal, and community interactions should not be evident in size distributions where all individuals are plotted regardless of their evolutionary history or which species they represent. Instead, the focus should be placed on the energetic hypothesis and the habitat hypothesis, which are both largely independent of taxonomy. It has been suggested that if body size distributions are controlled by energetic constraints, that this occurs on a large scale with habitat constraints

acting on a smaller scale (Kerr and Dickie 2001; Allen et al. 2006). It is possible that the patterns that we see in body size distributions are a result of the combined effects of spatial and energetic limitations.

*Energetic Hypothesis*

One of the main suggestions for energetic controls on size distributions is the rule of energetic equivalence. The energetic equivalence rule states that energy use per unit area is independent of body size (Damuth 1981, 1991) because density scales as mass to the -0.75 power (Marquet et al. 1995; Knouft 2002) whereas metabolic rate scales as mass$^{0.75}$. Thus, while all size classes have the same amount of energy available, there will be a higher density of small organisms because the energy requirements per individual are lower than that of large organisms. Loeuille and Loreau (2006) modeled the evolution of a food web, using nutrient availability and body size to predict density. Their model suggested that there is not equal resource use among body sizes, contradicting the energetic equivalence rule. Resource availability was not found to be static, but instead changed in relation to population size and community traits (Loeuille and Loreau 2006). The discrepancy between their results and the patterns that have been predicted based on energetic equivalence was most likely based on the fact that the energetic equivalence rule assumes that all organisms use a common energy source, which is not the case in a system with multiple trophic levels (Peters 1983; Jennings and Mackinson 2003; Loeuille and Loreau 2006). Ackerman et al. (2004) provided evidence from fish communities that they interpreted as support for the energetic equivalence rule, but they did not question the faulty assumption of a common resource.

Jennings and Mackinson (2003) provide an alternative theory to the energetic equivalence rule, suggesting that size is limited by the inefficiency with which energy is

transferred through trophic levels. If trophic level increases with mass, then large organisms (as predators) gain less energy from food than small organisms (Jennings and Mackinson 2003; Dinmore and Jennings 2004). This constraint on energy availability may lead to decreased abundance of large organisms. This theory provides a mechanistic explanation for the shape of size distributions that potentially applies to both aquatic and terrestrial organisms. However, there is currently little evidence that the relationship between trophic level and size can predict the shape of size distributions. Trophic level has been shown to increase with mass in several systems (Fry and Quiñones 1994; France et al. 1998; Jennings et al. 2002), but there has been some evidence that trophic level does not increase with mass in lotic and infaunal marine macroinvertebrates (Dinmore and Jennings 2004; Anderson and Cabana 2009).

*Habitat Hypothesis*

The habitat hypothesis states that space availability shapes size distributions (Morse et al. 1985; Sugihara and May 1990; Sinsabaugh et al. 1991; Gee and Warwick 1994). Many habitats, both terrestrial (Morse et al. 1985) and aquatic (Schmid 2000), have been described as fractal, meaning that the same patterns of complexity are evident at successively smaller scales, and therefore there is more available habitat at small scales than at large (Morse et al. 1985; Sugihara and May 1990; Gee and Warwick 1994; Halley et al. 2004). Because of the fractal nature of habitats, there should be an inverse relationship between the size of an organism and the amount of area it perceives (Kozlowski and Gawelczyk 2002). There is more space available to small organisms, therefore there should be more small than large organisms (Kozlowski and Gawelczyk 2002).

Results of studies considering the effect of habitat complexity on body size distributions have been mixed (Allen et al. 2006), in part due to differences in methodology and determination of complexity (Robson et al. 2005). But there have been some examples of studies in which the habitat hypothesis has been supported. Taniguchi and Tokeshi (2004) compared the macroinvertebrate communities on experimental plates differing in fractal complexity and Kostylev et al. (2005) measured the fractal dimension of marine shores on which they had sampled benthic organisms. Both groups of authors found that the slope of the size distribution increased with fractal dimension, indicating more small organisms in complex habitats. Both studies support the hypothesis that habitat complexity affects size in benthic organisms.

Allen et al. (2006) suggest that a comparison of body size distributions in adjacent areas with differing habitat structure would allow us to consider the effect of landscape while controlling for evolutionary and dispersal effects. In addition, these comparisons could be made in areas with similar food webs, and therefore similar energetic effects. The habitat hypothesis would predict significant differences between body size distributions in this case, while little to no differences would be predicted by the remaining hypothesis.

**Researching Body Size Distributions**

Examining individual body size distributions allows us to evaluate the mechanistic effects of both habitat and energy, while essentially controlling for factors that act at a species level. The resulting relationships may potentially be applied to other organisms, because they describe mechanisms that are not species-specific, and that act at a functional level. Few studies have examined the combined effects of the energetic and habitat hypotheses on body size distributions. Haskell et al. (2002) proposed a model to explain the

relationship of body size with home range based on the availability of resources. Their research suggested that organisms are limited both by the habitat that they perceive, and by the resources they perceive within that habitat, both of which are scale-dependent (Ritchie and Olff 1999; Haskell et al. 2002). This suggests that hypotheses based on habitat and energy availability are linked, and that it is the relative importance of each to the shape of body size distributions that must be determined (Kerr and Dickie 2001; Allen et al. 2006).

My research examined normalized biomass distributions of stream organisms, testing both the energy and habitat hypotheses for macroinvertebrates, crayfish, and fish. Body size research in lotic systems has rarely included all three groups of organisms, despite the potential importance of large organisms to ecosystem function. Morin and Nadon (1991) suggested that although small organisms are numerically the most abundant organisms, most of the stream benthic production is contributed by large organisms. Poff et al. (1993) provide the only example of a description of stream size distributions incorporating large organisms, but their observations were made on a single stream, and the widespread patterns in expanded size spectra remain unknown. The first objective of my research, presented in Chapter 3, was to compare size spectra among streams that covered a range of nutrient condition and substrate composition to determine whether similar patterns were observed when large macroinvertebrates (including crayfish) and fish were collected in addition to small- and medium-sized macroinvertebrates. As part of this objective, I modified and developed a method described by Taylor et al. (2001) to collect macroinvertebrates using an electroshocker (called electrobugging). Chapter 2 describes a comparison of the abilities of electrobugging and more traditional sampling methods to collect macroinvertebrates. I

predicted that electrobugging would lead to improved estimates of large mobile macroinvertebrate taxa.

My second and primary objective was to test the energy and habitat hypotheses using my size spectra data. The average trophic level per size class was used to as a measure of energy availability, while the physical space available to each size class was estimated as a measure of space availability. In order to complete this objective, I developed a method to estimate habitat space from through-water digital photographs of stream substrates. This method, described in Chapter 4, fit organisms of different sizes to substrate profiles to estimate the space available for each size class. The measures of energy and space availability were compared with normalized biomass estimates from the study streams in Chapter 5 in order to determine the role of each factor in controlling the shape of stream size spectra.

Overall, this research is intended to investigate the mechanisms that control the shape of size distributions of stream organisms. The strength of the observed patterns of size distributions suggests that all individuals, regardless of taxonomic class or ecosystem type, are in part controlled by a common force. This research represents the first simultaneous test of both the energetic and habitat hypotheses on lotic size spectra. The relationships between normalized biomass and both energy and space availability in the study streams may be applicable to other aquatic systems because of the universal nature of the factors I investigated. If the tested hypotheses are supported, this work will further the general understanding of size-based interactions in stream ecosystems.

## References


Ackerman, J.L., Bellwood, D.R., and Brown, J.H. 2004. The contribution of small individuals to density-body size relationships: examination of energetic equivalence in reef fishes. Oecologia. **139**: 568-571.

Allen, C.R. 2006. Discontinuities in ecological data. P. Natl. Acad. Sci. USA. **103**(16): 6083-6084.

Allen, C.R., Garmestani, A.S., Havlicek, T.D., Marquet, P.A., Peterson, G.D., Restrepo, C., Stow, C.A., and Weeks, B.E. 2006. Patterns in body mass distributions: sifting among alternative hypotheses. Ecol. Lett. **9**: 630-643.

Anderson, C., and Cabana, G. 2009. Anthropogenic alterations of lotic food web structure: evidence from the use of nitrogen isotopes. Oikos. **118**: 1929-1939.

Blackburn, T.M., and Gaston, K.J. 1994. Animal body size distributions: patterns, mechanisms and implications. Trends Ecol. Evol. **9**(12): 471-474.

Blackburn, T.M., and Gaston, K.J. 1997. A critical assessment of the form of the interspecific relationship between abundance and body size in animals. J. Anim. Ecol. **66**: 233-249.

Bourassa, N., and Morin, A. 1995. Relationships between size structure of invertebrate assemblages and trophy and substrate composition in streams. J. N. Am. Benthol. Soc. **14**(3): 393-403.

Brown, J.H., West, G.B., and Enquist, B.J. 2000. Scaling in biology: patterns and processes, causes and consequences. *In* Scaling in Biology. *Edited by* J.H. Brown, and G.B. West. Oxford University Press, Oxford. pp. 1-24.

Cattaneo, A. 1993. Size spectra of benthic communities in Laurentian streams. Can. J. Fish. Aquat. Sci. **50**: 2659-2666.

Cyr, H., Peters, R.H., and Downing, J.A. 1997. Population density and community size structure: comparison of aquatic and terrestrial studies. Oikos. **80**(1): 139-149.

Damuth, J. 1981. Populations density and body size in mammals. Nature. **290**: 699-700.

Damuth, J. 1987. Interspecific allometry of population density in mammals and other animals: the independence of body mass and population energy-use. Biol. J. Linn. Soc. **31**: 193-207.

Damuth, J. 1991. Of size and abundance. Nature. **351**: 268-269.

Dinmore, T.A., and Jennings, S. 2004. Predicting abundance-body mass relationships in benthic infaunal communities. Mar. Ecol.-Prog. Ser. **276**: 289-292.

France, R., Chandler, M., and Peters, R.H. 1998. Mapping trophic continua of benthic foodwebs: body size - ä$^{15}$N relationships. Mar. Ecol.-Prog. Ser. **174**: 301-306.

Fry, B., and Quiñones, R.B. 1994. Biomass spectra and stable isotope indicators of trophic level in zooplankton of the northwest Atlantic. Mar. Ecol.-Prog. Ser. **112**: 201-204.

Gee, J.M., and Warwick, R.M. 1994. Body-size distribution in a marine metazoan community and the fractal dimensions of macroalgae. J. Exp. Mar. Biol. Ecol. **178**: 247-259.

Halley, J.M., Hartley, S., Kallimanis, A.S., Kunin, W.E., Lennon, J.J., and Sgardelis, S.P. 2004. Uses and abuses of fractal methodology in ecology. Ecol. Lett. **7**: 254-271.

Haskell, J.P., Ritchie, M.E., and Olff, H. 2002. Fractal geometry predicts varying body size scaling relationships for mammal and bird home ranges. Nature. **418**: 527-530.

Jennings, S., Pinnegar, J.K., Polunin, N.V.C., and Warr, K.J. 2002. Linking size-based and trophic analyses of benthic community structure. Mar. Ecol.-Prog. Ser. **226**: 77-85.

Jennings, S., and Mackinson, S. 2003. Abundance-body mass relationships in size-structured food webs. Ecol. Lett. **6**: 971-974.

Jetz, W., Carbone, C., Fulford, J., and Brown, J.H. 2004. The Scaling of Animal Space Use. Science. **306**: 266-268.

Kerr, S.R., and Dickie, L.M. 2001. The biomass spectrum: a predator-prey theory of aquatic production. Columbia University Press, New York.

Knouft, J.H. 2002. Regional analysis of body size and population density in stream fish assemblages: testing predictions of the energetic equivalence rule. Can. J. Fish. Aquat. Sci. **59**: 1350-1360.

Kotsylev, V.E., Erlandsson, J., Ming, M.Y., and Williams, G.A. 2005. The relative importance of haitat comlexity and surface area in assessing biodiversity: fractal application on rocky shores. Ecol. Complex. **2**: 272-286.

Kozlowski, J., and Gawelczyk, A.T. 2002. Why are species' body size distributions usually skewed to the right? Funct. Ecol. **16**: 419-432.

Lawton, J.H. 1990. Species richness and population dynamics of animal assemblages. Patterns in body size: abundance space. Philos. T. Roy. Soc. B. **330**: 283-291.

Leaper, R., Raffaelli, D., Emes, C., and Manly, B. 2001. Constraints on body-size distributions: an experimental test of the habitat architecture hypothesis. J. Anim. Ecol. **70**: 248-259.

Loeuille, N., and Loreau, M. 2006. Evolution of body size in food webs: does the energetic equivalence rule hold? Ecol. Lett. **9**: 171-178.

Marquet, P.A., Navarrete, S.A., and Castilla, J.C. 1995. Body size, population density, and the energetic equivalence rule. J. Anim. Ecol. **64**: 325-332.

Morin, A., and Nadon, D. 1991. Size distribution of epilithic lotic invertebrates and implications for communtiy metabolism. J. N. Am. Benthol. Soc. **10**(3): 300-308.

Morin, A., Rodríguez, M.A., and Nadon, D. 1995. Temporal and environmental variation in the biomass spectrum of benthic invertebrates in streams: an application of thin-plate splines and relative warp analysis. Can. J. Fish. Aquat. Sci. **52**: 1881-1892.

Morse, D.R., Lawton, J.H., Dodson, M.M., and Williamson, M.H. 1985. Fractal dimension of vegetation and the distribution of arthropod body lengths. Nature. **314**: 731-733.

Peters, R.H. 1983. The Ecological Implications of Body Size. Cambridge University Press, Cambridge.

Platt, T., and Denman, K. 1975. Spectral analysis in ecology. Annu. Rev. Ecol. Syst. **6**: 189-210.

Poff, N.L., Palmer, M.A., Angermeier, P.L., Robert L. Vadas, J., Hakenkamp, C.C., Bely, A., Arensburger, P., and Martin, A.P. 1993. Size structure of the metazoan community in a Piedmont stream. Oecologia. **95**: 202-209.

Ritchie, M.E., and Olff, H. 1999. Spatial scaling laws yield a synthetic theory of biodiversity. Nature. **400**: 557-560.

Robson, B.J., Barmuta, L.A., and Fairweather, P.G. 2005. Methodological and conceptual issues in the search for a relationship between animal body-size distributions and benthic habitat architecture. Mar. Freshwater Res. **56**: 1-11.

Schmid, P.E. 2000. Fractal properties of habitat and patch structure in benthic ecosystems. Adv. Ecol. Res. **30**: 339-401.

Schmid, P.E., Tokeshi, M., and Schmid-Araya, J.M. 2000. Relation between population density and body size in stream communities. Science. **289**: 1557-1560.

Schmidt-Nielsen, K. 1984. Scaling: Why is Animal Size So Important? Cambridge University Press, Cambridge.

Sheldon, R.W., Prackash, A., and Sutcliffe, W.H.J. 1972. The size distribution of particles in the ocean. Limnol. Oceanogr. **17**(3): 327-340.

Sinsabaugh, R.L., Weiland, T., and Linkins, A.E. 1991. Epilithon patch structure in a boreal river. J. N. Am. Benthol. Soc. **10**(4): 419-429.

Solimini, A.G., Benvenuti, A., D'Olimpio, R., Cicco, M.d., and Carchini, G. 2001. Size structure of benthic invertebrate assemblages in a Mediterranean river. J. N. Am. Benthol. Soc. **20**(3): 421-431.

Sugihara, G., and May, R.M. 1990. Applications of fractals in ecology. Trends Ecol. Evol. **5**(3): 79-86.

Taniguchi, H., and Tokeshi, M. 2004. Effects of habitat complexity on benthic assemblages in a variable environment. Freshwater Biol. **49**: 1164-1178.

Taylor, B.W., McIntosh, A.R., and Peckarsky, B.L. 2001. Sampling stream invertebrates using electroshocking techniques: implications for basic and applied research. Can. J. Fish. Aquat. Sci. **58**: 437-445.

van der Meer, J. 2006. Metabolic theories in ecology. Trends Ecol. Evol. **21**(3): 136-140.

West, G.B., Brown, J.H., and Enquist, B.J. 1997. A general model for the origin of allometric scaling laws in biology. Science. **276**(5309): 122-126.

West, G.B., and Brown, J.H. 2005. The origin of allometric scaling laws in biology from genomes to ecosystems: towards a quantitative unifying theory of biological structure and organization. J. Exp. Biol. **208**: 1575-1592.

White, E.P., Ernest, S.K.M., Kerkhoff, A.J., and Enquist, B.J. 2007. Relationships between body size and abundance in ecology. Trends Ecol. Evol. **22**(6): 323-330.

Woodward, G., Ebenman, B., Emmerson, M., Montoya, J.M., Olesen, J.M., Valido, A., and Warren, P.H. 2005. Body size in ecological networks. Trends Ecol. Evol. **20**(7): 402-409.

# Chapter 2 – Completing Stream Macroinvertebrate Size Spectra With Electroshocking

## Introduction

The relationship between biomass or density and body size, plotted as biomass or density size spectra, has been widely used to describe benthic macroinvertebrate assemblages (e.g., Cattaneo 1993; Rasmussen 1993; Rodríguez and Magnan 1993; Bourassa and Morin 1995; Solimini et al. 2001; Basset et al. 2004). Size-based rather than taxon-based descriptions are beneficial because they can be used to estimate functional parameters such as production and metabolism (Peters 1983). In order to obtain an accurate estimate of the biomass across all body size classes, it is important to design a sampling protocol that efficiently collects both small and large invertebrates. However, the efficiency with which large invertebrates are sampled may be particularly critical. Morin and Nadon (1991) suggested that although density levels are highest in small organisms, more than 90% of the total biomass in the benthic community is from organisms longer than 2 mm. This implies that estimates of total biomass and the most important fraction of the size spectra will be highly affected if large invertebrates are not sampled accurately.

Many studies of size distributions in stream benthic macroinvertebrates describe assemblages sampled from randomly chosen cobbles (see Morin and Nadon 1991; Cattaneo 1993; Bourassa and Morin 1995; Morin et al. 1995; Solimini et al. 2001). However, the size of organisms that can be accurately sampled with this method may be limited. Many large organisms are quite mobile, and they may be able to evade capture by the cobble method. Moreover, depending on a cobble's size, large organisms may not be collected by this method because the cobble may not represent sufficient habitat space. The detection limit depends on sampled area, and because of the small area sampled by the cobble method

relative to other methods, large and less abundant organisms are likely to be at or below detection limit.

Large sampler areas should be used to accurately estimate density of large and relatively rare organisms, but samples from larger areas tend to contain more debris and be more costly to process unless organisms are separated from the substrate. Taylor et al. (2001) proposed a method to use a backpack electroshocker to collect macroinvertebrates over a large area by inducing them to enter the drift and float into a sample net. Their method, called electrobugging, was developed as a means to collect invertebrates from a range of habitats without physical disturbance. The primary benefit of the method as outlined by Taylor et al. (2001) was to reduce the amount of debris in samples (which results from physically disturbing the habitat) and thereby reduce sample processing time. They found that sample processing time was significantly reduced for electrobugging samples; there was a 40% reduction in processing time compared with Surber samples (Taylor et al. 2001). Density and species richness measurements from electrobugging samples were similar to those obtained using fixed-area samplers such as Hess and Surber samplers and cobble collection (Taylor et al. 2001). Electrobugging using a depletion method (similar to electrofishing by depletion) collected significantly more Ephemeroptera, Plecoptera, and Trichoptera taxa than the other sampling methods. However, Taylor et al. (2001) suggested that this may have been a result of the larger area and additional habitats sampled by depletion electrobugging compared to the other methods. They did note that electrobugging would be less efficient at collecting any organisms that were strongly attached to the substrate, such as case-making Trichoptera. However, due to the somewhat limited taxonomic diversity at their sampling sites (the sites were primarily dominated by

Ephemeroptera), this was not a large issue for their streams. Overall, they concluded that electrobugging could provide a viable and comparable alternative to more traditional macroinvertebrate sampling methods.

The purpose of this study was to compare the performance of electrobugging and cobble collection for estimation of taxa richness, biomass, and size distributions, to determine whether electrobugging could improve estimates of large organisms. We conducted this analysis in a set of streams covering a range of nutrient conditions, algal biomass, and habitat types. Our streams differed from those of Taylor et al. (2001) in terms of community composition, with much higher proportions of Diptera (particularly chironomids) and Trichoptera, and generally much lower proportions of Ephemeroptera and Plecoptera than their study streams. Because of the ability of electrobugging to immobilize organisms, we predicted that it would collect higher biomass of large macroinvertebrates than the cobble method, and would produce a different size distribution slope because of these increased biomass estimates. We also expected that electrobugging would collect more taxa than the cobble method because of the greater number of habitats and larger area it samples. In order to evaluate the accuracy of electrobugging biomass estimates, we used kick sampling to estimate the biomass not collected by electrobugging. We expected that electrobugging would be less efficient at collecting attached taxa (including case-making Trichoptera) than kick sampling. We also anticipated an effect of algal biomass on electrobugging efficiency, as electrobugging was not expected to collect organisms living within the biofilm as well as the cobble method or kick sampling.

## Methods

*Sampling and laboratory methods*

Samples were collected from 12 sites in 6 streams in eastern Ontario and western Quebec, Canada (Table 2-1). The streams were small, with a maximum width of 10 m, and were selected to cover a range of nutrient levels (Table 2-1). Sites were selected within the streams to represent different substrate compositions of primarily sand, gravel, cobble, or boulder, but all sites included cobble (particles with an approximate diameter ranging from 55 to 145 mm). Periphyton biomass varied, with no visible periphyton at some sites and large mats of filamentous algae at others; average periphyton chlorophyll *a* ranged from 8.24 $mg/m^2$ to 95.16 $mg/m^2$.

We used a modified version of the depletion electrobugging technique described by Taylor et al. (2001) to collect invertebrates. In this method, the electroshocker was used upstream of a stationary D-net (1 mm mesh), over an area of 30 x 60 cm. The width of the sampling area (30 cm) was the width of the D-net, and the length of the sampling area (60 cm) was determined by estimating how far the anode could be moved from the net and still shock invertebrates that would drift into the net with the current. We moved the anode through the sampling area for 30 seconds without disturbing the substrate, inducing drift by shocking the invertebrates in the area. The cathode was placed immediately downstream under the opening of the D-net to create an electrical gradient and direct drifting organisms into the net. After the 30 second sampling period, all organisms were removed from the net and placed in jars with 95% ethanol. This was repeated 3-5 times until attrition was noted. As recommended by Taylor et al. (2001), we used a Smith-Root LR-24 backpack electroshocker with a 15 cm (diameter) anode (instead of the standard 28 cm anode) to create a more concentrated pulse. We used the standard frequency and pulse width settings (30 Hz and a pulse width of 4ms), and a voltage ranging from 250-350 V DC depending on stream

conductivity (50 V higher than the voltage required to shock small fish). We did not set up nets surrounding our electrobugging area, and therefore may have had some movement of individuals in or out of the sampling area. However, we sampled over a smaller area than Taylor et al. (2001), and speculated that movement into the sampling area would be limited due the short-range pulse of the small anode. Immigration and emigration were expected to counterbalance each other, meeting the assumption of the depletion method that there was no net change in population size (Zippin 1958).

To examine the relative efficiency of electrobugging, we used two traditional invertebrate sampling methods (kick sampling and cobble collection) at the same stream sites to obtain data for comparison. Immediately following electrobugging, 2-3 kick samples (each lasting 30 seconds) were taken at the electrobugging locations to estimate the abundance of the remaining organisms. Six replicate cobbles (approximate diameter ranging from 55 to 145 mm) were collected at random from each stream site and placed in bags with 95% ethanol. All invertebrate samples were returned to the laboratory for processing.

In the laboratory, cobbles were brushed over a 1 mm sieve, and organisms retained on the sieve were identified. Electrobugging and kick samples were not sieved in the lab because the D-net mesh used in the field was 1 mm. When samples contained more than 200 individuals or large amounts of algae or debris (which often occurred in the case of kick samples), a Folsom plankton splitter was used to split samples. All invertebrate samples were identified to the level of family for insects and order or higher for non-insects. We measured the body length of each individual to the nearest 0.01 mm using an image analysis system (Optimas 6.5 Imaging Software; Media Cybernetics, Silver Springs, Maryland). Dry mass was estimated from body lengths by using taxon-specific length-mass regressions from

Benke et al. (1999). When there was no length-mass relationship information for a taxonomic group, dry mass (DM) was calculated as body length (L) cubed (DM [μg] = $L^3$ [$mm^3$]).

For the cobble samples, the number of organisms that were lost through the 1 mm sieve was predicted by using a sieve retention probability model. We used the overall (not taxon-specific) model of Gruenert et al. (2007) that incorporated chlorophyll *a* concentrations to predict the number of organisms in the cobble samples lost by sieving. Chlorophyll *a* concentrations were incorporated for the cobble samples because algae in the sample essentially trap organisms and prevent them from passing through the sieve, thereby inflating density estimates relative to sites with less algae.

The suitability of the sieve retention models to estimate organism counts for the electrobugging and kick samples was unknown, because it was unclear whether a 1 mm net held in flowing stream water would generate the same retention probabilities as a 1 mm sieve washed in the lab. To address this, we conducted a short experiment to evaluate the size retention of the net. Six cobbles were collected at random from a stream with a high abundance and richness of invertebrates (average abundance = 226, SE = 39.04; average richness = 13.17, SE = 0.70). The cobbles were gently brushed over a 63 μm sieve, all individuals were sorted and identified, and body lengths were measured. We then returned to the stream, separately placed each invertebrate sample in the 1 mm D-net, and held the net in the flowing stream water for 30 seconds, simulating an electrobugging or kick sampling pass. Samples were picked from the nets and returned to the lab to be re-processed. The retained organisms were again sorted, identified, and measured. Organisms were grouped according to body length, and the number of organisms of each length retained by the net was compared with the number originally collected for each cobble replicate. The net retained all

individuals larger than 6 mm in length. (Figure 2-1). Below 4 mm in length, more than 40% of individuals were lost through the net. When the sieve retention probability model of Morin et al. (2004) was applied to the number of organisms retained by the net, the estimated counts were improved to be within 6% of the original totals for all body lengths above 4 mm long (Figure 2-1). However, with the application of the sieve retention model, counts for individuals below 4 mm in length either remained much lower than original counts or became grossly overestimated.

From the results of the net retention test, we determined: (1) that the sieve retention probability models could be applied to electrobugging and kick sampling data for individuals greater than 4 mm in length to improve density and biomass estimates, and (2) that method comparisons with cobble samples should only be carried out for body lengths greater than 4 mm, due to the known loss of organisms below that size through the D-net. We applied the overall sieve retention probability model of Morin et al. (2004), which does not incorporate chlorophyll *a*, to the electrobugging data because the sampling method did not disturb the substrate and therefore did not dislodge algae. The retention model of Gruenert et al. (2007) was applied to the kick sampling data because the collection method did dislodge algae, and invertebrate retention was likely affected by algal biomass levels in those samples.

*Data Analysis*

Invertebrates collected in the cobble samples were grouped into $\log_2$ size classes based on dry mass. For each cobble, the total mass of individuals was summed for each taxon-size class combination and divided by the area of the cobble to provide estimates of biomass in $mg/m^2$ of cobble area. Cobble surface area was calculated by wrapping each cobble in aluminum foil, weighing the foil, and estimating the foil surface area from an area-

mass regression that was made using known surface areas of foil. In order to compare the cobble results with those from the other sampling methods, it was necessary to apply a correction factor to express biomass and density per unit stream area, rather than per unit cobble area. To create the correction factor, we wrapped all cobbles within a stream area of 1800 $cm^2$ (the size of the electrobugging and kick sampling area) and estimated the total cobble surface area from the weight of the foil. The cobble correction factor (cobble area per stream area) was then calculated as: correction = (cobble area $m^2$) / (0.18 $m^2$). We wrapped cobbles at two locations within each stream site to obtain an average cobble correction value for each site. The biomass in each taxon-size class combination was averaged across the number of replicate samples to provide average biomass estimates for each stream site.

Because the depletion method was used to collect electrobugging and kick samples, it was necessary to estimate the population size at each electrobugging site based on the number of individuals collected and the depletion in invertebrate counts with each additional pass. To create these estimates, we ran our data through MicroFish 3.0 (Van Deventer 1989), a program for estimating population size from electroshocking depletion data by using maximum-likelihood estimates. Because we were interested in comparing methods based on invertebrate size, we used count data that were summed over taxon-size class combinations for each pass (i.e., Baetidae size class 8, Baetidae size class 9, and so on). When population estimates were calculated, some of the invertebrate capture patterns did not display depletion as required by the MicroFish analysis. When a non-descending pattern was encountered from the first to the last pass, MicroFish was unable to provide an accurate population estimate, and set the total estimated count to 1.5 times the actual count. The presence of non-descending removal patterns was a by-product of our subdivision of the data into taxon-size

class combinations, rather than the standard taxon-based division, because it was difficult in the field to visually estimate the counts for each size class and determine whether attrition was visible.

The output from MicroFish was an estimated count for each taxon-size class combination based on the pass data. Electrobugging and kick sampling data were run separately through MicroFish for each site. Resulting counts were multiplied by the average dry mass of each taxon-size class combination (using sampling location-specific values) and divided by the area of the sampling location (0.18 $m^2$) to generate biomass values in $mg/m^2$ stream area. These values were averaged across the 3 replicates to provide average biomass estimates for electrobugging and kick samples for each stream site.

Electrobugging and kick sampling data were expected to provide a better estimate of biomass in large size classes when combined, because kick sampling was intended to collect the majority of individuals that electrobugging missed. However, because kick sampling potentially sampled a different portion of the population (including any organisms that were not induced to enter the drift by electroshocking), we combined the data in different ways depending on the number of individuals caught by each sampling method. We used the electrobugging estimates for all taxon-size class combinations that were only captured by that method, and similarly used the kick sample estimates for those that were only collected by kick sampling. For taxon-size class combinations that were collected by both sampling methods, we treated the kick sampling passes as additional electrobugging passes, essentially adding 2-3 more passes to the electrobugging data. We then ran those numbers through MicroFish to get estimates from the total number of passes. When MicroFish indicated a non-descending removal pattern, suggesting that kick sampling collected more individuals of

that taxon-size class combination, we did not treat the kick sampling data as additional electrobugging passes. In those cases, kick sampling was more efficient than electrobugging and collected individuals that were unable to enter the drift during electroshocking. For those taxon-size class combinations, we added the original electrobugging counts (without MicroFish population estimates) to the population estimates we obtained from the kick sampling data to get total counts for the stream site. The population estimates (from electrobugging and kick sampling data and a combination of the two) for all taxon-size class combinations were joined together for what will be termed the combined method of electrobugging and kick sampling. Resulting counts were multiplied by the average dry mass of each taxon-size class combination (using sampling location-specific values) and divided by the area of the sampling location (0.18 $m^2$) to generate biomass values ($mg/m^2$ stream area). These values were averaged across the 3 replicates to provide average biomass estimates for the combined method for each stream site.

*Method Comparison*

To evaluate the sampling accuracy of electrobugging, we examined the taxa and size classes collected by each method. We plotted the average biomass of each taxon collected by electrobugging and cobble collection to examine taxonomic overlap and compare density estimates from both methods. To account for any averages that may have been affected by extreme values, we also compared the number of sites at which electrobugging collected more biomass and the number of sites at which the cobble method collected more biomass for each taxon. We used chi-square analysis to determine whether the number of sites at which electrobugging or the cobble method collected more biomass was dependent on the taxonomic group (using insect orders and non-insects). If a significant result was found (at $\alpha$

= 0.05), we subdivided the contingency table to determine which taxa were collected at a significantly higher proportion of sites by one method (Zar 1999).

We used Fisher's exact test to compare the number of sites at which electrobugging or the cobble method collected more biomass of mobile or attached taxa. Mobile taxa were those deemed to be strong swimmers or fast crawlers by McCafferty (1998), while attached taxa included those noted to be strongly attached to the substrate and case-making Trichoptera, which were assumed to be slowed and partly anchored to the substrate by their cases. Electrobugging was expected to collect higher biomass of mobile taxa at a significant proportion of sites, and the cobble method was expected to collect higher biomass of attached taxa at a significant proportion of sites. To further examine the ability of electrobugging to collect mobile taxa, we plotted the average biomass across all sites of each mobile and attached taxon collected by electrobugging and kick sampling. Electrobugging was expected to collect more biomass than kick sampling because of the order in which the methods were used. Higher biomass in the kick samples was an indication that a taxon was not collected efficiently by electrobugging, because more biomass was left behind than was collected. The emphasis on mobility in this analysis was due to the fact that kick sampling, which physically disturbed the substrate, was expected to be more efficient at collecting attached taxa.

To determine whether algal biomass affected sampling efficiency, we compared the invertebrate biomass collected by electrobugging, kick sampling, and cobble collection as a function of the chlorophyll *a* concentration at each site. Because invertebrates may use algae as a refuge, we predicted that cobble collection and kick sampling (which both physically disturb the substrate) would collect higher biomass at sites with high chlorophyll *a* concentrations than the more passive electrobugging. Initially, we used least squares

regressions to determine whether invertebrate biomass increased significantly as a function of chlorophyll *a* for each sampling method. To compare sampling efficiencies, we used a general linear model (GLM) to test whether the slope of the relationship between invertebrate biomass (BM; $mg/m^2$) and chlorophyll *a* (Chl *a*; $mg/m^2$) was significantly different among sampling methods. The GLM model was: $\log_{10}$ BM = *b* + *c* ($\log_{10}$ Chl *a*) + method + ($\log_{10}$ Chl *a* * method), where *b* was the intercept and *c* was a coefficient describing the slope. The interaction term ($\log_{10}$ Chl *a* * method) tested whether slopes differed among sampling methods, which would suggest that the relative sampling efficiencies of the methods differed as a function of chlorophyll *a*.

We plotted size spectra to compare the biomass collected in each size class by the sampling methods. For this analysis, we compared the cobble method with the combined method, because the combination of electrobugging and kick sampling (collecting both mobile and attached taxa) was expected to provide a better estimate of the total biomass in each size class than electrobugging alone. Size spectra were created by summing the biomass (standardized per $m^2$ stream area) in each $\log_2$ size class (irrespective of taxon). The biomass size spectrum was plotted as the $\log_{10}$ biomass (BM; $mg/m^2$) against the $\log_{10}$ body length (length; mm). The body length used for each $\log_2$ size class (SC) was a rough estimate calculated as the cube root of the dry mass of that size class: length = $(2^{SC})^{1/3}$. We expected that the combined method would collect higher biomass in the large size classes because of the detection limit of the cobble collection method. To test this, we used a GLM to compare the combined and cobble biomass size spectra. Because several of the biomass spectra were best described by a second-order regression, the GLM model contained a squared body length term. We tested the model: $\log_{10}$ BM = *a* + *b* ($\log_{10}$ length) + *c* ($\log_{10}$ length)$^2$ +

method + ($\log_{10}$ length * method) + (($\log_{10}$ length)$^2$ * method). The interaction terms ($\log_{10}$ length * method) and (($\log_{10}$ length)$^2$ * method) tested whether the slopes were significantly (at $\alpha = 0.05$) different between methods, and therefore whether the effectiveness of each sampling method differed depending on body size. The method term tested whether the intercepts were significantly (at $\alpha = 0.05$) different. We visually assessed the spectra to determine the lengths at which the combined method collected higher biomass than the cobble method.

The final analysis was intended to examine whether the biomass collected in the large size classes represented a similar number of taxa for each method. We plotted the richness within each size class (as $\log_{10}$(body length)) for the cobble collection and combined methods to compare the number of taxa collected by each. This comparison was intended to evaluate whether differences in biomass spectra could be related to the number of taxa collected by each method.

**Results**

Average biomass values from the cobble method were higher than those from electrobugging for the majority of the taxa that were collected by both methods (Figure 2-2). The disparity in biomass estimates was particularly evident in Trichoptera families, which generally had higher average biomass in cobble samples than electrobugging samples. This may have been due in part to the effect of Trichoptera cases, which were expected to prevent the organisms from entering the drift. The only Trichoptera families that were collected more effectively by electrobugging were two families of free-living caddisflies that were not collected by the cobble method. The taxa that had higher average biomass in electrobugging samples were primarily mobile organisms (Amphipoda, Baetidae, Corydalidae,

Coenagrionidae, and Perlidae), in accordance with the prediction that electrobugging would collect mobile taxa that could evade collection by the cobble method. Furthermore, there were 18 taxa that were collected only by the electrobugging method. The biomass collected by electrobugging ranged from 0.5 to 1095 $mg/m^2$ for those taxa (Figure 2-2), which indicated that they were not only rare or insignificant taxa. Therefore, although the cobble method collected higher average biomass of the majority of taxa that were sampled by both methods, there was a large portion of the community that the cobble method missed.

In order to test whether the average biomass values presented in Figure 2-2 were unduly influenced by extreme values at a small number of sites, we compared the number of sites at which electrobugging collected higher biomass with the number of sites at which the cobble method collected higher biomass for each taxon. There were 7 taxa that had a higher average biomass in cobble samples, but for which more sites had higher biomass in electrobugging samples than in cobble samples (Table 2-2; Figure 2-2). One notable example was Hydropsychidae (Trichoptera) which had higher biomass in electrobugging samples at 9 sites and higher biomass in cobble samples at only 3 sites, yet which had a higher average biomass in cobble samples. The average biomass values for Hydropsychidae were clearly affected by extremely high values at a small number of sites, and did not represent the true capture probability of the two methods. In addition, there were 4 taxa that had higher average biomass values in cobble samples, but that had more biomass in cobble samples or more biomass in electrobugging samples at an even number of sites (Table 2-2; Figure 2-2). These results suggest that the cobble method did not consistently collect higher biomass than electrobugging for the taxa captured by both methods. In contrast, taxa that had higher average biomass in electrobugging samples were all found to have higher biomass in

electrobugging samples in more sites, indicating that the high average biomass values for electrobugging were not a result of extreme values at a small number of sites.

Based on the number of sites in which it collected higher biomass, electrobugging sampled families of Ephemeroptera, Hemiptera, Megaloptera, Odonata, and Plecoptera better than the cobble method (Table 2-2). These orders were primarily made up of mobile taxa (Table 2-2), supporting the prediction that electrobugging would collect more biomass of mobile taxa. The remaining groups of taxa were not clearly sampled better by one method or the other. Although Trichoptera appeared to be sampled more effectively by the cobble method based on average biomass values (Figure 2-2), the number of sites at which electrobugging collected higher biomass was close to the number of sites at which the cobble method collected higher biomass for most families (Table 2-2). The proportion of sites at which the cobble or electrobugging method collected more biomass was not independent on the major taxonomic group ($\chi^2 = 22.32$, df = 6, $p = 0.001$). When we subdivided the contingency table, we found that neither the cobble method nor electrobugging collected higher biomass of Coleoptera, Diptera, Trichoptera, and non-insects at a significant proportion of sites ($\chi^2 = 4.074$, df = 3, $p = 0.25$), confirming that these taxonomic groups were not sampled better by one method over the other. The number of sites at which the cobble method or electrobugging collected higher biomass for the remaining three taxa (Ephemeroptera, Odonata, and Plecoptera) was compared with the sum of the number of sites for Coleoptera, Diptera, Trichoptera, and non-insects. Ephemeroptera and Plecoptera were both found to be collected in higher biomass by electrobugging at a significant proportion of sites (Ephemeroptera one-tailed $p < 0.001$; Plecoptera one-tailed $p = 0.01$), confirming the trend that was evident in Table 2-2. Odonata were not found to be collected in higher

biomass at a significant proportion of sites by electrobugging (one-tailed $p$ =0.05), in contrast with the patterns evident in Table 2-2. However, this last result may have been affected by low frequencies; in total, the cobble method collected higher biomass of Odonata at 1 site and electrobugging collected higher biomass at 5 sites. Although many of the mobile taxa were represented in the taxonomic groups that were found to be better sampled by electrobugging (Ephemeroptera, Odonata, and Plecoptera), we compared the frequencies with which the cobble method or electrobugging collected higher biomass of all mobile or attached taxa. The proportion of sites at which electrobugging or the cobble method collected higher biomass depended on whether mobile or attached taxa were considered ($p < 0.001$), which indicated that electrobugging collected mobile taxa at a higher proportion of sites than the cobble method, and the cobble method collected attached taxa at a higher proportion of sites than electrobugging.

When compared with kick sampling, there was further evidence that electrobugging was appropriate for collecting mobile taxa, because kick sampling only collected higher biomass of three of the highly mobile taxa (Figure 2-3). Although we cannot conclude that electrobugging was significantly better than kick sampling because of the non-independence of the samples, it collected more biomass of the majority of mobile taxa than was left behind. In addition, electrobugging collected 8 mobile taxa that were not found in kick samples. Kick sampling was more effective at collecting attached taxa than electrobugging. Kick sampling collected higher biomass than electrobugging for 14 of the 18 attached taxa (including 5 taxa that were not found in electrobugging samples). As expected, electrobugging did not cause the attached taxa to enter the drift, and collected lower biomass estimates for those taxa than the physical disturbance of the kick sampling method.

The total biomass collected at each site by the cobble method, electrobugging, and kick sampling was plotted as a function of the average chlorophyll *a* concentration at each site to examine whether algal biomass affected sampling relative performance (Figure 2-4). There was a weak and statistically non significant increase in invertebrate biomass with an increase in chlorophyll *a* for samples collected by the cobble and kick sampling methods, and no trend for electrobugging. There was a great deal of scatter in the data, and no clear visible trend to suggest that either cobble collection or kick sampling was more efficient than electrobugging in high algal biomass compared to low algal biomass. This was confirmed when we tested the GLM to compare the sampling methods. There was no significant interaction between method and chlorophyll *a* ($p = 0.80$), nor was there a significant effect of chlorophyll *a* ($p = 0.87$). These results indicated that the relative performance of the 3 methods did not vary significantly with increasing periphyton biomass. Physical disturbance sampling methods (cobble and kick sampling) were not better than the more passive electrobugging at collecting invertebrates at sites with high algal biomass.

The biomass spectra from the cobble method were compared with the combined method (electrobugging and kick sampling) spectra because the combined method provided a better estimate of total biomass for both mobile and attached taxa than electrobugging alone. There was very little consistency in the differences between biomass spectra across all of the sampling sites: at several sites, the cobble method collected more biomass, while at other sites, the combined method collected more biomass in the majority of size classes (Figure 2-5). In general, the combined method appeared to be more effective in the sites where chlorophyll *a* levels were lowest (indicated by the arrangement of spectra in Figure 2-5). This was evidenced by higher biomass totals for the combined method in size classes sampled by

both methods (particularly in DT1, BRA2, and C2; Figure 2-5), and more noticeably by an increase in the number of size classes collected by the combined method relative to the cobble method (particularly in C3, BRA2, C6, C9a, and C2; Figure 2-5). In four sites, the combined method captured invertebrates in 3 or more size classes beyond the largest size class collected by the cobble method. However, the additional size classes were not solely in the longest body lengths, but were spread throughout the spectrum, down to 4 mm in length. The larger number of size classes collected by the cobble method in the sites with high chlorophyll *a* concentrations may have been a result of organisms living within the algae and therefore being more susceptible to collection by the cobble method. In sites where chlorophyll *a* levels were low, the cobble method may have collected a limited number of size classes because of the lack of algal biomass. The combined method was more consistent with regards to the number of size classes sampled, collecting organisms from a large number of size classes at all sites irrespective of chlorophyll *a* concentrations, and only collecting fewer size classes than the cobble method at one site (a difference of one class).

There was a strong similarity in spectrum shape between the cobble and combined method at most sites (Figure 2-5). Biomass differences between the two methods were generally consistent across all size classes, and did not suggest that one method sampled a particular portion of the size spectrum better than the other. Therefore, despite overall biomass differences between the two methods, the slopes of the size spectra produced by the cobble and combined methods did not appear to differ. This was confirmed by the results of the GLM. The interaction terms in the model were not significant ($\log_{10}$ length $p = 0.09$; $(\log_{10}\text{ length})^2$ $p = 0.09$), suggesting that the biomass spectrum slopes did not differ between methods. The reduced model (without the interaction term) showed that there was a

significant difference in intercepts ($p = 0.04$), which indicated that biomass levels differed between the cobble and combined method. These results indicate that although biomass levels differed between the two methods, the general shape of the biomass spectrum remained the same. However, the lower number of size classes collected by the cobble method in the sites with low chlorophyll *a* suggests that the biomass spectrum shape could be affected by the chosen sampling method under conditions of low algal biomass.

We explored how the taxonomic richness differed among size classes for the cobble and combined methods because taxonomic discrepancies had already been indicated in Figure 2-2, and were expected to account for some of the differences in biomass seen in the spectra in Figure 2-5. There were large differences in the number of taxa collected in each size class, particularly in the sites with low concentrations of chlorophyll *a*, where the combined method generally collected 2-3 times as many taxa as the cobble method (see C3, BRA2, C6, C9a, and C2; Figure 2-6). However, the combined method collected more taxa than the cobble method even in the sites with high chlorophyll *a* concentrations. Overall, the patterns in Figure 2-6 suggest that the cobble method only samples a portion of the community, missing the majority of taxa, especially in oligotrophic sites. This was particularly evident for Chelsea Stream 6 (C6): the cobble method collected higher biomass than the combined method for size classes sampled by both methods (Figure 2-5), but Figure 2-6 showed that the cobble method only collected one taxon in each size class, while the combined method collected 2-14 taxa in each size class. The cobble method biomass spectrum therefore represented an underestimate of the overall biomass across all size classes.

**Discussion**

Many of the merits of electrobugging were outlined by Taylor et al. (2001) in their description and test of the method. First and foremost, electrobugging is beneficial because of the extent to which it simplifies the sample sorting process by eliminating much of the debris commonly collected by other sampling methods. Although the depletion method of electrobugging may require a larger time commitment in the field to ensure that a sufficient number of passes has been collected, the reduced sorting time still makes this method faster than many others. It is also less disruptive to the benthic habitat than other more physical methods such as kick sampling and cobble collection. Furthermore, electrobugging can be used to collect organisms from a wider range of habitats than cobble collection, and the larger-scale samples can incorporate multiple habitat types for a more complete description of the benthic community.

Our study identified additional benefits of electrobugging that were more specifically related to its use in body size analysis. We found that electrobugging collected many more taxa than the cobble method. As suggested by Taylor et al. (2001), this may have been partly a result of the larger area and the additional habitats sampled by electrobugging. Any taxon in interstitial spaces, or on sand, bedrock, or boulders would not have been sampled by the cobble method, but could have been induced by electrobugging to drift into the sample net. The increased number of taxa collected by electrobugging may also have resulted from the efficiency of the method to sample highly mobile taxa. Electrobugging collected higher biomass of mobile taxa than the cobble method at a significant proportion of sites. Electrobugging also collected more biomass of mobile taxa than was left behind and collected by kick sampling, and sampled several mobile taxa that were not found in any kick sampling passes. The combination of electrobugging and kick sampling greatly increased the

number of taxa collected per size class relative to the cobble method, which resulted in increased numbers of taxa in all size classes. These results have large implications for biomass measurements in body size studies, because they suggest that size distributions that are created using only data from cobble collection do not represent the entire benthic community. Such studies can underestimate not only the total biomass in the community, but also the biomass in each size class in which taxa have been missed.

One limitation of the method was evident when we compared our electrobugging and kick sampling results, as we found that the electrobugging method left more biomass of attached taxa than it collected. The cobble method was also found to collect higher biomass of attached taxa than electrobugging at a significant proportion of sites. The inability of electrobugging to efficiently collect attached taxa was pointed out by Taylor et al. (2001) as a weakness of the method, but was not explicitly tested because their study sites were dominated by more mobile taxa. Because of the large proportion of attached taxa that were inefficiently collected by electrobugging at our study sites, it cannot be recommended as the sole collection method if the aim of sampling is to obtain an accurate estimate of biomass in both mobile and attached taxa. However, cobble collection does not provide an ideal method to supplement electrobugging, because it samples a more restricted habitat and was shown to miss a large number of taxa. Therefore, we suggest that kick sampling be performed after electrobugging in order to obtain the most complete measure of the biomass of mobile and attached taxa. The data from the two methods may then be merged as we have described for the combined method.

We predicted that electrobugging would collect more biomass of large organisms than the cobble method because it sampled a larger area and therefore had a lower detection

limit than the cobble method. We found that as well as collecting more taxa, the combination of electrobugging and kick sampling added to the biomass estimates for large organisms by sampling additional size classes that were not included in the cobble method biomass distributions. The use of these sampling methods particularly improved the description of biomass in large organisms in the sites with low algal biomass, where the cobble method collected very few size classes. Although the combined method did not add a large number of size classes to the extreme end of the spectrum (in the longest body lengths) at all of our sites, size classes were added throughout the entire range of the biomass spectrum included in this study at the majority of sites. Morin and Nadon (2001) hypothesized that 90% of the biomass in the macroinvertebrate community was contributed by organisms greater than 2 mm in length. Therefore, the addition of new size classes at any body length along our cobble biomass spectrum (which only contained large organisms that were greater than 4 mm in length) contributed to a more accurate estimate of density and biomass in the most important part of the size spectrum. When combined with data for organisms less than 4 mm in length, this improved estimate of large organisms could lead to a better description of body size distribution shape in stream macroinvertebrates.

A second limitation of electrobugging was evident when we compared the biomass collected per taxon. When average biomass values per taxon were plotted for electrobugging and the cobble method, it appeared that the cobble method collected higher biomass for the majority of taxa sampled by both methods. Examination of the number of sites at which the cobble method collected more biomass indicated that the average biomass results for several taxa were influenced by a small number of sites with extreme values. While this indicates that the cobble method did not collect more biomass at a large proportion of sites for those

taxa, it also suggests that electrobugging collected much less biomass than the cobble method at those sites. There were several possible reasons for the apparent inferiority of electrobugging and the combined method. Our electrobugging and kick sampling estimates may have been affected by the lack of enclosure around the sampling area, or the lack of attrition at several sampling locations. The non-enclosed sampling area may have allowed organisms to leave the sampling area, resulting in reduced capture rates and reduced population estimates. The lack of attrition may have introduced further error into our population estimates, as an estimate of 1.5 times the captured abundance was used when a taxon-size class combination displayed a non-descending trend. The resulting estimate could have been an over- or underestimate of the actual total population size, but given the much higher biomass estimates produced by the cobble method, we suspect that it was generally an underestimate.

One noticeable effect of the gradient in chlorophyll *a* concentrations among our sites was that the number of taxa and size classes collected by the cobble method decreased with decreasing algal biomass, while the combined method continued to collect large numbers of taxa and size classes even when chlorophyll *a* levels were low. This suggests that the importance of non-cobble habitat increases when algal biomass (and therefore refuge) decreases, and a more wide-ranging sampling method like electrobugging is required to ensure that the entire biomass spectrum is sampled. However, despite the differences in the number of taxa and size classes represented, the shape of the biomass distribution was not significantly different between the cobble and combined methods. This indicates that although the cobble method only sampled a portion of the invertebrate community, the relative biomass from one size class to the next remained the same, resulting in no change in

distribution slope. The additional data provided by the combined method are therefore more important for biomass totals than for distribution shape.

Our estimates of small organisms would have been improved by the use of a smaller mesh size. This would have allowed us to compare smaller size classes with the cobble method. However, the main point of this research was to evaluate the ability of electrobugging to sample large organisms that may be inefficiently collected by the cobble method. Therefore, the use of a smaller mesh size would have increased processing time and may not have contributed meaningful results to our analysis. A larger problem came from creating population estimates based on attrition. The lack of attrition in many of our taxon-size class combinations may have introduced further error into our population estimates, as an estimate of 1.5 times the captured abundance was used when there was a non-descending trend. The resulting estimate could have been an over- or underestimate of the actual total population size, but given the much higher biomass estimates produced by the cobble method for some taxa (notably Trichoptera families) and for some size classes (especially in Raisin River 2 and Des Trembles 2), we suspect that this value was generally an underestimate. This is a problem without a clear solution, because the issue is due to the estimation of population size using taxon-size class combinations; increasing sampling effort did not appear to have a large effect on attrition patterns. In order to create a size distribution, you must have a population estimate for each body size. Because different sampling methods will preferentially collect different taxa, there must be separate population estimates for each taxon-body size combination, causing further subdivision that affects depletion patterns and makes it very difficult in the field to estimate whether you've achieved attrition or not. The best recommendation for this problem is to try to optimize sampling efforts to attain what

appears to be (in the field) the best possible depletion pattern. The size spectra including the combination of electrobugging and kick sampling were similar in terms of biomass levels for the majority of the sites. A more quantitative method such as cobble collection could be used in conjunction with the combined method in order to further ensure the best estimates have been obtained.

The use of kick sampling following electrobugging passes may seem to negate the benefits of electrobugging by introducing habitat disruption and producing samples with a large amount of debris to be sorted through. However, in the recommended methodology, kick sampling is used as a supplement to electrobugging rather than as the primary method. Therefore, fewer kick samples will be required and the samples will contain less organisms than if electrobugging had not been performed first. It was not possible to test whether electrobugging was more efficient at collecting mobile organisms than kick sampling by reversing the order in which they were performed. The process of collecting a kick sample is very destructive to the habitat, and the mobile taxa collected by electrobugging would presumably have moved away during the kick sampling passes if they were not collected. Because of this, we do not have strong evidence that electrobugging collects mobile taxa more efficiently than kick sampling and is therefore a superior method. The choice to use electrobugging must therefore be based on a desire to ensure all taxa are collected while reducing the required number of kick samples.

It would be ideal to recommend electrobugging alone as a viable option to sample benthic macroinvertebrates for body size studies. This method was found to improve estimates of biomass in large organisms by sampling additional taxa and size classes not collected by the cobble method. However, this method was unable to provide an unbiased

estimate of the biomass across all taxa and size classes because of the inefficiency with which it collected attached taxa. Our results showed that the more commonly used cobble method was also not an ideal sampling method because of the large number of taxa and size classes that it did not collect (particularly in sites with low algal biomass). Because of the problems with electrobugging, we recommend that each set of electrobugging passes be followed by 2-3 passes of kick sampling, to ensure that attached taxa are collected. Furthermore, because of the low biomass estimates for some taxon-size class combinations sampled by the combined method of electrobugging and kick sampling, we recommend that this method be accompanied by the more traditional cobble collection method. To create a merged biomass size distribution from these two sets of data, the higher biomass estimate from the two methods should be selected for each taxon-size class combination to make certain that data for all taxa and sizes are incorporated. Although this has the possibility to result in overestimates if sampling methods are equivalent, our results showed that the combination of electrobugging and kick sampling collected a large number of taxa that were not collected by the cobble method, but underestimated the densities of organisms that were collected by both methods. The recommended procedures will therefore ensure that the most complete description of the biomass spectrum has been obtained.

**References**

Basset, A., Sangiorgio, F., and Pinna, M. 2004. Monitoring with benthic macroinvertebrates: advantages and disadvantages of body size descriptors. Aquat. Conserv. **14**: S43-S58.

Benke, A.C., Huryn, A.D., Smock, L.A., and Wallace, J.B. 1999. Length-mass relationships for freshwater macroinvertebrates in North America with particular reference to the southeastern United States. J. N. Am. Benthol. Soc. **18**(3): 308-343.

Bourassa, N., and Morin, A. 1995. Relationships between size structure of invertebrate assemblages and trophy and substrate composition in streams. J. N. Am. Benthol. Soc. **14**(3): 393-403.

Cattaneo, A. 1993. Size spectra of benthic communities in Laurentian streams. Can. J. Fish. Aquat. Sci. **50**: 2659-2666.

Gruenert, U., Carr, G., and Morin, A. 2007. Reducing the cost of benthic sample processing by using sieve retention probability models. Hydrobiologia. **589**: 79-90.

McCafferty, W.P. 1998. Aquatic Entomology: The Fisherman's and Ecologist's Illustrated Guide to Insects and Their Relatives. Jones & Bartlett Publishers.

Morin, A., and Nadon, D. 1991. Size distribution of epilithic lotic invertebrates and implications for communtiy metabolism. J. N. Am. Benthol. Soc. **10**(3): 300-308.

Morin, A., Rodríguez, M.A., and Nadon, D. 1995. Temporal and environmental variation in the biomass spectrum of benthic invertebrates in streams: an application of thin-plate splines and relative warp analysis. Can. J. Fish. Aquat. Sci. **52**: 1881-1892.

Morin, A., Stephenson, J., and Strike, J. 2004. Sieve retention probabilities of stream benthic invertebrates. J. N. Am. Benthol. Soc. **23**(2): 383-391.

Peters, R.H. 1983. The Ecological Implications of Body Size. Cambridge University Press, Cambridge.

Rasmussen, J.B. 1993. Patterns in the size structure of littoral zone macroinvertebrate communities. Can. J. Fish. Aquat. Sci. **50**: 2192-2207.

Rodríguez, M.A., and Magnan, P. 1993. Community structure of lacustrine macrobenthos: do taxon-based and size-based approaches yield similar insights? Can. J. Fish. Aquat. Sci. **50**: 800-815.

Solimini, A.G., Benvenuti, A., D'Olimpio, R., Cicco, M.d., and Carchini, G. 2001. Size structure of benthic invertebrate assemblages in a Mediterranean river. J. N. Am. Benthol. Soc. **20**(3): 421-431.

Taylor, B.W., McIntosh, A.R., and Peckarsky, B.L. 2001. Sampling stream invertebrates using electroshocking techniques: implications for basic and applied research. Can. J. Fish. Aquat. Sci. **58**: 437-445.

Van Deventer, J.S. 1989. Microcomputer Software System for Generating Population Statistics from Electrofishing Data -- User's Guide for MicroFish 3.0. USDA Forest Service, General Technical Report INT-254.

Zar, J.H. 1999. Biostatistical Analysis. Prentice-Hall, Inc., Upper Saddle River, NJ.

Zippin, C. 1958. The removal method of population estimation. J. Wildlife Manage. **22**(1): 82-90.

Table 2-1. Physical and biological characteristics of the study sites.

| Site | Abbreviation | Lat (N) | Long (W) | Conductivity (uS/cm) | Average TP (mg/L) | Average TN (mg/L) | Average Chl a (mg/m2) |
|---|---|---|---|---|---|---|---|
| Beckett's Creek | BEC | 45.5212 | 75.3589 | 560 | 0.12 | 1.55 | 223.18 |
| Brassil's Creek 2 | BRA2 | 44.9850 | 75.8013 | 370 | 0.02 | 0.71 | 18.37 |
| Chelsea Stream 2 | C2 | 45.5076 | 75.8129 | 320 | 0.02 | 0.48 | 9.81 |
| Chelsea Stream 3 | C3 | 45.5020 | 75.8113 | 365 | 0.04 | 0.54 | 31.95 |
| Chelsea Stream 6 | C6 | 45.4960 | 75.8144 | 365 | 0.07 | 0.59 | 17.52 |
| Chelsea Stream 9a | C9a | 45.4953 | 75.7854 | 475 | 0.05 | 0.50 | 11.37 |
| Des Trembles 1 | DT1 | 45.4290 | 75.7616 | 815 | 0.20 | 1.30 | 74.49 |
| Des Trembles 2 | DT2 | 45.4201 | 75.7529 | 895 | 0.11 | 1.07 | 94.04 |
| Leamy midstream | LMS | 45.4674 | 75.7470 | 775 | 0.21 | 1.97 | 76.77 |
| Leamy downstream | LDS | 45.4625 | 75.7287 | 760 | 0.16 | 1.18 | 96.16 |
| Leamy downstream 2 | LDS2 | 45.4595 | 75.7323 | 1255 | 0.15 | 1.96 | 44.65 |
| Raisin River 2 | RR2 | 45.1867 | 74.8556 | 550 | 0.04 | N/A | 189.76 |

Table 2-2. A comparison of the electrobugging and cobble methods, with a list of the collected taxa and their mobility (for those taxa that were rated; M = mobile, A = attached), and for each taxon: the sample with the higher average biomass value (E = electrobugging, C = cobble; see Figure 2-1), the number of sites where it was found, and the number of sites where the cobble or electrobugging method collected more biomass (BM; larger number of sites is marked in bold).

| | Taxa | | Mobility | Method with higher average value | Number of sites where | | |
|---|---|---|---|---|---|---|---|
| | | | | | taxon was found | cobble BM was higher | electrobugging BM was higher |
| Insects | | | | | | | |
| Coleoptera | C1 | Chrysomelidae larva | | E | 1 | 0 | **1** |
| | C2 | Dytiscidae larva | M | E | 2 | 0 | **2** |
| | C3 | Elmidae adult | A | C | 1 | **1** | 0 |
| | C4 | Elmidae larva | A | C | 7 | **5** | 2 |
| | C5 | Hydrophilidae adult | M | E | 1 | 0 | **1** |
| | C6 | Psephenidae larva | A | C | 3 | **3** | 0 |
| Diptera | D1 | Ceratopogonidae | | E | 1 | 0 | **1** |
| | D2 | Chironominae | A | C | 12 | **8** | 4 |
| | D3 | Ephydridae | | E | 3 | 0 | **3** |
| | D4 | Muscidae-Anthomyiidae | | E | 1 | 0 | **1** |
| | D5 | Orthocladiinae | A | C | 10 | **9** | 1 |
| | D6 | Simuliidae larva | A | C | 9 | 3 | **6** |
| | D7 | Simuliidae pupa | A | C | 1 | **1** | 0 |
| | D8 | Tanypodinae | | C | 10 | **8** | 2 |
| | D9 | Tipulidae | | C | 10 | 5 | 5 |
| | D10 | unknown pupa | A | C | 6 | **4** | 2 |
| Ephemeroptera | E1 | Baetidae | M | E | 9 | 1 | **8** |
| | E2 | Caenidae | | C | 6 | 3 | 3 |
| | E3 | Ephemerellidae | | E | 2 | 0 | **2** |
| | E4 | Heptageniidae | A | E | 9 | 2 | **7** |
| | E5 | Leptophebiidae | | C | 4 | 2 | 2 |
| | E6 | Oligoneuriidae | M | E | 4 | 0 | **4** |
| | E7 | Tricorythidae | | E | 3 | 0 | **3** |
| Hemiptera | H1 | Veliidae | M | E | 1 | 0 | **1** |
| Megaloptera | M1 | Corydalidae | M | E | 4 | 1 | **3** |
| Odonata | O1 | Aeshnidae | M | C | 3 | 1 | **2** |
| | O2 | Coenagrionidae | M | E | 1 | 0 | **1** |
| | O3 | Cordulegastridae | M | E | 1 | 0 | **1** |
| | O4 | Gomphidae | M | E | 1 | 0 | **1** |
| Plecoptera | P1 | Leuctridae | M | E | 3 | 0 | **3** |
| | P2 | Nemouridae | M | E | 1 | 0 | **1** |
| | P3 | Perlidae | M | E | 6 | 2 | **4** |
| | P4 | Perlodidae | M | E | 1 | 0 | **1** |
| Trichoptera | T1 | Brachycentridae | A | C | 3 | 1 | **2** |
| | T2 | Glossomatidae | A | C | 4 | 2 | 2 |
| | T3 | Helicopsychidae | A | C | 4 | **4** | 0 |
| | T4 | Hydropsychidae | | C | 12 | 3 | **9** |
| | T5 | Hydroptilidae | A | C | 2 | **2** | 0 |
| | T6 | Lepidostomatidae | A | C | 3 | **2** | 1 |
| | T7 | Leptoceridae | A | C | 1 | **1** | 0 |
| | T8 | Philopotamidae | | C | 7 | **4** | 3 |
| | T9 | Polycentropodidae | | C | 6 | **4** | 2 |
| | T10 | Psychomyiidae | | E | 2 | 0 | **2** |
| | T11 | Rhyacophilidae | | E | 1 | 0 | **1** |
| | T12 | unknown pupa | A | C | 4 | **3** | 1 |
| Non-Insects | | | | | | | |
| Amphipoda | N1 | | M | E | 3 | 0 | **3** |
| Isopoda | N2 | | | C | 7 | 1 | **6** |
| Gastropoda | N3 | | A | C | 4 | **4** | 0 |
| Turbellaria | N4 | | | C | 5 | 2 | **3** |
| Nematoda | N5 | | | C | 4 | **3** | 1 |
| Oligochaeta | N6 | | | C | 7 | 3 | **4** |
| Hirudinea | N7 | | | E | 3 | 0 | **3** |

**Figure Captions**

Figure 2-1. The percent of individuals of each length from the initial cobble samples retained by the 1 mm mesh D-net (open squares) and predicted by the model of Morin et al. (2004; open triangles), averaged across the 6 replicate samples used in the electrobugging retention study. Lengths on the x-axis represent the lower limit for each length class (i.e., length 1 includes organisms 1-2 mm long). Data are omitted for lengths below 1 mm because predicted percents greatly exceeded 100%.

Figure 2-2. The biomass of each taxon (denoted by a one-letter code for the broad taxonomic group and a subscript number to indicate family or order; see Table 2-2 for legend) collected by electrobugging and cobble collection. The diagonal represents a 1:1 line. Biomass values are averages for all sampling sites where the taxon was found. A value of 0.1 $mg/m^2$ was used when a taxon was not collected by one method. One-letter codes are as follows: C – Coleoptera, D – Diptera, E – Ephemeroptera, M – Megaloptera, O – Odonata, P – Plecoptera, T – Trichoptera, N – non-insect.

Figure 2-3. The biomass of mobile (M) and attached (A) taxa collected by electrobugging and kick sampling. The diagonal represents a 1:1 line. Biomass values are averages for all sampling sites where the taxon was found. A value of 0.1 $mg/m^2$ was used when a taxon was not collected by one method.

Figure 2-4. Total invertebrate biomass collected by each sampling method as a function of chlorophyll *a* standing stock at the stream site. Linear regression lines are shown for each sampling method.

Figure 2-5. The biomass collected in each size class by the cobble method (open squares) and the combined method (closed circles) at each site. A LOESS curve is shown for each method. Sites are arranged in order of decreasing algal biomass (as measured by chlorophyll *a*); BEC has the highest levels while C2 has the lowest levels of algal biomass.

Figure 2-6. The number of taxa collected in each size class by the cobble method (open squares) and the combined method (closed circles) at each site. A LOESS curve is shown for each method. Sites are arranged in order of decreasing algal biomass (as measured by chlorophyll *a*); BEC has the highest levels while C2 has the lowest levels of algal biomass.

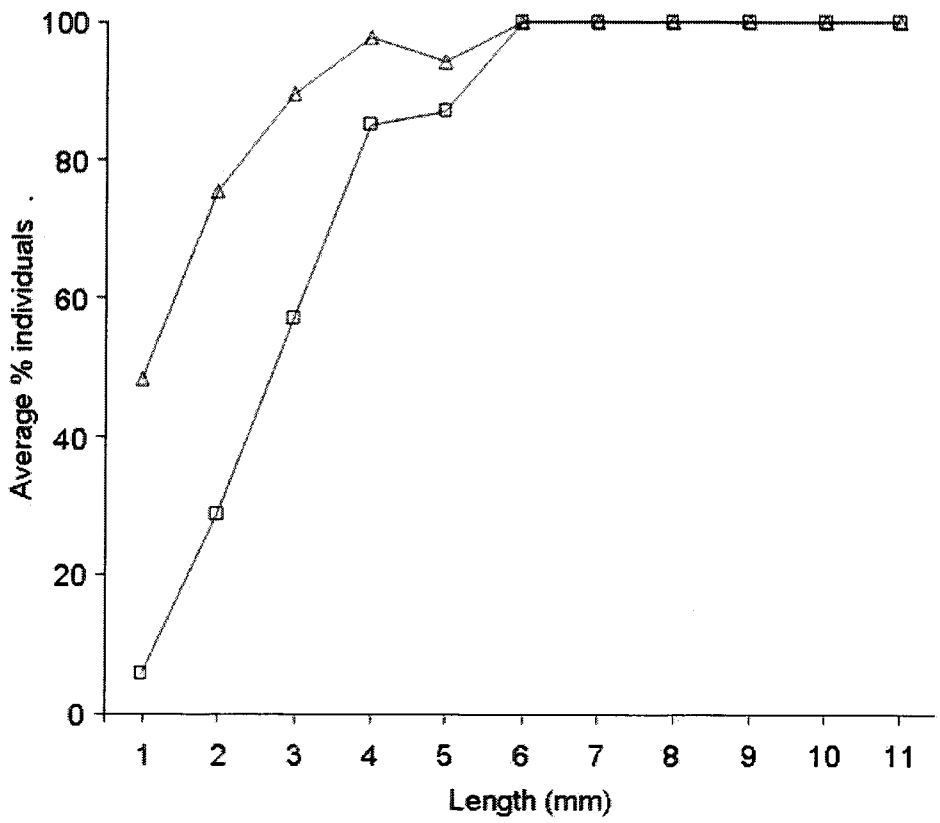
100
80
60
40
20
0
Average % individuals
1
2
3
4
5
6
7
8
9
10
11
Length (mm)

Figure 2-1

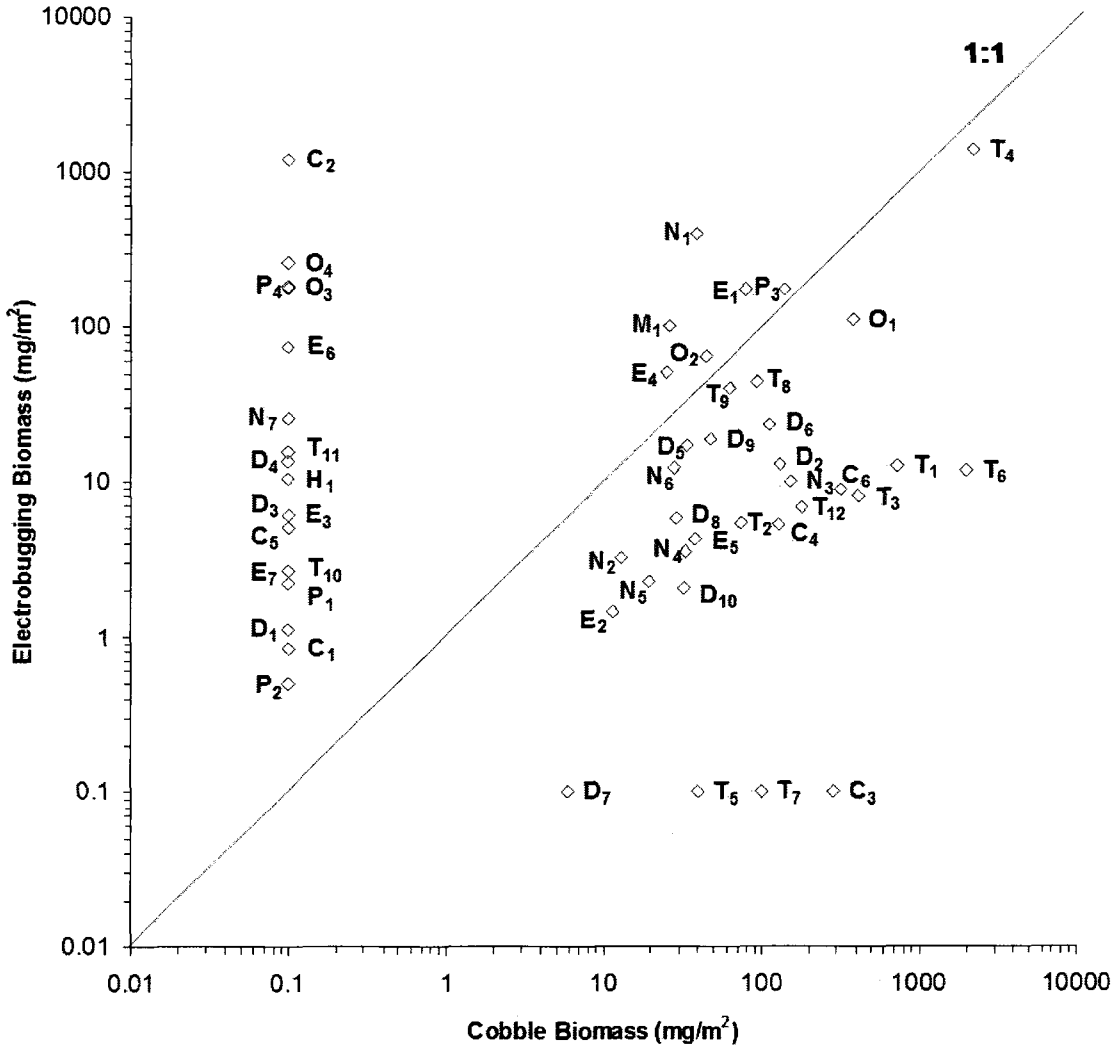
1:1
Electrobugging Biomass (mg/m²)
Cobble Biomass (mg/m²)
10000
1000
100
10
1
0.1
0.01
0.01
0.1
1
10
100
1000
10000
C2
O4
P4
O3
E6
N7
D4
T11
H1
D3
E3
C5
E7
T10
P1
D1
C1
P2
N1
E1
P3
M1
O2
E4
T9
T8
D6
D5
D9
D2
N6
N3
C6
T1
T6
T3
T12
D8
T2
C4
E5
N4
N2
N5
D10
E2
T4
O1
D7
T5
T7
C3

Figure 2-2

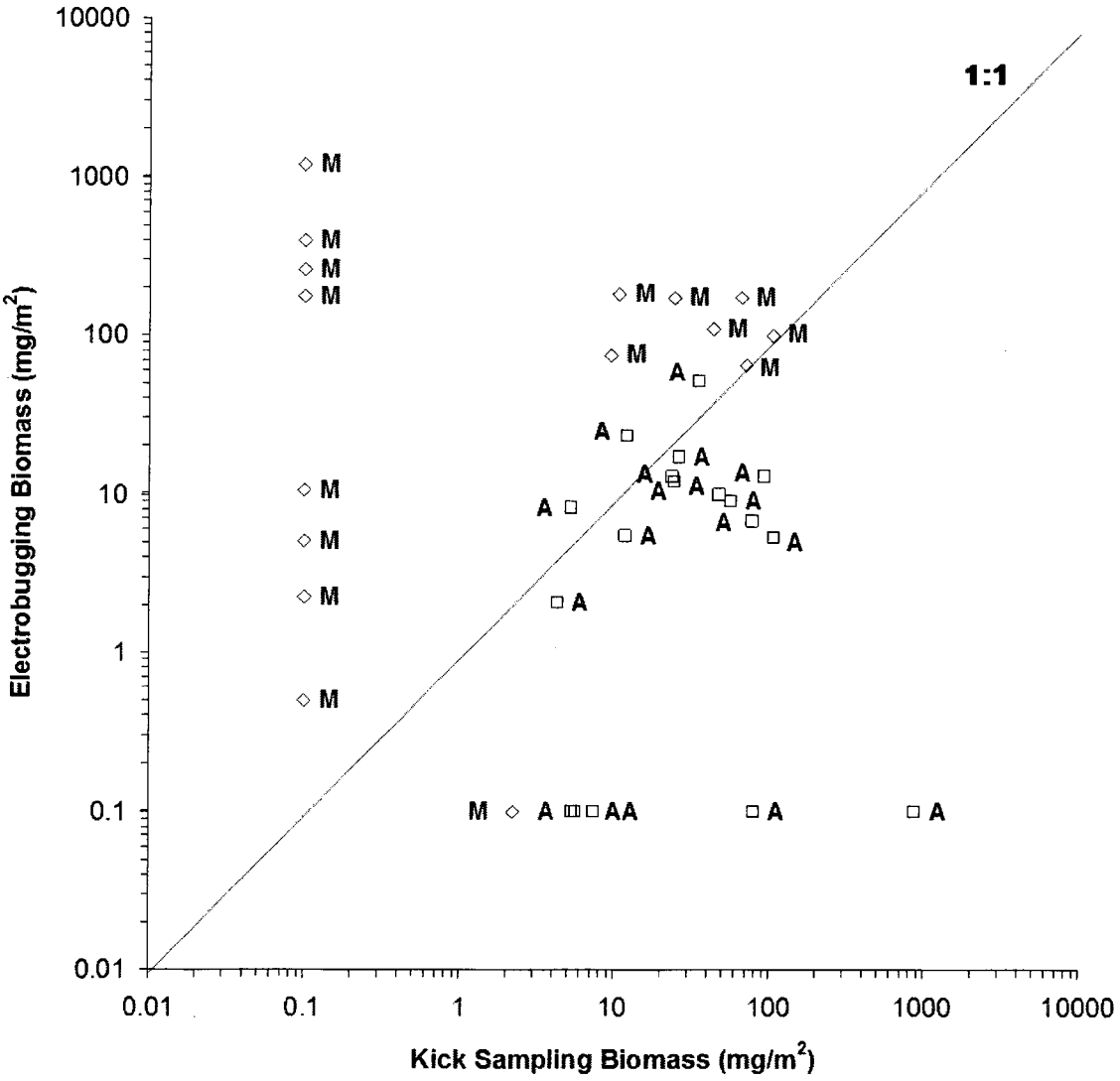
1:1
Electrobugging Biomass (mg/m2)
Kick Sampling Biomass (mg/m2)
10000
1000
100
10
1
0.1
0.01
0.01
0.1
1
10
100
1000
10000

Figure 2-3

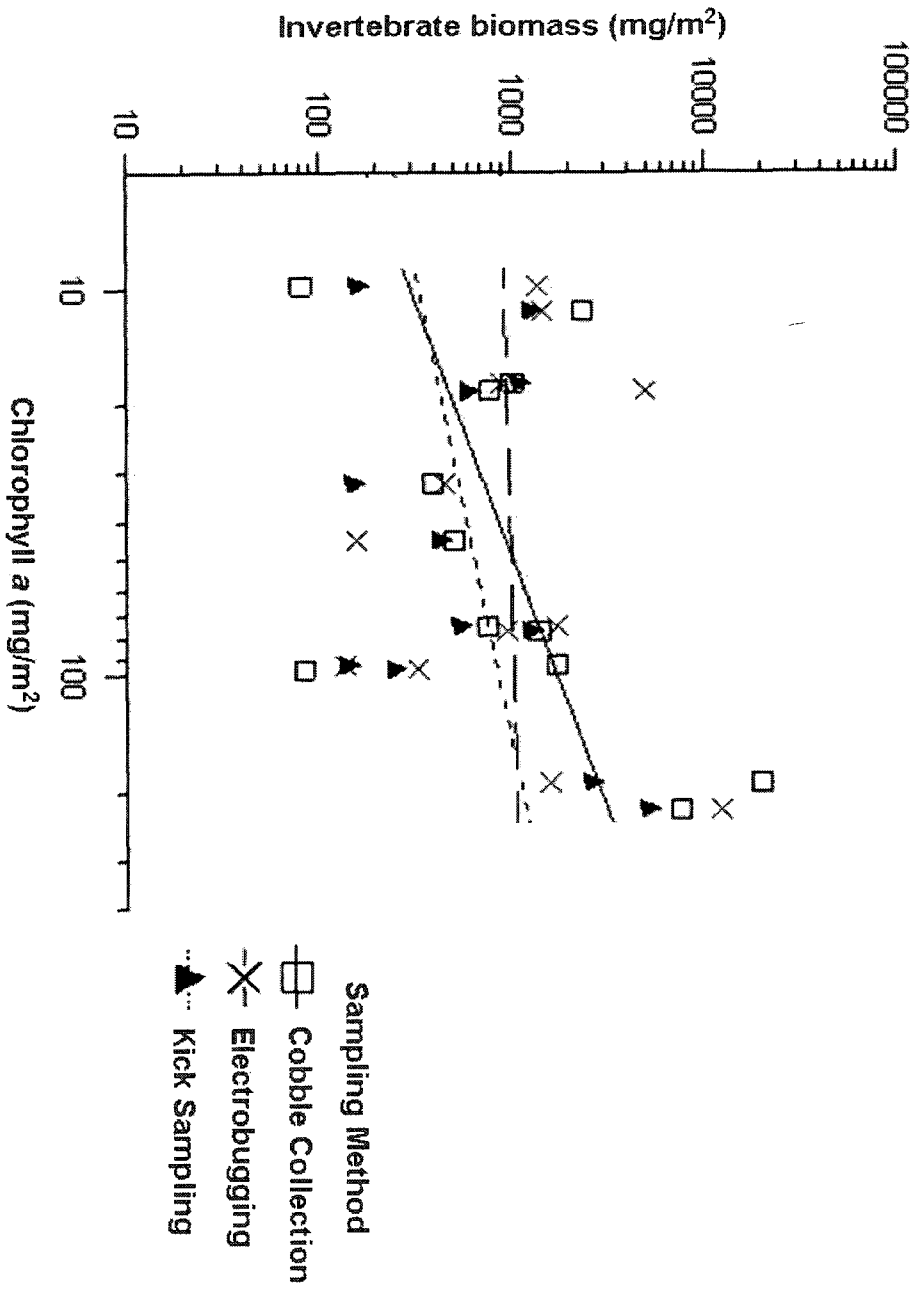
Invertebrate biomass (mg/m2)
10
100
1000
10000
100000
Chlorophyll a (mg/m2)
10
100
Sampling Method
Cobble Collection
Electrobugging
Kick Sampling

Figure 2-4

BEC
RR2
LDS
DT2
LMS
DT1
LDS2
C3
BRA2
C6
C9a
C2
Log10 Biomass (mg/m2)
Log10 Body Length (mm)

Figure 2-5

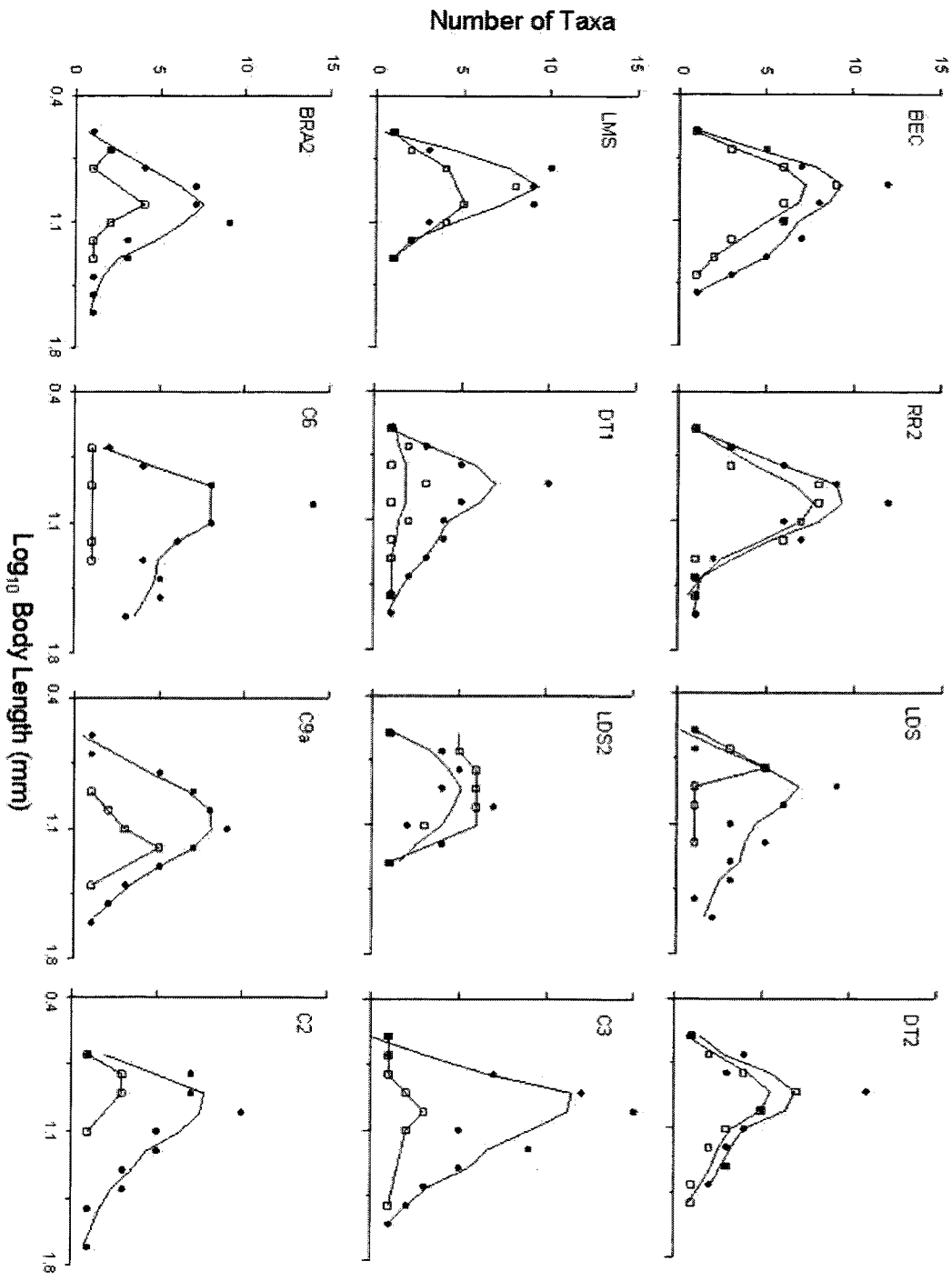
Number of Taxa
Log10 Body Length (mm)
BEC
LMS
RR2
DT1
LDS
LDS2
DT2
C3
BRA2
C6
C9a
C2

Figure 2-6

# Chapter 3 – Expanding Lotic Size Spectra to Include Large Macroinvertebrates, Crayfish, and Fish

## Introduction

Size distributions of organisms are important characteristics of natural communities because size determines fundamental rate processes such as metabolism, production, and excretion (Peters 1983; Rasmussen 1993; White et al. 2007). Body size also has implications for the use of food resources, the transfer of energy, and the selection of prey (Kerr and Dickie 2001; White et al. 2007). Individual-based size spectra, which group organisms into body size classes regardless of taxonomy, provide a species-independent method for comparing communities across habitats and large spatial scales (Kerr and Dickie 2001; Basset et al. 2004). This form of the size spectrum has been the focus of size-based analyses in aquatic systems (Kerr and Dickie 2001; White et al. 2007), where the use of an average size value for a species (as is commonly plotted in other forms of the size distribution; White et al. 2007) may not be an appropriate way to represent larval and nymphal body forms (in the case of macroinvertebrates) or species with indeterminate growth (in the case of fish). Many studies have compared individual-based size spectra in aquatic systems in order to better understand how the shape of the distribution changes in relation to physical, chemical, and biological influences (see review in Kerr and Dickie 2001). The most notable result of these studies has been a strong consistency of size spectrum shape across sites and among different groups of organisms (Kerr and Dickie 2001; White et al. 2007).

In stream systems, size spectra comparisons have been made over gradients in nutrient levels and habitat complexity, with little evidence of variation in spectrum shape in most studies. For example, Morin and Nadon (1991) noted a strong similarity in benthic macroinvertebrate size spectrum shape among streams despite the presence of a

nutrient gradient. Bourassa and Morin (1995) did find a significant effect of total phosphorus and substrate particle size on macroinvertebrate size spectra, but still noted that spectra were similar among sites. Solimini et al. (2001) also compared benthic macroinvertebrate size spectra on different substrate types in sites with different levels of nutrients and found a strong stability in size spectrum shape despite differences in environmental variables. Together, these results suggest that the shape of the size spectrum is largely unaffected by variation in habitat structure or nutrient levels in stream benthic communities.

Most of the research on stream size spectra has focused on small- to medium-sized macroinvertebrates. However, Morin and Nadon (1991) suggested that although density levels are highest in small organisms, greater than 90% of the total biomass in the benthic macroinvertebrate community is contributed by organisms longer than 2 mm. This dominance of invertebrates > 2mm is such that, although metabolic rate declines with size, these size classes are energetically the most important fraction of the benthic macroinvertebrate community for which size distributions are currently described. However, although many large invertebrates live in streams, they are generally inefficiently sampled, and are therefore underrepresented in most studies. Similarly, though crayfish and fish represent a large proportion of the production in stream ecosystems, descriptions of size spectra have rarely extended into the larger size classes to include them. This suggests that the most important portion of the size spectrum in terms of biomass and energy flow has been largely overlooked in previous research in stream systems. The energetic importance of large organisms to the benthic community necessitates their inclusion in the measurement of size distributions.

The expansion of size spectra to include more than one group of organisms has previously been found to affect spectrum shape in stream systems. When Morin and Nadon (1991) added data for algae, bacteria, and protozoans to their unimodal stream benthic macroinvertebrate size spectrum, they found that the size spectrum took on a negative linear trend with a slope close to -1. This pattern was further confirmed when Cattaneo (1993) plotted size spectra for stream algae, protozoans, and benthic macroinvertebrates and obtained slopes close to -1. Cattaneo (1993) found that the shape of the size spectrum remained remarkably stable when small organisms were added, however, it is unknown whether the same would be true if large organisms were added to stream size spectra.

In one example of a study that shifted focus to include large organisms, Poff et al. (1993) sampled meiofauna, macroinvertebrates, and aquatic vertebrates (including fish) in a single stream, and provided a description of an expanded stream size spectrum. They obtained a regression slope of -0.82 for their size spectrum, which was within the range of slopes obtained by Cattaneo (1993) in her research on stream algae, protozoans, and macroinvertebrates. However, Poff et al. (1993) only had data for one stream, and their results may not be representative of the general trend in combined size distributions of small and large organisms. Furthermore, their study did not address whether the size spectrum stability that has been noted in studies of small organisms is also evident when size spectra are expanded, nor did it examine the effects of environmental variables on expanded size spectra. Because of the potential importance of large organisms to ecosystem function, it is necessary to study the patterns of such expanded size spectra further to determine whether they are affected by fluctuations in environmental variables.

In this study, we sampled stream sites covering a range of environmental conditions in order to examine the variability in stream size spectra when large organisms were included. The main objectives of this research were to create expanded stream size spectra by sampling crayfish and fish and increasing sampling efforts for large macroinvertebrates, and to compare expanded size spectra among sites with varying levels of nutrients and substrate composition to determine whether spectrum slopes and intercepts differed. We speculated that the stability in size spectra that had been apparent in previous research would still be evident when large organisms were added. We also expected that if the biomass patterns described by Morin and Nadon (1991) continued into larger size classes, then there would be more biomass in the large size classes that we sampled than in the size classes that were considered to be large by Morin and Nadon (1991).

## Methods

### *Sampling and laboratory methods*

Samples were collected from 17 sites in 6 streams in eastern Ontario and western Québec in Canada (see Table 3-1 for site details). The streams were sampled during the summer of 2006, with the exception of Brassil's creek and Chelsea Stream 9a and 9b, which were sampled during the summer of 2007. The streams were all small, with a maximum width of 10 m, and were selected to cover a range of nutrient levels (Table 3-1). Sites were selected within the streams to represent different substrate compositions of sand, gravel, cobble, or boulder (Table 3-1). Substrate composition was homogeneous throughout the sampled stream reach; as a result, some sampling sites constituted riffle habitat (those sites with complex substrate) while other sampling sites constituted pool or

run habitat (generally those sampling sites with flat substrate). Periphyton biomass varied, with no visible periphyton at some sites and large mats of filamentous algae at others; average chlorophyll *a* concentrations ranged from 0.36 mg/m$^2$ to 286.2 mg/m$^2$ (Table 3-1).

Water chemistry samples were collected from all sites except those at Beckett's Creek on 3 occasions during the summer sampling season to obtain average values. Samples were submitted to the Ottawa-Carleton Water Quality Laboratory in Ottawa, Ontario for analysis. Water chemistry results for Beckett's Creek were obtained from the City of Ottawa. Several water chemistry parameters were measured, but this study focused on total nitrogen (TN) and total phosphorus (TP).

We used four different sampling methods (cobble collection, Hess sampling, electrobugging, and kick sampling) to collect benthic macroinvertebrates. For the cobble method, six replicate cobbles (approximate diameter ranging from 55 to 145 mm) were collected at random from each stream site and placed in bags with 95% ethanol. Six Hess samples (each sampling an area of 0.036 m$^2$) were collected at sites without cobbles (flat sites; Table 3-1) and placed in jars with 95% ethanol. At stream sites where cobble was not the dominant substrate type, 3-6 replicate Hess samples were collected (in addition to the cobble samples).

In order to increase our sampling efforts for large macroinvertebrates, we used a modified version of the depletion electrobugging technique described by Taylor et al. (2001). In combination with kick sampling, electrobugging was found to collect additional taxa and size classes of large invertebrates that were not captured by the cobble method (Chapter 2). To electrobug, we used a Smith-Root LR-24 backpack

electroshocker upstream of a stationary D-net (1 mm mesh), over an area of 30 x 60 cm. The width of the sampling area (30 cm) was the width of the D-net, and the length of the sampling area (60 cm) was determined by estimating how far the anode could be moved from the net and still shock invertebrates that would drift into the net with the current. A 15 cm (diameter) anode was used instead of the standard 28 cm anode in order to create a more concentrated pulse. We moved the anode through the sampling area for 30 seconds without disturbing the substrate, inducing drift by shocking the invertebrates in the area. The cathode was placed immediately downstream under the opening of the D-net to create an electrical gradient and direct drifting organisms into the net. After the 30 second sampling period, all organisms were removed from the net and placed in jars with 95% ethanol. This was repeated 3-5 times until attrition was noted. We did not set up nets surrounding our electrobugging area, and therefore may have had some movement of individuals in or out of the sampling area. However, we sampled over a smaller area than Taylor et al. (2001), and speculated that movement into the sampling area would be limited due to the short-range pulse of the small anode. Immigration and emigration were expected to counterbalance each other, meeting the assumption of the depletion method that there was no net change in population size (Zippin 1958). Immediately following electrobugging, 2-3 kick samples (each lasting 30 seconds) were taken at the electrobugging locations until attrition was noted. Kick sampling was performed in order to collect the attached taxa (such as case-making Trichoptera) that were not efficiently collected by electrobugging (Chapter 2). All invertebrate samples (from the cobble method, Hess sampler, electrobugging, and kick sampling) were returned to the laboratory for processing.

Fish and crayfish were collected from a 10 m length of stream by depletion electroshocking with a standard 28 cm (diameter) anode. Seine nets were set up immediately upstream and downstream of the 10 m sampling area to block immigration and emigration of fish and crayfish. Each electroshocking pass was completed by moving through the sampling area from upstream to downstream while shocking and collecting fish and crayfish with dip nets. After each pass, we measured the collected fish and crayfish, identified them to species level, and returned them to the stream downstream of the sampling area. At each site, we completed 3-5 passes of electroshocking until 50% attrition was noted in both the fish and crayfish.

In the laboratory, cobbles were brushed over a 1 mm sieve, and organisms retained on the sieve were identified. Hess samples were also rinsed over a 1 mm sieve to collect and identify any retained organisms. Electrobugging and kick samples were not sieved in the lab prior to identification because the D-net mesh used in the field was 1 mm. When samples contained more than 200 individuals or large amounts of algae or debris (which often occurred in the case of kick samples), a Folsom plankton splitter was used to split samples. All invertebrate samples were identified to the level of family for insects and order or higher for non-insects. We measured the body length of each individual to the nearest 0.01 mm using an image analysis system (Optimas 6.5 Imaging Software; Media Cybernetics, Silver Springs, Maryland). Dry mass (in μg) was estimated from body lengths by using taxon-specific length-mass regressions from Benke et al. (1999). When there was no length-mass relationship information for a taxonomic group, dry mass (DM) was calculated as body length (L) cubed (DM $[\mu g] = L^3\ [mm^3]$).

For the cobble and Hess samples, the number of organisms that were lost through the 1 mm sieve was predicted by using sieve retention probability models. We used the overall (not taxon-specific) model of Gruenert et al. (2007) that incorporated chlorophyll *a* concentrations to predict the number of organisms in the cobble samples lost by sieving. Chlorophyll *a* concentrations were incorporated for the cobble samples because algae in the sample essentially trap organisms and prevent them from passing through the sieve, thereby inflating density estimates relative to sites with no algae. For the Hess samples, which rarely included algal biomass, we used the overall sieve retention probability model of Morin et al. (2004) which did not incorporate chlorophyll *a*. The suitability of the sieve retention models to estimate organism counts for the electrobugging and kick samples was tested in Chapter 2. The sieve retention probability model of Morin et al. (2004) predicted the number of individuals lost through the D-net within 6% for all body lengths above 4 mm long, but under- or over-estimated counts for individuals below 4 mm in length by more than 15% (Chapter 2). The sieve retention probability models were therefore applied to electrobugging and kick samples for all individuals longer than 4 mm, and data for individuals shorter than 4 mm long were disregarded from these samples. We applied the overall sieve retention probability model of Morin et al. (2004) to the electrobugging data because the sampling method did not disturb the substrate and therefore did not dislodge algae. The retention model of Gruenert et al. (2007) was applied to the kick sampling data because the collection method did dislodge algae, and invertebrate retention was likely affected by algal biomass levels in those samples.

*Data Analysis*

Invertebrates collected in the cobble and Hess samples were grouped into $\log_2$ size classes based on dry mass (μg), and the total mass of individuals was summed for each taxon-size class combination. For the Hess samples, this mass value was divided by the area of the sampler (0.036 $m^2$) to provide estimates of biomass in $\mu g/m^2$ of stream area. For each cobble, the total mass of individuals in each taxon-size class combination was divided by the area of the cobble to provide estimates of biomass in $\mu g/m^2$ of cobble area. Cobble surface area was calculated by wrapping each cobble in aluminum foil, weighing the foil, and estimating the foil surface area from an area-mass regression that was made using known surface areas of foil. In order to combine the cobble results with those from the other sampling methods, we estimated the cobble surface area per $m^2$ of stream substrate covered with cobble to express biomass and density per unit stream area, rather than per unit cobble area. For both the Hess and cobble samples, the biomass in each taxon-size class combination was averaged across the number of replicate samples to provide average biomass estimates for each stream site on cobble and non-cobble substrates. We used a weighted average to combine the biomass estimates from the cobble and Hess samples, weighting the cobble estimates by the proportion of cobble habitat and weighting the Hess estimates by the proportion of non-cobble habitat in each site.

Similar to the cobble and Hess samples, invertebrates collected in electrobugging and kick samples were grouped into $\log_2$ size classes based on dry mass (μg). Because the depletion method was used to collect electrobugging and kick samples, it was necessary to estimate the population size at each electrobugging site based on the number of individuals collected and the depletion in invertebrate counts with each additional pass.

To create these estimates, we entered total counts of each taxon-size class combination into MicroFish 3.0 (Van Deventer 1989), a program for estimating population size from electroshocking depletion data by using maximum-likelihood estimates. Because kick sampling potentially sampled a different portion of the population (including any organisms that were not induced to enter the drift by electroshocking), we combined the data for kick sampling and electrobugging in different ways depending on the number of individuals caught by each sampling method. Initially, electrobugging and kick sampling data were run separately through MicroFish for each site. We used the electrobugging estimates for all taxon-size class combinations that were only captured by that method, and similarly used the kick sample estimates for those that were only collected by kick sampling. For taxon-size class combinations that were collected by both sampling methods, we treated the kick sampling passes as additional electrobugging passes, essentially adding 2-3 more passes to the electrobugging data. We then ran those numbers through MicroFish to get estimates from the combined passes. When there was a non-descending removal pattern, suggesting that kick sampling collected more individuals of that taxon-size class combination, we did not treat the kick sampling data as additional electrobugging passes. In those cases, kick sampling was more effective than electrobugging and collected individuals that were unable to enter the drift during electroshocking. For those taxon-size class combinations, we added the original electrobugging counts (without MicroFish population estimates) to the population estimates we obtained from the kick sampling data to get total counts for the stream site.

The output from MicroFish was an estimated count for each taxon-size class combination based on the pass data. The population estimates for all taxon-size class

combinations at each site were multiplied by the average dry mass of each taxon-size class combination (using sampling location-specific values) and divided by the area of the sampling location (0.18 $m^2$) to generate biomass values in $\mu g/m^2$ stream area. These values were averaged across the 3 sampling locations to provide average biomass estimates for electrobugging and kick samples for each stream site.

Biomass estimates for all invertebrates less than 4 mm long were obtained from Hess and cobble samples. For invertebrates longer than 4 mm, we used the estimate either from cobble/Hess or electrobugging/kick depending on which gave the highest biomass for each taxon-size class combination that was collected at the sample sites. Once the data had been combined for all sampling methods, we summed the biomass in each size class across taxa to obtain biomass values for creating the size spectra.

Crayfish and fish data were run through MicroFish to obtain population estimates from the pass depletion data. Crayfish dry mass (in μg) was estimated from carapace length by using the average Decapoda length-mass regression from Benke et al. (1999) because of the absence of regression information for the species we collected (primarily *Orconectes virilis, O. obscurus*, and *O. rusticus*). Crayfish were grouped into $\log_2$ size classes based on their dry mass. Population estimates from MicroFish were obtained by entering counts for each taxon-size class combination. Resulting estimated counts were multiplied by the average dry mass of the taxon-size class combination (using site-specific averages) and divided by the stream area ($m^2$) sampled at each site to calculate biomass estimates. The biomass in each size class was summed across taxa to obtain biomass values for creating the size spectra.

Fish wet mass (in μg) was estimated from total length or standard length using species-specific length-mass regressions from Randall and Minns (2000) and Schneider et al. (2000). In order to convert wet mass to dry mass, we found examples in the literature of the relationship between wet mass and dry mass for a range of fish species; the average relationship for species similar to those we collected was dry mass = 0.25 * wet mass (Berry et al. 1982; Whicker et al. 1990; Lantry and O'Gorman 2007). Fish were grouped into $\log_2$ size classes based on their dry mass, and population estimates from MicroFish were obtained by entering counts for each taxon-size class combination. The resulting estimated counts were multiplied by the average dry mass of the taxon-size class combination (using site-specific averages) and divided by the stream area ($m^2$) sampled at each site to calculate biomass estimates. The biomass in each size class was summed across taxa to obtain biomass values for creating the size spectra.

Normalized biomass values were calculated for invertebrates, crayfish, and fish by dividing the biomass concentration ($\mu g/m^2$) in each size class by the width of that size class (i.e., for $\log_2$ size class intervals, the width of a size class is the lower limit of the size class interval). Data for invertebrates, crayfish, and fish were combined, and normalized biomass values were summed for any overlapping size classes. Normalized biomass size spectra were plotted for each site as the $\log_{10}$ normalized biomass against the $\log_{10}$ body size (the upper biomass limit for the size class in μg). The biomass for each size class was transformed to a $\log_{10}$ scale to linearize the normalized biomass-body size relationship.

*Size Spectra Comparison*

A linear regression was calculated for each size spectrum to describe the general trend in the relationship between body size and normalized biomass. Each linear regression was of the form $(\log_{10}D) = a + b\ (\log_{10}M)$, where D was the normalized biomass within a size class, M was the upper limit of the mass (μg) of the size class, $a$ was the intercept, and $b$ was a coefficient describing the slope of the relationship. These regressions provided only a rough description of the relationship between normalized biomass and body size, while not accounting for any deviations from linearity. However, the primary focus of this study was to examine the general trends in size spectra shape.

To evaluate the similarity of distribution shape among sampling sites, we tested the model $(\log_{10}D) = a + b(\log_{10}M) + \text{Site} + (\log_{10}M) * \text{Site}$, in which Site was a categorical variable. In this model, the interaction term $((\log_{10}M) * \text{Site})$ tested whether slopes differed among size distributions (Zar 1999). If the interaction was not found to be significant (at $\alpha = 0.05$), a reduced model (without the interaction term) was tested. In the reduced model, the site term tested whether size distribution intercepts differed among sites (Zar 1999).

To explore the possible relationship between variability in normalized biomass spectra and environmental variables, we used GLMs to test whether total phosphorus (TP), total nitrogen (TN), or substrate (a categorical variable: flat or primarily small, medium, or large particles) had an effect on the slopes and intercepts of the size spectra. The GLMs were of the form $(\log_{10}D) = a + b(\log_{10}M) + c(X) + (\log_{10}M) * (X)$, where X was $(\log_{10}TP)$, $(\log_{10}TN)$, or substrate, and $(\log_{10}M) * (X)$ was an interaction term. A significant interaction term (at a Bonferroni-corrected $\alpha = 0.016$ because we tested the effect of 3 environmental variables) was indicative of a difference in size spectra slopes

that could be attributed to the chosen variable. If the interaction term was not found to be significant, a reduced model (without the interaction term) was tested. A significant term for TP, TN, or substrate (at a Bonferroni-corrected $\alpha = 0.016$) in the reduced model was indicative of a difference in size spectra intercepts that could be attributed to that variable. The GLM for TN excluded Raisin River sites 2 and 3 because TN data were unavailable for those sites.

To quantify the contribution of the large organisms that were previously not included in size spectra to the overall biomass of the entire assemblage, we plotted the biomass of macroinvertebrates, crayfish, and fish collected in small, medium, and large body size ranges. The body size ranges were defined based on the size spectra presented by Morin and Nadon (1991). Small organisms were defined as those that were less than or equal to 1 μg, which was the mode of the size spectra plotted by Morin and Nadon. Medium organisms were between 1 μg (above which Morin and Nadon classified organisms as "large") and $10^4$ μg (the maximum body size collected by Morin and Nadon). Finally, large organisms were those that were larger than $10^4$ μg, which represented the previously unsampled size classes that we added in this study. We used a one-way paired *t*-test to compare the percent of the total biomass that was contributed by macroinvertebrates in the medium and large size ranges in all sites, to determine whether more biomass was collected in the large size classes as expected. The same analysis was completed with the sum of the percent of the total biomass contributed by macroinvertebrates and crayfish in the medium and large size ranges, to determine whether the addition of crayfish resulted in the collection of more biomass in the large size classes. In both analyses, percent data were arcsin transformed in order to meet the

assumptions of the paired *t*-test. We did not complete the analysis with the inclusion of fish data, because the objective was to determine the relative contributions of small, medium, and large invertebrates to benthic biomass estimates (as in Morin and Nadon 1991). To further evaluate the distribution of biomass across size classes, we plotted the cumulative proportion of density, biomass, and production potential in each size class. Production potential was estimated from density and body size by assuming that somatic growth scales as $mass^{0.75}$.

**Results**

The normalized biomass size spectra displayed a negative trend that appeared similar among sites (Figure 3-1). The spectrum for Leamy downstream site 2 did appear to differ from the other sites, but this was largely due to a lack of fish and crayfish at that site; the lack of large organisms resulted in a much shallower slope. When linear regressions were calculated for each site, the average slope (± SE) was found to be -0.66 ± 0.03 (Table 3-2). Leamy downstream site 2 was found to have a very shallow slope compared to the other sites (slope = -0.38), while Beckett's creek site b was found to have a steeper slope than the other sites (slope = -0.87). The shallow slope at Leamy downstream site 2 was due to a lack of large organisms combined with low normalized biomass of small macroinvertebrates (possibly due to undersampling of small organisms). In contrast, higher than average normalized biomass of small macroinvertebrates was collected at Beckett's site b, contributing to the steeper than average slope. The range of slopes excluding those sites was -0.53 to -0.76 (Table 3-2).

Size spectra slopes and intercepts varied among sites, but slope variability was mainly because of 2 sites. When we compared all sites using the GLM model with the

Site term, we found a significant interaction term ($p = 0.01$; Table 3-3), which indicated a significant difference in size spectra slopes among sites. However, this result was due to the steep slope of Beckett's creek b and the shallow slope of Leamy downstream 2; when these sites were removed, the interaction term was not found to be significant ($p = 0.49$). This result confirmed the similarity in size spectra slopes that was evident across the remaining 15 sites. We tested the reduced model (without the interaction term) with BECb and LDS2 removed, and found that there was a significant Site term ($p < 0.001$), indicating a significant difference in density levels among sites.

Size spectra slopes did not vary with nutrient concentrations or substrate type. Total phosphorus was not found to have an effect on either the size spectrum slopes (interaction term $p = 0.50$) or intercepts (reduced model TP term $p = 0.636$; Table 3-3). Similar to TP, TN was not found to have an effect on size spectrum slopes (interaction term $p = 0.81$; sites RR2 and RR3 excluded because of a lack of data). However, there was a significant effect of TN on spectra intercepts when the reduced model was tested (TN term $p < 0.01$; Table 3-3), suggesting that TN had an effect on overall normalized biomass levels of the size spectra, although it did not affect the relative proportions of small and large organisms. When the GLM for substrate type was tested, we found no significant difference in spectrum slopes among substrate types (interaction term $p = 0.72$), suggesting that the substrate type did not affect the relative proportions of small and large organisms at a site. However, there was a significant difference in intercepts ($p < 0.01$), which indicated that the type of substrate (flat or primarily small, medium, or large particles) had an effect on overall normalized biomass levels in our sites. The highest normalized biomass values were found in the substrate that was primarily

composed of small particles, while the lowest normalized biomass values were found in the flat substrate.

In several sites, there was a decrease in normalized biomass in the smallest macroinvertebrate size classes, resulting in a unimodal appearance to the macroinvertebrate portion of the size spectra. In addition, there was a decrease in normalized biomass in several sites in the size range of 65,000 to 262,000 μg (4.8 to 5.4 on the $\log_{10}$ scale in Figure 3-1). This size range contained small fish, medium-sized crayfish, and the largest size classes of macroinvertebrates, and was a transition area between the macroinvertebrate-dominated and the fish-dominated portions of the spectrum (Figure 3-2). The dip in the size spectra appeared to reflect a large drop in macroinvertebrate normalized biomass in the largest size classes, coupled with low normalized biomass in the small fish (Figure 3-2). The largest macroinvertebrates we collected were 262,000 μg, but they were only found at 2 sites in the size range of 131,000 to 262,000 μg, and a sharp decline in normalized biomass of macroinvertebrates was evident in most sites after 16,000 or 32,000 ug. The average spectrum showed a dip in the fish size distribution across the size range of 65,000 to 262,000 μg (Figure 3-2). Crayfish densities were generally low across all size classes at the sites at which they were collected. In the largest size classes, average normalized biomass of crayfish was similar to that of fish, but in the remaining size classes, crayfish displayed much lower normalized biomass on average.

Small organisms contributed an insignificant amount to the total biomass at each site (Figure 3-3). However, when the biomass collected in the medium and large size ranges was compared, no clear pattern emerged. When all organisms (including fish)

were compared, there appeared to be more biomass collected in the large size range at most sites (Figure 3-3). But when fish were excluded and only benthic organisms were considered (macroinvertebrates and crayfish), the biomass appeared to be more evenly distributed between the medium and large size ranges (Figure 3-3). When only macroinvertebrates were considered, there was more biomass collected in the medium than in the large size range (Figure 3-3). The latter two observations were confirmed by the paired *t*-test analysis. When only macroinvertebrates were considered, the medium size range contained a higher proportion of the biomass than the large size range (one-tailed $t = 2.52$, df = 16, $p = 0.01$). Moreover, the large size range still did not contain a higher proportion of the biomass when crayfish were considered in addition to macroinvertebrates (one-tailed $t = 0.88$, df = 16, $p = 0.80$). However, while there was higher biomass in the medium than in the large size range when macroinvertebrates alone were considered (one-tailed $p = 0.01$), when crayfish were added there was no significant difference between the proportion of the biomass collected in the medium and large size ranges (two-tailed $p = 0.39$).

Figure 3-4 confirmed the insignificant contribution of small organisms to stream assemblage biomass. Although small organisms were numerically the most abundant, medium- and large-sized organisms contributed the most biomass and production in our stream sites (Figure 3-4). In most sites, more than 80% of density was due to organisms less than 100 μg in size, but these organisms contributed less than 20% of the benthic secondary production in the streams. The proportion of secondary production that was due to organisms that we classified as large in Figure 3-3 (organisms greater than $10^4$ μg) ranged from less than 10% to greater than 80%, depending on the site (Figure 3-4).

## Discussion

The slopes of expanded size spectra that included small and large macroinvertebrates, crayfish, and fish were consistent across sites, similar to previous studies of small organisms in streams (e.g., Morin and Nadon 1991; Cattaneo 1993; Bourassa and Morin 1995; Solimini et al. 2001). There was a strong stability in spectrum slopes among our sites, despite differences in habitat architecture and nutrient levels. The spectra from our streams covered a body size range that was similar to the expanded size spectrum presented by Poff et al. (1993). However, our spectra generally displayed stronger linear trends with a less prominent modality than the spectrum described by Poff et al. (1993). The clearly multimodal spectrum of Poff et al. (1993) may have resulted primarily from the presence of an invasive species, the asiatic clam (*Corbicula fluminea*), which dominated the size range of the large macroinvertebrates and small fish. The spectra we presented may therefore be more indicative of what would be expected in a system lacking such an invasive species.

The slopes of our size spectra were less steep than -1, indicating that there was relatively more biomass in the large size classes. Moreover, the slopes of our size spectra were much shallower than has been noted in stream systems in previous studies (e.g., Morin and Nadon 1991; Cattaneo 1993; Poff et al. 1993), providing stronger evidence that there is increased biomass in the large size classes. The increase in biomass relative to small organisms was clearly evident when we compared the percent of the total biomass contributed by the small, medium and large size ranges; the small size range accounted for an insignificant proportion of the biomass in comparison with the medium and large size ranges. Moreover, when density, biomass, and production curves were

compared for each site, small organisms were found to contribute to less than 20% of benthic secondary production in our streams. These results support Morin and Nadon's (1991) conclusion that small organisms contribute little to secondary production in streams despite their numerical dominance. However, if the largest organisms were energetically the most important fraction of the size spectrum, we would have expected to see significantly higher biomass in the large size range than in the medium, to compensate for the decline in metabolic rate with increased body size. Instead, we found that when only benthic organisms were considered, there was approximately equal biomass in the medium and large size ranges. The contribution of large organisms to secondary production differed greatly among streams, but on average was approximately 30%, while medium-sized organisms contributed an average of 55% of the secondary production. This indicates that medium-sized organisms (from 1 μg to $10^4$ μg) contribute more to body size-mediated processes such as metabolism and production in stream benthic communities, and are more important for ecosystem function than small or large organisms. However, this does not suggest that large organisms should be excluded from stream size spectra. The inclusion of large macroinvertebrates and crayfish resulted in a doubling of biomass in most sites. Moreover, when fish were included, there was more biomass in the large size classes than in the medium in the majority of sites. In several sites, large organisms contributed to the largest proportion of secondary production (as much as 80%), indicating that the relative importance of each body size group to ecosystem function may be strongly site dependent. Large organisms in streams contribute a great deal to the total biomass and secondary production in the system, and should be included in size-related studies.

We sampled several of the same streams as Bourassa and Morin (1995), but we did not find that total phosphorous had a significant effect on the slopes or intercepts of our stream size spectra as they did in their study. We sampled different phosphorus ranges (our TP ranged from 0.020 to 0.210 mg/L, while Bourassa and Morin's TP ranged from 0.002 to 0.054 mg/L and indicated that sites might be nutrient-limited) and a much larger range of body sizes, either of which may have accounted for the different results. Lavoie et al. (2010) examined benthic diatom size spectra from streams that covered an agricultural gradient and, similarly to our study, found no effect of either TP or TN on size spectra slopes, but a significant effect on spectra intercepts. The lack of significant effect of either TP or TN on the slope of the size spectra suggests that the relationship between body size and normalized biomass is not driven by nutrient levels in stream systems. Instead, nutrients appear to affect densities of organisms in all size classes, resulting in a positive shift in size spectrum intercepts across sites. We also found no difference in size spectrum slopes among substrate types, despite the fact that several authors have suggested that the shape of the size distribution may be related to substrate complexity and habitat availability (Morse et al. 1985; Sugihara and May 1990; Sinsabaugh et al. 1991; Gee and Warwick 1994). Moreover, Bourassa and Morin (1995) found a significant effect of substrate size on stream size spectra slopes in addition to the nutrient effect. In addition, Macpherson et al. (2002) found very different size spectra slopes for demersal fish in two marine habitats with different architectures (rocky bottom vs. sea grass habitat), suggesting that habitat complexity might affect size spectra slopes in fish populations. Our lack of significant results may have been due to the rough

estimate of substrate type and complexity that we used. A more exact measurement of habitat complexity may indicate a substrate effect on size spectra slopes.

Many of the deviations from linearity in the size spectra appeared to be a result of inadequate sampling of two groups of size classes. There was a unimodal appearance to the size spectra in the small size classes (small macroinvertebrates) in several of our sites. These results suggest that the linear trend in the size spectra may have continued had data been included for meiofauna or algae. Morin and Nadon (1991) found that the inclusion of algae, protozoans, and bacteria into the unimodal macroinvertebrate size spectrum resulted in a negative linear trend. Cattaneo (1993) confirmed this trend with a more extensive algal dataset. If the linear trend in the large size classes was continued in the small size classes with the inclusion of algal data, it is possible that our size spectra slopes could have been steeper (and closer to -1).

The other deviation from linearity that was evident in our size spectra was a dip in normalized biomass in the transition area between macroinvertebrates, crayfish, and fish. This dip occurred in the body size range of 65,000 to 262,000 μg in a large proportion of our sites, and appeared to be largely the result of a decline in fish density. The overlap between macroinvertebrates and fish began at 16,000 μg for most sites, but there was a clear drop in normalized biomass levels of fish at size class 65,000 μg. This may have occurred because of the difficulties inherent in colleting small fish with a dip net from rocky habitat or from within filamentous algae. However, the dip in the size spectra was evident even at sites without rocky habitat or large amounts of algae (such as BRA1, C9b, and LDSb), suggesting that it may not have been entirely due to sampling error. Instead, this dip in normalized biomass may represent a natural pattern within stream

systems. Interestingly, Poff et al. (1993) found a peak in their size spectrum in the same biomass range in which we noted a dip in our size spectra. But the peak in their spectrum was due to the presence of the introduced asiatic clam (*Corbicula fluminea*). In the absence of such a proliferate species, it is unclear whether this size range could be exploited by other large macroinvertebrates or small fish.

The shape of the size distribution in the large size classes might have been different if crayfish had been sampled more effectively. In the largest size classes, average normalized biomass of crayfish was similar to that of fish. However, densities of medium- and small-sized crayfish were found to be much lower on average than those of fish. Because of the difficulties inherent in collecting crayfish, particularly in complex habitats where crayfish may actively evade capture (Rabeni et al. 1997), it seems likely that the low densities of crayfish compared to fish may have reflected ineffective sampling. Although there should have been an overlap of macroinvertebrates and crayfish starting at 4,000 μg (the smallest size of crayfish that we found), we only collected crayfish of that size at 2 sites, and the smallest crayfish we caught at most sites were 65,000 or 131,000 μg in mass. It is possible that we collected few small crayfish because of our sampling method; Rabeni et al. (1997) found that electroshocking collected lower numbers of small crayfish than quadrat sampling. Small crayfish were very difficult to see, complicating their capture with the dip net. In addition, we found that crayfish were generally not as strongly affected by electroshocking as fish, and often moved faster as a result of shocking, rather than being immobilized. However, we could not increase the electroshocker voltage sufficiently to immobilize crayfish without killing the fish that were present in the stream (because of the higher sensitivity of fish to the shocking).

Additional passes (once the majority of fish have been collected) with a higher voltage to try to collect any remaining crayfish could improve population estimates in the large size classes, though an additional method such as quadrat sampling might still be necessary for accurate population estimates of small crayfish.

By adding large macroinvertebrates, crayfish, and fish to stream size spectra, our study showed that the stability in size spectrum shape that has been observed in previous studies of small organisms is still evident when size spectra are expanded to include large organisms. Although we did not find evidence to support the idea that the largest organisms are energetically the most important fraction of the size spectrum in all of our streams, our results clearly showed that small organisms ($\leq$ 1 μg) contribute little to stream biomass, and that the inclusion of large organisms represents at least a doubling of biomass and production estimates. Overall, our results suggest that the inclusion of large organisms is vital for the most accurate description of stream size spectra and biomass levels.

**References**

Basset, A., Sangiorgio, F., and Pinna, M. 2004. Monitoring with benthic macroinvertebrates: advantages and disadvantages of body size descriptors. Aquat. Conserv. **14**: S43-S58.

Benke, A.C., Huryn, A.D., Smock, L.A., and Wallace, J.B. 1999. Length-mass relationships for freshwater macroinvertebrates in North America with particular reference to the southeastern United States. J. N. Am. Benthol. Soc. **18**(3): 308-343.

Berry, P.F., van der Elst, R.P., Joubert, C.S.W., and Smale, M.J. 1982. Density and biomass of the ichthyofauna of a natal littoral reef. Mar. Ecol.-Prog. Ser. **10**: 49-55.

Bourassa, N., and Morin, A. 1995. Relationships between size structure of invertebrate assemblages and trophy and substrate composition in streams. J. N. Am. Benthol. Soc. **14**(3): 393-403.

Cattaneo, A. 1993. Size spectra of benthic communities in Laurentian streams. Can. J. Fish. Aquat. Sci. **50**: 2659-2666.

Gee, J.M., and Warwick, R.M. 1994. Body-size distribution in a marine metazoan community and the fractal dimensions of macroalgae. J. Exp. Mar. Biol. Ecol. **178**: 247-259.

Gruenert, U., Carr, G., and Morin, A. 2007. Reducing the cost of benthic sample processing by using sieve retention probability models. Hydrobiologia. **589**: 79-90.

Kerr, S.R., and Dickie, L.M. 2001. The biomass spectrum: a predator-prey theory of aquatic production. Columbia University Press, New York.

Lantry, B.F., and O'Gorman, R. 2007. Drying temperature effects on fish dry mass measurements. J. Great Lakes Res. **33**: 606-616.

Lavoie, I., Lento, J., and Morin, A. 2010. Inadequacy of size distributions of stream benthic diatoms for environmental monitoring. J. N. Am. Benthol. Soc. **29**(2): 586-601.

Macpherson, E., Gordoa, A., and García-Rubies, A. 2002. Biomass size spectra in littoral fishes in protected and unprotected areas in the NW Mediterranean. Estuar. Coast. Shelf S. **55**: 777-788.

Morin, A., and Nadon, D. 1991. Size distribution of epilithic lotic invertebrates and implications for communtiy metabolism. J. N. Am. Benthol. Soc. **10**(3): 300-308.

Morin, A., Stephenson, J., and Strike, J. 2004. Sieve retention probabilities of stream benthic invertebrates. J. N. Am. Benthol. Soc. **23**(2): 383-391.

Morse, D.R., Lawton, J.H., Dodson, M.M., and Williamson, M.H. 1985. Fractal dimension of vegetation and the distribution of arthropod body lengths. Nature. **314**: 731-733.

Peters, R.H. 1983. The Ecological Implications of Body Size. Cambridge University Press, Cambridge.

Poff, N.L., Palmer, M.A., Angermeier, P.L., Robert L. Vadas, J., Hakenkamp, C.C., Bely, A., Arensburger, P., and Martin, A.P. 1993. Size structure of the metazoan community in a Piedmont stream. Oecologia. **95**: 202-209.

Rabeni, C.F., Collier, K.J., Parkyn, S.M., and Hicks, B.J. 1997. Evaluating techniques for sampling stream crayfish (*Paranephrops planifrons*). New Zeal. J. Mar. Fresh. . **31**: 693-700.

Randall, R.G., and Minns, C.K. 2000. Use of fish production per unit biomass ratios for measuring the productive capacity of fish habitats. Can. J. Fish. Aquat. Sci. **57**: 1657-1667.

Rasmussen, J.B. 1993. Patterns in the size structure of littoral zone macroinvertebrate communities. Can. J. Fish. Aquat. Sci. **50**: 2192-2207.

Schneider, J.C., Laarman, P.W., and Gowing, H. 2000. Chapter 17: Length-weight relationships. *In* Manual of fisheries survey methods II: with periodic updates. *Edited by* J.C. Schneider. Michigan Department of Natural Resources, Fisheries Special Report 25, Ann Arbor, MI.

Sinsabaugh, R.L., Weiland, T., and Linkins, A.E. 1991. Epilithon patch structure in a boreal river. J. N. Am. Benthol. Soc. **10**(4): 419-429.

Solimini, A.G., Benvenuti, A., D'Olimpio, R., Cicco, M.d., and Carchini, G. 2001. Size structure of benthic invertebrate assemblages in a Mediterranean river. J. N. Am. Benthol. Soc. **20**(3): 421-431.

Sugihara, G., and May, R.M. 1990. Applications of fractals in ecology. Trends Ecol. Evol. **5**(3): 79-86.

Taylor, B.W., McIntosh, A.R., and Peckarsky, B.L. 2001. Sampling stream invertebrates using electroshocking techniques: implications for basic and applied research. Can. J. Fish. Aquat. Sci. **58**: 437-445.

Van Deventer, J.S. 1989. Microcomputer Software System for Generating Population Statistics from Electrofishing Data -- User's Guide for MicroFish 3.0. USDA Forest Service, General Technical Report INT-254.

Whicker, F.W., Pinder, J.E.I., Bowling, J.W., Alberts, J.J., and Brisbin, I.L.J. 1990. Distribution of long-lived radionuclides in an abandoned reactor colling reservoir. Ecol. Monogr. **60**(4): 471-496.

White, E.P., Ernest, S.K.M., Kerkhoff, A.J., and Enquist, B.J. 2007. Relationships between body size and abundance in ecology. Trends Ecol. Evol. **22**(6): 323-330.

Zippin, C. 1958. The removal method of population estimation. J. Wildlife Manage. **22**(1): 82-90.

Table 3-1. Physical, chemical, and biological characteristics of the study sites.

| Site | Abbreviation | Lat (N) | Long (W) | Substrate Type | Average TP (mg/L) | Average TN (mg/L) | Average Chl *a* ($mg/m^2$) |
|---|---|---|---|---|---|---|---|
| Beckett's Creek | BEC | 45.5212 | 75.3589 | Medium-large cobble | 0.12 | 1.55 | 223.18 |
| Beckett's Creek b | BECb | 45.5208 | 75.3584 | Flat shale | 0.12 | 1.55 | 286.20 |
| Brassil's Creek 1 | BRA1 | 44.9855 | 75.8018 | Flat bedrock | 0.02 | 0.71 | 17.32 |
| Brassil's Creek 2 | BRA2 | 44.9850 | 75.8013 | Medium-large cobble, boulders | 0.02 | 0.71 | 18.37 |
| Chelsea Stream 2 | C2 | 45.5076 | 75.8129 | Medium-large cobble, boulders | 0.02 | 0.48 | 9.81 |
| Chelsea Stream 3 | C3 | 45.5020 | 75.8113 | Small-large cobble | 0.04 | 0.54 | 31.95 |
| Chelsea Stream 6 | C6 | 45.4960 | 75.8144 | Gravel, small cobble | 0.07 | 0.59 | 17.52 |
| Chelsea Stream 9a | C9a | 45.4953 | 75.7854 | Gravel, small-large cobble | 0.05 | 0.50 | 11.37 |
| Chelsea Stream 9b | C9b | 45.4943 | 75.7842 | Flat bedrock | 0.05 | 0.50 | 0.36 |
| Des Trembles 1 | DT1 | 45.4290 | 75.7616 | Medium-large cobble | 0.20 | 1.30 | 74.49 |
| Des Trembles 2 | DT2 | 45.4201 | 75.7529 | Small-large cobble | 0.11 | 1.07 | 94.04 |
| Leamy midstream | LMS | 45.4674 | 75.7470 | Small-large cobble | 0.21 | 1.97 | 76.77 |
| Leamy downstream | LDS | 45.4625 | 75.7287 | Medium-large cobble | 0.16 | 1.18 | 96.16 |
| Leamy downstream b | LDSb | 45.4626 | 75.7293 | Flat pavement | 0.16 | 1.18 | 50.38 |
| Leamy downstream 2 | LDS2 | 45.4595 | 75.7323 | Sand, gravel, small cobble | 0.15 | 1.96 | 44.65 |
| Raisin River 2 | RR2 | 45.1867 | 74.8556 | Gravel, small-medium cobble | 0.04 | N/A | 189.76 |
| Raisin River 3 | RR3 | 45.1772 | 74.8338 | Small-large cobble | 0.03 | N/A | 56.38 |

Table 3-2. Intercept, slope, residual mean square (RMS), and $R^2$ value for each of the normalized biomass size spectrum linear regressions. Each linear regression fits the model $\log_{10}D = a + b\ (\log_{10}M)$, where D is normalized biomass, $a$ is the intercept, $b$ is the coefficient describing the slope, and M is mass in μg.

| Site | Intercept | Slope | RMS | $R^2$ |
|---|---|---|---|---|
| BEC | 4.52 | -0.73 | 1.10 | 0.76 |
| BECb | 4.94 | -0.87 | 0.57 | 0.89 |
| BRA1 | 4.01 | -0.71 | 0.39 | 0.85 |
| BRA2 | 4.80 | -0.76 | 0.55 | 0.78 |
| C2 | 3.93 | -0.72 | 0.38 | 0.89 |
| C3 | 3.64 | -0.69 | 0.47 | 0.84 |
| C6 | 3.39 | -0.53 | 0.43 | 0.75 |
| C9a | 4.17 | -0.71 | 0.50 | 0.82 |
| C9b | 3.43 | -0.65 | 0.19 | 0.92 |
| DT1 | 3.58 | -0.60 | 0.51 | 0.80 |
| DT2 | 4.02 | -0.65 | 0.51 | 0.83 |
| LDS | 4.03 | -0.73 | 0.22 | 0.93 |
| LDS2 | 3.80 | -0.38 | 0.36 | 0.49 |
| LDSb | 2.90 | -0.55 | 0.15 | 0.92 |
| LMS | 4.17 | -0.66 | 0.62 | 0.77 |
| RR2 | 4.92 | -0.73 | 0.70 | 0.80 |
| RR3 | 3.71 | -0.62 | 0.50 | 0.81 |

Table 3-3. Summary of GLMs to test site and nutrient effects on normalized biomass size spectra, showing the *p*-values for the model terms (interaction term for full model, and site, TP, TN, or substrate term for reduced model), residual means square (RMS), and $R^2$ value for each model. Models were tested using data from all sites[a], with the exception of the TN model that excluded RR2 and RR3 because of a lack of data. The full model was $\log_{10}D = a + b\ (\log_{10}M) + c\ (X) + (\log_{10}M) * (X)$, where D was normalized biomass, M was mass, X was site, substrate, or $\log_{10}$(nutrient variable), *a* was the intercept, and *b* and *c* were coefficients describing the slope (with *c* omitted from the categorical site and substrate terms). The reduced model (with the removal of the non-significant interaction term) was $\log_{10}D = a + b\ (\log_{10}M) + c\ (X)$. Significant *p*-values ($\alpha = 0.05$ for site model, Bonferroni-corrected $\alpha = 0.017$ for environmental variable models) are indicated in bold.

| Model Terms | Full model | | | Reduced model | | |
|---|---|---|---|---|---|---|
| | Interaction *p*-value | RMS | $R^2$ | Variable *p*-value | RMS | $R^2$ |
| Log$_{10}$M | | 0.61 | 0.79 | | | |
| log$_{10}$M + site + interaction | **0.01** | 0.49 | 0.85 | | | |
| log$_{10}$M + log$_{10}$TP + interaction | 0.50 | 0.62 | 0.79 | 0.64 | 0.61 | 0.79 |
| log$_{10}$M + log$_{10}$TN + interaction | 0.81 | 0.56 | 0.81 | **< 0.01** | 0.56 | 0.81 |
| log$_{10}$M + substrate + interaction | 0.72 | 0.59 | 0.80 | **< 0.01** | 0.59 | 0.80 |

[a] Results presented for the site model were obtained using data for all sites. However, when the site model was tested without the inclusion of BECb and LDS2, the interaction *p*-value was 0.49. When the reduced model was tested without the inclusion of BECb and LDS2, the variable *p*-value was < 0.01.

**Figure captions**

Figure 3-1. Normalized biomass size spectra, including data for macroinvertebrates, crayfish, and fish, for 17 stream sites. A linear regression line for each site (solid line) and an average linear regression line (dashed line) are shown on each plot; see Table 3-2 for regression coefficients.

Figure 3-2. Average normalized biomass spectrum for the 17 sampling sites, showing the density of macroinvertebrates, crayfish, and fish in each size class.

Figure 3-3. The percent of the total biomass in each site collected as small, medium, or large macroinvertebrates, crayfish, and fish. Small organisms are $\leq 1$ μg, medium organisms are between 1 μg and $10^4$ μg, and large organisms are $> 10^4$ μg (see Methods for details on size classification).

Figure 3-4. The distribution of density, biomass, and production potential in relation to body size for each stream site. Production potential was estimated from density by assuming it scales as mass$^{0.75}$.

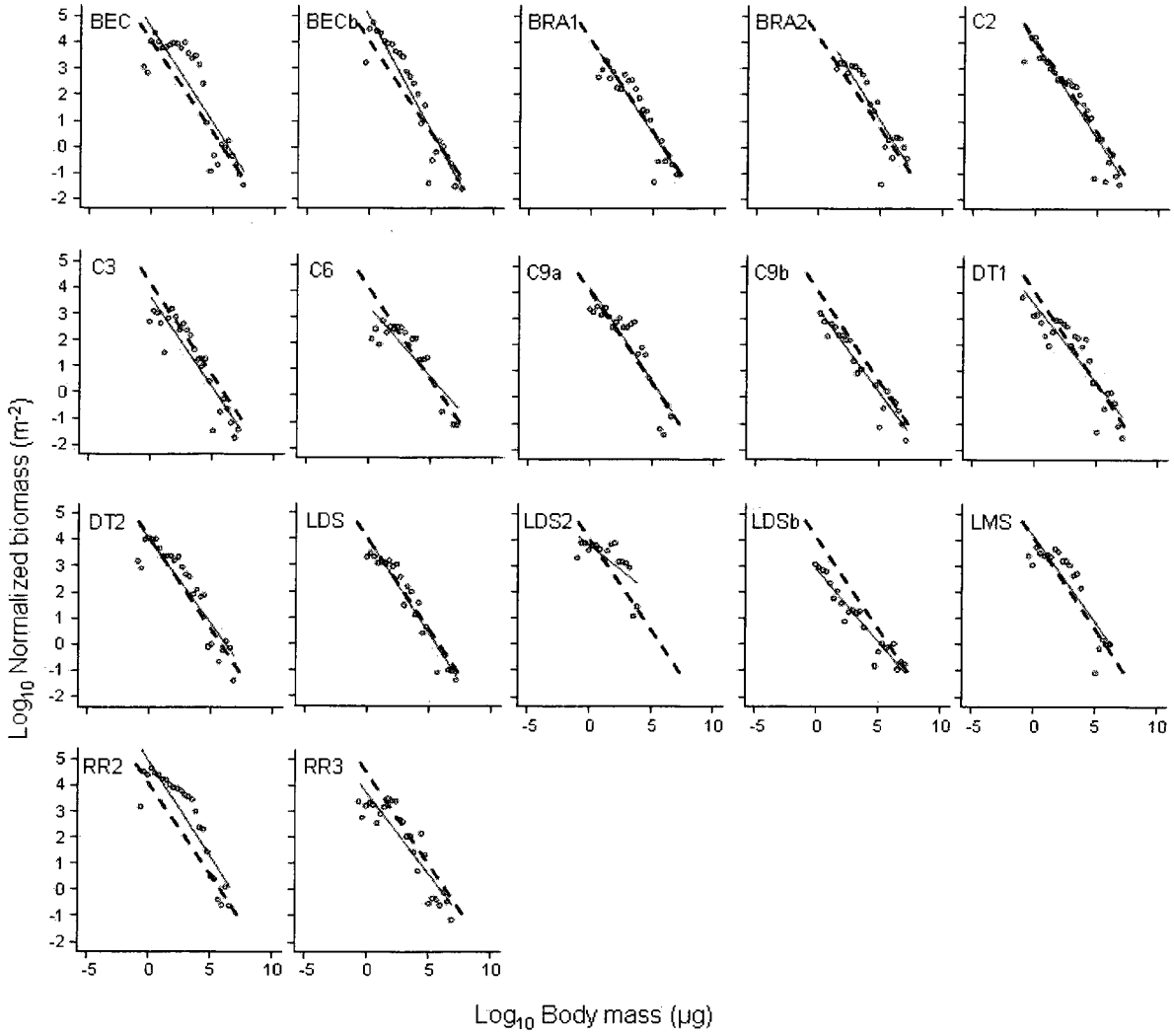
BEC
BECb
BRA1
BRA2
C2
C3
C6
C9a
C9b
DT1
DT2
LDS
LDS2
LDSb
LMS
RR2
RR3
Log10 Normalized biomass (m-2)
Log10 Body mass (µg)

Figure 3-1

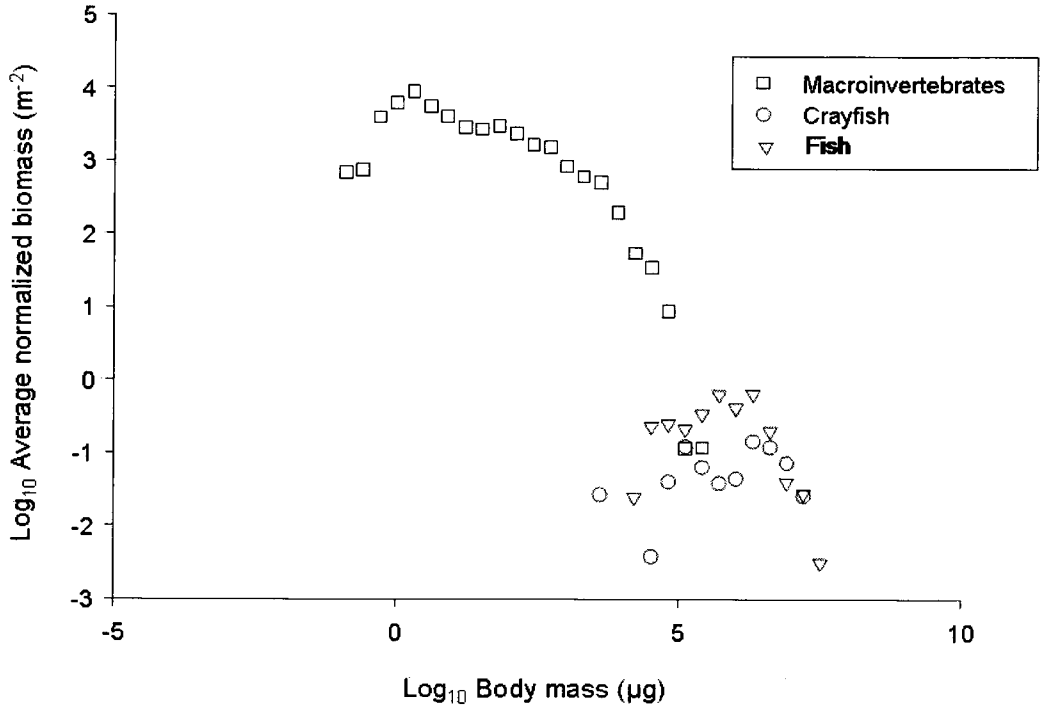
Log10 Average normalized biomass (m-2)
Log10 Body mass (µg)
Macroinvertebrates
Crayfish
Fish
5
4
3
2
1
0
-1
-2
-3
-5
0
5
10

Figure 3-2

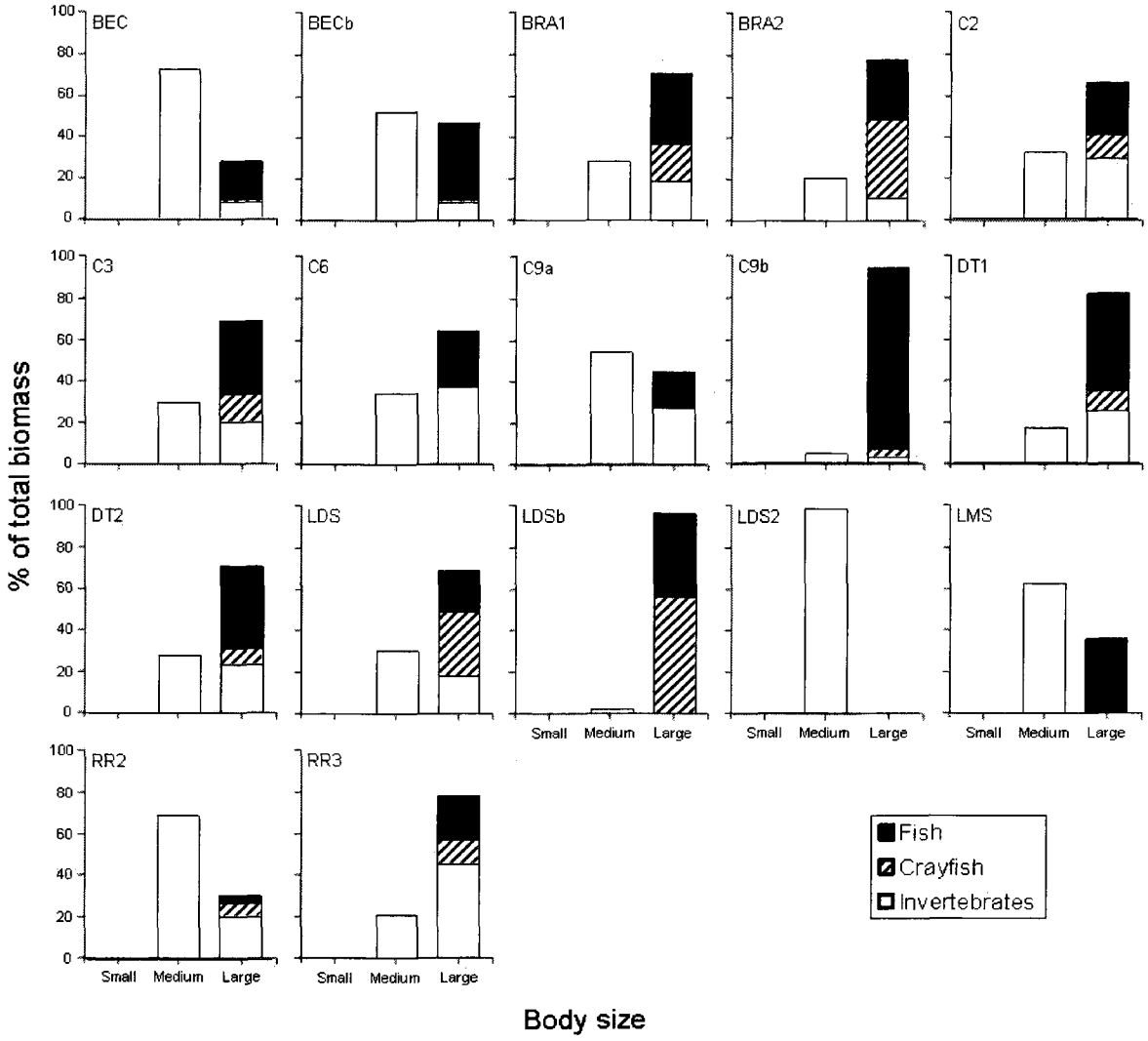
BEC
BECb
BRA1
BRA2
C2
C3
C6
C9a
C9b
DT1
DT2
LDS
LDSb
LDS2
LMS
RR2
RR3
% of total biomass
Small
Medium
Large
Fish
Crayfish
Invertebrates
Body size

Figure 3-3

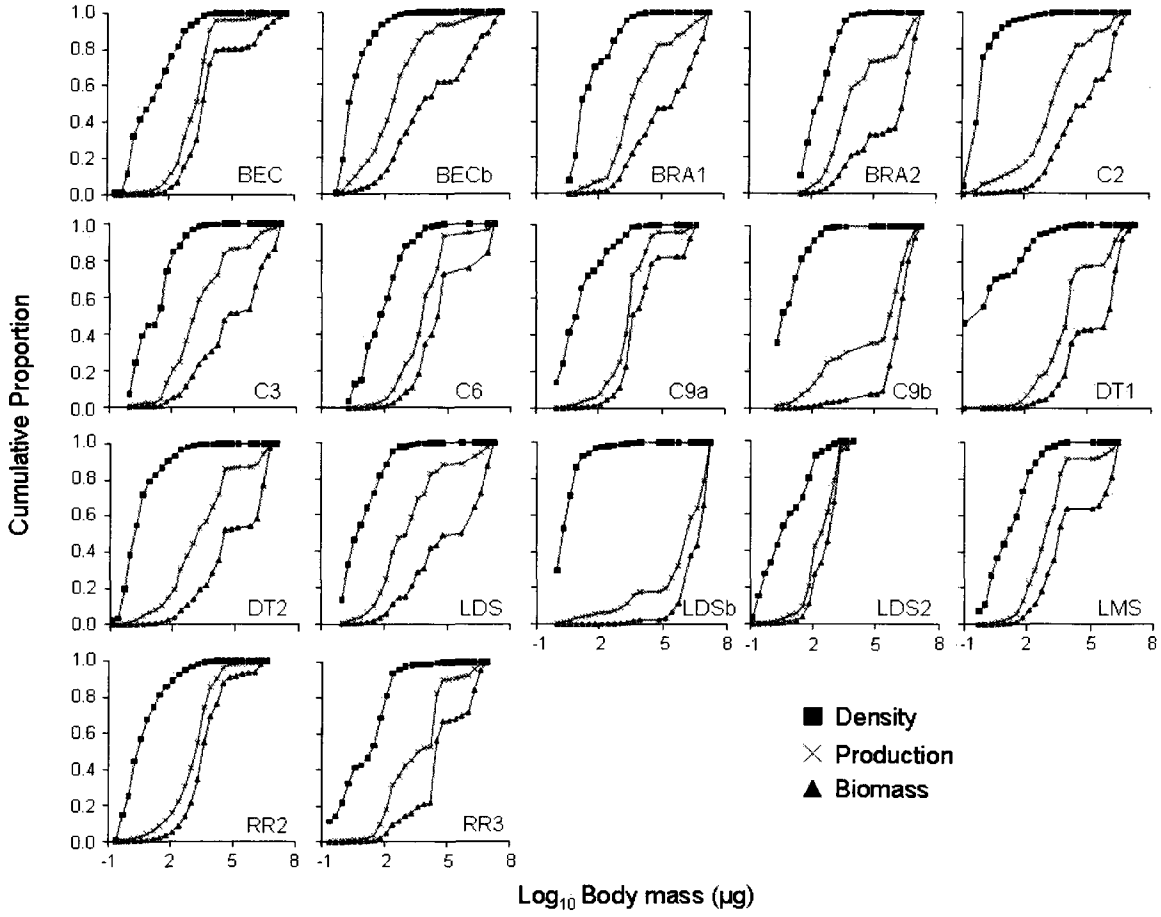
Cumulative Proportion
BEC
BECb
BRA1
BRA2
C2
C3
C6
C9a
C9b
DT1
DT2
LDS
LDSb
LDS2
LMS
RR2
RR3
Density
Production
Biomass
Log10 Body mass (µg)

Figure 3-4

# Chapter 4 – A Photographic Method to Quantify Available Space for Benthic Organisms in Streams

## Introduction

Habitat space has been suggested by several authors to be a factor controlling the abundance of various size classes, and hence body size distributions of benthic assemblages (Sinsabaugh et al. 1991; Holling 1992; Gee and Warwick 1994; Downes et al. 1998; Schmid 2000; Taniguchi and Tokeshi 2004). In particular, relative densities of small and large organisms may be related to the complexity of the habitat in which they live. Complex surfaces include small spaces that may act as refuge for small organisms, but may limit the ability of large organisms to access resources. At the upper limit, organisms are restricted by the amount of space available to them, and in the case of large organisms, that amount may decrease as a result of surface complexity (Sanson et al. 1995; Downes et al. 1998).

The relationship between body size and surface complexity forms the basis for the habitat hypothesis, which states that space availability shapes body size distributions. The slope of size distributions is predicted to change in relation to habitat space availability. In complex habitats, where small organisms have the largest amount of available space due to small crevices and interstitial spaces that large organisms cannot access, steep size distribution slopes are predicted, with high densities of small organisms and low densities of large organisms. In simple habitats, where all space is available to all size classes of organisms, relatively more shallow size distribution slopes are predicted because small organisms do not benefit from the presence of habitat patches that are inaccessible to large organisms. There are numerous studies that have attempted to determine whether habitat space affects body size distributions as predicted by the habitat hypothesis, but the results of such studies have been mixed (Robson et al. 2005). Many of these studies have

relied on indirect measurements of habitat space or complexity (e.g., Bourassa and Morin 1995; Solimini et al. 2001), suggesting the need for a direct measurement of size and habitat space that is easily repeatable.

Habitat space is often described in terms of substrate complexity, which has most often been quantified by measuring the fractal dimension of surfaces (Gee and Warwick 1994; Schmid 2000; Halley et al. 2004; Taniguchi and Tokeshi 2004; Kotsylev et al. 2005). The fractal dimension of a surface is a measure of the amount of roughness or texture on a surface; a high fractal dimension is indicative of high substrate complexity and only results in increased habitat for small organisms (Morse et al. 1985; Sugihara and May 1990; Gee and Warwick 1994; Halley et al. 2004). However, the fractal dimension of a surface is an abstract measure that does not provide quantitative information about the amount of habitat space available. Substrates with different spatial arrangements of particles and differently sized habitat spaces can have the same fractal dimension (Sanson et al. 1995; Halley et al. 2004), calling to question the meaningfulness of the fractal dimension as a descriptor of habitat space.

A more simple and direct measurement of habitat space may provide a better way to quantify habitat complexity and relate it to body size distributions than using fractal dimensions. Although particle size has been used as a measure of habitat space in previous studies (Bourassa and Morin 1995; Duplisea and Drgas 1999; Solimini et al. 2001), the shape and spatial arrangement of particles (often described as habitat architecture) are important aspects of habitat complexity and may be more important to benthic organisms than the size distribution of particles alone (Robson et al. 2002; Robson et al. 2005). However, the amount of available habitat space on a benthic

substrate is extremely difficult to measure when the spatial arrangement of particles and the presence of interstitial refuges must be taken into account (Robson et al. 2005).

In order to obtain accurate estimates of the amount of habitat space given habitat architecture, measurements must be made without removing particles from the substrate. Image analysis of photographs may provide a means to obtain such measurements. Through-water photographs of substrates, taken using photogrammetric methods, have been shown to be of high enough quality to allow the extraction of digital elevation models (Westaway et al. 2001; Butler et al. 2002). Unfortunately, the level of expertise required to extract digital elevation models from such photos does not make this a viable method for easily obtaining a measure of habitat space. But similar photographic methods may be employed to take through-water photographs of stream substrates that may be analyzed by simpler methods.

Our objective was to develop a simple method to measure habitat space in stream substrates using through-water digital photographs. We extracted profile information from the photographs by estimating the vertical height of particles (z-values) through the use of image analysis software. In order to estimate habitat space for benthic organisms, we fit invertebrates of different sizes to the profiles, predicting the maximum possible density of organisms if all available space was utilized.

## Methods

### *Field Methods*

We collected data from 5 sites in Chelsea Stream in western Québec in Canada (see Table 4-1 for site details). Chelsea Stream is a small 1$^{st}$ through 3$^{rd}$ order stream running through deciduous forests of Gatineau Park, with a maximum width of 10 m.

Sample sites were separated along the length of the stream by a distance of at least 50 m, and were selected to represent different levels of habitat complexity. The least complex substrate was at C9b, which was primarily composed of flat bedrock. More complex substrates were composed of combinations of sand, gravel, cobble, and boulder (Table 4-1). The most complex substrate was at C6, which was primarily composed of gravel and small cobbles. This substrate was deemed to contain the greatest amount of habitat for small organisms, but the least habitat for large organisms.

At each sampling site, we took through-water digital photos in multiple locations that were representative of the dominant substrate composition. In order to control reflections and flatten the water surface, we floated a viewing box on the water above the photo location. This box was constructed with plywood sides and a 3 mm thick perspex base through which the stream substrate could be viewed and photographed. The thin layer of perspex has been recommended to reduce refraction and approximate a more simplified air/water interface at the water surface (Butler et al. 2002). A tripod was placed in the water just downstream of the photo location and clamps on the tripod legs were used to hold the viewing box in place. A Nikon D200 digital camera on a ball head was attached to the tripod center column that was held parallel to the water surface. The camera was rotated until the lens was parallel to the substrate, and a bubble level was used to ensure that the photos were not taken at an angle. To allow the photos to be scaled in later processing, a thin metal ruler was placed on the substrate within the frame of the photo. To control glare and block sky reflections on the perspex, we held a 3 m by 3 m piece of heavy black photographer's cloth above the camera and photo location while the photos were taken.

We took 4 to 7 photos per stream site depending on the depth and water clarity of each site. The water was too shallow for photos to be taken in a location if rocks broke the water surface, because the glare could not be controlled in such cases. There was also a maximum depth at which photos could be taken, as the camera was set up on a tripod in the stream to stabilize the equipment. The maximum allowable depth of the water decreased in high turbidity, because in deeper depths the substrate was not visible in the photos. The substrate area photographed in each location differed depending on the vertical position of the camera (which varied with water depth); the maximum length of substrate included in each photo ranged between approximately 50 and 70 cm.

*Estimating z-values*

In order to extract profile data from the photos, we needed a way to estimate the height of each rock (the z-value) from the aerial view of the rocks. Estimations that required the substrate particles to be removed and measured would not allow us to describe the configuration of the substrate, and therefore were not of use. However, in their review of methods to estimate surface area of stream substrates, Bergey and Getty (2006) noted several examples of equations that had been derived to estimate surface area from measured parameters such as the longest and shortest perpendicular axes on a rock. Furthermore, Bunte and Abt (2001) suggested that the relationship between particle axes could be used to describe substrate size. We used this approach to approximate z-values for our substrate profiles by exploring the relationship between z and particle properties that could be measured using the photos.

We measured a set of cobbles from all sampling sites (range of sizes: 55 to 145 mm longest axis). On each cobble, we measured the height (z-value) and the length of

perpendicular axes (longest axis and perpendicular short axis) across the particle when viewed from above. The longest axis was defined as perpendicular to the short axis (as defined by Gordon et al. 1992), and not necessarily as the longest distance between two points on the particle. Although many previous studies assumed that all particles had one particular shape (most commonly spherical for ease of calculation, as reviewed by Bergey and Getty 2006), the cobbles that we measured had 4 general shapes: ellipsoid, rectangular, cubic, and triangular-based pyramid. Because these shapes appeared to influence the relationship between z and the long and short axes, we made separate measurements for each particle shape and determined relationships with z separately for each. Ellipsoid, cubic, and pyramid particles generally had a z-value that was similar to the length of the short perpendicular axis. Rectangular particles were generally broken rock or shale, and had a z-value that was much shorter than the length of the short axis.

The relationship between z and both the long and short axes was examined in order to determine which relationship provided the most accurate descriptor of z. For each particle shape, z was best described by an average proportion of the long axis (0.39 to 0.70; Table 4-2), with standard deviations ranging from 0.10 to 0.11 (Table 4-2). To determine whether this relationship held for larger particles, we measured large cobbles and boulders (range of sizes: 145 to 425 mm longest axis), ensuring that measurements were obtained for all particle shapes. When large rocks were included, the SD changed only slightly for the average calculation of z as a proportion of the long axis (Table 4-2). This proportion was used for small and large particles to predict z values.

*Profile extraction*

Image analysis software was used to make measurements on the substrate photos (Image-Pro Plus v6.0; Media Cybernetics, Bethesda, Maryland). Within the program, each photo was initially calibrated by setting up a measurement scale based on the number of pixels per 20 mm length in the photo (as measured by the ruler that was on the substrate in all photos). Once the photo was calibrated, 1-6 straight lines were drawn across the photo to represent the profiles along which particles were to be measured. The lines were selected at random, but were drawn parallel to each other in order to avoid duplicate measurements within the same substrate area. The length of the profile lines was limited by the particles present along the edges of each photo; a particle towards the edge of the photo was only included as part of the profile if enough of the longest axis was visible to allow z-values to be estimated. Profiles were also limited to areas of the photograph where the substrate particles were clearly visible.

Measurements were made on each particle that the profile line crossed, excluding particles < 5 mm in diameter, which were generally too small to be clearly measured in the photos. Lengths along the profile that were composed of bedrock, sand, or particles < 5 mm in diameter were treated as flat habitat, and were measured and assigned a z-value of 0. To estimate the remaining z-values, each particle along the profile was assigned a shape (cubic, rectangular, ellipsoid, or pyramid), and was described as partially buried or fully emerged from any underlying sand. In order to minimize variability in z-values caused by different users describing the substrata as different shapes, all measurements, and therefore all decisions about particle shape, were completed by one researcher (J.L.).

A different set of measurements was required for each particle depending on its shape, orientation, and placement across the profile. For all particles, the long axis was

measured in order to estimate the maximum z-value. The length of the particle crossed by the horizontal profile was also measured on all particles regardless of shape. No additional measurements were required for cubic or rectangular rocks because of the simplicity of their profile shapes. However, several more measurements were required for ellipsoid and pyramid particles. The z-value for each of these two shapes had the potential to differ from the maximum z-value for the particle if the profile crossed it in a non-lengthwise direction or close to its edge rather than at the center (or the apex, in the case of a pyramid). Geometric relationships for ellipses (Weisstein 2010a) and pyramids (Weisstein 2010b) were used to obtain the actual z-value for each particle.

When the profile cut across an ellipsoid particle in a non-lengthwise direction away from the center (and therefore maximum z-value), a new z-value was calculated by using the distance ($t$) from the edge of the particle to the point ($P$) where the profile cut across (Figure 4-1a). The distance ($r$) from the focus of the ellipse ($F$) to point $P$ on the curve of the ellipse formed the hypotenuse of a right triangle which had a height equal to half the z-value for the point where the profile cut across the particle (Figure 4-1a). The hypotenuse was calculated as $r = a * (1 - e^2) - e * (x - c)$, where $a$ was the length of the semimajor axis (half the length of the long axis of the rock), $e$ was the eccentricity of the ellipse (defined as $c/a$), $x$ was the horizontal distance from the center of the ellipse to $P$ (calculated as $a - t$), and $c$ was the distance from $F$ to the center of the ellipse (calculated as $\sqrt{(a^2 - b^2)}$, where $b$ was the semiminor axis (half the maximum z-value for the particle); Figure 4-1a). The new max z-value was then calculated as $z/2 = r * \sin \theta$, where $\theta$ was the angle opposite z in the right triangle formed by z and $r$.

When a profile cut across a pyramid anywhere other than the apex, the new z-value was calculated using the side and edge lengths of the pyramid. The edge of the pyramid along which the profile cut was calculated as $(\text{edge length})^2 = (\text{max z})^2 + (1/3)*(\text{side length})^2$, where the side length was measured on the photo and max z was calculated as a proportion of the longest axis (Figure 4-1b). The new z-value was then calculated by creating a right triangle from the edge length and the max z-value (Figure 4-1b). The base of the right triangle was calculated as $(\text{base})^2 = \sqrt{((\text{edge length})^2 - (\text{max z})^2)}$. The new max z-value was obtained by using the angle formed by the base and edge ($\theta$) and the horizontal distance to where the profile crossed the particle (cut) as $z = \tan \theta * \text{cut}$ (Figure 4-1b).

We created a Visual Basic program to automatically extract (x,z) coordinates along the length of each profile. The program moved along the x-axis of each profile in increments of 0.1 mm, calculating a z-value for each x-value. The z-value remained at 0 for the entire length of flat substrates. When a cubic or rectangular particle was encountered, the program set z equal to the calculated max z-value (or half of the calculated max z-value if the particle was buried) for the entire length that the profile crossed the particle, and subsequently set z equal to zero before moving on to the next particle. When an ellipsoid particle was encountered, the z-value for each x-value was estimated by calculating *r* as described above. On each particle, we measured the horizontal length along the profile until the maximum z-value on the particle was reached. This length was used as the *a*-value for the first half of the ellipse, and was subtracted from the total particle length crossed by the profile to calculate the *a*-value for the second half of the ellipse. The *b*-value for the calculation of z was half of the max z-

value (as calculated for either a lengthwise or non-lengthwise ellipse). When the ellipsoid particle was not buried, ((max z) / 2) was added to each calculated z-value. Although this resulted in straight sides for the lower half of the particle, the majority of ellipsoid particles encountered at our sites had a rounded upper surface and straight sides. The length to the maximum z-value was also measured for pyramid-shaped particles to indicate the halfway point of the pyramid. For the first half of the pyramid (when z increased as x increased), the angle of increase was calculated as $\tan \theta = (\max z) / (\text{length to max})$. For each 0.1 mm increment of x, the increase in z was calculated as $\Delta z = \tan \theta * 0.1$, and it was added to the previous value of z to obtain the (x,z) coordinate. For the second half of the pyramid (when z decreased as x increased), the length to the end of the pyramid was calculated by subtracting the length to the maximum z from the total length that the profile crossed the particle. The angle of decrease was calculated as $\tan \theta = (\max z) / (\text{length to end of particle})$. For each 0.1 mm increment of x, the decrease in z was calculated as $\Delta z = \tan \theta * 0.1$, and it was subtracted from the previous value of z to obtain the (x,z) coordinate. No alterations were made to z when a pyramid-shaped particle was buried, because the long axis appeared shorter in such cases, resulting in a smaller maximum z-value. The output from the program was a series of (x,z) coordinates that covered the range of the entire horizontal profile.

*Fitting organisms to profiles*

The profile coordinates were used to quantify habitat space for benthic organisms by estimating the maximum number of individuals of each body size that could fit along the profile end-to-end. The number of organisms that could fit along a profile was calculated for the range of $\log_2$ size classes (calculated as $\log_2$(dry mass in μg)) that was

observed in the benthic macroinvertebrate communities in our study streams (size classes -3 to 18, corresponding to 0.125 to 265000 μg dry mass). The maximum body length for each size class was used to fit organisms to the profiles. Maximum body length was estimated by averaging the length-mass regressions described by Benke et al. (1999), weighting the taxon-specific regression coefficients by the proportion of the total biomass in the stream samples that was contributed by each taxon.

Organisms in all size classes were fit to the profiles under different levels of body "flexibility." At one extreme, organisms were considered to be infinitely flexible, meaning that they could bend in any direction as much as necessary to use all of the available habitat space. This was equivalent to dividing the total length of habitat space by the length of the organism. At the other extreme, organisms were considered to be infinitely inflexible. With this level of flexibility, they were unable to bend at all, and could only inhabit spaces that had no change in angle over an expanse at least as long as the organism's body length. In order to fit organisms using this rule, the angle of increase or decrease of the substrate profile across each 0.1 mm x-interval was calculated from a right triangle with a height equal to $\Delta z$. If the angle of x-interval$_{n+1}$ equaled the angle of x-interval$_n$, then the length of the hypotenuse of triangle$_{n+1}$ was added to the length of the hypotenuse of triangle$_n$ to represent the length of habitable space. This continued, with individuals fit to the habitable space, until the angle of x-interval$_{n+1}$ did not equal the angle of x-interval$_n$, at which point the length of habitable space was reset to zero and the angle comparisons restarted. Three intermediate flexibility levels were also used: 10 degrees flexible, 25 degrees flexible, and 45 degrees flexible. Under these levels of flexibility, organisms could bend a maximum of 10, 25, or 45 degrees to fit into available

habitat space The same algorithm was used to fit organisms under these rules as for the infinitely inflexible rule, except that for each angle comparison, there was an allowable difference of 10, 25, or 45 degrees. For each flexibility level and each profile, the number of organisms fit was standardized by the horizontal length of the profile and expressed as the maximum possible density ($m^{-1}$).

*Sensitivity analysis*

In order to evaluate the uncertainty in the maximum possible density distribution for each site that was attributable to fitting organisms by using different levels of flexibility, we compared the mean maximum possible density in each size class across flexibility levles. For each site, the average of the maximum possible density (the number of organisms / m) was plotted on a $\log_{10}$ scale as a function of $\log_{10}$ body size (mass in μg) for each profile and level of flexibility. Error bars were plotted in order to quantify the variation in maximum possible density values across profiles for each size class under each level of flexibility.

We estimated spatial variation on maximum possible densities by quantifying variability due to differences between substrate profiles and variability due to our estimation of z-values. To examine the variability due to profile heterogeneity, we calculated the coefficient of variation for densities across profiles. The coefficient of variation was calculated separately for each size class and each site in order to compare the effects of heterogeneity on the maximum possible density of organisms across body sizes. To quantify the uncertainty in maximum possible density that was caused by variable z-ratios, we conducted a Monte Carlo simulation. For each rock shape (rectangle, square, ellipse, and pyramid), a set of random normal deviates was produced

that had a mean of 0 and a standard deviation equal to that of the z-ratio for the rock shape (see Table 4-2). For all sites other than C9b (which was flat), we picked a representative profile on which to test the effects of varying the z-ratio. A maximum z-value was estimated for each particle along the profiles by adding a random normal deviate to the proportion of the long axis that described z. This was repeated to obtain 6 alternate sets of z-values for each profile. Profile coordinates were extracted for each replicate as previously described, and organisms were fit to the profiles. We calculated the coefficient of variation for the density of organisms fit to the profiles extracted using the original and altered z-ratios in order to examine the uncertainty in maximum possible density distributions that could be attributed to our estimation of z using a constant ratio of z to longest axis. Coefficients of variation were calculated separately for each size class at each site to determine whether the effect of variable z-ratios differed by size.

Maximum possible density distributions were compared among sites in order to determine whether they differed among habitat complexities as predicted. For all other analyses, the body lengths used to fit size classes to the profiles were site-specific, as was the range of size classes fit to each profile. Both the range of size classes and the body lengths were based on macroinvertebrate data collected from these sites, in order to restrict predictions to the size range observed at each site. However, to facilitate the comparison of the average distribution of maximum possible densities among sites, we used a single set of size classes and body lengths for all sites, so that differences among distributions could not be attributed to differences in the lengths used to fit organisms to the profiles. The GLM model $\log_{10}$ (maximum possible density) = $a + b$ ($\log_{10}$ mass) + site + ($\log_{10}$ mass) * site, where $a$ was the intercept and $b$ was a coefficient describing the

slope, was used to compare density distributions among sites, with profiles as replicates. The interaction term ($(\log_{10}$ mass) * site) tested whether the distribution slopes differed significantly (at $\alpha = 0.05$) among sites, while the site term tested whether the density differed significantly (at $\alpha = 0.05$) among sites. The density in each size class was averaged across profiles for each site and plotted for a visual comparison of the differences between predicted densities for each habitat complexity level.

**Results**

Figure 4-2 provides examples of the profiles extracted from photos of sites C2 (boulder), C9a (mixed substrate), and C6 (gravel and cobbles). The profiles looked as expected, with the largest z-values in site C2, and the smallest in site C6 (Figure 4-2). The combination of small z-values and a large number of rocks in C6 contributed to its high substrate complexity, while site C9a displayed intermediate complexity levels between sites C2 and C6.

There was a difference in maximum possible density distributions that was primarily evident between infinitely flexible and all other flexibility levels (Figure 4-3). The difference was most prominent in the more complex sites (the mixed substrates at C9a and the gravel and cobble at C6), where there was a sharp decline in maximum potential densities of large organisms for all levels of flexibility except infinitely flexible (maximum possible densities for organisms of 131,000 to 262,000 μg mass (largest size class): C9a infinitely flexible = 23 individuals $m^{-1}$, C9a infinitely inflexible = 4 individuals $m^{-1}$, C6 infinitely flexible = 24 individuals $m^{-1}$, C6 infinitely inflexible = 1 individuals $m^{-1}$; Figure 4-3). The error bars on each density distribution were small, which suggested that the differences in maximum possible densities in the large size

classes due to differences in flexibility level was much larger than spatial variation among profiles. However, there did appear to be more variance (evidenced by larger error bars) in the large size classes than in small size classes, which suggested that the number of large organisms fit under each flexibility level was more sensitive to the spatial variation among profiles.

The maximum possible densities for the infinitely inflexible and intermediate levels (10, 25, and 45 degrees flexible) appeared very similar for each size class. The maximum possible densities for the infinitely inflexible rule only appeared to differ from the intermediate flexibility levels in the most complex site (C6; Figure 4-3), while the three intermediate flexibility levels did not appear to differ in terms of maximum possible densities at any site (Figure 4-3). The level of flexibility was expected to have a greater impact on predicted densities in the most complex site, because large organisms were expected to have limited space in a complex habitat when they were not infinitely flexible. However, the similarity of the maximum possible densities among the intermediate flexibility levels at all sites suggested that any of the chosen intermediate rules could be used to predict invertebrate densities. For all subsequent analyses, we chose to use the 45 degree flexible rule.

Examination of the coefficients of variation for each size class revealed that more of the uncertainty in the maximum possible density distributions was related to spatial heterogeneity among profiles than to the estimation of z. Because the substrates were not completely homogenous and profiles were selected at random from the photos, there was variation in terms of the number of organisms that could be fit to the profiles at each site. The coefficient of variation was highest in the largest size classes for all sites because the

density of the largest invertebrates was most affected by differences in the size and arrangement of particles. For example, the coefficient of variation ranged from 12 to 20% for the small size classes in the gravel site (C6), but in the largest size classes it was found to be over 100% because some profiles fit 1 or 2 invertebrates while others fit no organisms. Overall, the coefficient of variation was highest for the boulder site (C2), where it ranged from 35 to 45% in the small size classes. Because of the large z-values for the majority of particles at that site (leading to large amounts of habitat in the vertical dimension for each particle), the maximum possible density of invertebrates was more highly affected by the number of particles crossed by a profile in site C2 than in other sites. In contrast, the coefficients of variation for the C2 profiles extracted using the original and altered z-ratios ranged from 7 to 10%, suggesting that the variability in z-ratios contributed little to the uncertainty in maximum possible densities. At all sites, the coefficients of variation for the variability in z-ratios were less than half as large as the coefficients of variation for profile heterogeneity. When compared across size classes, coefficients of variation for the variability in z-ratios were largest in the largest size classes, but they were still found to be less than half of what was calculated for the largest size classes for the profile heterogeneity data.

The density distributions of organisms fit to the profiles at the four sites matched the patterns that were expected based on habitat complexity levels. Overall, there was a significant difference in distribution slopes ($p < 0.001$) and intercepts ($p < 0.001$) between sites. The flat habitat had the lowest maximum possible density of small organisms; there was more space available for small organisms in the more complex habitats. In contrast, there were higher maximum possible densities of large organisms in

the flat habitat than in the more complex mixed or gravel substrates (Figure 4-4). The decrease in maximum possible density levels in the large size classes led to a curved distribution for the more complex sites (C6 and C9a; Figure 4-4). The distribution of maximum possible densities in the boulder habitat (site C2) was more similar in shape to the distribution for the flat habitat (site C9b) than the more complex sites (Figure 4-4). However, overall maximum possible density levels were higher in the boulder substrate than all other substrate types because of the extra habitat space in the vertical direction.

**Discussion**

The substrate analysis method presented in this paper was used to extract profiles from digital photos of stream substrates and estimate the maximum number of macroinvertebrates that could fit along those substrate profiles. The density of macroinvertebrates predicted by this method for each size class matched the patterns expected based on the habitat complexity levels at the sample sites. The maximum possible density distributions indicated that small organisms have more potential space available to them in complex habitats because they can fit into small spaces between particles. According to the predictions of the substrate analysis, large organisms should be present at lower densities in complex substrates because much of the habitat space is too small for them to utilize, but they have the potential to be present in higher densities in habitats with low complexity (including flat habitats and those dominated by large particles such as boulders) because they should be able to access the entire habitat.

From the results of the substrate analysis, we made several predictions about what patterns we expected to see in size distributions if the normalized biomass in size classes was affected by habitat space. The predictions were (1) that the size spectrum for the

boulder site (C2) should have higher normalized biomass in all size classes than the size spectrum for the flat site (C9b) because the large amount of habitat space in the vertical dimension at C2 was expected to lead to higher overall densities if invertebrates utilized available space; (2) that the steepest slope would be found in the most complex site (C6, the gravel site) because a large amount of the habitat space was expected to be inaccessible to large organisms, while small organisms were expected to have increased space; and (3) that the size spectra in the more complex habitats (mixed substrate in C9a and gravel in C6) should be more curved than those in the simple habitats (flat substrate in C9b and boulder in C2) as in Figure 4-4 because of low normalized biomass of large organisms in the complex substrate.

We used size spectra data collected from the four sample sites to test these predictions (see Chapter 3 for details on data collection and the construction of normalized size spectra). When the observed size spectra were examined, not all of the predictions made from the substrate analysis were supported by the data. There was significantly higher normalized biomass in the boulder habitat (C2) that in the flat habitat (C9b; $t_{0.05(1),11} = 4.49, p < 0.001$). The boulder site did have higher normalized biomass in all size classes than the flat site, congruent with the increased habitat space in the vertical dimension contributed by the large particles. The third prediction was also supported by the observed normalized size spectra. Adding a second order $\log_{10}$ mass term to regression models fit to the normalized spectra for each site had the largest effect in the most complex habitats (site C9a with mixed substrate and site C6 with gravel substrate; Table 4-3). The change in $R^2$ and residual mean square (RMS) values from the first order to the second order model was largest for the complex sites (C9a and C6; Table 4-3).

These results suggested that the normalized size spectra for the complex sites were more curved than for the simple sites. However, visual inspection of the spectra revealed that this was not purely due to reduced densities of large organisms as had been predicted. Although site C9a appeared to have a curved distribution due to lower normalized biomass of large organisms, much of the curvature in the spectrum for site C6 was due to low normalized biomass in the small size classes (Figure 4-5).

The lower than expected normalized biomass of small organisms in site C6 also affected the test of the second prediction that this site (with the most complex substrate) would have the steepest slope. Because of low normalized biomass of small organisms in the observed size spectrum for site C6, this site was found to have the most shallow size distribution slope (slope = -0.215). It's possible that small organisms at C6 are not utilizing all of the available space because they are limited by some other factor such as food availability or predation. However, it is unclear why the normalized biomass of small organisms would have been more affected by factors other than space availability at C6 than they were at the other sample sites.

The steepest overall slopes in the observed spectra were actually found to be in the most simple habitats (sites C9b and C2, slope = -0.61 and -0.56, respectively) even though the substrate analysis predicted that those sites would have the most shallow slopes. There was a decrease in normalized biomass of large organisms in these sites. Although not a large decrease, it was sufficient to result in steep size spectrum slopes in both sites. This decrease may have occurred because large organisms were limited by some factor other than space, such as food availability. Alternatively, this might reflect an interactive effect of habitat complexity and predation. Bartholomew (2002) suggested

that organisms would preferentially choose habitat space that was suitable for their body size but excluded larger predators, and predicted that organisms would not be found in high densities in areas sufficiently larger than their own body size to allow predator access. In the flat habitat, all of the substrate space was potentially available to the large organisms, but it was all open space with no refuges. In such an open habitat, large organisms would be particularly susceptible to predation because any larger-sized predators would not be excluded from the habitat on the basis of size. Similarly, although refuge space may have existed in the boulder habitat, the refuge space may still have been large enough for predators to access it due to the generally large particle size at this site, thereby offering little protection from predation. The decreased densities of large organisms we observed in the flat and boulder sites may have been a result of this tradeoff between habitat space availability and predator susceptibility.

The mixed substrate habitat at C9a appeared to show the closest fit between predicted and observed size spectrum patterns. Although low normalized biomass of small organisms resulted in a less steep slope at this site than in the more simple habitats, C9a clearly showed a decrease in normalized biomass in the large size classes and overall displayed a curved distribution shape because of the decrease in large organisms. The results for this site provided the strongest evidence that size spectrum shape is related to habitat space, and suggested that our substrate analysis method may provide a viable means to evaluate space availability in stream benthic habitats.

One of the merits of our substrate method was its simplicity compared to other methods. Our simple photographic technique took very little time in the field, providing data for a large number of profiles with little effort. In contrast, other studies have used a

contour gauge in the field to obtain profile information, either tracing and digitizing the resulting profile (Kotsylev et al. 2005), or photographing the profile (Sanson et al. 1995). Although the use of a contour gauge may provide more accurate estimates of z-values then our use of z-ratios, the larger number of profiles that we obtain through our photographic method may lead to a better description of the overall substrate at a site. Moreover, we found that spatial variation at our sampling site (evidenced as variation among profiles) had a larger effect on our measurement of space availability than the variability in z-ratios.

The method of profile extraction that we used was highly simplified compared to the photogrammetric methods required to obtain digital elevation models from similar photographs (for examples, see Westaway et al. 2001; Carbonneau et al. 2003). We used geometric properties of the particles, including the relationship between z and the longest axis as well as the physical shape of the particles, to estimate habitat space. The simplicity of the profile extraction technique makes it a viable option for other researchers lacking a photogrammetric background. If the relationship between z and the long and short axis is known for particles in a study area, our substrate method could easily be applied. Moreover, the use of this type of profile data provides a better description of habitat space than methods that don't incorporate the spatial arrangement of substrate particles. Our estimated profiles provide information about particle size as well as the size of interstitial spaces, leading to a better estimate of usable habitat space that can be used to test predictions about the relationship between space and body size.

Our description of habitat space allowed us to clearly identify the potential effects of habitat space on body size because we were able to fit organisms to the profiles and

determine how many individuals could potentially utilize the available space. Because we extracted profile coordinates from our sample photos, it would have been possible to have focused our analysis on relating the fractal dimension of the surface to body size. But we felt that the best variable to describe the relationship between body size and habitat space was a direct measurement of available space. The fractal dimension of a surface only provides information about how total space changes with scale. Although it may be useful to provide the total surface length at a particular scale, any information about how that surface is arranged has been lost (Sanson et al. 1995). Our method uses the spatial arrangement of particles in addition to the total surface length to actually attempt to fit organisms to the surface and provide a more accurate assessment of available space. Moreover, our description of space is easily comparable across habitats, and can be used to directly compare space availability at any number of sites.

The results of the analysis of the described method to estimate habitat space suggested several possible patterns in the relationship between space and body size in stream benthic macroinvertebrates. When we examined observed stream size spectra, we found higher normalized biomass in the boulder habitat than in the flat habitat, as was expected based on the habitat analysis. Furthermore, one of the complex habitats showed a decrease in normalized biomass in the large size classes as was expected based on the habitat space analysis. However, the importance of considering other factors was emphasized by size spectrum patterns that did not match our expectations about the effects of space limitations. Overall, the results of our study suggest that our simplified method of measuring available space in stream substrates is a viable technique to assess habitat space.

## References


Bartholomew, A. 2002. Faunal colonization of artificial seagrass plots: the importance of surface area versus space size relative to body size. Estuaries. **25**(5): 1045-1052.

Benke, A.C., Huryn, A.D., Smock, L.A., and Wallace, J.B. 1999. Length-mass relationships for freshwater macroinvertebrates in North America with particular reference to the southeastern United States. J. N. Am. Benthol. Soc. **18**(3): 308-343.

Bergey, E.A., and Getty, G.M. 2006. A review of methods for measuring the surface area of stream substrates. Hydrobiologia. **556**: 7-16.

Bourassa, N., and Morin, A. 1995. Relationships between size structure of invertebrate assemblages and trophy and substrate composition in streams. J. N. Am. Benthol. Soc. **14**(3): 393-403.

Bunte, K., and Abt, S.R. 2001. Sampling surface and subsurface particle-size distributions in wadable gravel- and cobble-bed streams for analyses in sediment transport, hydraulics, and streambed monitoring. Department of Agriculture, Forest Service, Rocky Mountain Research Station. Gen. Tech. Rep. RMRS-GTR-74, Fort Collins, CO, USA.

Butler, J.B., Lane, S.N., Chandler, J.H., and Porfiri, E. 2002. Through-water close range digital photogrammetry in flume and field environments. Photogramm. Rec. **17**(99): 419-439.

Carbonneau, P.E., Lane, S.N., and Bergeron, N.E. 2003. Cost-effective non-metric close-range digital photogrammetry and its application to a study of coarse gravel river beds. Int. J. Remote Sens. **24**(14): 2837-2854.

Downes, B.J., Lake, P.S., Schreiber, E.S.G., and Glaister, A. 1998. Habitat structure and regulation of local species diversity in a stony, upland stream. Ecol. Monogr. **68**(2): 237-257.

Duplisea, D.E., and Drgas, A. 1999. Sensitivity of a benthic, metazoan, biomass size spectrum to differences in sediment granulometry. Mar. Ecol.-Prog. Ser. **177**: 73-81.

Gee, J.M., and Warwick, R.M. 1994. Body-size distribution in a marine metazoan community and the fractal dimensions of macroalgae. J. Exp. Mar. Biol. Ecol. **178**: 247-259.

Gordon, N.D., McMahon, T.A., and Finlayson, B.L. 1992. Stream Hydrology. An Introduction for Ecologists. John Wiley and Sons, Chichester, GB.

Halley, J.M., Hartley, S., Kallimanis, A.S., Kunin, W.E., Lennon, J.J., and Sgardelis, S.P. 2004. Uses and abuses of fractal methodology in ecology. Ecol. Lett. **7**: 254-271.

Holling, C.S. 1992. Cross-scale morphology, geometry, and dynamics in ecosystems. Ecol. Monogr. **62**: 447-502.

Kotsylev, V.E., Erlandsson, J., Ming, M.Y., and Williams, G.A. 2005. The relative importance of haitat comlexity and surface area in assessing biodiversity: fractal application on rocky shores. Ecol. Complex. **2**: 272-286.

Morse, D.R., Lawton, J.H., Dodson, M.M., and Williamson, M.H. 1985. Fractal dimension of vegetation and the distribution of arthropod body lengths. Nature. **314**: 731-733.

Robson, B.J., Chester, E.T., and Barmuta, L.A. 2002. Using fractal geometry to make rapid fiels measurements of riverbed topography at ecologically useful spatial scales. Mar. Freshwater Res. **53**: 999-1003.

Robson, B.J., Barmuta, L.A., and Fairweather, P.G. 2005. Methodological and conceptual issues in the search for a relationship between animal body-size distributions and benthic habitat architecture. Mar. Freshwater Res. **56**: 1-11.

Sanson, G.D., Stolk, R., and Downes, B.J. 1995. A new method for characterizing surface roughness and available space in biological systems. Funct. Ecol. **9**: 127-135.

Schmid, P.E. 2000. Fractal properties of habitat and patch structure in benthic ecosystems. Adv. Ecol. Res. **30**: 339-401.

Sinsabaugh, R.L., Weiland, T., and Linkins, A.E. 1991. Epilithon patch structure in a boreal river. J. N. Am. Benthol. Soc. **10**(4): 419-429.

Solimini, A.G., Benvenuti, A., D'Olimpio, R., Cicco, M.d., and Carchini, G. 2001. Size structure of benthic invertebrate assemblages in a Mediterranean river. J. N. Am. Benthol. Soc. **20**(3): 421-431.

Sugihara, G., and May, R.M. 1990. Applications of fractals in ecology. Trends Ecol. Evol. **5**(3): 79-86.

Taniguchi, H., and Tokeshi, M. 2004. Effects of habitat complexity on benthic assemblages in a variable environment. Freshwater Biol. **49**: 1164-1178.

Weisstein, Eric W. 2010a. Ellipse. From MathWorld - A Wolfram Web Resource. http://mathworld.wolfram.com/Ellipse.html.

Weisstein, Eric W. 2010b. Triangular Pyramid. From Mathworld - A Wolfram web resource. http://mathworld.wolfram.com/TriangularPyramid.html.

Westaway, R.M., Lane, S.N., and Hicks, D.M. 2001. Remote sensing of clear-water, shallow, gravel-bed rivers using digital photogrammetry. Photogramm. Eng. Rem. S. **67**(11): 1271-1281.

Table 4-1. Physical characteristics of the study sites, including the number of photos taken at each site and the number of profiles that were extracted from the photos.

| Site | Abbreviation | Lat (N) | Long (W) | Substrate Type | Number of photos | Number of profiles extracted |
|---|---|---|---|---|---|---|
| Chelsea Stream 2 | C2 | 45.5076 | 75.8129 | Medium-large cobble, boulders | 7 | 31 |
| Chelsea Stream 6 | C6 | 45.4960 | 75.8144 | Gravel, small cobble | 4 | 21 |
| Chelsea Stream 9a | C9a | 45.4953 | 75.7854 | Gravel, small-large cobble | 6 | 30 |
| Chelsea Stream 9b | C9b | 45.4943 | 75.7842 | Flat bedrock | 5 | 25 |

Table 4-2. The mean proportion of the long axis used to calculate z-values for each rock shape, with the sample size (N) and standard deviation around the mean (SD). Means and standard deviations were calculated for small rocks only (range of lengths of the long axis: 55 to 145 mm) and for the combination of small and large rocks (range of lengths of the long axis: 55 to 425 mm).

| | Small rocks | | | Small and large rocks | | |
|---|---|---|---|---|---|---|
| Shape | Mean Proportion of Long Axis | N | SD | Mean Proportion of Long Axis | N | SD |
| Rectangular | 0.391 | 37 | 0.106 | 0.374 | 46 | 0.112 |
| Cubic | 0.702 | 22 | 0.114 | 0.687 | 30 | 0.135 |
| Ellipsoid | 0.510 | 16 | 0.100 | 0.511 | 25 | 0.105 |
| Pyramid | 0.627 | 9 | 0.113 | 0.626 | 12 | 0.115 |

Table 4-3. The change in $R^2$ and residual mean square (RMS) values for the normalized size spectrum for each site when a second order regression model is fitted to the data instead of a first order model. The first order model was $\log_{10}$ (normalized biomass) = $a$ + $b$ ($\log_{10}$ mass), and the second order model was $\log_{10}$ (normalized biomass) = $a + b$ ($\log_{10}$ mass) + $c$ ($\log_{10}$ mass)$^2$, where $a$ was the intercept and $b$ and $c$ were coefficients describing the slope.

| | $R^2$ | | | RMS | | |
|---|---|---|---|---|---|---|
| Site | 1st order model | 2nd order model | Increase | 1st order model | 2nd order model | Decrease |
| C9b (flat) | 0.891 | 0.900 | 0.009 | 0.085 | 0.086 | -0.001 |
| C2 (boulder) | 0.901 | 0.940 | 0.039 | 0.126 | 0.080 | 0.046 |
| C9a (mixed) | 0.750 | 0.864 | 0.114 | 0.152 | 0.089 | 0.063 |
| C6 (gravel) | 0.423 | 0.757 | 0.334 | 0.138 | 0.063 | 0.075 |

**Figure captions**

Figure 4-1. Diagram of measurements and angles used to calculate z-values for (a) ellipse-shaped rocks and (b) pyramid-shaped rocks.

Figure 4-2. Examples of substrate photos (with measured profiles drawn in white) and plots of the extracted profiles for (a) site C2, (b) site C9a, and (c) site C6. Profile axes units are mm.

Figure 4-3. A comparison of the average maximum possible density distributions (±SE) for the 5 flexibility levels at each site, with substrate complexity indicated on each plot.

Figure 4-4. A comparison of the average maximum possible density distribution for each site, with substrate complexity indicated.

Figure 4-5. A comparison of (a) the maximum possible normalized biomass distribution and (b) the observed normalized biomass distribution for each site. Observed normalized biomass were calculated per $m^2$ while maximum possible normalized biomass (calculated from the substrate analysis) were per m.

a)

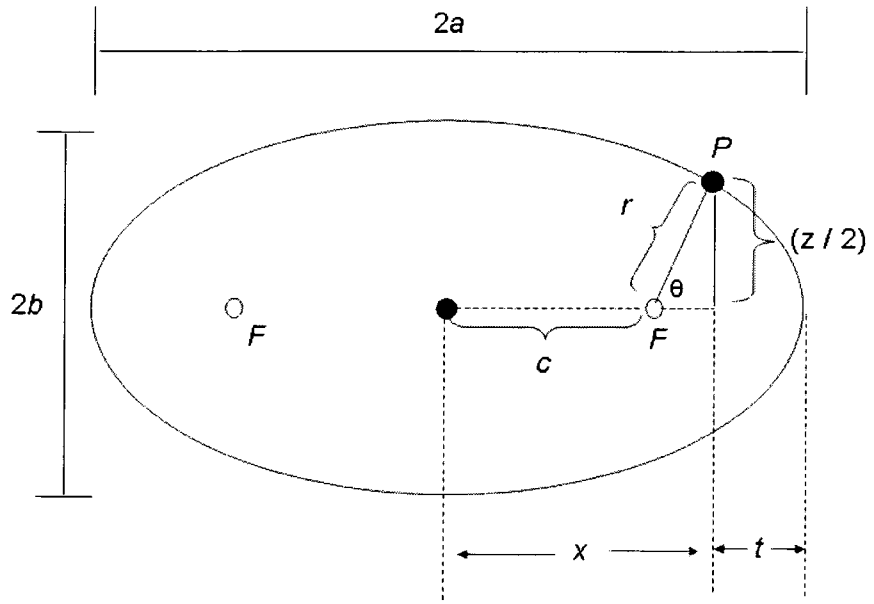
2a
2b
P
r
(z / 2)
θ
F
F
c
x
t

b)

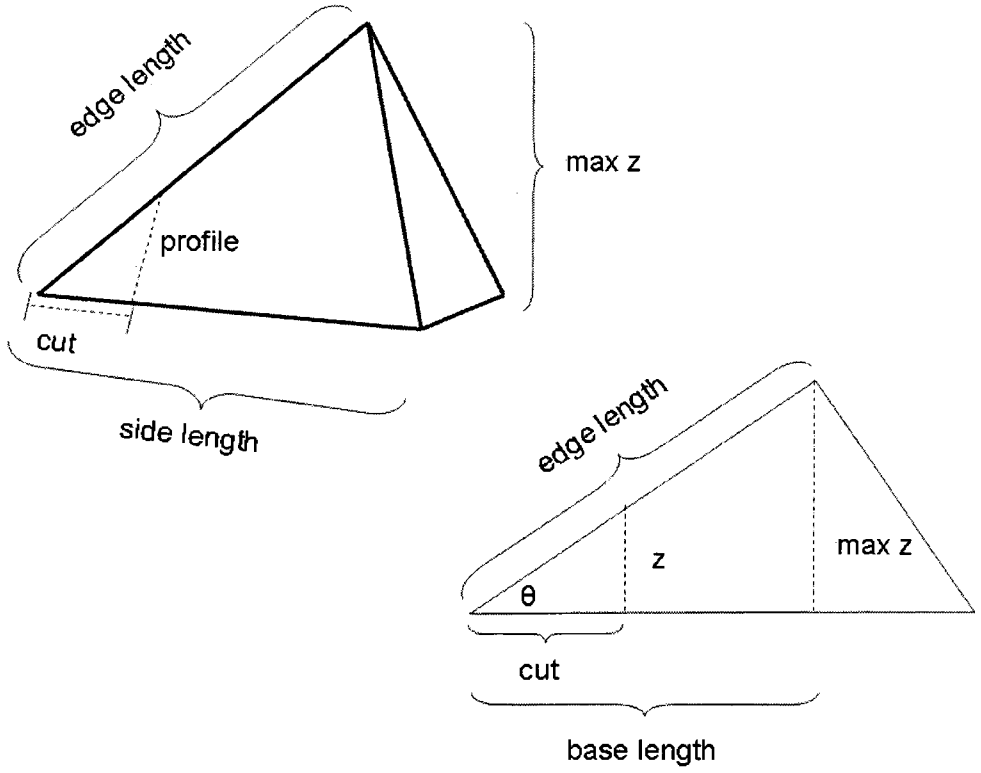
edge length
max z
profile
cut
side length
edge length
z
max z
θ
cut
base length

Figure 4-1

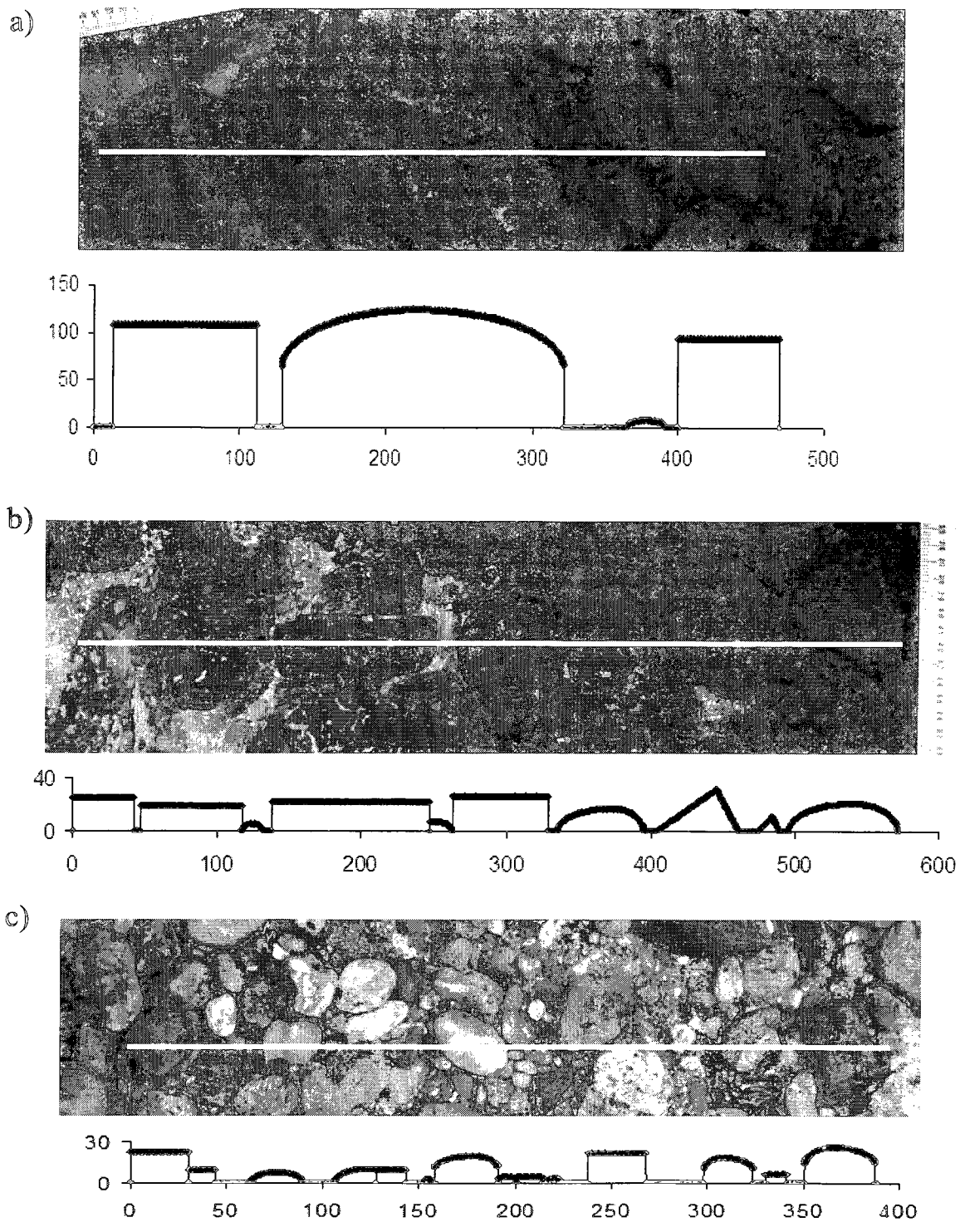
a)
150
100
50
0
0
100
200
300
400
500
b)
40
0
0
100
200
300
400
500
600
c)
30
0
0
50
100
150
200
250
300
350
400

Figure 4-2

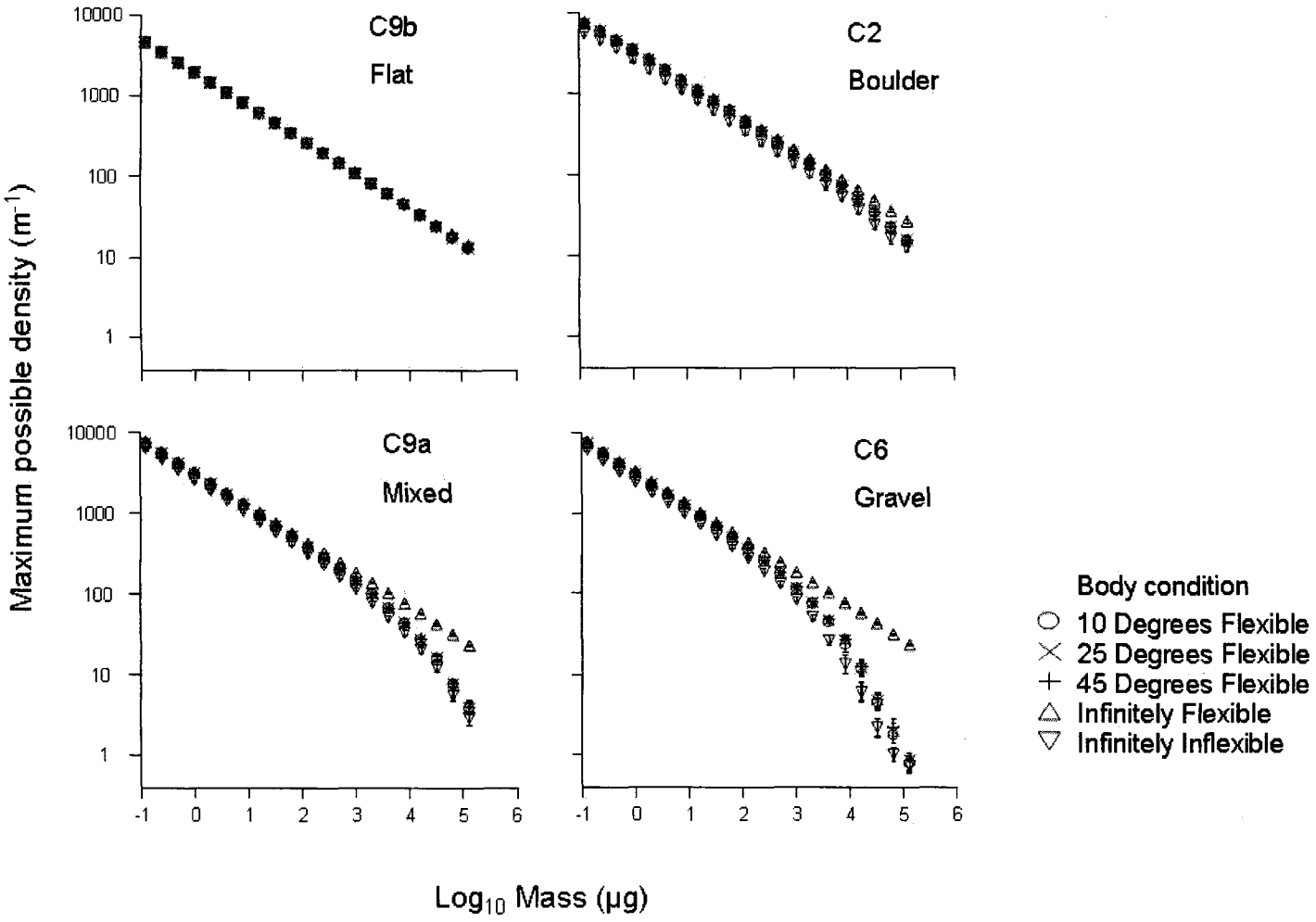
C9b
Flat
C2
Boulder
C9a
Mixed
C6
Gravel
Maximum possible density ($m^{-1}$)
$Log_{10}$ Mass (µg)
Body condition
10 Degrees Flexible
25 Degrees Flexible
45 Degrees Flexible
Infinitely Flexible
Infinitely Inflexible

Figure 4-3

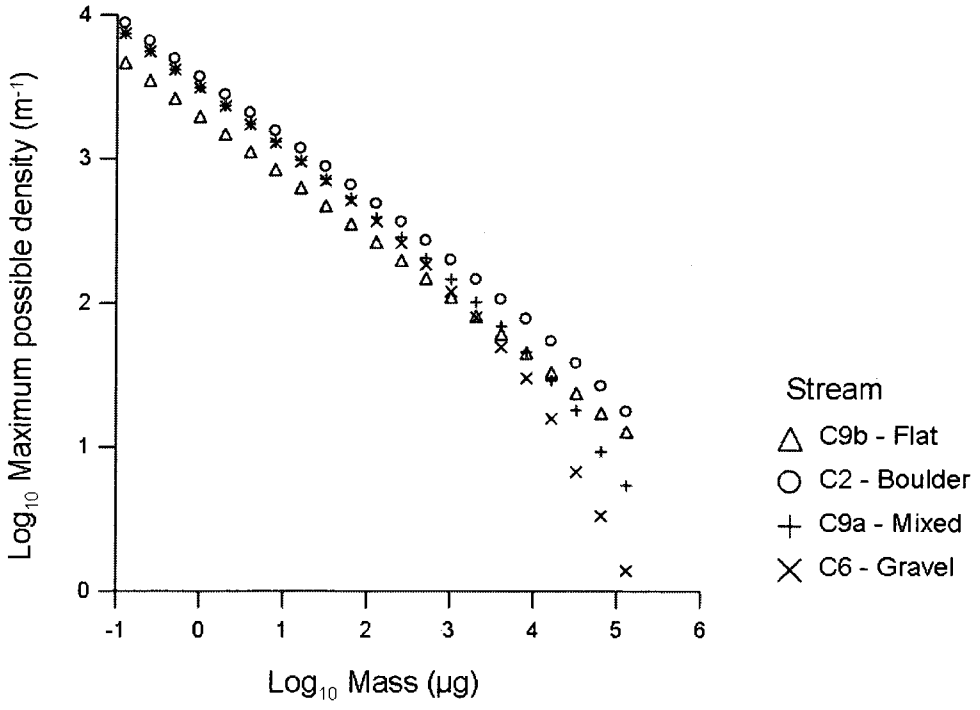
Log10 Maximum possible density (m-1)
Log10 Mass (µg)
Stream
C9b - Flat
C2 - Boulder
C9a - Mixed
C6 - Gravel

Figure 4-4

a)

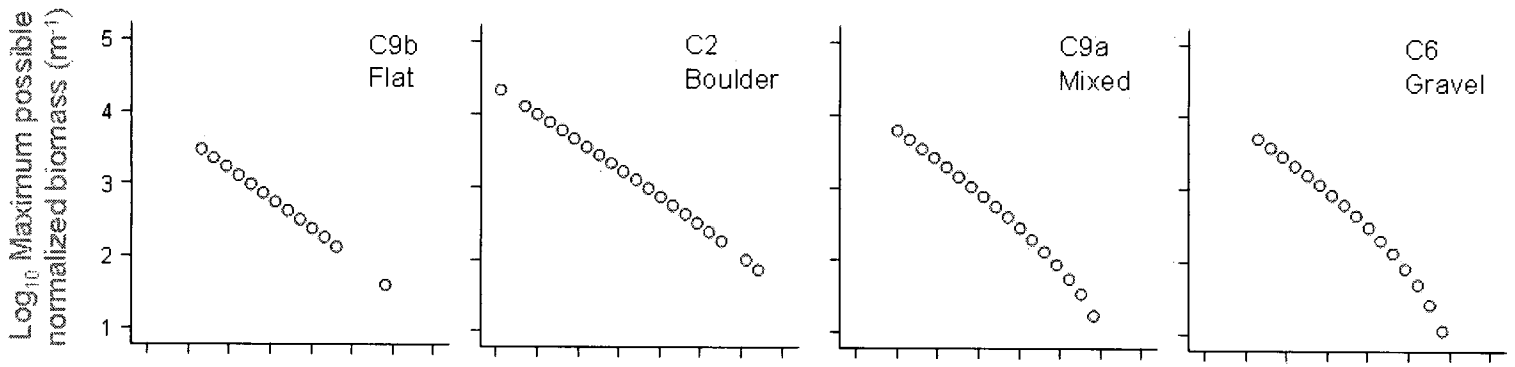
Log10 Maximum possible normalized biomass (m-1)
C9b Flat
C2 Boulder
C9a Mixed
C6 Gravel

b)

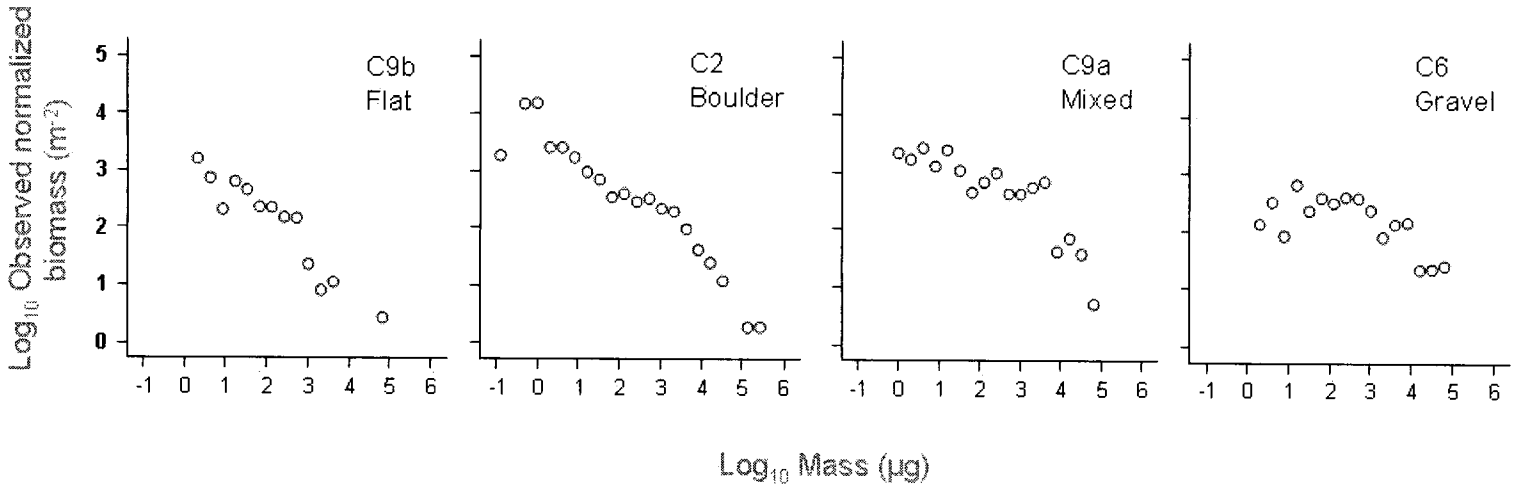
Log10 Observed normalized biomass (m-2)
C9b Flat
C2 Boulder
C9a Mixed
C6 Gravel
Log10 Mass (µg)

Figure 4-5

# Chapter 5 - The Effects of Energy and Space Availability on Lotic Size Distributions

## Introduction

Several functional and structural properties of organisms and assemblages scale with body size in a predictable manner (Peters 1983; Kerr and Dickie 2001; Woodward et al. 2005). In particular, the relationship between normalized biomass of aquatic individuals and body size has been shown to be highly stable across a range of environmental conditions (Morin and Nadon 1991; Cattaneo 1993; Bourassa and Morin 1995; Kerr and Dickie 2001; Solimini et al. 2001; White et al. 2007; Chapter 4). Body size distributions display log-linear negative slopes which indicate higher normalized biomass of small organisms than large. Though attempts have been made to explain these patterns, their cause is still a subject of debate (Kerr and Dickie 2001; Allen et al. 2006; Maxwell and Jennings 2006). Two main hypotheses have been proposed to explain the shape of size distributions: one hypothesis based on energy availability, and the other on space availability.

The hypothesis of energetic constraints on body size distributions stems from the inefficient transfer of energy between trophic levels (Jennings and Mackinson 2003). If trophic level increases with mass, large organisms (as predators) have less energy per unit habitat than small organisms because only a fraction of the energy available as food to small organisms (their prey) can be consumed, assimilated, and converted into consumable biomass (Jennings and Mackinson 2003; Dinmore and Jennings 2004; Maxwell and Jennings 2006). This constraint on energy availability may lead to decreased abundance of large organisms, resulting in the size distribution patterns that have been widely observed. This theory provides a mechanistic explanation for the shape of size distributions that potentially applies to both aquatic and terrestrial organisms.

If trophic level increases with size, an organism's trophic position can be used as an estimate of energy availability because of the inefficient transfer of energy between trophic levels (Maxwell and Jennings 2006). Trophic level has been shown to increase with body size in marine (Fry and Quiñones 1994) and lentic (France et al. 1998) communities. But a recent study of trophic structure in lotic communities found some evidence that trophic level may not increase with size in macroinvertebrates (Anderson and Cabana 2009), while Maxwell and Jennings (2006) found a decrease in trophic level with size in marine infaunal invertebrates. Moreover, the hypothesis of energy limitation due to trophic position has not been explicitly tested in stream communities.

The second hypothesis that has been suggested to explain the shape of size distributions is a habitat hypothesis that states that space availability shapes size distributions (Morse et al. 1985; Sugihara and May 1990; Sinsabaugh et al. 1991; Gee and Warwick 1994). Since small organisms can occupy small crevices or interstitial spaces that larger organisms cannot access, there should be an inverse relationship between the size of an organism and the amount of area it perceives (Kozlowski and Gawelczyk 2002). There is more space available to small organisms, therefore there should be more small than large organisms (Kozlowski and Gawelczyk 2002). However, there have been mixed results in studies of the habitat hypothesis, largely due to differences in methodology (Robson et al. 2005) and indirect measurements of habitat space (Chapter 4). Furthermore, studies of the effects of habitat space on benthic macroinvertebrates have excluded larger organisms such as crayfish. Habitat complexity has been shown to influence crayfish abundance in streams (Lodge and Hill 1994), and may be particularly important for small crayfish (Olsson and Nyström 2009).

The energetic hypothesis predicts a decline of density with increasing trophic level because of the inefficient transfer of energy between trophic levels. The habitat hypothesis states that the density of organisms per size class is proportional to the space available for organisms of that size. The purpose of this research was to simultaneously test both hypotheses for size distributions of stream organisms. To test the hypothesis of energy availability, we used stable nitrogen isotopes to estimate the average trophic position per size class of stream organisms. Stable nitrogen isotope analysis has become a common method to determine trophic linkages within a community (for examples, see Cabana and Rasmussen 1996; France et al 1998; Anderson and Cabana 2009) because there is an enrichment of nitrogen isotope signatures ($\delta^{15}N$) with an increase in trophic position (Jardine et al. 2003). Stable isotopes provide a more integrated estimate of an organism's trophic position than gut content analysis because nitrogen signatures reflect food that has been assimilated over a long period of time (Pinnegar and Polunin 1999; Jardine et al. 2003). To test the habitat hypothesis, habitat space was estimated for each size class by fitting organisms to substrate profiles extracted from digital photographs of the stream substrate.

**Methods**

*Study area*

Samples were collected from 17 sites in 6 streams in eastern Ontario and western Québec in Canada (see Table 5-1 for site details). The streams were sampled during the summer of 2006, with the exception of Brassil's creek and Chelsea Stream 9a and 9b, which were sampled during the summer of 2007. The streams were all small, with a maximum width of 10 m, and were selected to cover a range of nutrient levels (Table 5-

1). Sites were selected within the streams to represent different levels of habitat complexity. The least complex substrates were composed of flat bedrock or concrete. More complex substrates were composed of combinations of sand, gravel, cobble, and boulder (Table 5-1). Periphyton biomass varied, with no visible periphyton at some sites and large mats of filamentous algae at others; average chlorophyll *a* concentrations ranged from 0.36 mg/m$^2$ to 286.2 mg/m$^2$ (Table 5-1).

*Size spectra*

Field and laboratory methods

To properly estimate densities of organisms over the full range of substrates and organism sizes, we used four different sampling methods (cobble collection, Hess sampling, electrobugging, and kick sampling) to collect benthic macroinvertebrates. For the cobble method, six replicate cobbles (approximate diameter ranging from 55 to 145 mm) were collected at random from each stream site and placed in bags with 95% ethanol. Six Hess samples were collected at sites without cobbles (flat sites; Table 5-1) and placed in jars with 95% ethanol. At stream sites where cobble was not the dominant substrate type, 3-6 replicate Hess samples were collected (in addition to the cobble samples). In order to increase our sampling efforts for large macroinvertebrates, we used a modified version of the depletion electrobugging technique described by Taylor et al. (2001). In combination with kick sampling, electrobugging was found to collect additional taxa and size classes of large invertebrates that were not captured by the cobble method (Chapter 2). To electrobug, we used a Smith-Root LR-24 backpack electroshocker upstream of a stationary D-net (1 mm mesh), over triplicate areas of 30 x 60 cm. A 15 cm (diameter) anode was used instead of the standard 28 cm anode in order

to create a more concentrated pulse. We moved the anode through the sampling area for 30 seconds without disturbing the substrate, inducing drift by shocking the invertebrates in the area. The cathode was placed immediately downstream under the opening of the D-net to create an electrical gradient and direct drifting organisms into the net. After the 30 second sampling period, all organisms were removed from the net and placed in jars with 95% ethanol. This was repeated 3-5 times until attrition was noted. Immediately following electrobugging, 2-3 kick samples (each lasting 30 seconds) were taken at the electrobugging locations until attrition was noted. Kick sampling was performed in order to collect the attached taxa (such as case-making Trichoptera) that were not efficiently collected by electrobugging (Chapter 2). All invertebrate samples (from the cobble method, Hess sampler, electrobugging, and kick sampling) were returned to the laboratory for processing.

Fish and crayfish were collected from a 10 m length of stream by depletion electroshocking with a standard 28 cm (diameter) anode. Seine nets were set up immediately upstream and downstream of the 10 m sampling area to block immigration and emigration of fish and crayfish. Each electroshocking pass was completed by moving through the sampling area from upstream to downstream while shocking and collecting fish and crayfish with dip nets. After each pass, we measured the collected fish and crayfish, identified them to species level, and returned them downstream of the sampling area. At each site, we completed 3-5 passes of electroshocking until 50% attrition was noted in both the fish and crayfish.

In the laboratory, cobbles were brushed over a 1 mm sieve, and organisms retained on the sieve were identified. Hess samples were also rinsed over a 1 mm sieve to

collect and identify any retained organisms. Electrobugging and kick samples were not sieved in the lab prior to identification because the D-net mesh used in the field was 1 mm. When samples contained more than 200 individuals or large amounts of algae or debris (which often occurred in the case of kick samples), a Folsom plankton splitter was used to split samples. All invertebrate samples were identified to the level of family for insects and order or higher for non-insects. We measured the body length of each individual to the nearest 0.01 mm using an image analysis system (Optimas 6.5 Imaging Software; Media Cybernetics, Silver Springs, Maryland). Dry mass (in μg) was estimated from body lengths by using taxon-specific length-mass regressions from Benke et al. (1999). When there was no length-mass relationship information for a taxonomic group, dry mass (DM) was calculated as body length (L) cubed (DM [μg] = $L^3$ [$mm^3$]).

For the cobble and Hess samples, the number of organisms that were lost through the 1 mm sieve was predicted by using sieve retention probability models. We used the overall (not taxon-specific) model of Gruenert et al. (2007) that incorporated chlorophyll *a* concentrations to predict the number of organisms in the cobble samples lost by sieving. For the Hess samples, which rarely included algal biomass, we used the overall sieve retention probability model of Morin et al. (2004) which did not incorporate chlorophyll *a*. The suitability of the sieve retention models to estimate organism counts for the electrobugging and kick samples was tested in Chapter 2. The sieve retention probability model of Morin et al. (2004) predicted the number of individuals lost through the D-net for all body lengths above 4 mm long within 6%, but under- or over-estimated counts for individuals below 4 mm in length by more than 15% (Chapter 2). The sieve retention probability models were therefore applied to electrobugging and kick samples

for all individuals longer than 4 mm, and data for individuals shorter than 4 mm long were disregarded from these samples. We applied the overall sieve retention probability model of Morin et al. (2004) to the electrobugging data because this sampling method did not dislodge algae, and applied the retention model of Gruenert et al. (2007) to the kick sampling data because this collection method did dislodge algae.

Spectrum calculation

Invertebrates collected in the cobble and Hess samples were grouped into $\log_2$ size classes based on dry mass (μg), and the total mass of individuals was summed for each taxon-size class combination. For the Hess samples, this mass value was divided by the area of the sampler (0.036 $m^2$) to provide estimates of biomass in $\mu g/m^2$ of stream area. For each cobble, the total mass of individuals in each taxon-size class combination was divided by the area of the cobble (see Chapter 3) to provide estimates of biomass in $\mu g/m^2$ of cobble area. In order to combine the cobble results with those from the other sampling methods, we estimated the cobble surface area per $m^2$ of stream substrate covered with cobble to express biomass and density per unit stream area. For both the Hess and cobble samples, the biomass in each taxon-size class combination was averaged across the number of replicate samples to provide average biomass estimates for each stream site on cobble and non-cobble substrates. We used a weighted average to combine the biomass estimates from the cobble and Hess samples, weighting the cobble estimates by the proportion of cobble habitat and weighting the Hess estimates by the proportion of non-cobble habitat in each site.

Similar to the cobble and Hess samples, invertebrates collected in electrobugging and kick samples were grouped into $\log_2$ size classes based on dry mass (μg). Because the

depletion method was used to estimate density from electrobugging and kick samples, it was necessary to estimate the population size at each site based on the number of individuals collected and the depletion in invertebrate counts with each additional pass. To create these estimates, we entered total counts of each taxon-size class combination into MicroFish 3.0 (Van Deventer 1989), a program for estimating population size from electroshocking depletion data by using maximum-likelihood estimates. Kick sampling occurred after the electrobugging passes and over the same sampling area, and was primarily intended to collect any organisms missed by electrobugging. Therefore, because kick sampling potentially sampled a different portion of the population (including any organisms that were not induced to enter the drift by electroshocking), we combined the data for kick sampling and electrobugging in different ways depending on the number of individuals caught by each sampling method. Initially, electrobugging and kick sampling data were run separately through MicroFish for each site. We used the electrobugging estimates for all taxon-size class combinations that were only captured by that method, and similarly used the kick sample estimates for those that were only collected by kick sampling. For taxon-size class combinations that were collected by both sampling methods, we treated the kick sampling passes as additional electrobugging passes, essentially adding 2-3 more passes to the electrobugging data. We then ran those numbers through MicroFish to get estimates from the combined passes. When there was a non-descending removal pattern in the data, suggesting that kick sampling collected more individuals of that taxon-size class combination, we did not treat the kick sampling data as additional electrobugging passes. In those cases, kick sampling was more effective than electrobugging and collected individuals that did not enter the drift during

electroshocking. For those taxon-size class combinations, we added the original electrobugging counts (without MicroFish population estimates) to the population estimates we obtained from the kick sampling data to get total counts for the stream site.

The output from MicroFish was an estimated count for each taxon-size class combination based on the pass data. The population estimates from electrobugging and kick sampling data and the combination of the two were joined together for all taxon-size class combinations at each site. Resulting counts were multiplied by the average dry mass of each taxon-size class combination (using sampling location-specific values) and divided by the area of the sampling location (0.18 $m^2$) to generate biomass values in $\mu g/m^2$ stream area. These values were averaged across the triplicates to provide average biomass estimates for electrobugging and kick samples for each stream site.

Biomass estimates for all invertebrates less than 4 mm long were obtained from Hess and cobble samples. For invertebrates longer than 4 mm, we used the estimate either from cobble/Hess or electrobugging/kick depending on which gave the highest biomass for each taxon-size class combination that was collected at the sample sites. Once the data had been combined for all sampling methods, we summed the biomass in each size class across taxa to obtain biomass values for creating the size spectra.

Crayfish and fish data were run through MicroFish to obtain population estimates from the pass depletion data. Crayfish dry mass (in μg) was estimated from carapace length by using the average Decapoda length-mass regression from Benke et al. (1999). Crayfish were grouped into $\log_2$ size classes based on their dry mass. Population estimates from MicroFish were obtained by entering counts for each taxon-size class combination. Resulting estimated counts were multiplied by the average dry mass of the

taxon-size class combination (using site-specific averages) and divided by the stream area ($m^2$) sampled at each site to calculate biomass estimates. The biomass in each size class was summed across taxa to obtain biomass values for creating the size spectra.

Fish wet mass (in μg) was estimated from total length or standard length using species-specific length-mass regressions from Randall and Minns (2000) and Schneider et al. (2000). In order to convert wet mass to dry mass, we found examples in the literature of the relationship between wet mass and dry mass for a range of fish species; the average relationship for species similar to those we collected was dry mass = 0.25 * wet mass (Berry et al. 1982; Whicker et al. 1990; Lantry and O'Gorman 2007). Fish were grouped into $\log_2$ size classes based on their dry mass, and population estimates from MicroFish were obtained by entering counts for each taxon-size class combination. The resulting estimated counts were multiplied by the average dry mass of the taxon-size class combination (using site-specific averages) and divided by the stream area ($m^2$) sampled at each site to calculate biomass estimates. The biomass in each size class was summed across taxa to obtain biomass values for creating the size spectra.

Normalized biomass values were calculated for invertebrates, crayfish, and fish by dividing the biomass concentration ($\mu g/m^2$) in each size class by the width of that size class (i.e., for $\log_2$ size class intervals, the width of a size class is the lower limit of the size class interval). Data for invertebrates, crayfish, and fish were combined, and normalized biomass values were summed for any overlapping size classes. Normalized biomass size spectra were plotted for each site as the $\log_{10}$ normalized biomass against the $\log_{10}$ body size (the upper biomass limit of the size class in μg).

*Trophic data*

Sampling and laboratory methods

Stable N isotope ($\delta^{15}N$) composition of biomass was used to determine relative trophic position for biofilm and each size class of macroinvertebrates, crayfish, and fish. At each site, 3 cobbles were selected at random from within the 10 m sampling area. Biofilm scrapes were taken from each rock with a scalpel, and the material scraped from each rock replicate was placed in a vial with water from the stream. For invertebrate samples, a minimum of three cobbles was collected and placed in sample bags with water, and a minimum of three Hess samples was collected and placed in sample jars with water at each site for stable isotope analysis. Electrobugging and kick sampling were used at several locations throughout the 10 m sampling area in order to collect additional macroinvertebrates for stable isotope analysis. Electrobugging and kick samples were placed in sample jars filled with water. For both biofilm and macroinvertebrate samples, efforts were made to maximize biomass collection in order to meet minimum sample weight requirements for stable isotope analysis. All samples were returned to the lab and frozen.

As fish and crayfish samples were identified and measured in the field between electroshocking passes, we selected individuals to retain for stable isotope analysis based on taxon and size. We used a conversion chart in the field to estimate each individual's $\log_2$ size class based on total or standard length for fish and carapace length for crayfish. We retained two individuals of each species-size class combination when possible (more than two individuals for the smallest size classes, to ensure sufficient biomass was collected). Crayfish and fish samples were returned to the laboratory and frozen.

In the lab, samples were thawed for sorting, identification, and dissection. Biofilm samples were sorted under a dissecting microscope in order to remove any invertebrates that might have been trapped within the algae, potentially affecting stable isotope results. Invertebrate sample processing proceeded in a similar manner as for the size spectra. Cobbles were scrubbed gently over a 63 μm sieve to remove all invertebrates, and cobble, Hess, electrobugging, and kick samples were identified to the level of family for insects and order or higher for non-insects. The body length of each individual was measured to the nearest 0.01 mm using an image analysis system. After an individual's length was measured, it was placed in a vial based on its $\log_2$ size class (determined using taxon-specific length-mass regressions). Organisms were grouped in vials on the basis of size class, regardless of taxon. Crayfish and fish were dissected to obtain muscle for stable isotope analysis. Abdominal muscle was cut from crayfish and dorsal muscle was cut from fish. When fish or crayfish were too small to dissect, the entire organism was used for the stable isotope sample.

All samples (biofilm, invertebrates, crayfish, and fish) were placed in a drying oven at 60°C for at least 24 hours, until samples were dried and no longer changed weight over time. Samples were ground into a homogeneous powder. Fish samples were combined by size class (regardless of taxon) similar to invertebrate samples in order to reduce sample size. Submission material was weighed out to obtain approximately 0.1 mg of nitrogen in each sample; required sample weights were based on the % N in each type of organism. Average % N values from previous samples taken in these streams were used to determine sample weight requirements: biofilm was on average 0.74% N (requiring 13.5 mg of material for submission), macroinvertebrates and crayfish were on

average 11.05% N (requiring 0.9 mg of material), and fish were on average 14.85% N (requiring ~0.7 mg of material). All samples were submitted to the G.G. Hatch Stable Isotope Laboratory at the University of Ottawa for stable isotope analysis using continuous flow isotope ratio mass spectrometry. Samples and standards were weighed into tin capsules, then passed through a CE 1110 Elemental Analyser for combustion followed by a Thermo Finnigan DeltaPlus Advantage isotope ratio mass spectrometer (IRMS) coupled with a ConFlo III interface for isotopic analysis. The $^{15}N$ composition of the samples was expressed in delta notation as $\delta^{15}N$: the $^{15}N/^{14}N$ in the sample relative to $^{15}N/^{14}N$ in air.

When $\delta^{15}N$ results were compared for each group of organisms, the standard deviation for replicate samples of fish was 0.11‰, and for replicate samples of crayfish the standard deviation was 0.07‰. Because it was difficult to obtain sufficient weights of macroinvertebrate material for many of the small size classes, we ran a group of samples at half-weights (~0.05 mg N and half the normal weight for each standard), and a group of samples at a five-fold decrease in weight that were analyzed by using modified tubing (with samples weighed to contain ~0.02 mg N and a five-fold decrease in the normal weight for each standard). To evaluate the effect of varying sample weights on $\delta^{15}N$ results, we ran duplicates of 6 invertebrate samples as full-weight, half-weight, and five-fold decreased weight. The standard deviation of $\delta^{15}N$ for the full-weight samples was 0.28‰, for the full and half-weight samples together was 0.27‰, and for the full and five-fold decreased weight samples together was 0.32‰.

Although the biofilm samples were intended to provide baseline data to scale the remaining $\delta^{15}N$ results, we found that the biofilm $\delta^{15}N$ was highly elevated in several of

the samples, and was actually higher than $\delta^{15}N$ values for invertebrates and even fish in some sites. The $\delta^{15}N$ in the biofilm was highly correlated with water column nitrate/nitrite concentrations ($r = 0.72$ when one outlier (site LMS, which had much lower $\delta^{15}N$ values than all other sites) was excluded), suggesting that the N enrichment in the biofilm might have been due to uptake from the water column. However, the fact that the biofilm $\delta^{15}N$ was higher than many of the consumer $\delta^{15}N$ values indicated that it may not have been a food source for consumers, and shouldn't be used as a baseline value. Because we were more interested in examining the change in $\delta^{15}N$ with increasing body size at a site rather than comparing trophic levels among sites, we suspected that the use of a baseline correction level would be unnecessary for our analyses. We ran our analyses with all $\delta^{15}N$ data unaltered, adjusted by subtracting the average $\delta^{15}N$ of the 3 smallest size classes of invertebrates, and adjusted by subtracting the overall average $\delta^{15}N$ of all sizes, to see if the choice of baseline (or lack of baseline in the case of the unaltered data) affected our results. The same results were obtained with all three sets of data, and we therefore left the data unaltered for subsequent analyses.

*Substrate data*

Sampling methods

At each sampling site, we took through-water digital photos in multiple locations that were representative of the dominant substrate composition. In order to control reflections and flatten the water surface, we floated a viewing box on the water above the photo location. This box was constructed with plywood sides and a 3 mm thick perspex base through which the stream substrate could be viewed and photographed. The thin layer of perspex has been recommended to reduce refraction and approximate a more

simplified air/water interface at the water surface (Butler et al. 2002). A tripod was placed in the water just downstream of the photo location and clamps on the tripod legs were used to hold the viewing box in place. A Nikon D200 digital camera on a ball head was attached to the tripod center column that was held parallel to the water surface. The camera was rotated until the lens was parallel to the substrate, and a bubble level was used to ensure that the photos were not taken at an angle. To allow the photos to be scaled in later processing, a thin metal ruler was placed on the substrate within the frame of the photo. To control glare and block sky reflections on the perspex, we held a 3 m by 3 m piece of heavy black photographer's cloth above the camera and photo location while the photos were snapped.

The number of photos per stream site differed depending on the depth and water clarity of each site. The water was too shallow for photos to be taken in a location if rocks broke the water surface, because the glare could not be controlled in such cases. There was also a maximum depth at which photos could be taken, as the camera was set up on a tripod in the stream to stabilize the equipment. The maximum allowable depth of the water decreased in high turbidity, because in deeper depths the substrate was not visible in the photos. The substrate area photographed in each location differed depending on the height of the camera (which varied with water depth); the maximum length of substrate included in each photo ranged between approximately 50 and 70 cm. We were unable to take photos at four sites (BEC, BECb, LDS, and LDSb) because the turbidity levels were too high for the substrate to be visible. For each, we chose another site with a morphologically similar substrate and used the profile data from that site to predict space. Both BECb and LDSb had flat substrate, and profiles from BRA1 were

used for those sites. BEC was most similar to BRA2, while LDS was most similar to DT1 in terms of substrate composition.

Estimating z-values

In order to extract profile data from the photos, we needed a way to estimate the height of each particle (the z-value) from the aerial view of the substrate. We measured a range of small – large particles from our study sites. On each particle, we measured the height (z-value) and the length of perpendicular axes (longest axis and perpendicular short axis) across the particle when viewed from above. The longest axis was defined as perpendicular to the short axis as defined in Gordon et al. (1992), and not necessarily as the longest distance between two points on the particle. Although many previous studies assumed that all particles had one particular shape (most commonly spherical for ease of calculation, as reviewed by Bergey and Getty 2006), the particles that we measured had 4 general shapes evident: ellipsoid, rectangular, cubic, and triangular pyramid. Because these shapes appeared to influence the relationship between z and the long and short axes, we made separate measurements for each particle shape and determined relationships with z separately for each. Ellipsoid, cubic, and pyramid particles generally had a z-value that was similar to the length of the short perpendicular axis. Rectangular particles were generally broken rock or shale, and had a z-value that was much shorter than the length of the short axis. For each particle shape, z was best described by an average proportion of the long axis (ranging from 0.37 to 0.69), with standard deviations ranging from 0.10 to 0.14. We tested whether the variance around the z-ratios affected our results by conducting Monte Carlo simulations (Chapter 4). The results of our analysis suggested

that the variance around our z-ratios did not have a significant effect our estimates of habitat space (Chapter 4).

Extracting profiles

Image analysis software was used to make measurements on the substrate photos (Image-Pro Plus v6.0; Media Cybernetics, Bethesda, Maryland). Within the program, each photo was initially calibrated by setting up a measurement scale that was based on the number of pixels per 20 mm length in the photo (as measured by the ruler that was on the substrate in all photos). Once the photo was calibrated, 1-6 straight lines were drawn across the photo to represent the profiles along which particles were to be measured. The lines were selected at random, but were drawn parallel to each other in order to avoid duplicate measurements within the same substrate area. The length of the profile lines was limited by the particles present along the edges of each photo; a particle towards the edge of the photo was only included as part of the profile if enough of the longest axis was visible to allow z-values to be estimated. Profiles were also limited to areas of the photograph where the substrate particles were clearly visible.

Measurements were made on each particle that the profile line crossed, excluding particles < 5 mm in diameter, which were generally too small to be clearly measured in the photos. Lengths along the profiles that were composed of bedrock, sand, or particles < 5 mm in diameter were treated as flat habitat, and were measured and assigned a z-value of 0. To estimate the remaining z-values, each particle along the profile was assigned a shape (cubic, rectangular, ellipsoid, or pyramid), and was described as partially buried or fully emerged from any underlying sand. In order to minimize variability in z-values caused by different users describing the substrata as different

shapes, all measurements, and therefore all decisions about particle shape, were completed by one researcher (J.L.).

A different set of measurements was required for each particle depending on its shape, orientation, and placement across the profile. For all particles, the long axis was measured in order to estimate the maximum z-value. The length of the particle crossed by the horizontal profile was also measured on all particles regardless of shape. No additional measurements were required for cubic or rectangular particles because of the simplicity of their profile shapes. However, several more measurements were required for ellipsoid and pyramid particles. The z-value for each of these shapes had the potential to differ from the maximum z-value for the particle if the profile crossed it close to its edge rather than at the center (or the apex, in the case of a pyramid). Geometric relationships for ellipses (Weisstein 2010a) and pyramids (Weisstein 2010b) were used to obtain the actual z-value for each particle. When the profile cut across an ellipsoid particle in a non-lengthwise direction away from the center (and therefore maximum z-value), a new z-value was calculated by using the distance from the edge of the particle to the point where the profile cut across and applying principles of ellipse geometry to determine the new maximum z-value (Chapter 4). When a profile cut across a pyramid anywhere other than the apex, the new z-value was calculated using the side and edge lengths of the pyramid and using triangle geometry to estimate the new maximum z-value (Chapter 4).

We created a Visual Basic program to automatically extract (x,z) coordinates along the length of each profile. The program moved along the x-axis of each profile in increments of 0.1 mm, calculating a z-value for each x-value. The z-value remained at 0 for the entire length of flat substrates. When a cubic or rectangular particle was

encountered, the program set z equal to the calculated max z-value (or half of the calculated max z-value if the particle was buried) for the entire length that the profile crossed the particle, and subsequently set z equal to zero before moving on to the next particle. When an ellipsoid particle was encountered, the z-value for each x-value was estimated to create a curved profile by using principles of ellipse geometry as before (Chapter 4). When the ellipse was not buried, ((max z) / 2) was added to each calculated z-value. Although this resulted in straight sides for the lower half of the particle, the majority of ellipsoid particles encountered at our sites had a rounded upper surface and straight sides. Triangle geometry was used to calculate the change in z for each x-value for the initial increasing and subsequent decreasing portions of profiles of pyramid-shaped particles (Chapter 4). No alterations were made to z when a pyramid-shaped particle was buried, because the long axis appeared shorter in such cases, resulting in a smaller maximum z-value. When all particles had been encountered, the output from the program was a series of (x,z) coordinates that covered the range of the entire horizontal profile.

Estimating habitat space

The profile coordinates were used to quantify habitat space for organisms by predicting the maximum number of individuals of each body size that could fit along the profile end-to-end if all the available habitat space was utilized, and using those predictions to quantify the amount of habitable space along each profile. The number of organisms that could fit along a profile was calculated for the range of $\log_2$ size classes (calculated as $\log_2$(dry mass in μg)) that was observed in the benthic macroinvertebrate communities in our study streams (the range differed depending on the site, but the

overall range covered size classes -3 to 18, corresponding to 0.125 to 265000 μg dry mass). The site-specific maximum body length for each size class was used to fit organisms to the profiles. Maximum body length was estimated by averaging the length-mass regressions described by Benke et al. (1999), weighting the taxon-specific regression coefficients by the proportion of the total biomass in the stream samples that was contributed by each taxon.

We compared the effects of fitting benthic macroinvertebrates to the profiles under different levels of body "flexibility." Organisms were fit under two extreme conditions (infinitely flexible and infinitely inflexible) and three intermediate conditions (10, 25, and 45 degrees flexible) by measuring the change in angle of the substrate surface across x-values (Chapter 4). We compared the densities predicted for each size class under the different levels of flexibility, and found that although the infinitely flexible rule fit much higher densities of large organisms to the profiles than the other rules, the infinitely inflexible rule only differed from the intermediate flexibility levels in the most complex habitats (Chapter 4). Moreover, the densities fit to the profiles did not appear to differ among the intermediate flexibility levels for any size classes or levels of habitat complexity, suggesting that 10, 25, or 45 degrees flexibility could be used with no difference in predicted space. We chose to complete all future analyses with the 45 degree flexibility level for macroinvertebrates. For macroinvertebrates, space was quantified for each size class by first multiplying the number of organisms fit along the profile by the body length of the organisms in order to calculate the length of habitat that could be used by individuals in that size class. This length was then standardized by

dividing by the horizontal length of the profile. Finally, we squared the term in order to calculated the estimated maximum habitable area.

Crayfish and fish were not believed to use the habitat in the same manner as macroinvertebrates, and different methods were used to fit individuals to the profiles. Observations of crayfish in streams suggested that they tended to straddle substrates smaller than their body size, rather than being limited to particles longer than their maximum body length. Initially, we used the macroinvertebrate model with 45 degree flexibility to obtain a crayfish distribution for comparison. We then designed a separate program to fit crayfish to the habitat space by assuming that they could straddle multiple particles as long as the difference in z-values between the particles did not exceed a maximum limit. We estimated the number of crayfish that could fit along a profile by using two different limits for the range in z-values: the maximum body width and the maximum carapace length for each size class. The maximum habitable area was calculated from the number of organisms fit to the profiles by each of the three substrate methods as it was for macroinvertebrates.

Although some fish species at our stream sites were benthic, the majority of species were not. While these non-benthic fish species fed within the benthic habitat, they were not expected to be affected by space availability in the same way as macroinvertebrates or crayfish because they did not inhabit the substrates. However, we fit fish to the substrate profiles using three different methods to represent their use of the habitat space. The first two methods assumed that fish would be able to make use of the entire horizontal length of the profile by floating just above the substrate (and would therefore not be limited by small habitat spaces). Fish were fit along the profile by first

dividing the horizontal length of the profile by the maximum total body length for each size class, and then by dividing the horizontal length of the profile by the maximum body depth (vertical height from ventral to dorsal) for each size class because many species of fish were expected to turn their bodies perpendicular to the substrate in order to feed off of it. The third method used to fit fish to the profile was similar to the substrate straddling method used for crayfish, with fish body depth fit to habitat space whenever the range of z-values in that space was less than the body depth length. Individuals in each size class were fit to the profiles using each of the three methods, and the maximum habitable area was calculated as it was for the crayfish and macroinvertebrates.

*Statistical Analysis*

A linear regression was calculated for each size spectrum to describe the general trend in the relationship between body size and normalized biomass. Each linear regression was of the form $(\log_{10}D) = a + b\ (\log_{10}M)$, where D was the normalized biomass within a size class, M was the upper limit of the mass (μg) of the size class, $a$ was the intercept, and $b$ was a coefficient describing the slope of the relationship.

For crayfish and fish, we compared the 3 methods used to estimate habitable space in order to determine which provided the best fit to observed normalized biomass. We tested the regression model $\log_{10}$ (normalized biomass) = $\log_{10}$ space separately for each of the three fitting methods. For both fish and crayfish, residual mean square (RMS) values for the models were compared to determine which space estimate provided the best fit to the data. For the crayfish, the RMS was similar for the first and third fitting methods (the macroinvertebrate 45 degrees flexible method, and the straddling method with carapace length as the z range limit; RMS = 0.233). The second method, which

applied the substrate straddling method with a maximum z range equal to body width, provided a slightly better fit to the data (RMS = 0.195). This method was used for subsequent analyses because it provided the best fit to the data. The three substrate models used to predict fish densities had a very weak relationship with the normalized biomass data. The methods that divided the horizontal profile length by total length and body depth provided a better fit to the data than the method that applied the straddling model (horizontal profile divided by total length, RMS = 0.303; horizontal profile divided by body depth, RMS = 0.305; straddling method with body depth as the z range limit, RMS= 0.332). Because the method of dividing the horizontal profile by total length provided a slightly better fit, it was used for subsequent analyses.

In order to test an overall model with all data combined, it was necessary to calculate average values for space and energy availability for size classes that contained more than one group of organisms (e.g., size classes where macroinvertebrates, crayfish, or fish overlapped). We used weighted averages to combine the data in these size classes, weighting the space estimate or $\delta^{15}N$ value for each group (macroinvertebrates, crayfish, or fish) by the proportion of the total biomass in the size class that was contributed by that group of organisms.

The relationship between $\delta^{15}N$ and body size was plotted in order to determine whether the food webs in our study sites were size-structured. We compared the change in average $\delta^{15}N$ as a function of body size across sites by testing the GLM: $\delta^{15}N = a + b$ ($\log_{10}$ mass) + site + $\log_{10}$ mass * site, where the interaction term ($\log_{10}$ mass * site) tested whether the slope of the relationship between $\delta^{15}N$ and body size differed significantly (at $\alpha = 0.05$) among sites. A similar analysis was not performed for space

availability because the relationship between body size and estimated space was shown to differ among sites in Chapter 4.

We plotted $\log_{10}$ normalized biomass as a function of $\log_{10}$ space and as a function of $\delta^{15}N$ to evaluate whether normalized biomass changed predictably with space and energy availability. To examine the combined effects of space and energy availability on the body size spectra, we tested a GLM that included both factors: $\log_{10}$ (normalized biomass) = $a + b$ ($\log_{10}$ space) + $c$ ($\delta^{15}N$) + site. The categorical site term was included in the model to account for site-specific differences in overall abundance. In order to evaluate the individual effect of each variable on the size spectra, we examined the partial $R^2$ for each variable.

**Results**

The normalized biomass size spectra displayed a negative trend that appeared similar among sites (Figure 5-1). The spectrum for Leamy downstream site 2 (LDS2) did appear to differ from the other sites, but this was largely due to a lack of fish and crayfish at that site; the lack of large organisms resulted in a much shallower slope. When linear regressions were calculated for each site, the average slope (± SE) was found to be -0.66 ± 0.03 (Table 5-2). Leamy downstream site 2 was found to have a very shallow slope compared to the other sites (slope = -0.38), while Beckett's creek site b (BECb) was found to have a steeper slope than the other sites (slope = -0.87). The range of slopes excluding those sites was -0.53 to -0.76 (Table 5-2). Analysis of these size distributions in Chapter 3 indicated that slopes were not significantly different among sites when sites LDS2 and BECb were excluded.

The food webs in the study sites were size-structured, with evidence of a positive relationship between size and $\delta^{15}N$ (Figure 5-2). The pattern was remarkably similar among sites (with the exception of site LMS, which displayed a wider range of $\delta^{15}N$ across size classes). This was confirmed when we tested the GLM; when LMS was excluded from the analysis, there was no significant difference in the slope of the relationship between $\delta^{15}N$ and body size among sites ($F_{15,227} = 1.235$, $p = 0.247$). The range of slopes was 0.52 to 1.18 (excluding LMS, which had a slope of 1.98; Table 5-3). The body size range in most sites covered approximately 2 trophic levels (assuming an average fractionation of 3.4‰ between trophic levels; Post 2002).

In most sites, taxa (e.g., macroinvertebrates, crayfish, or fish) that overlapped in body size displayed similar $\delta^{15}N$, which suggested that food choice was more closely related to body size than taxonomic group (Figure 5-3). However, there were clear exceptions to this when fish overlapped in size with invertebrates or crayfish in sites BEC, BECb, RR2, and RR3. In the case of the Becket's Creek sites (BEC and BECb) and Raisin River site 2 (RR2), this may have been an indication that fish were feeding on biofilm while macroinvertebrates and crayfish had a different source of food; the biofilm $\delta^{15}N$ was elevated in these sites, but remained below that of the fish (Figure 5-3).

Space availability declined with increasing body size (Figure 5-4). , The relationship between space and body size showed much stronger deviations from linearity than were evident for the $\delta^{15}N$-size relationship. The largest deviations were in the size range corresponding to the overlap between large macroinvertebrates and small to medium crayfish, both of which had low estimated space availability in complex habitats.

The slope of the relationship between estimated space and body size ranged from -0.50 to -0.04 (Table 5-3).

There was a positive relationship between normalized biomass and estimated space, showing that as the available space for a size class increased, the normalized biomass of organisms in that size class also increased (Figure 5-5). The slopes for the relationship between normalized biomass and space ranged from 0.95 to 11.53 (Table 5-4). In contrast, there was a negative relationship between normalized biomass and $\delta^{15}N$; as the trophic position increased (and available energy therefore decreased), the normalized biomass of organisms within a size class decreased (Figure 5-6). The slopes of the relationship between normalized biomass and $\delta^{15}N$ ranged from -1.18 to -0.38 (Table 5-4); there was a more narrow range of slopes and the relationship was more linear than that observed between normalized biomass and space.

When the overall GLM that included both space and energy availability was tested, there was a significant effect (at $\alpha = 0.05$) of all variables (space $F_{1,253} = 106.0$, $p < 0.001$; $\delta^{15}N$ $F_{1,253} = 295.4$, $p < 0.001$; site $F_{1,253} = 13.9$, $p < 0.001$). The $R^2$ for the full model was 0.779. When partial $R^2$ values were calculated, we found that the site term and $\delta^{15}N$ explained the greatest amount of the variability in normalized biomass (partial $R^2$ = 0.287 and 0.258, respectively), while the space term explained less than half as much variability as $\delta^{15}N$ (space partial $R^2 = 0.093$).

**Discussion**

Our results suggested that both energy availability (measured as $\delta^{15}N$) and space availability affected the normalized biomass of organisms in our study sites, although energy availability explained more of the variation in normalized biomass. These results

are consistent with the suggestion that it is the combined effect of multiple factors that controls size distribution shape. Allen et al. (2006) suggested that if body size distributions are controlled by energetic constraints, it occurs on a large scale with some other factor acting on a smaller scale, citing the differences in distribution shape that occur in differing landscapes. This could be the mechanism in our study area, as very little variation was evident in trophic relationships among sites, whereas differences in space availability were clearly evident among our streams. Kerr and Dickie (2001) suggested that energy availability is the primary force structuring aquatic size distributions, while space availability is responsible for secondary structuring, resulting in deviations from the general pattern among sites. The results of our analysis are consistent with this hypothesis.

This idea of primary and secondary structuring can be related to measurable aspects of the size spectra. The patterns that we observed in the relationships between body size and $\delta^{15}N$ as well as body size and space availability suggest that these two factors may influence different aspects of stream size distributions. There was a strong linear trend evident when $\delta^{15}N$ was plotted as a function of body size, while the patterns in space availability displayed stronger deviations from linearity. Given the stability of the patterns in $\delta^{15}N$ across sites and the high partial $R^2$ for this term in the model, it's possible that energy constraints may affect the general slope of the size spectra, leading to the negative linear relationship that was evident across sites, with higher densities of small organisms because of energy limitations higher in the trophic network. In contrast, space availability spectra were quite variable among sites and substrates. In the more complex habitats, there was a strong curvature to the relationship between space and

body size, particularly in the large macroinvertebrate size classes. This pattern, combined with the weaker effect of space on normalized biomass suggests that space availability may therefore be more responsible for deviations from linearity in the stream size spectra. The size spectrum has been described as multimodal in some benthic habitats (Kerr and Dickie 2001), and this deviation from linearity may reflect habitat space constraints on large size classes of benthic organisms.

The positive relationship between $\delta^{15}N$ and body size at all of our study sites suggested that the food webs were strongly size-structured, as has been noted in previous studies (e.g., Fry and Quiñones 1994; France et al. 1998; Anderson and Cabana 2009; Arim et al. 2010). Moreover, our results confirmed two observations made by France et al. (1998) in their study of the trophic structure of lentic food webs. Firstly, we observed a similar continuum of $\delta^{15}N$ across size classes and taxonomic groups. France et al. (1998) noted that this pattern was in sharp contrast to the idea that there should be discrete trophic levels within a community, instead suggesting that organisms occupy all possible trophic positions and display a more gradual increase in $\delta^{15}N$ with size, a pattern that our results supported. Secondly, we observed a strong similarity in the relationship between $\delta^{15}N$ and body size among our sites, with similar slopes at 16 of the 17 sites. France et al. (1998) noted similar patterns in the relationship between $\delta^{15}N$ and body size even when compared between lentic and coastal communities, and suggested that the stability in this relationship could be due to the strength of the size-structured predation in those communities. Although the slopes of our $\delta^{15}N$-body size relationships were less steep than those found by France et al. (1998), suggesting that our food webs were less

strongly size-structured, our results still indicate a similar dominance of size-structured predation in small streams.

The relationship between $\delta^{15}N$ and body size can be used to make predictions about the slopes that we would expect to see in normalized size spectra that were energy limited. The slope of the relationship between $\delta^{15}N$ and size can be used to estimate the difference in mass between a predator and its prey by assuming enrichment of 3.4‰ per trophic level (Post 2002; Maxwell and Jennings 2006). Using this slope, an estimate of trophic transfer efficiencies, and the exponent of the allometric relationship between metabolism and body size it is possible to predict the change in density that would be expected over the body size range covered by one trophic level. We used the average slope of the relationship between $\delta^{15}N$ and body size in our sites (0.88) to predict normalized spectrum slopes. The change in mass with one trophic level was determined by $\Delta\ \delta^{15}N$ / slope (calculated as 3.4 / 0.88 for our sites). On average, there was a change in mass of $10^{3.88}$ between prey and predators in our streams. Because metabolism scales as $mass^{0.75}$ (Peters 1983), predators consume $(10^{3.88} * mass_{prey})^{0.75}$, or $10^{2.91}$ more than prey due to their size difference. Density can be estimated for a size class by the total available energy divided by the energy that has been consumed by that size class. Assuming a trophic transfer efficiency of 1/10 (Maxwell and Jennings 2006), density for predators should scale as (total energy) / (10 * ($10^{2.91}$ * prey energy consumption)), and therefore predators should have densities that are $10^{3.91}$ lower than those of prey. This translates to a predicted change in $\log_{10}$ normalized biomass of -3.91 with an increase in $\log_{10}$ mass of 3.88 (from prey to predator), or a size spectrum slope of approximately -1.

The patterns observed in our size spectra slopes did not match what would have been expected if normalized biomass was controlled by energy availability alone. The average slope of our stream size spectra (-0.66) was more shallow than the slope of -1 predicted from the relationship between $\delta^{15}N$ and body size. In order to predict a size spectrum slope as shallow as we observed, a change in $\delta^{15}N$ equivalent to one trophic level (3.4 ‰) would have had to occur over a wider size range than in our study sites. These results indicated that although there was a strong correlation between normalized biomass and trophic position, energy availability alone did not control normalized biomass because the relationship between trophic position and body size predicted a steeper size spectrum slope than we observed.

This difference between the predicted and observed size spectrum slopes may have occurred because of problems with the estimation of observed size spectra slopes. The low normalized biomass of small macroinvertebrates contributed to shallow slopes at our sites. When small size classes were excluded from the analysis, regression slopes were found to be steeper; the average size spectrum slope was -0.83, and 7 sites had size spectrum slopes in the range of -1.06 to -0.90. The removal of small size classes brought our observed slopes closer to the slope predicted based on $\delta^{15}N$. Furthermore, our size spectrum slopes may have been more similar to the predicted slope if we had accounted for error in our estimation of body size by evaluating our size spectra using type II regressions. Type II regressions would have provided more accurate estimates of the relationship between normalized density and body size, and would have resulted in steeper slopes that were more in accordance with the slopes predicted by energy availability.

The difference between predicted and observed size spectrum slopes may also have reflected an influence of space availability on normalized biomass. There was a steep relationship between available space and normalized biomass in our streams, consistent with the slopes that would be expected if normalized biomass was space-limited. In the flat habitat, there was the same amount of space available to organisms of all sizes due to the absence of surface complexity, and the relationship between normalized biomass and space was expected to show a vertical distribution. As surface complexity increased, the slope was expected to be greater than 1 if small organisms had more space than large organisms because of the negative scaling of density with body size. The slope was greater than 1 in all but one of our sites, consistent with the fact that small organisms had more habitat space than large organisms (Table 5-3). Although the effect of space availability on normalized biomass was weak, the slopes of the relationship between normalized biomass and space availability were consistent with the habitat hypothesis. Because there was a break in the distribution slope in many sites due to the vertical distribution in the highest densities, we evaluated whether the inclusion of a squared $\log_{10}$ space term would improve the fit of the GLM and the partial $R^2$ for space. However, the improvement to the GLM model was minimal, and the partial $R^2$ for space only increased by 0.02.

The overall weaker effect of space availability on normalized biomass may have been partially due to the weak relationship between fish normalized biomass and predicted space. Because of the three-dimensional nature in which fish use space, it's difficult to predict their relationship with habitat complexity, as evidenced by the weak relationship we observed between estimated space and fish normalized biomass (for the

model $\log_{10}$ (normalized biomass) = $a$ + $b$ ($\log_{10}$ space) + site + ($\log_{10}$ space) * site, using only fish data, $R^2$ = 0.08). In contrast, space explained a large amount of the variation in invertebrate normalized biomass (for the model $\log_{10}$ (normalized biomass) = $a$ + $b$ ($\log_{10}$ space) + site + ($\log_{10}$ space) * site, using only invertebrate data, $R^2$ = 0.81), suggesting that our method was effective at estimating space for that group of organisms. Although the benthic habitat is certainly important for fish in terms of feeding, the complexity of that habitat (and the ability of the fish to access resources within the habitat) may not be as important as other factors in structuring fish size distributions. This is particularly true if fish are not feeding in the benthic habitat, but instead are consuming drifting organisms or material.

In contrast, we believed habitat space to be an important factor for structuring crayfish size distributions because past studies have shown a strong effect of habitat complexity on crayfish abundance (Lodge and Hill 1994; Olsson and Nyström 2009). However, our estimates of space for crayfish provided only a moderate fit to observed normalized biomass (for the model $\log_{10}$ (normalized biomass) = $a$ + $b$ ($\log_{10}$ space) + site + ($\log_{10}$ space) * site, using only crayfish data, $R^2$ = 0.57). Crayfish rely heavily on refuge space, particularly when molting (Lodge and Hill 1994; Olsson and Nyström 2009). But our use of one-dimensional profiles to estimate habitat space would not allow us to differentiate refuge space (protected from predators) from open habitat. Habitat space for crayfish may be better estimated by examining patches of usable habitat and areas of interstitial space, rather than lengths of habitat space as with the other macroinvertebrates.

One of the issues in determining the factors controlling size distribution shape is collinearity between the factors of interest. Although body mass is a strong predictor of normalized biomass, mass was not included in our model because of high collinearity between mass and both space ($r$ = -0.62) and $\delta^{15}N$ ($r$ = -0.61). Although the inclusion of mass in the model would have improved the overall fit, it would have been difficult to disentangle the effects of each of the factors. Space and $\delta^{15}N$ were only weakly correlated ($r$ = -0.34). Although there was a combined effect of space and $\delta^{15}N$ on normalized biomass in our streams, we were still able to evaluate the relative effects of these factors.

Previous research on the relationship between trophic position and body size have assigned organisms to size classes by separating the samples with different-sized sieves (Fry and Quiñones 1994; Anderson and Cabana 2009), or have sampled a subset of organisms to assign body sizes to species groups (France et al. 1998). Those researchers who have measured all organisms prior to stable isotope analysis have focused on marine ecosystems (Jennings et al. 2002) and infaunal communities (Dinmore and Jennings 2004; Maxwell and Jennings 2006). This study is the only one to our knowledge to include a species-independent evaluation of the relationship between $\delta^{15}N$ and body size that was attained by measuring all individuals. Moreover, studies have rarely examined the combined effects of energy and space availability on aquatic size distributions. The merits of our method of habitat space estimation have been noted elsewhere (see Chapter 4). Together, our estimates of energy availability and space availability provide a more complete test of the mechanisms controlling size distributions than has been completed for stream benthic communities.

Kerr and Dickie (2001) suggested that predator-prey interactions are responsible for the primary structuring of size spectra. We found evidence of size-structured food webs in our streams, and there was a significant effect of $\delta^{15}N$ on normalized biomass, suggesting that energy availability controlled size spectra. However, the size distribution slope predicted from the relationship between $\delta^{15}N$ and body size was more steep than we observed at our sites, suggesting that energy availability alone did not control size spectrum slopes. Space availability also explained variability in normalized biomass, albeit to a lesser extent than $\delta^{15}N$, and may have contributed to size spectrum structuring. Slopes of the relationship between normalized density and space availability were similar to patterns that were expected if organisms were space-limited. The deviations from linearity that were evident in our space-size distributions suggested that space may be more responsible for secondary structuring of size spectra. However, further research into the mechanisms controlling secondary structuring would be necessary to confirm this speculation. Our research on the mechanisms controlling the primary linear trend in size spectra suggests that both energy and space availability play a role in shaping stream size spectra.

**References**

Allen, C.R., Garmestani, A.S., Havlicek, T.D., Marquet, P.A., Peterson, G.D., Restrepo, C., Stow, C.A., and Weeks, B.E. 2006. Patterns in body mass distributions: sifting among alternative hypotheses. Ecol. Lett. **9**: 630-643.

Anderson, C., and Cabana, G. 2009. Anthropogenic alterations of lotic food web structure: evidence from the use of nitrogen isotopes. Oikos. **118**: 1929-1939.

Arim, M., Abades, S.R., Laufer, G., Loureiro, M., and Marquet, P.A. 2010. Food web structure and body size: trophic position and resource acquisition. Oikos. **119**: 147-153.

Benke, A.C., Huryn, A.D., Smock, L.A., and Wallace, J.B. 1999. Length-mass relationships for freshwater macroinvertebrates in North America with particular

reference to the southeastern United States. J. N. Am. Benthol. Soc. **18**(3): 308-343.

Bergey, E.A., and Getty, G.M. 2006. A review of methods for measuring the surface area of stream substrates. Hydrobiologia. **556**: 7-16.

Berry, P.F., van der Elst, R.P., Joubert, C.S.W., and Smale, M.J. 1982. Density and biomass of the ichthyofauna of a natal littoral reef. Mar. Ecol.-Prog. Ser. **10**: 49-55.

Bourassa, N., and Morin, A. 1995. Relationships between size structure of invertebrate assemblages and trophy and substrate composition in streams. J. N. Am. Benthol. Soc. **14**(3): 393-403.

Butler, J.B., Lane, S.N., Chandler, J.H., and Porfiri, E. 2002. Through-water close range digital photogrammetry in flume and field environments. Photogramm. Rec. **17**(99): 419-439.

Cabana, G., and J. B. Rasmussen. 1996. Comparison of aquatic food chains using nitrogen isotopes. P. Natl. Acad. Sci. U.S.A. **93:** 10844-10847.

Cattaneo, A. 1993. Size spectra of benthic communities in Laurentian streams. Can. J. Fish. Aquat. Sci. **50**: 2659-2666.

Dinmore, T.A., and Jennings, S. 2004. Predicting abundance-body mass relationships in benthic infaunal communities. Mar. Ecol.-Prog. Ser. **276**: 289-292.

France, R., Chandler, M., and Peters, R.H. 1998. Mapping trophic continua of benthic foodwebs: body size – $\delta^{15}N$ relationships. Mar. Ecol.-Prog. Ser. **174**: 301-306.

Fry, B., and Quiñones, R.B. 1994. Biomass spectra and stable isotope indicators of trophic level in zooplankton of the northwest Atlantic. Mar. Ecol.-Prog. Ser. **112**: 201-204.

Gee, J.M., and Warwick, R.M. 1994. Body-size distribution in a marine metazoan community and the fractal dimensions of macroalgae. J. Exp. Mar. Biol. Ecol. **178**: 247-259.

Gordon, N.D., McMahon, T.A., and Finlayson, B.L. 1992. Stream Hydrology. An Introduction for Ecologists. John Wiley and Sons, Chichester, GB.

Gruenert, U., Carr, G., and Morin, A. 2007. Reducing the cost of benthic sample processing by using sieve retention probability models. Hydrobiologia. **589**: 79-90.

Jardine, T.D., S.A. McGeachy, C.M. Paton, M. Savoie, and R.A. Cunjak. 2003. Stable isotopes in aquatic systems: Sample preparation, analysis, and interpretation. Can. Manuscr. Rep. Fish. Aquat. Sci. No. 2656: 39 p.

Jennings, S., Pinnegar, J.K., Polunin, N.V.C., and Warr, K.J. 2002. Linking size-based and trophic analyses of benthic community structure. Mar. Ecol.-Prog. Ser. **226**: 77-85.

Jennings, S., and Mackinson, S. 2003. Abundance-body mass relationships in size-structured food webs. Ecol. Lett. **6**: 971-974.

Kerr, S.R., and Dickie, L.M. 2001. The biomass spectrum: a predator-prey theory of aquatic production. Columbia University Press, New York.

Kozlowski, J., and Gawelczyk, A.T. 2002. Why are species' body size distributions usually skewed to the right? Funct. Ecol. **16**: 419-432.

Lantry, B.F., and O'Gorman, R. 2007. Drying temperature effects on fish dry mass measurements. J. Great Lakes Res. **33**: 606-616.

Lodge, D.M., and Hill, A.M. 1994. Factors governing species composition, population size, and productivity of cool-water crayfishes. Nordic J. Freshw. Res. **69**: 111-136.

Maxwell, T.A.D., and Jennings, S. 2006. Predicting abundance-body size relationships in functional and taxonomic subsets of food webs. Oecologia. **150**: 282-290.

Morin, A., and Nadon, D. 1991. Size distribution of epilithic lotic invertebrates and implications for communtiy metabolism. J. N. Am. Benthol. Soc. **10**(3): 300-308.

Morin, A., Stephenson, J., and Strike, J. 2004. Sieve retention probabilities of stream benthic invertebrates. J. N. Am. Benthol. Soc. **23**(2): 383-391.

Morse, D.R., Lawton, J.H., Dodson, M.M., and Williamson, M.H. 1985. Fractal dimension of vegetation and the distribution of arthropod body lengths. Nature. **314**: 731-733.

Olsson, K., and Nyström, P. 2009. Non-interactive effects of habitat complexity and adult crayfish on survival and growth of juvenile crayfish (*Pacifastacus leniusculus*). Freshwater Biol. **54**: 35-46.

Peters, R.H. 1983. The Ecological Implications of Body Size. Cambridge University Press, Cambridge.

Pinnegar, J. K., and N. V. C. Polunin. 1999. Differential fractionation of $\delta^{13}C$ and $\delta^{15}N$ among fish tissues: implications for the study of trophic interactions. Funct. Ecol. 13: 225-231

Post, D.M. 2002. Using stable isotopes to estimate trophic position: models, methods and assumptions. Ecology. **83**: 703-718.

Randall, R.G., and Minns, C.K. 2000. Use of fish production per unit biomass ratios for measuring the productive capacity of fish habitats. Can. J. Fish. Aquat. Sci. **57**: 1657-1667.

Robson, B.J., Barmuta, L.A., and Fairweather, P.G. 2005. Methodological and conceptual issues in the search for a relationship between animal body-size distributions and benthic habitat architecture. Mar. Freshwater Res. **56**: 1-11.

Schneider, J.C., Laarman, P.W., and Gowing, H. 2000. Chapter 17: Length-weight relationships. *In* Manual of fisheries survey methods II: with periodic updates. *Edited by* J.C. Schneider. Michigan Department of Natural Resources, Fisheries Special Report 25, Ann Arbor, MI.

Sinsabaugh, R.L., Weiland, T., and Linkins, A.E. 1991. Epilithon patch structure in a boreal river. J. N. Am. Benthol. Soc. **10**(4): 419-429.

Solimini, A.G., Benvenuti, A., D'Olimpio, R., Cicco, M.d., and Carchini, G. 2001. Size structure of benthic invertebrate assemblages in a Mediterranean river. J. N. Am. Benthol. Soc. **20**(3): 421-431.

Sugihara, G., and May, R.M. 1990. Applications of fractals in ecology. Trends Ecol. Evol. **5**(3): 79-86.

Taylor, B.W., McIntosh, A.R., and Peckarsky, B.L. 2001. Sampling stream invertebrates using electroshocking techniques: implications for basic and applied research. Can. J. Fish. Aquat. Sci. **58**: 437-445.

Van Deventer, J.S. 1989. Microcomputer Software System for Generating Population Statistics from Electrofishing Data -- User's Guide for MicroFish 3.0. USDA Forest Service, General Technical Report INT-254.

Weisstein, Eric W. 2010a. Ellipse. From MathWorld - A Wolfram Web Resource. http://mathworld.wolfram.com/Ellipse.html.

Weisstein, Eric W. 2010b. Triangular Pyramid. From Mathworld - A Wolfram web resource. http://mathworld.wolfram.com/TriangularPyramid.html.

Whicker, F.W., Pinder, J.E.I., Bowling, J.W., Alberts, J.J., and Brisbin, I.L.J. 1990. Distribution of long-lived radionuclides in an abandoned reactor colling reservoir. Ecol. Monogr. **60**(4): 471-496.

White, E.P., Ernest, S.K.M., Kerkhoff, A.J., and Enquist, B.J. 2007. Relationships between body size and abundance in ecology. Trends Ecol. Evol. **22**(6): 323-330.

Woodward, G., Ebenman, B., Emmerson, M., Montoya, J.M., Olesen, J.M., Valido, A., and Warren, P.H. 2005. Body size in ecological networks. Trends Ecol. Evol. **20**(7): 402-409.

Table 5-1. Physical, chemical, and biological characteristics of the study sites.

| Site | Abbreviation | Lat (N) | Long (W) | Substrate Type | Average TP (mg/L) | Average TN (mg/L) | Average Chl *a* ($mg/m^2$) |
|---|---|---|---|---|---|---|---|
| Beckett's Creek | BEC | 45.5212 | 75.3589 | Medium-large cobble | 0.12 | 1.55 | 223.18 |
| Beckett's Creek b | BECb | 45.5208 | 75.3584 | Flat shale | 0.12 | 1.55 | 286.20 |
| Brassil's Creek 1 | BRA1 | 44.9855 | 75.8018 | Flat bedrock | 0.02 | 0.71 | 17.32 |
| Brassil's Creek 2 | BRA2 | 44.9850 | 75.8013 | Medium-large cobble, boulders | 0.02 | 0.71 | 18.37 |
| Chelsea Stream 2 | C2 | 45.5076 | 75.8129 | Medium-large cobble, boulders | 0.02 | 0.48 | 9.81 |
| Chelsea Stream 3 | C3 | 45.5020 | 75.8113 | Small-large cobble | 0.04 | 0.54 | 31.95 |
| Chelsea Stream 6 | C6 | 45.4960 | 75.8144 | Gravel, small cobble | 0.07 | 0.59 | 17.52 |
| Chelsea Stream 9a | C9a | 45.4953 | 75.7854 | Gravel, small-large cobble | 0.05 | 0.50 | 11.37 |
| Chelsea Stream 9b | C9b | 45.4943 | 75.7842 | Flat bedrock | 0.05 | 0.50 | 0.36 |
| Des Trembles 1 | DT1 | 45.4290 | 75.7616 | Medium-large cobble | 0.20 | 1.30 | 74.49 |
| Des Trembles 2 | DT2 | 45.4201 | 75.7529 | Small-large cobble | 0.11 | 1.07 | 94.04 |
| Leamy midstream | LMS | 45.4674 | 75.7470 | Small-large cobble | 0.21 | 1.97 | 76.77 |
| Leamy downstream | LDS | 45.4625 | 75.7287 | Medium-large cobble | 0.16 | 1.18 | 96.16 |
| Leamy downstream b | LDSb | 45.4626 | 75.7293 | Flat pavement | 0.16 | 1.18 | 50.38 |
| Leamy downstream 2 | LDS2 | 45.4595 | 75.7323 | Sand, gravel, small cobble | 0.15 | 1.96 | 44.65 |
| Raisin River 2 | RR2 | 45.1867 | 74.8556 | Gravel, small-medium cobble | 0.04 | N/A | 189.76 |
| Raisin River 3 | RR3 | 45.1772 | 74.8338 | Small-large cobble | 0.03 | N/A | 56.38 |

Table 5-2. Intercept, slope, residual mean square (RMS), and $R^2$ value for each of the normalized biomass size spectrum linear regressions. Each linear regression fits the model $\log_{10}D = a + b\ (\log_{10}M)$, where D is normalized biomass, $a$ is the intercept, $b$ is the coefficient describing the slope, and M is the upper limit of mass (in μg) for each size class.

| Site | Intercept | Slope | RMS | $R^2$ |
|---|---|---|---|---|
| BEC | 4.52 | -0.73 | 1.10 | 0.76 |
| BECb | 4.94 | -0.87 | 0.57 | 0.89 |
| BRA1 | 4.01 | -0.71 | 0.39 | 0.85 |
| BRA2 | 4.80 | -0.76 | 0.55 | 0.78 |
| C2 | 3.93 | -0.72 | 0.38 | 0.89 |
| C3 | 3.64 | -0.69 | 0.47 | 0.84 |
| C6 | 3.39 | -0.53 | 0.43 | 0.75 |
| C9a | 4.17 | -0.71 | 0.50 | 0.82 |
| C9b | 3.43 | -0.65 | 0.19 | 0.92 |
| DT1 | 3.58 | -0.60 | 0.51 | 0.80 |
| DT2 | 4.02 | -0.65 | 0.51 | 0.83 |
| LDS | 4.03 | -0.73 | 0.22 | 0.93 |
| LDSb | 2.90 | -0.55 | 0.15 | 0.92 |
| LDS2 | 3.80 | -0.38 | 0.36 | 0.49 |
| LMS | 4.17 | -0.66 | 0.62 | 0.77 |
| RR2 | 4.92 | -0.73 | 0.70 | 0.80 |
| RR3 | 3.71 | -0.62 | 0.50 | 0.81 |

Table 5-3. Intercept, slope, residual mean square (RMS), and $R^2$ value for the linear regression of body size on average $\delta^{15}N$ and estimated space for each stream site. The linear regressions were (average $\delta^{15}N$) = $a + b \log_{10} M$ and $\log_{10}$ (estimated space) = $a + b \log_{10} M$, where $a$ was the intercept, $b$ was the coefficient describing the slope, and M was the upper limit of mass (in μg) for each size class.

| | Average $\delta^{15}N$ | | | | Estimated space | | | |
|---|---|---|---|---|---|---|---|---|
| Site | Intercept | Slope | RMS | $R^2$ | Intercept | Slope | RMS | $R^2$ |
| BEC | 7.63 | 0.82 | 0.72 | 0.78 | 1.13 | -0.21 | 0.02 | 0.88 |
| BECb | 7.66 | 0.82 | 0.31 | 0.89 | 0.11 | -0.04 | 0.01 | 0.45 |
| BRA1 | 2.32 | 0.88 | 1.04 | 0.72 | 0.19 | -0.08 | 0.10 | 0.19 |
| BRA2 | 0.97 | 1.18 | 1.46 | 0.77 | 1.41 | -0.27 | 0.05 | 0.84 |
| C2 | 3.84 | 0.66 | 0.56 | 0.70 | 1.41 | -0.27 | 0.17 | 0.56 |
| C3 | 4.26 | 0.75 | 1.53 | 0.59 | 0.73 | -0.18 | 0.15 | 0.46 |
| C6 | 4.57 | 0.52 | 0.83 | 0.59 | 0.31 | -0.08 | 0.05 | 0.37 |
| C9a | 3.24 | 0.97 | 2.06 | 0.53 | 0.57 | -0.13 | 0.04 | 0.49 |
| C9b | 4.95 | 0.72 | 0.47 | 0.83 | 0.13 | -0.04 | 0.00 | 0.65 |
| DT1 | 5.26 | 0.90 | 0.21 | 0.93 | 1.12 | -0.20 | -0.02 | 0.88 |
| DT2 | 6.04 | 0.75 | 1.37 | 0.61 | 1.00 | -0.24 | 0.12 | 0.65 |
| LDS | 3.27 | 0.96 | 0.59 | 0.86 | 1.83 | -0.44 | 0.39 | 0.66 |
| LDSb | 5.48 | 0.54 | 1.15 | 0.42 | 0.62 | -0.20 | 0.28 | 0.29 |
| LDS2 | 5.42 | 0.60 | 0.54 | 0.30 | 0.91 | -0.50 | 0.00 | 0.99 |
| LMS | -3.24 | 1.98 | 1.62 | 0.86 | 0.60 | -0.12 | 0.00 | 0.96 |
| RR2 | 4.96 | 1.02 | 1.33 | 0.69 | 0.75 | -0.25 | 0.11 | 0.62 |
| RR3 | 6.48 | 0.80 | 1.89 | 0.55 | 0.68 | -0.15 | 0.01 | 0.89 |

Table 5-4. Intercept, slope, residual mean square (RMS), and $R^2$ value for the linear regressions of average $\delta^{15}N$ and estimated space on normalized biomass for each stream site. The linear regressions were $\log_{10}$ (normalized biomass) = $a + b$ (average $\delta^{15}N$) and $\log_{10}$ (normalized biomass) = $a + b \log_{10}$ (estimated space), where $a$ was the intercept and $b$ was the coefficient describing the slope.

| | Average $\delta^{15}N$ | | | | Estimated space | | | |
|---|---|---|---|---|---|---|---|---|
| Site | Intercept | Slope | RMS | $R^2$ | Intercept | Slope | RMS | $R^2$ |
| BEC | 12.22 | -0.95 | 1.77 | 0.62 | 0.41 | 5.08 | 0.19 | 0.96 |
| BECb | 14.49 | -1.18 | 0.36 | 0.92 | 1.98 | 10.59 | 2.64 | 0.39 |
| BRA1 | 5.03 | -0.66 | 0.92 | 0.64 | 1.44 | 2.86 | 1.54 | 0.40 |
| BRA2 | 4.83 | -0.53 | 0.33 | 0.84 | 1.04 | 2.38 | 0.40 | 0.81 |
| C2 | 7.45 | -0.98 | 0.78 | 0.70 | 0.45 | 1.99 | 1.02 | 0.61 |
| C3 | 6.04 | -0.69 | 1.62 | 0.53 | 0.94 | 2.20 | 2.11 | 0.38 |
| C6 | 6.98 | -0.86 | 1.74 | 0.47 | 1.11 | 3.09 | 2.56 | 0.22 |
| C9a | 5.69 | -0.58 | 0.95 | 0.60 | 1.43 | 3.13 | 1.55 | 0.35 |
| C9b | 6.53 | -0.73 | 0.78 | 0.65 | 1.34 | 11.53 | 0.50 | 0.78 |
| DT1 | 9.15 | -0.87 | 0.60 | 0.79 | 0.17 | 3.97 | 0.40 | 0.86 |
| DT2 | 8.10 | -0.72 | 1.07 | 0.63 | 1.50 | 2.39 | 0.96 | 0.67 |
| LDS | 6.65 | -0.76 | 0.60 | 0.80 | 1.10 | 1.37 | 0.90 | 0.70 |
| LDSb | 3.22 | -0.38 | 0.63 | 0.31 | 0.50 | 0.95 | 0.56 | 0.39 |
| LDS2 | 8.30 | -0.76 | 0.49 | 0.47 | 3.81 | 1.98 | 0.29 | 0.69 |
| LMS | 3.85 | -0.47 | 0.43 | 0.86 | 0.61 | 8.12 | 0.51 | 0.83 |
| RR2 | 9.16 | -0.78 | 0.89 | 0.74 | 2.69 | 2.26 | 2.04 | 0.41 |
| RR3 | 7.46 | -0.63 | 1.02 | 0.79 | 1.06 | 4.54 | 0.74 | 0.72 |

**Figure Captions**

Figure 5-1. Normalized biomass size spectra, including data for macroinvertebrates, crayfish, and fish, for 17 stream sites. A linear regression line for each site (solid line) and an average linear regression line (dashed line) are shown on each plot; see Table 5-2 for regression coefficients.

Figure 5-2. The average $\delta^{15}N$ (‰) for each size class (averaged across macroinvertebrates, crayfish, and fish) as a function of body size (μg) for 17 stream sites. A linear regression line is shown on each plot; see Table 5-3 for regression coefficients.

Figure 5-3. The change in $\delta^{15}N$ (‰) with body size (μg) for each group of organisms (macroinvertebrates, crayfish, and fish represented separately) for 17 stream sites. Biofilm was arbitrarily assigned a mass of 1 μg to facilitate its inclusion on the plot.

Figure 5-4. The change in $\log_{10}$ estimated space ($m^2$; averaged across macroinvertebrates, crayfish, and fish) with body size (μg) for 17 stream sites. A linear regression line is shown on each plot; see Table 5-3 for regression coefficients.

Figure 5-5. The relationship between $\log_{10}$ normalized biomass ($m^{-2}$) and $\log_{10}$ estimated space ($m^2$) for 17 stream sites. A linear regression line is shown on each plot; see Table 5-4 for regression coefficients.

Figure 5-6. The relationship between $\log_{10}$ normalized biomass ($m^{-2}$) and the average $\delta^{15}N$ (‰) for 17 stream sites. A linear regression line is shown on each plot; see Table 5-4 for regression coefficients.

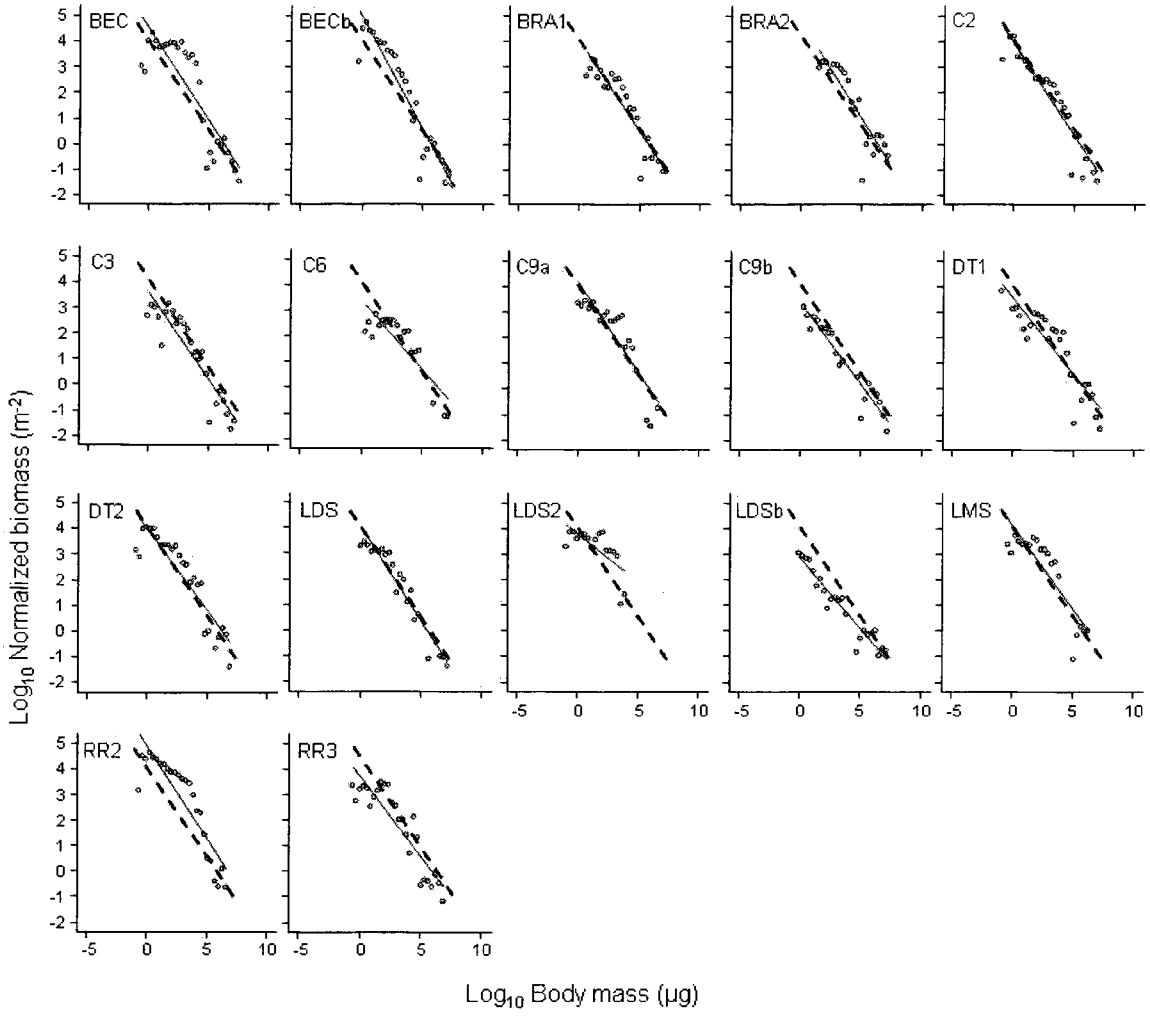
BEC
BECb
BRA1
BRA2
C2
C3
C6
C9a
C9b
DT1
DT2
LDS
LDS2
LDSb
LMS
RR2
RR3
Log10 Normalized biomass (m-2)
Log10 Body mass (µg)

Figure 5-1

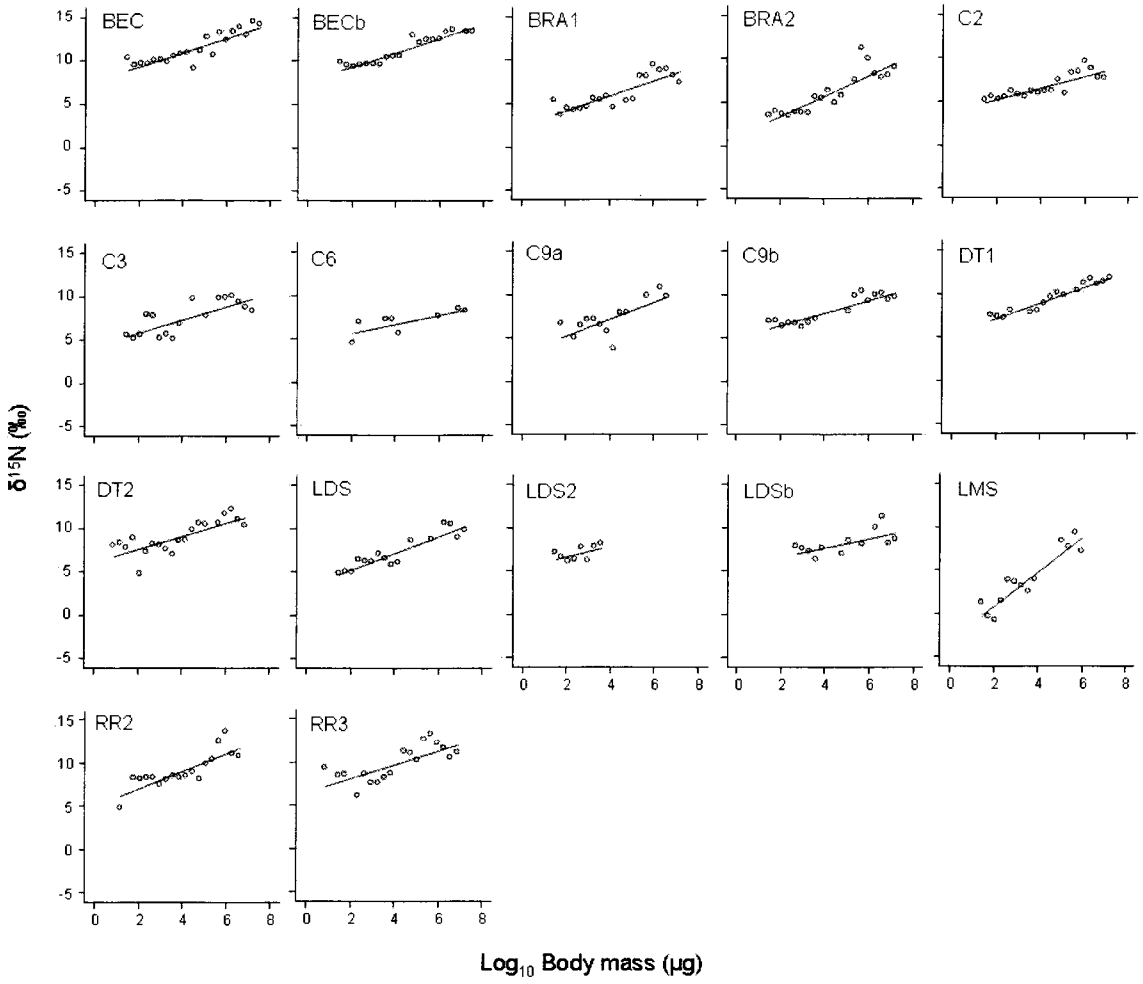
BEC
BECb
BRA1
BRA2
C2
C3
C6
C9a
C9b
DT1
DT2
LDS
LDS2
LDSb
LMS
RR2
RR3
δ15N (‰)
Log10 Body mass (µg)

Figure 5-2

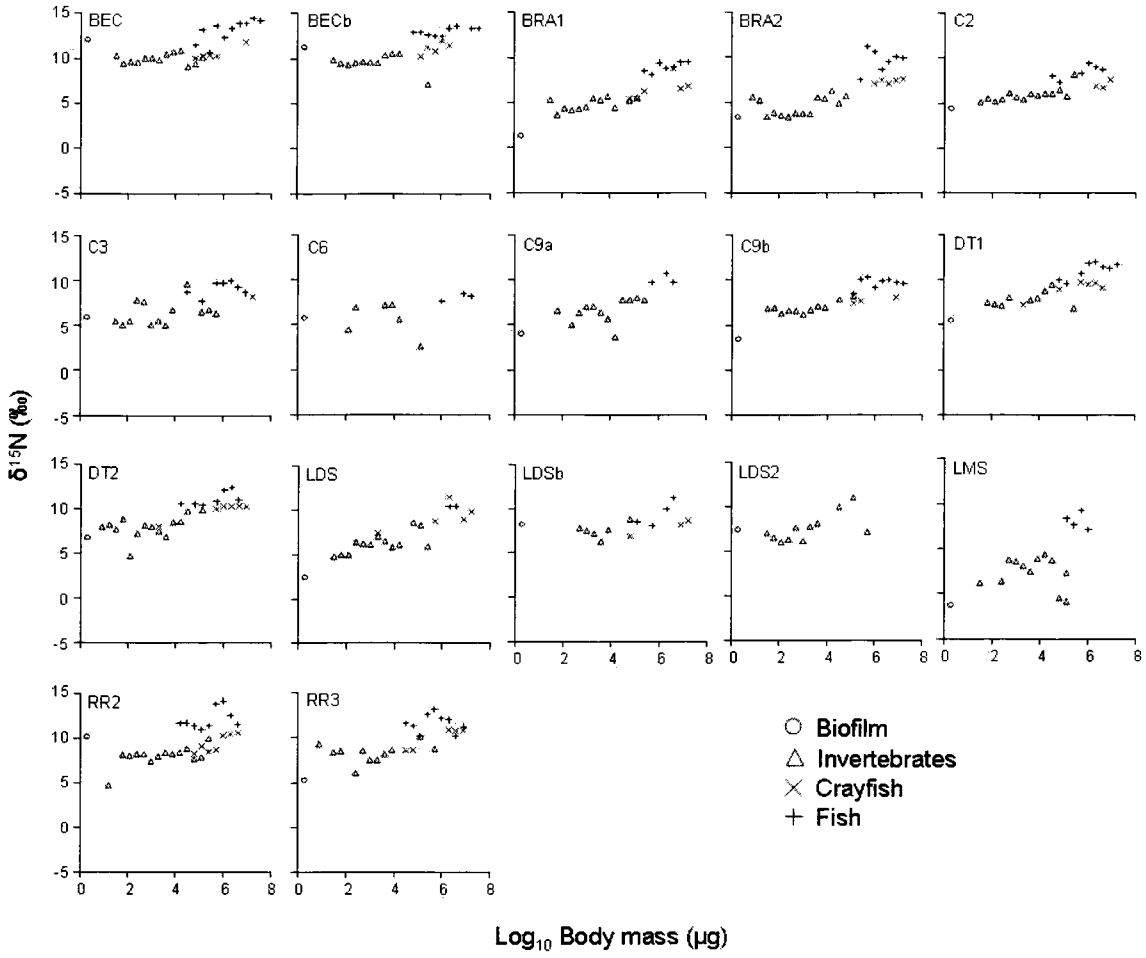
BEC
BECb
BRA1
BRA2
C2
C3
C6
C9a
C9b
DT1
DT2
LDS
LDSb
LDS2
LMS
RR2
RR3
δ15N (‰)
Log10 Body mass (µg)
Biofilm
Invertebrates
Crayfish
Fish

Figure 5-3

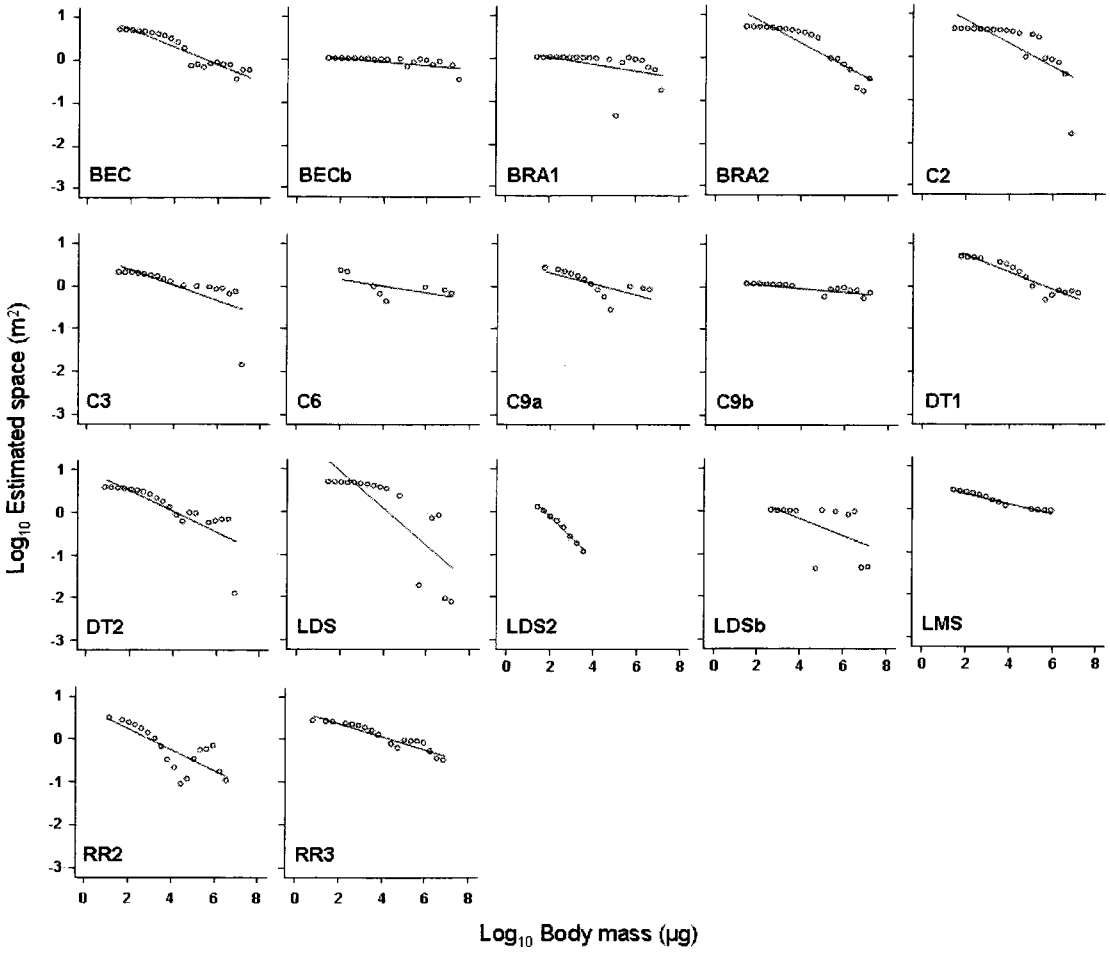
BEC
BECb
BRA1
BRA2
C2
C3
C6
C9a
C9b
DT1
DT2
LDS
LDS2
LDSb
LMS
RR2
RR3
Log10 Estimated space (m2)
Log10 Body mass (µg)

Figure 5-4

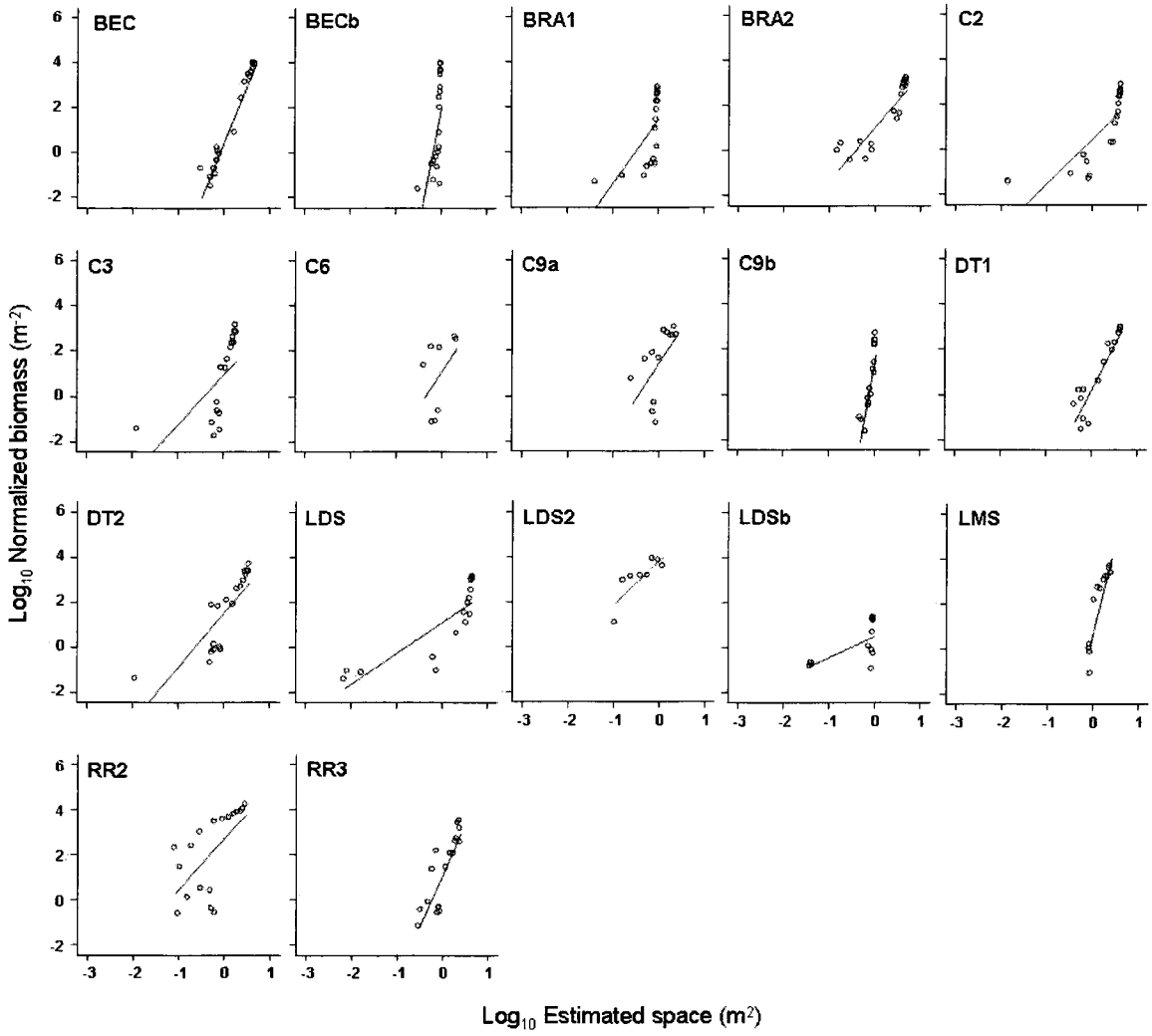
BEC
BECb
BRA1
BRA2
C2
C3
C6
C9a
C9b
DT1
DT2
LDS
LDS2
LDSb
LMS
RR2
RR3
Log10 Normalized biomass (m-2)
Log10 Estimated space (m2)

Figure 5-5

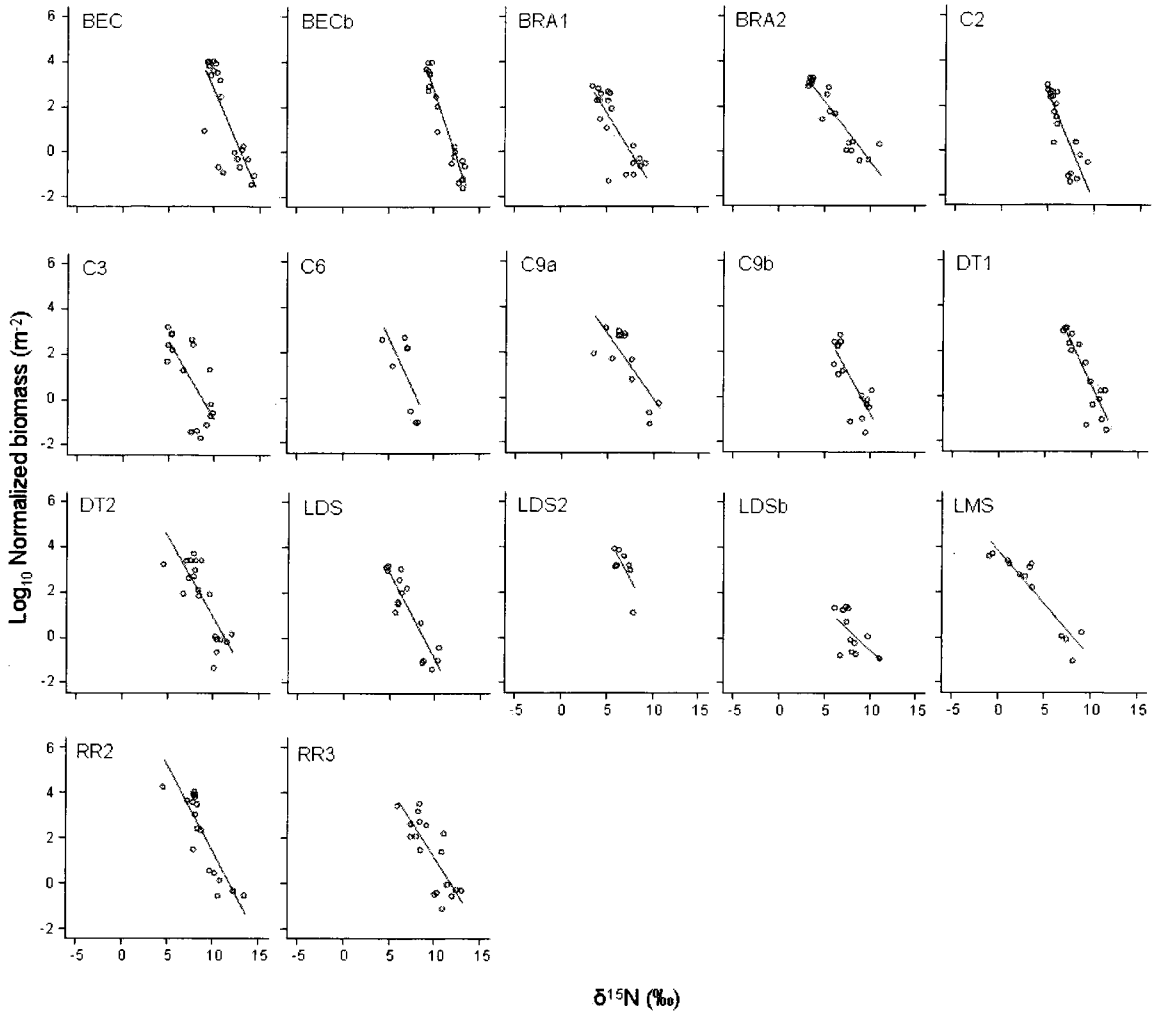
BEC
BECb
BRA1
BRA2
C2
C3
C6
C9a
C9b
DT1
DT2
LDS
LDS2
LDSb
LMS
RR2
RR3
Log10 Normalized biomass (m-2)
δ15N (‰)

Figure 5-6

# Chapter 6 – General Conclusions

This research provides the first description of spatial variability of stream size spectra extending from macroinvertebrates to fish. Previous research on stream size spectra has primarily focused on macroinvertebrates alone or in combination with algae (Morin and Nadon 1991; Cattaneo 1993; Bourassa and Morin 1995; Solimini et al. 2001), with the exception of one study that examined the size spectrum of macroinvertebrates and fish in a single stream (Poff et al. 1993). There was an added emphasis on large organisms in my analysis because of the suggestion that large organisms might contribute more to community biomass than small organisms (Morin and Nadon 1991). Although macroinvertebrate biomass was primarily contributed by medium-sized organisms (body mass range 1 μg to $10^4$ μg), when crayfish and fish were considered, large organisms (body mass larger than $10^4$ μg) were found to contribute the largest proportion of biomass in several streams, while the contribution of small organisms (less than 1 μg) to biomass totals was negligible in all streams. Moreover, production potential was minimal in the small size classes in our streams, in accordance with the suggestion that despite being present at higher densities, small organisms contribute little to the energetics of benthic communities (Morin and Nadon 1991).

Size spectra have been shown to be remarkably stable across a range of environmental conditions, with a strong consistency in size spectrum slope (Bourassa and Morin 1995; Morin et al. 1995; Kerr and Dickie 2001; Solimini et al. 2001; Sprules 2008). This stability was further evident among the sampling sites when I compared expanded size spectra (with macroinvertebrates, crayfish, and fish data). Despite differences in nutrient levels and substrate composition, normalized biomass size spectrum slopes were similar among the sampled stream sites. The consistency of size

spectra patterns not only within the study sites but also across other systems and taxa suggests the effect of a strong underlying mechanism.

Several authors have suggested that a combination of energy and space availability is responsible for structuring size spectra in benthic systems (Kerr and Dickie 2001; Allen et al. 2006). My research represents a rare test of the effects of both factors in stream systems. Energy availability emerged as the stronger factor affecting normalized biomass in these streams; normalized biomass was more strongly correlated with $\delta^{15}N$ than with space. $\delta^{15}N$ increased with size, suggesting that the food webs were size-structured. Because of the inefficient transfer of energy between trophic levels, this increase in $\delta^{15}N$ with size indicated that large organisms had less energy per unit habitat than small organisms. Consequently, normalized biomass declined with increasing $\delta^{15}N$, indicating that normalized biomass in large organisms may have been limited by energy availability. The strength of the linear relationship between these variables suggested that energy availability might be responsible for primary structuring of size spectra, contributing to the negative linear relationship between normalized biomass and body size that indicates lower normalized biomass of large organisms than small. However, the patterns observed in the stream size spectra did not match what would be expected if the normalized biomass in a size class was mediated by energy availability alone. The normalized size spectra slope that was predicted based on the relationship between $\delta^{15}N$ and body size was steeper than the spectrum slopes we observed at our sites.

The discrepancy between predicted and observed size spectrum slopes may have been due in part to an effect of space availability on normalized biomass. Space availability had a weaker effect on normalized biomass, and showed many deviations

from linearity when plotted as a function of body size. However, the slopes of the relationship between normalized density and estimated space were consistent with the patterns that were expected if organisms were limited by habitat space. In flat habitats, distributions were roughly vertical due to the similarity of space estimates for all size classes. As complexity increased, the distribution shifted to reflect an increase in normalized biomass with increasing habitat space, the slope of which was greater than 1, consistent with the observation that large organisms had less available space than small organisms. The results of this analysis supported the habitat hypothesis, but the weaker effect of this factor indicated that it had less of an effect on size spectrum shape than energy availability. Moreover, the variability in the relationship between normalized biomass and space suggested that space availability might influence a different aspects of size spectra. As suggested by Kerr and Dickie (2001), space availability might be more responsible for secondary structuring of size spectra, contributing to the deviations from linearity observed in the relationship between normalized biomass and body size.

The effect of space availability on normalized biomass may have been mediated by the weak relationship between fish normalized biomass and estimated space. The space estimates for macroinvertebrates provided a good fit to normalized biomass data, suggesting that the substrate analysis method worked well to predict space for small benthic organisms. However, despite trying various methods to fit both crayfish and fish to the available habitat space, the fit to the normalized biomass data for both groups of organisms was weaker. This was particularly true for fish, which feed within the benthic habitat, but may be less limited by space availability than purely benthic organisms. Further work to develop a more accurate estimate of space use could benefit the

description of habitat space for crayfish, as these organisms are known to rely on refuge space for protection from predation (Lodge and Hill 1994; Olsson and Nyström 2009). However, habitat space may be less important for fish because of the three dimensional manner in which they perceive space. Estimates of space availability may generally be uncorrelated to fish normalized biomass.

The hypotheses tested here describe mechanisms that may be applicable over a range of habitats and taxa, and it's possible that the results of this analysis could be extrapolated to other systems as well. An effect of energy availability on normalized biomass may be expected in any food web (aquatic or terrestrial) that is size-structured, because the resultant decrease in energy availability for large organisms should give rise to lower normalized biomass. In aquatic systems, similarly size-structured food webs have been noted in lentic (France et al. 1998; Arim et al. 2010) and marine (Fry and Quiñones 1994; Jennings et al. 2001; Jennings et al. 2002) organisms including zooplankton, macroinvertebrates, crayfish, and fish. Moreover, predator-prey interactions have been proposed as the primary factor controlling size spectra in marine pelagic systems (see review in Kerr and Dickie 2001). However, in benthic habitats (whether marine or freshwater), size spectra may be additionally affected by space availability. Although I found a weaker effect of space availability on normalized size spectra, this effect may be perceptible as deviations from the linear relationship between normalized biomass and body size (Kerr and Dickie 2001). If terrestrial systems function similarly to aquatic systems, size distributions of organisms that live on the ground may be controlled by a combination of energy and habitat constraints, as in benthic aquatic systems. Noted differences between aquatic and terrestrial size distributions suggest that energy use may

differ between the two systems (Cyr et al. 1007). However, general similarities in aquatic and terrestrial size distribution patterns support the possibility of similar mechanistic controls in both systems.

This research was the first to compare expanded lotic size spectra and evaluate the effect of adding large macroinvertebrates, crayfish, and fish to body size analyses, and it provides an early test of the hypotheses of energy availability and space availability. To further this research, I described two new methods that can be used to measure and study size spectra: a sampling method (electrobugging) that can be used to increase the accuracy of macroinvertebrate size spectra, and a substrate analysis method that can be used to estimate habitat space for benthic organisms from digital photographs of stream substrates. Overall, the results of this research suggested that in habitats where food webs are size-structured and organisms rely on habitat space for refuge or to access resources, energy availability contributes to the primary structuring of normalized biomass spectra (leading to negative linear slopes) while space availability contributes to secondary structuring of spectra (influencing deviations from linearity).

**References**

Allen, C.R., Garmestani, A.S., Havlicek, T.D., Marquet, P.A., Peterson, G.D., Restrepo, C., Stow, C.A., and Weeks, B.E. 2006. Patterns in body mass distributions: sifting among alternative hypotheses. Ecol. Lett. **9**: 630-643.

Arim, M., Abades, S.R., Laufer, G., Loureiro, M., and Marquet, P.A. 2010. Food web structure and body size: trophic position and resource acquisition. Oikos. **119**: 147-153.

Bourassa, N., and Morin, A. 1995. Relationships between size structure of invertebrate assemblages and trophy and substrate composition in streams. J. N. Am. Benthol. Soc. **14**(3): 393-403.

Cattaneo, A. 1993. Size spectra of benthic communities in Laurentian streams. Can. J. Fish. Aquat. Sci. **50**: 2659-2666.

Cyr, H., R. H. Peters, and J. A. Downing. 1997. Population density and community size structure: comparison of aquatic and terrestrial studies. Oikos **80:** 139-149.

France, R., Chandler, M., and Peters, R.H. 1998. Mapping trophic continua of benthic foodwebs: body size - ä$^{15}$N relationships. Mar. Ecol.-Prog. Ser. **174**: 301-306.

Fry, B., and Quiñones, R.B. 1994. Biomass spectra and stable isotope indicators of trophic level in zooplankton of the northwest Atlantic. Mar. Ecol.-Prog. Ser. **112**: 201-204.

Jennings, S., Pinnegar, J.K., Polunin, N.V.C., and Boon, T.W. 2001. Weak cross-species relationships between body size and trophic level belie powerful size-based trophic structuring in fish communities. J. Anim. Ecol. **70**: 934-944.

Jennings, S., Pinnegar, J.K., Polunin, N.V.C., and Warr, K.J. 2002. Linking size-based and trophic analyses of benthic community structure. Mar. Ecol.-Prog. Ser. **226**: 77-85.

Kerr, S.R., and Dickie, L.M. 2001. The biomass spectrum: a predator-prey theory of aquatic production. Columbia University Press, New York.

Lodge, D.M., and Hill, A.M. 1994. Factors governing species composition, population size, and productivity of cool-water crayfishes. Nordic J. Freshw. Res. **69**: 111-136.

Morin, A., and Nadon, D. 1991. Size distribution of epilithic lotic invertebrates and implications for communtiy metabolism. J. N. Am. Benthol. Soc. **10**(3): 300-308.

Morin, A., Rodríguez, M.A., and Nadon, D. 1995. Temporal and environmental variation in the biomass spectrum of benthic invertebrates in streams: an application of thin-plate splines and relative warp analysis. Can. J. Fish. Aquat. Sci. **52**: 1881-1892.

Olsson, K., and Nyström, P. 2009. Non-interactive effects of habitat complexity and adult crayfish on survival and growth of juvenile crayfish (*Pacifastacus leniusculus*). Freshwater Biol. **54**: 35-46.

Poff, N.L., Palmer, M.A., Angermeier, P.L., Robert L. Vadas, J., Hakenkamp, C.C., Bely, A., Arensburger, P., and Martin, A.P. 1993. Size structure of the metazoan community in a Piedmont stream. Oecologia. **95**: 202-209.

Solimini, A.G., Benvenuti, A., D'Olimpio, R., Cicco, M.d., and Carchini, G. 2001. Size structure of benthic invertebrate assemblages in a Mediterranean river. J. N. Am. Benthol. Soc. **20**(3): 421-431.

Sprules, W.G. 2008. Ecological change in Great Lake communities - a matter of perspective. Can. J. Fish. Aquat. Sci. **65**: 1-9.

# Appendix A – Raw Data

Table 1 – Electrobugging retention test results, showing initial and second counts for each body length (mm) for each replicate cobble sample

| Replicate | Body length | Initial count | Second count |
|---|---|---|---|
| 1 | 0.7 | 7 | 1 |
| 1 | 2 | 52 | 3 |
| 1 | 3 | 39 | 11 |
| 1 | 4 | 15 | 8 |
| 1 | 5 | 5 | 5 |
| 1 | 6 | 4 | 3 |
| 1 | 8 | 1 | 1 |
| 2 | 0.9 | 4 | 1 |
| 2 | 2 | 33 | 1 |
| 2 | 3 | 25 | 7 |
| 2 | 4 | 13 | 3 |
| 2 | 5 | 4 | 4 |
| 2 | 6 | 1 | 1 |
| 2 | 9 | 1 | 1 |
| 3 | 0.6 | 4 | 1 |
| 3 | 0.7 | 7 | 1 |
| 3 | 0.9 | 14 | 2 |
| 3 | 2 | 132 | 17 |
| 3 | 3 | 102 | 31 |
| 3 | 4 | 45 | 26 |
| 3 | 5 | 16 | 16 |
| 3 | 6 | 15 | 15 |
| 3 | 7 | 3 | 3 |
| 3 | 8 | 2 | 2 |
| 3 | 10 | 1 | 1 |
| 3 | 11 | 1 | 1 |
| 3 | 12 | 1 | 1 |
| 4 | 0.6 | 1 | 1 |
| 4 | 2 | 81 | 2 |
| 4 | 3 | 52 | 10 |
| 4 | 4 | 16 | 9 |
| 4 | 5 | 5 | 4 |
| 4 | 6 | 5 | 3 |
| 4 | 7 | 1 | 1 |
| 4 | 9 | 1 | 1 |

| Replicate | Body length | Initial count | Second count |
|---|---|---|---|
| 5 | 0.6 | 1 | 1 |
| 5 | 1 | 10 | 1 |
| 5 | 2 | 132 | 7 |
| 5 | 3 | 73 | 25 |
| 5 | 4 | 39 | 31 |
| 5 | 5 | 14 | 9 |
| 5 | 6 | 5 | 5 |
| 5 | 7 | 3 | 3 |
| 5 | 8 | 2 | 2 |
| 5 | 9 | 1 | 1 |
| 6 | 0.8 | 6 | 1 |
| 6 | 1 | 14 | 1 |
| 6 | 2 | 85 | 4 |
| 6 | 3 | 46 | 15 |
| 6 | 4 | 25 | 18 |
| 6 | 5 | 6 | 4 |
| 6 | 6 | 8 | 7 |
| 6 | 7 | 4 | 4 |
| 6 | 8 | 1 | 1 |

Table 2 – The total biomass (BM) collected by each sampling method (cobble, electrobugging, and kick sampling) at each site, with chlorophyll *a* (chla) data (only including biomass for organisms with body length > 4mm).

| Method | Stream | Chla ($mg/m^2$) | BM ($mg/m^{2)}$ |
|---|---|---|---|
| Cobble | 06BEC | 223.18 | 7594.63 |
| Cobble | 06C2 | 9.81 | 80.63 |
| Cobble | 06C3 | 31.95 | 387.03 |
| Cobble | 06C6 | 17.52 | 1012.17 |
| Cobble | 06DT1 | 74.49 | 750.01 |
| Cobble | 06DT2 | 94.04 | 1725.76 |
| Cobble | 06LDS | 96.16 | 83.81 |
| Cobble | 06LDS2 | 44.65 | 506.08 |
| Cobble | 06LMS | 76.77 | 1384.52 |
| Cobble | 06RR2 | 189.76 | 19551.52 |
| Cobble | 07BRA2 | 18.37 | 773.88 |
| Cobble | 07C9a | 11.37 | 2349.38 |
| EB | 06BEC | 223.18 | 12250.42 |
| EB | 06C2 | 9.81 | 1368.13 |
| EB | 06C3 | 31.95 | 452.63 |
| EB | 06C6 | 17.52 | 892.25 |
| EB | 06DT1 | 74.49 | 1722.15 |
| EB | 06DT2 | 94.04 | 137.05 |
| EB | 06LDS | 96.16 | 329.04 |
| EB | 06LDS2 | 44.65 | 157.64 |
| EB | 06LMS | 76.77 | 946.07 |
| EB | 06RR2 | 189.76 | 1576.07 |
| EB | 07BRA2 | 18.37 | 4958.13 |
| EB | 07C9a | 11.37 | 1441.96 |
| KS | 06BEC | 223.18 | 5199.98 |
| KS | 06C2 | 9.81 | 162.32 |
| KS | 06C3 | 31.95 | 154.03 |
| KS | 06C6 | 17.52 | 1124.15 |
| KS | 06DT1 | 74.49 | 555.68 |
| KS | 06DT2 | 94.04 | 143.91 |
| KS | 06LDS | 96.16 | 252.70 |
| KS | 06LDS2 | 44.65 | 436.88 |
| KS | 06LMS | 76.77 | 1282.17 |
| KS | 06RR2 | 189.76 | 2655.91 |
| KS | 07BRA2 | 18.37 | 612.10 |
| KS | 07C9a | 11.37 | 1290.81 |

Table 3 – Total biomass (BM) of each taxon collected by cobble and electrobugging (EB) at each site (including only organisms with body length > 4mm).

| Stream | Order | Family | Cobble BM ($mg/m^2$) | EB BM ($mg/m^2$) | KS BM ($mg/m^2$) |
|---|---|---|---|---|---|
| BEC | Amphipoda | | 67.71 | 1169.30 | |
| BEC | Bivalvia | | | | 142.65 |
| BEC | Coleoptera | Elmidae (larva) | 19.72 | 4.93 | 509.55 |
| BEC | Coleoptera | Psephenidae | 478.39 | | 110.08 |
| BEC | Diptera | Chironominae | 468.51 | 70.07 | 94.87 |
| BEC | Diptera | Orthocladiinae | 138.36 | 34.31 | 17.76 |
| BEC | Diptera | Simuliidae | 556.30 | 203.35 | 52.19 |
| BEC | Diptera | Simuliidae Pupa | 10.43 | | |
| BEC | Diptera | Tanypodinae | 13.45 | 9.65 | |
| BEC | Diptera | Tipulidae | 42.28 | 44.73 | 13.83 |
| BEC | Diptera | unknown pupa | 4.16 | 0.29 | 6.36 |
| BEC | Ephemeroptera | Baetidae | 448.97 | 1355.89 | 71.62 |
| BEC | Ephemeroptera | Caenidae | 10.09 | 0.83 | |
| BEC | Ephemeroptera | Heptageniidae | 34.38 | 5.70 | |
| BEC | Isopoda | | | 2.10 | |
| BEC | Oligochaeta | | | | 2.86 |
| BEC | Trichoptera | Glossomatidae | | 8.35 | |
| BEC | Trichoptera | Helicopsychidae | 78.85 | | |
| BEC | Trichoptera | Hydropsychidae | 10335.98 | 9313.76 | 3883.97 |
| BEC | Trichoptera | Philopotamidae | 110.03 | 12.96 | 30.57 |
| BEC | Trichoptera | Polycentropodidae | 34.96 | 7.47 | |
| BEC | Trichoptera | unknown pupa | 407.25 | 2.27 | 247.17 |
| BEC | Turbellaria | | 37.39 | 4.43 | 16.51 |
| BRA2 | Coleoptera | Dytiscidae larva | | 2377.52 | |
| BRA2 | Coleoptera | Elmidae (larva) | | | 36.88 |
| BRA2 | Diptera | Chironominae | | 0.94 | |
| BRA2 | Diptera | Orthocladiinae | 4.80 | 0.19 | 4.89 |
| BRA2 | Diptera | Simuliidae | | 1.77 | 2.81 |
| BRA2 | Diptera | Tanypodinae | 70.76 | 1.61 | 1.90 |
| BRA2 | Diptera | Tipulidae | | 6.77 | |
| BRA2 | Ephemeroptera | Baetidae | | 85.34 | 0.58 |
| BRA2 | Ephemeroptera | Heptageniidae | 58.22 | 345.42 | 35.65 |
| BRA2 | Ephemeroptera | Leptophebiidae | 48.49 | | |
| BRA2 | Ephemeroptera | Oligoneuriidae | | 7.42 | |
| BRA2 | Ephemeroptera | Tricorythidae | | 2.51 | |
| BRA2 | Gastropoda | | 533.47 | 16.62 | 3.66 |
| BRA2 | Hirudinea | | | 1.54 | |
| BRA2 | Isopoda | | | 2.22 | |
| BRA2 | Odonata | Coenagrionidae | 63.78 | 64.83 | 130.69 |
| BRA2 | Trichoptera | Hydropsychidae | 50.80 | 1981.83 | 355.04 |
| BRA2 | Trichoptera | Philopotamidae | | 52.74 | 33.85 |
| BRA2 | Trichoptera | Polycentropodidae | 275.22 | | |
| BRA2 | Turbellaria | | | 8.85 | 6.15 |
| C2 | Coleoptera | Elmidae (larva) | | 0.84 | |
| C2 | Diptera | Chironominae | 54.10 | | 0.26 |
| C2 | Diptera | Orthocladiinae | | | 0.35 |
| C2 | Diptera | Tanypodinae | 25.46 | | |
| C2 | Diptera | Tipulidae | 8.82 | 4.69 | |

Table 3 (cont.)

| Stream | Order | Family | Cobble BM ($mg/m^2$) | EB BM ($mg/m^2$) | KS BM ($mg/m^2$) |
|---|---|---|---|---|---|
| C2 | Diptera | unknown pupa | | 0.30 | |
| C2 | Ephemeroptera | Caenidae | | 2.57 | |
| C2 | Ephemeroptera | Ephemerellidae | | 1.16 | |
| C2 | Ephemeroptera | Heptageniidae | | 24.82 | |
| C2 | Ephemeroptera | Leptophebiidae | | 7.57 | 0.73 |
| C2 | Ephemeroptera | Oligoneuriidae | | 137.60 | 4.36 |
| C2 | Ephemeroptera | Tricorythidae | | 3.93 | |
| C2 | Megaoloptera | Corydalidae | | 18.59 | 12.87 |
| C2 | Odonata | Gomphidae | | 260.61 | |
| C2 | Plecoptera | Leuctridae | | 0.82 | |
| C2 | Plecoptera | Perlidae | | 367.74 | 18.35 |
| C2 | Trichoptera | Brachycentridae | | 1.00 | |
| C2 | Trichoptera | Glossomatidae | | | 9.08 |
| C2 | Trichoptera | Hydropsychidae | 70.32 | 530.14 | 100.06 |
| C2 | Trichoptera | Philopotamidae | | 3.88 | 16.25 |
| C2 | Trichoptera | Polycentropodidae | 20.47 | | |
| C2 | Trichoptera | Psychomyiidae | | 1.50 | |
| C2 | Turbellaria | | | 0.38 | |
| C3 | Coleoptera | Dytiscidae larva | | 1.06 | |
| C3 | Coleoptera | Elmidae (larva) | | | 0.87 |
| C3 | Coleoptera | Hydrophilidae (Larva) | | | 3.77 |
| C3 | Diptera | Chironominae | | 1.11 | 2.87 |
| C3 | Diptera | Orthocladiinae | 1.94 | | 1.30 |
| C3 | Diptera | Simuliidae | | 2.42 | |
| C3 | Diptera | Tanypodinae | 12.78 | 0.69 | 0.94 |
| C3 | Diptera | Tipulidae | 4.36 | 11.82 | 0.35 |
| C3 | Diptera | unknown pupa | | | 0.56 |
| C3 | Ephemeroptera | Baetidae | | 63.16 | 1.80 |
| C3 | Ephemeroptera | Ephemerellidae | | | 1.36 |
| C3 | Ephemeroptera | Heptageniidae | | 25.51 | |
| C3 | Ephemeroptera | Leptophebiidae | | 2.58 | |
| C3 | Ephemeroptera | Oligoneuriidae | | 21.09 | |
| C3 | Ephemeroptera | Tricorythidae | | 1.64 | |
| C3 | Hemiptera | Veliidae | | 10.50 | |
| C3 | Odonata | Aeshnidae | | | 4.13 |
| C3 | Oligochaeta | | | 40.83 | 1.31 |
| C3 | Plecoptera | Leuctridae | | 4.36 | |
| C3 | Plecoptera | Perlidae | 540.39 | 145.02 | 1.01 |
| C3 | Trichoptera | Brachycentridae | | 1.42 | |
| C3 | Trichoptera | Glossomatidae | 57.55 | | 6.85 |
| C3 | Trichoptera | Hydropsychidae | 52.45 | 99.87 | 22.00 |
| C3 | Trichoptera | Philopotamidae | 26.83 | 10.55 | 44.15 |
| C3 | Trichoptera | Polycentropodidae | | 5.10 | |
| C3 | Trichoptera | Psychomyiidae | | 3.90 | |
| C3 | Trichoptera | Rhyacophilidae | | | 46.28 |
| C3 | Trichoptera | unknown pupa | | | 14.47 |
| C6 | Coleoptera | Elmidae (larva) | | | 18.85 |
| C6 | Diptera | Ceratopogonidae | | | 2.58 |
| C6 | Diptera | Chironominae | | 0.32 | 0.92 |

Table 3 (cont.)

| Stream | Order | Family | Cobble BM ($mg/m^2$) | EB BM ($mg/m^2$) | KS BM ($mg/m^2$) |
|---|---|---|---|---|---|
| C6 | Diptera | Ephydridae | | 13.74 | |
| C6 | Diptera | Orthocladiinae | 7.23 | 0.49 | |
| C6 | Diptera | Simuliidae | | 0.33 | |
| C6 | Diptera | Tipulidae | | 36.24 | 11.52 |
| C6 | Ephemeroptera | Baetidae | | 16.01 | 46.01 |
| C6 | Ephemeroptera | Ephemerellidae | | 11.08 | 25.82 |
| C6 | Ephemeroptera | Heptageniidae | | 4.70 | |
| C6 | Isopoda | | | 1.20 | |
| C6 | Nematoda | | | 2.24 | |
| C6 | Odonata | Aeshnidae | | 206.04 | 81.54 |
| C6 | Odonata | Cordulegastridae | | 175.94 | |
| C6 | Oligochaeta | | | 4.73 | 8.54 |
| C6 | Plecoptera | Leuctridae | | 1.52 | |
| C6 | Plecoptera | Nemouridae | | 0.50 | |
| C6 | Plecoptera | Perlodidae | | 180.74 | 10.72 |
| C6 | Trichoptera | Glossomatidae | | 2.52 | 1.25 |
| C6 | Trichoptera | Hydropsychidae | 1207.15 | 90.63 | 12.31 |
| C6 | Trichoptera | Lepidostomatidae | | 11.83 | 24.67 |
| C6 | Trichoptera | Limniphilidae | | | 801.39 |
| C6 | Trichoptera | Philopotamidae | 50.83 | 11.06 | |
| C6 | Trichoptera | Polycentropodidae | | 109.09 | |
| C6 | Trichoptera | Rhyacophilidae | | | 60.69 |
| C6 | Trichoptera | unknown pupa | | 11.31 | 17.34 |
| C9a | Coleoptera | Elmidae (larva) | | 0.87 | 16.57 |
| C9a | Coleoptera | Psephenidae | 252.34 | 15.81 | 55.11 |
| C9a | Diptera | Ceratopogonidae | | | 2.20 |
| C9a | Diptera | Chironominae | | 0.42 | 2.68 |
| C9a | Diptera | Orthocladiinae | | | 0.89 |
| C9a | Diptera | Simuliidae | | 0.62 | |
| C9a | Diptera | Tipulidae | 127.10 | 44.35 | 0.25 |
| C9a | Ephemeroptera | Baetidae | | 1.27 | |
| C9a | Ephemeroptera | Heptageniidae | | 0.93 | |
| C9a | Megaloptera | Corydalidae | | 156.16 | 313.93 |
| C9a | Megaloptera | Sialidae | | | 2.22 |
| C9a | Odonata | Aeshnidae | 428.41 | | |
| C9a | Plecoptera | Perlidae | | 384.17 | 237.86 |
| C9a | Trichoptera | Brachycentridae | 807.21 | 35.93 | 179.19 |
| C9a | Trichoptera | Glossomatidae | 129.84 | | 46.28 |
| C9a | Trichoptera | Hydropsychidae | 586.30 | 575.12 | 94.23 |
| C9a | Trichoptera | Philopotamidae | 279.24 | 210.55 | 312.10 |
| C9a | Trichoptera | Polycentropodidae | | | 14.31 |
| C9a | Trichoptera | Rhyacophilidae | | 15.76 | 12.99 |
| DT1 | Coleoptera | Elmidae (larva) | | | 195.98 |
| DT1 | Diptera | Chironominae | 33.92 | 2.08 | 21.02 |
| DT1 | Diptera | Orthocladiinae | 10.13 | 9.39 | 62.45 |
| DT1 | Diptera | Simuliidae | | | 3.04 |
| DT1 | Diptera | Tanypodinae | | 9.45 | 14.38 |
| DT1 | Diptera | Tipulidae | 8.45 | 1.49 | |

Table 3 (cont.)

| Stream | Order | Family | Cobble BM ($mg/m^2$) | EB BM ($mg/m^2$) | KS BM ($mg/m^2$) |
|---|---|---|---|---|---|
| DT1 | Diptera | unknown pupa | | | 0.48 |
| DT1 | Ephemeroptera | Baetidae | 13.56 | 13.72 | |
| DT1 | Ephemeroptera | Caenidae | | 1.38 | |
| DT1 | Ephemeroptera | Heptageniidae | | 42.58 | |
| DT1 | Isopoda | | | 7.13 | |
| DT1 | Megaoloptera | Corydalidae | | 124.71 | |
| DT1 | Oligochaeta | | | 0.35 | 1.29 |
| DT1 | Plecoptera | Perlidae | 104.99 | 109.30 | |
| DT1 | Trichoptera | Helicopsychidae | 416.86 | | |
| DT1 | Trichoptera | Hydropsychidae | 35.72 | 1399.97 | 257.05 |
| DT1 | Trichoptera | unknown pupa | 283.45 | | |
| DT1 | Turbellaria | | | 0.62 | |
| DT2 | Coleoptera | Elmidae (larva) | 176.26 | 16.71 | 4.79 |
| DT2 | Diptera | Chironominae | 274.48 | 3.39 | 20.04 |
| DT2 | Diptera | Orthocladiinae | 48.83 | 6.04 | 4.17 |
| DT2 | Diptera | Simuliidae | 16.62 | 0.91 | 0.64 |
| DT2 | Diptera | Tanypodinae | 17.72 | 2.22 | 2.14 |
| DT2 | Diptera | Tipulidae | | | 0.52 |
| DT2 | Diptera | unknown pupa | | | 4.37 |
| DT2 | Ephemeroptera | Baetidae | 45.48 | 27.20 | 1.38 |
| DT2 | Ephemeroptera | Heptageniidae | | 10.85 | |
| DT2 | Isopoda | | 22.90 | | 0.94 |
| DT2 | Megaoloptera | Corydalidae | | | 23.11 |
| DT2 | Oligochaeta | | | 2.58 | 5.64 |
| DT2 | Plecoptera | Perlidae | 61.69 | 28.40 | 4.01 |
| DT2 | Trichoptera | Glossomatidae | | | 1.89 |
| DT2 | Trichoptera | Helicopsychidae | 1291.54 | | |
| DT2 | Trichoptera | Hydropsychidae | 978.35 | 38.76 | 70.26 |
| DT2 | Trichoptera | Lepidostomatidae | 36.71 | | |
| DT2 | Trichoptera | unknown pupa | 134.27 | | |
| LDS | Amphipoda | | | 11.58 | |
| LDS | Coleoptera | Elmidae (adult) | | | 7.51 |
| LDS | Diptera | Ceratopogonidae | | 1.11 | |
| LDS | Diptera | Chironominae | 5.26 | 0.88 | 10.71 |
| LDS | Diptera | Orthocladiinae | 28.41 | 4.19 | 0.19 |
| LDS | Diptera | Simuliidae | | 0.37 | |
| LDS | Diptera | Tanypodinae | 46.48 | 9.28 | 11.91 |
| LDS | Diptera | Tipulidae | 2.85 | | |
| LDS | Diptera | unknown pupa | | 3.15 | 2.87 |
| LDS | Ephemeroptera | Caenidae | | 1.32 | |
| LDS | Gastropoda | | 147.18 | 3.37 | 90.50 |
| LDS | Hirudinea | | | 65.62 | 20.42 |
| LDS | Isopoda | | | 0.61 | |
| LDS | Megaoloptera | Corydalidae | | | 70.06 |
| LDS | Nematoda | | 8.53 | | |
| LDS | Odonata | Aeshnidae | | 13.29 | |
| LDS | Odonata | Coenagrionidae | | | 10.25 |
| LDS | Oligochaeta | | 15.05 | | 5.20 |

Table 3 (cont.)

| Stream | Order | Family | Cobble BM ($mg/m^2$) | EB BM ($mg/m^2$) | KS BM ($mg/m^2$) |
|---|---|---|---|---|---|
| LDS | Trichoptera | Hydropsychidae | | 214.25 | 23.08 |
| LDS2 | Amphipoda | | | 6.55 | |
| LDS2 | Coleoptera | Chrysomelidae (larva) | | 0.84 | |
| LDS2 | Coleoptera | Elmidae (larva) | 10.28 | | |
| LDS2 | Diptera | Chironominae | 1039.00 | 43.82 | 56.95 |
| LDS2 | Diptera | Muscidae-Anthomyiidae | | 13.55 | |
| LDS2 | Diptera | Orthocladiinae | 432.82 | 57.43 | 44.10 |
| LDS2 | Diptera | Simuliidae | 32.10 | 1.81 | 2.79 |
| LDS2 | Diptera | Tanypodinae | 130.49 | | 16.11 |
| LDS2 | Diptera | unknown pupa | 256.09 | 6.22 | 12.57 |
| LDS2 | Gastropoda | | 100.11 | | |
| LDS2 | Nematoda | | 46.98 | | 13.27 |
| LDS2 | Oligochaeta | | 346.09 | 25.55 | 291.08 |
| LDS2 | Trichoptera | Hydropsychidae | | 1.87 | |
| LMS | Bivalvia | | | | 15.71 |
| LMS | Coleoptera | Elmidae (larva) | 587.20 | | 62.71 |
| LMS | Diptera | Chironominae | 125.98 | | 12.65 |
| LMS | Diptera | Ephydridae | | 0.34 | |
| LMS | Diptera | Muscidae-Anthomyiidae | | | 5.34 |
| LMS | Diptera | Orthocladiinae | 229.40 | 39.72 | 151.86 |
| LMS | Diptera | Simuliidae | | 0.29 | |
| LMS | Diptera | Tanypodinae | 50.92 | 1.85 | 4.32 |
| LMS | Diptera | Tipulidae | 445.95 | 20.68 | 78.75 |
| LMS | Diptera | unknown pupa | 35.96 | 0.39 | 2.92 |
| LMS | Ephemeroptera | Baetidae | | 1.20 | |
| LMS | Ephemeroptera | Caenidae | 50.51 | 1.14 | |
| LMS | Hirudinea | | | 9.22 | 94.31 |
| LMS | Isopoda | | | 5.93 | 12.53 |
| LMS | Megaloptera | Corydalidae | 67.03 | | |
| LMS | Nematoda | | 116.19 | | |
| LMS | Oligochaeta | | 16.59 | 0.44 | 14.26 |
| LMS | Trichoptera | Hydropsychidae | 1636.58 | 864.86 | 821.46 |
| LMS | Trichoptera | Hydroptilidae | 159.99 | | 5.34 |
| RR2 | Coleoptera | Elmidae (adult) | 354.52 | | |
| RR2 | Coleoptera | Elmidae (larva) | 374.63 | 3.39 | 120.36 |
| RR2 | Coleoptera | Hydrophilidae | | 5.04 | |
| RR2 | Coleoptera | Psephenidae | 582.71 | 2.13 | 4.38 |
| RR2 | Diptera | Athericidae | | | 4.32 |
| RR2 | Diptera | Chironominae | 382.71 | 6.34 | 40.16 |
| RR2 | Diptera | Ephydridae | | 4.30 | |
| RR2 | Diptera | Orthocladiinae | 22.47 | 3.65 | 2.67 |
| RR2 | Diptera | Tanypodinae | 138.22 | 12.22 | 4.51 |
| RR2 | Diptera | Tipulidae | 70.01 | 0.65 | 25.30 |
| RR2 | Diptera | unknown pupa | 71.83 | | |
| RR2 | Ephemeroptera | Baetidae | 24.00 | 1.79 | |
| RR2 | Ephemeroptera | Caenidae | 10.91 | | |
| RR2 | Ephemeroptera | Heptageniidae | 17.65 | 0.92 | |
| RR2 | Ephemeroptera | Leptophebiidae | 51.65 | 2.65 | |

Table 3 (cont.)

| Stream | Order | Family | Cobble BM ($mg/m^2$) | EB BM ($mg/m^2$) | KS BM ($mg/m^2$) |
|---|---|---|---|---|---|
| RR2 | Ephemeroptera | Oligoneuriidae | | 132.70 | 14.67 |
| RR2 | Gastropoda | | 209.51 | | |
| RR2 | Oligochaeta | | | | 70.10 |
| RR2 | Plecoptera | Perlidae | | 6.60 | |
| RR2 | Trichoptera | Brachycentridae | | | 6.71 |
| RR2 | Trichoptera | Glossomatidae | | | 6.61 |
| RR2 | Trichoptera | Helicopsychidae | 681.38 | 8.10 | 5.22 |
| RR2 | Trichoptera | Hydropsychidae | 16312.97 | 1381.00 | 1340.71 |
| RR2 | Trichoptera | Hydroptilidae | 20.60 | | |
| RR2 | Trichoptera | Lepidostomatidae | 4958.52 | | |
| RR2 | Trichoptera | Leptoceridae | 123.94 | | 5.66 |
| RR2 | Trichoptera | Limniphilidae | | | 966.69 |
| RR2 | Trichoptera | Philopotamidae | | 4.58 | |
| RR2 | Trichoptera | Polycentropodidae | 37.26 | | |
| RR2 | Trichoptera | unknown pupa | | | 31.82 |
| RR2 | Turbellaria | | 55.90 | | 6.01 |

Table 4 – Total biomass (BM) of each size class collected by the cobble and combined methods in each site.

| Stream | Size Class | Length (mm) | Cobble BM ($mg/m^2$) | Combined BM ($mg/m^2$) |
|---|---|---|---|---|
| BEC | 6 | 4.00 | 76.40 | 34.45 |
| BEC | 7 | 5.04 | 121.64 | 53.67 |
| BEC | 8 | 6.35 | 434.59 | 216.69 |
| BEC | 9 | 8.00 | 1586.53 | 1911.04 |
| BEC | 10 | 10.08 | 545.85 | 1615.78 |
| BEC | 11 | 12.70 | 2073.57 | 1758.10 |
| BEC | 12 | 16.00 | 2661.30 | 5580.68 |
| BEC | 13 | 20.16 | 3052.84 | 5141.93 |
| BEC | 14 | 25.40 | 2744.51 | 1967.07 |
| BEC | 15 | 32.00 | | 121.42 |
| BRA2 | 6 | 4.00 | | 1.83 |
| BRA2 | 7 | 5.04 | 13.80 | 5.15 |
| BRA2 | 8 | 6.35 | 19.12 | 24.13 |
| BRA2 | 9 | 8.00 | | 291.54 |
| BRA2 | 10 | 10.08 | 213.13 | 410.73 |
| BRA2 | 11 | 12.70 | 267.89 | 494.51 |
| BRA2 | 12 | 16.00 | 316.38 | 926.37 |
| BRA2 | 13 | 20.16 | 275.22 | 950.33 |
| BRA2 | 14 | 25.40 | | 339.65 |
| BRA2 | 15 | 32.00 | | 379.22 |
| BRA2 | 16 | 40.32 | | 1671.98 |
| C2 | 7 | 5.04 | 5.37 | 0.22 |
| C2 | 8 | 6.35 | 58.66 | 6.57 |
| C2 | 9 | 8.00 | 44.82 | 51.57 |
| C2 | 10 | 10.08 | | 115.88 |
| C2 | 11 | 12.70 | 70.32 | 206.99 |
| C2 | 12 | 16.00 | | 200.09 |
| C2 | 13 | 20.16 | | 177.01 |
| C2 | 14 | 25.40 | | 214.65 |
| C2 | 15 | 32.00 | | 203.79 |
| C2 | 17 | 50.80 | | 127.28 |
| C2 | 18 | 64.00 | | 260.61 |
| C3 | 6 | 4.00 | 1.94 | 0.09 |
| C3 | 7 | 5.04 | 4.36 | 0.15 |
| C3 | 8 | 6.35 | 4.51 | 4.48 |
| C3 | 9 | 8.00 | 17.87 | 85.20 |
| C3 | 10 | 10.08 | 97.16 | 72.41 |
| C3 | 11 | 12.70 | 133.18 | 65.40 |
| C3 | 12 | 16.00 | | 83.04 |
| C3 | 13 | 20.16 | | 67.84 |
| C3 | 14 | 25.40 | | 71.79 |
| C3 | 15 | 32.00 | 437.29 | 83.86 |
| C3 | 16 | 40.32 | | 75.42 |
| C6 | 7 | 5.04 | 7.23 | 1.41 |
| C6 | 8 | 6.35 | | 11.48 |
| C6 | 9 | 8.00 | 50.83 | 39.84 |
| C6 | 10 | 10.08 | | 123.65 |

Table 4 (cont.)

| Stream | Size Class | Length (mm) | Cobble BM ($mg/m^2$) | Combined BM ($mg/m^2$) |
|---|---|---|---|---|
| C6 | 11 | 12.70 | | 82.90 |
| C6 | 12 | 16.00 | 393.79 | 110.92 |
| C6 | 13 | 20.16 | 813.36 | 240.69 |
| C6 | 14 | 25.40 | | 182.24 |
| C6 | 15 | 32.00 | | 369.33 |
| C6 | 16 | 40.32 | | 849.16 |
| C9a | 6 | 4.00 | | 0.29 |
| C9a | 7 | 5.04 | | 0.60 |
| C9a | 8 | 6.35 | | 6.69 |
| C9a | 9 | 8.00 | 111.94 | 98.69 |
| C9a | 10 | 10.08 | 89.81 | 217.58 |
| C9a | 11 | 12.70 | 476.85 | 394.15 |
| C9a | 12 | 16.00 | 1503.42 | 765.65 |
| C9a | 13 | 20.16 | | 175.09 |
| C9a | 14 | 25.40 | 428.41 | 238.90 |
| C9a | 15 | 32.00 | | 641.87 |
| C9a | 16 | 40.32 | | 173.45 |
| DT1 | 6 | 4.00 | 4.59 | 5.16 |
| DT1 | 7 | 5.04 | 12.89 | 16.69 |
| DT1 | 8 | 6.35 | 16.83 | 43.70 |
| DT1 | 9 | 8.00 | 31.74 | 105.98 |
| DT1 | 10 | 10.08 | 10.59 | 49.02 |
| DT1 | 11 | 12.70 | 89.57 | 170.88 |
| DT1 | 12 | 16.00 | 104.99 | 341.00 |
| DT1 | 13 | 20.16 | 219.01 | 163.01 |
| DT1 | 14 | 25.40 | | 1334.93 |
| DT1 | 15 | 32.00 | 416.86 | 60.94 |
| DT1 | 16 | 40.32 | | 119.04 |
| DT2 | 6 | 4.00 | 19.45 | 3.46 |
| DT2 | 7 | 5.04 | 45.06 | 13.80 |
| DT2 | 8 | 6.35 | 203.76 | 8.00 |
| DT2 | 9 | 8.00 | 194.55 | 60.22 |
| DT2 | 10 | 10.08 | 225.60 | 30.56 |
| DT2 | 11 | 12.70 | 199.13 | 21.19 |
| DT2 | 12 | 16.00 | 152.73 | 63.18 |
| DT2 | 13 | 20.16 | 435.27 | 41.17 |
| DT2 | 14 | 25.40 | 473.03 | 39.44 |
| DT2 | 15 | 32.00 | 1156.26 | |
| LDS | 6 | 4.00 | 19.15 | 1.72 |
| LDS | 7 | 5.04 | 29.33 | 0.89 |
| LDS | 8 | 6.35 | 32.74 | 5.69 |
| LDS | 9 | 8.00 | 16.49 | 31.39 |
| LDS | 10 | 10.08 | 8.86 | 13.35 |
| LDS | 11 | 12.70 | | 8.92 |
| LDS | 12 | 16.00 | 147.18 | 35.97 |
| LDS | 13 | 20.16 | | 48.06 |
| LDS | 14 | 25.40 | | 269.19 |

Table 4 (cont.)

| Stream | Size Class | Length (mm) | Cobble BM ($mg/m^2$) | Combined BM ($mg/m^2$) |
|---|---|---|---|---|
| LDS | 15 | 32.00 | | 37.74 |
| LDS | 16 | 40.32 | | 130.81 |
| LDS2 | 6 | 4.00 | 89.70 | 16.64 |
| LDS2 | 7 | 5.04 | 370.92 | 100.52 |
| LDS2 | 8 | 6.35 | 150.09 | 108.26 |
| LDS2 | 9 | 8.00 | 343.84 | 53.24 |
| LDS2 | 10 | 10.08 | 598.58 | 135.16 |
| LDS2 | 11 | 12.70 | 740.73 | 138.22 |
| LDS2 | 12 | 16.00 | | 22.25 |
| LDS2 | 13 | 20.16 | 100.11 | 9.40 |
| LMS | 6 | 4.00 | 113.31 | 69.03 |
| LMS | 7 | 5.04 | 136.55 | 132.46 |
| LMS | 8 | 6.35 | 186.31 | 57.94 |
| LMS | 9 | 8.00 | 473.92 | 103.15 |
| LMS | 10 | 10.08 | 863.25 | 248.09 |
| LMS | 11 | 12.70 | 719.47 | 261.43 |
| LMS | 12 | 16.00 | 593.90 | 951.58 |
| LMS | 13 | 20.16 | 435.58 | 561.97 |
| RR2 | 6 | 4.00 | 20.08 | 5.65 |
| RR2 | 7 | 5.04 | 95.94 | 9.80 |
| RR2 | 8 | 6.35 | 346.29 | 38.01 |
| RR2 | 9 | 8.00 | 1443.12 | 307.12 |
| RR2 | 10 | 10.08 | 2126.98 | 563.59 |
| RR2 | 11 | 12.70 | 3562.37 | 503.81 |
| RR2 | 12 | 16.00 | 6650.25 | 636.82 |
| RR2 | 13 | 20.16 | 4602.34 | 687.09 |
| RR2 | 14 | 25.40 | 2184.20 | 70.10 |
| RR2 | 15 | 32.00 | 3469.80 | 208.38 |
| RR2 | 16 | 40.32 | | 758.31 |

Table 5 –Taxa collected by the cobble and combined methods in each site (only including organisms with body length > 4mm).

| Stream | Size class | Number of taxa - cobble samples | Number of taxa - combined samples |
|---|---|---|---|
| BEC | 6 | 1 | 1 |
| BEC | 7 | 3 | 5 |
| BEC | 8 | 6 | 7 |
| BEC | 9 | 9 | 12 |
| BEC | 10 | 6 | 8 |
| BEC | 11 | 6 | 6 |
| BEC | 12 | 3 | 7 |
| BEC | 13 | 2 | 5 |
| BEC | 14 | 1 | 3 |
| BEC | 15 | 0 | 1 |
| BRA2 | 6 | 0 | 1 |
| BRA2 | 7 | 2 | 2 |
| BRA2 | 8 | 1 | 4 |
| BRA2 | 9 | 0 | 7 |
| BRA2 | 10 | 4 | 7 |
| BRA2 | 11 | 2 | 9 |
| BRA2 | 12 | 1 | 3 |
| BRA2 | 13 | 1 | 3 |
| BRA2 | 14 | 0 | 1 |
| BRA2 | 15 | 0 | 1 |
| BRA2 | 16 | 0 | 1 |
| C2 | 7 | 1 | 1 |
| C2 | 8 | 3 | 7 |
| C2 | 9 | 3 | 7 |
| C2 | 10 | 0 | 10 |
| C2 | 11 | 1 | 5 |
| C2 | 12 | 0 | 5 |
| C2 | 13 | 0 | 3 |
| C2 | 14 | 0 | 3 |
| C2 | 15 | 0 | 1 |
| C2 | 17 | 0 | 1 |
| C2 | 18 | 0 | 1 |
| C3 | 6 | 1 | 1 |
| C3 | 7 | 1 | 1 |
| C3 | 8 | 1 | 7 |
| C3 | 9 | 2 | 12 |
| C3 | 10 | 3 | 15 |
| C3 | 11 | 2 | 5 |
| C3 | 12 | 0 | 9 |
| C3 | 13 | 0 | 5 |
| C3 | 14 | 0 | 3 |
| C3 | 15 | 1 | 2 |
| C3 | 16 | 0 | 1 |
| C6 | 7 | 1 | 2 |
| C6 | 8 | 0 | 4 |
| C6 | 9 | 1 | 8 |
| C6 | 10 | 0 | 14 |

Table 5 (cont.)

| Stream | Size class | Number of taxa - cobble samples | Number of taxa - combined samples |
|---|---|---|---|
| C6 | 11 | 0 | 8 |
| C6 | 12 | 1 | 6 |
| C6 | 13 | 1 | 4 |
| C6 | 14 | 0 | 5 |
| C6 | 15 | 0 | 5 |
| C6 | 16 | 0 | 3 |
| C9a | 6 | 0 | 1 |
| C9a | 7 | 0 | 1 |
| C9a | 8 | 0 | 5 |
| C9a | 9 | 1 | 7 |
| C9a | 10 | 2 | 8 |
| C9a | 11 | 3 | 9 |
| C9a | 12 | 5 | 7 |
| C9a | 13 | 0 | 5 |
| C9a | 14 | 1 | 3 |
| C9a | 15 | 0 | 2 |
| C9a | 16 | 0 | 1 |
| DT1 | 6 | 1 | 1 |
| DT1 | 7 | 2 | 3 |
| DT1 | 8 | 1 | 5 |
| DT1 | 9 | 3 | 10 |
| DT1 | 10 | 1 | 5 |
| DT1 | 11 | 2 | 4 |
| DT1 | 12 | 1 | 4 |
| DT1 | 13 | 1 | 3 |
| DT1 | 14 | 0 | 2 |
| DT1 | 15 | 1 | 1 |
| DT1 | 16 | 0 | 1 |
| DT2 | 6 | 1 | 1 |
| DT2 | 7 | 2 | 4 |
| DT2 | 8 | 4 | 3 |
| DT2 | 9 | 7 | 11 |
| DT2 | 10 | 5 | 5 |
| DT2 | 11 | 3 | 4 |
| DT2 | 12 | 2 | 3 |
| DT2 | 13 | 3 | 3 |
| DT2 | 14 | 1 | 2 |
| DT2 | 15 | 1 | 0 |
| LDS | 6 | 1 | 1 |
| LDS | 7 | 3 | 1 |
| LDS | 8 | 5 | 5 |
| LDS | 9 | 1 | 9 |
| LDS | 10 | 1 | 6 |
| LDS | 11 | 0 | 3 |
| LDS | 12 | 1 | 5 |
| LDS | 13 | 0 | 3 |
| LDS | 14 | 0 | 3 |

Table 5 (cont.)

| Stream | Size class | Number of taxa - cobble samples | Number of taxa - combined samples |
|---|---|---|---|
| LDS | 15 | 0 | 1 |
| LDS | 16 | 0 | 2 |
| LDS2 | 6 | 1 | 1 |
| LDS2 | 7 | 5 | 4 |
| LDS2 | 8 | 6 | 5 |
| LDS2 | 9 | 6 | 4 |
| LDS2 | 10 | 6 | 7 |
| LDS2 | 11 | 3 | 2 |
| LDS2 | 12 | 0 | 4 |
| LDS2 | 13 | 1 | 1 |
| LMS | 6 | 1 | 1 |
| LMS | 7 | 2 | 3 |
| LMS | 8 | 4 | 10 |
| LMS | 9 | 8 | 9 |
| LMS | 10 | 5 | 9 |
| LMS | 11 | 4 | 3 |
| LMS | 12 | 2 | 2 |
| LMS | 13 | 1 | 1 |
| RR2 | 6 | 1 | 1 |
| RR2 | 7 | 3 | 3 |
| RR2 | 8 | 3 | 6 |
| RR2 | 9 | 8 | 9 |
| RR2 | 10 | 8 | 13 |
| RR2 | 11 | 8 | 6 |
| RR2 | 12 | 6 | 7 |
| RR2 | 13 | 1 | 2 |
| RR2 | 14 | 1 | 1 |
| RR2 | 15 | 1 | 1 |
| RR2 | 16 | 0 | 1 |

Table 6 – Invertebrate normalized biomass in each size class for each site.

| Site | Size class | Mass (ug) | Normalized biomass ($m^{-2}$) |
|---|---|---|---|
| BEC | 0 | 1.00 | 9997.69 |
| BEC | 1 | 2.00 | 21318.68 |
| BEC | 10 | 1024.00 | 3458.84 |
| BEC | 11 | 2048.00 | 2133.87 |
| BEC | 12 | 4096.00 | 2830.70 |
| BEC | 13 | 8192.00 | 1286.22 |
| BEC | 14 | 16384.00 | 240.12 |
| BEC | 15 | 32768.00 | 7.41 |
| BEC | 2 | 4.00 | 9596.19 |
| BEC | 3 | 8.00 | 5465.12 |
| BEC | 4 | 16.00 | 6014.34 |
| BEC | 5 | 32.00 | 7195.86 |
| BEC | 6 | 64.00 | 8563.73 |
| BEC | 7 | 128.00 | 8157.68 |
| BEC | 8 | 256.00 | 5399.23 |
| BEC | 9 | 512.00 | 8943.22 |
| BEC | -1 | 0.50 | 617.31 |
| BEC | -2 | 0.25 | 1068.66 |
| BECb | 0 | 1.00 | 31321.07 |
| BECb | 1 | 2.00 | 54469.83 |
| BECb | 10 | 1024.00 | 723.86 |
| BECb | 11 | 2048.00 | 466.24 |
| BECb | 12 | 4096.00 | 254.00 |
| BECb | 13 | 8192.00 | 94.80 |
| BECb | 14 | 16384.00 | 7.36 |
| BECb | 15 | 32768.00 | 35.77 |
| BECb | 2 | 4.00 | 25295.50 |
| BECb | 3 | 8.00 | 21488.16 |
| BECb | 4 | 16.00 | 10421.67 |
| BECb | 5 | 32.00 | 8560.18 |
| BECb | 6 | 64.00 | 7991.51 |
| BECb | 7 | 128.00 | 4293.63 |
| BECb | 8 | 256.00 | 3613.69 |
| BECb | 9 | 512.00 | 2673.74 |
| BECb | -1 | 0.50 | 1543.29 |
| C2 | 0 | 1.00 | 15802.69 |
| C2 | 1 | 2.00 | 2583.49 |
| C2 | 10 | 1024.00 | 226.32 |
| C2 | 11 | 2048.00 | 202.14 |
| C2 | 12 | 4096.00 | 97.70 |
| C2 | 13 | 8192.00 | 43.22 |
| C2 | 14 | 16384.00 | 26.20 |
| C2 | 15 | 32768.00 | 12.44 |
| C2 | 17 | 131072.00 | 1.94 |
| C2 | 18 | 262144.00 | 1.99 |
| C2 | 2 | 4.00 | 2589.61 |
| C2 | 3 | 8.00 | 1764.11 |
| C2 | 4 | 16.00 | 975.49 |

Table 6 (cont.)

| Site | Size class | Mass (ug) | Normalized biomass ($m^{-2}$) |
|---|---|---|---|
| C2 | 5 | 32.00 | 721.48 |
| C2 | 6 | 64.00 | 361.91 |
| C2 | 7 | 128.00 | 411.49 |
| C2 | 8 | 256.00 | 294.01 |
| C2 | 9 | 512.00 | 339.52 |
| C2 | -1 | 0.50 | 15208.04 |
| C2 | -3 | 0.13 | 1879.07 |
| C3 | 0 | 1.00 | 468.03 |
| C3 | 1 | 2.00 | 1186.97 |
| C3 | 10 | 1024.00 | 220.66 |
| C3 | 11 | 2048.00 | 137.02 |
| C3 | 12 | 4096.00 | 40.55 |
| C3 | 13 | 8192.00 | 16.56 |
| C3 | 14 | 16384.00 | 8.76 |
| C3 | 15 | 32768.00 | 17.50 |
| C3 | 16 | 65536.00 | 2.30 |
| C3 | 2 | 4.00 | 1000.42 |
| C3 | 3 | 8.00 | 404.96 |
| C3 | 4 | 16.00 | 30.56 |
| C3 | 5 | 32.00 | 634.69 |
| C3 | 6 | 64.00 | 1394.91 |
| C3 | 7 | 128.00 | 708.68 |
| C3 | 8 | 256.00 | 222.44 |
| C3 | 9 | 512.00 | 390.19 |
| C6 | 1 | 2.00 | 137.62 |
| C6 | 10 | 1024.00 | 241.51 |
| C6 | 11 | 2048.00 | 80.95 |
| C6 | 12 | 4096.00 | 136.17 |
| C6 | 13 | 8192.00 | 145.15 |
| C6 | 14 | 16384.00 | 22.25 |
| C6 | 15 | 32768.00 | 22.54 |
| C6 | 16 | 65536.00 | 25.91 |
| C6 | 2 | 4.00 | 334.12 |
| C6 | 3 | 8.00 | 84.16 |
| C6 | 4 | 16.00 | 669.19 |
| C6 | 5 | 32.00 | 235.31 |
| C6 | 6 | 64.00 | 398.03 |
| C6 | 7 | 128.00 | 320.99 |
| C6 | 8 | 256.00 | 407.37 |
| C6 | 9 | 512.00 | 388.94 |
| DT1 | 0 | 1.00 | 1309.24 |
| DT1 | 1 | 2.00 | 1441.03 |
| DT1 | 10 | 1024.00 | 95.75 |
| DT1 | 11 | 2048.00 | 219.32 |
| DT1 | 12 | 4096.00 | 180.06 |
| DT1 | 13 | 8192.00 | 84.36 |
| DT1 | 14 | 16384.00 | 162.96 |

Table 6 (cont.)

| Site | Size class | Mass (ug) | Normalized biomass ($m^{-2}$) |
|---|---|---|---|
| DT1 | 15 | 32768.00 | 24.92 |
| DT1 | 16 | 65536.00 | 3.63 |
| DT1 | 2 | 4.00 | 694.09 |
| DT1 | 3 | 8.00 | 217.58 |
| DT1 | 4 | 16.00 | 90.51 |
| DT1 | 5 | 32.00 | 304.64 |
| DT1 | 6 | 64.00 | 887.26 |
| DT1 | 7 | 128.00 | 829.71 |
| DT1 | 8 | 256.00 | 635.85 |
| DT1 | 9 | 512.00 | 482.92 |
| DT1 | -3 | 0.13 | 6607.27 |
| DT2 | 0 | 1.00 | 11326.49 |
| DT2 | 1 | 2.00 | 9713.37 |
| DT2 | 10 | 1024.00 | 444.31 |
| DT2 | 11 | 2048.00 | 360.48 |
| DT2 | 12 | 4096.00 | 76.53 |
| DT2 | 13 | 8192.00 | 112.64 |
| DT2 | 14 | 16384.00 | 60.56 |
| DT2 | 15 | 32768.00 | 70.57 |
| DT2 | 2 | 4.00 | 10206.14 |
| DT2 | 3 | 8.00 | 4476.25 |
| DT2 | 4 | 16.00 | 2252.68 |
| DT2 | 5 | 32.00 | 2269.61 |
| DT2 | 6 | 64.00 | 2247.47 |
| DT2 | 7 | 128.00 | 1498.24 |
| DT2 | 8 | 256.00 | 2123.59 |
| DT2 | 9 | 512.00 | 847.73 |
| DT2 | -1 | 0.50 | 9700.82 |
| DT2 | -2 | 0.25 | 763.90 |
| DT2 | -3 | 0.13 | 1404.39 |
| LDS | 0 | 1.00 | 1827.43 |
| LDS | 1 | 2.00 | 2645.99 |
| LDS | 10 | 1024.00 | 27.24 |
| LDS | 11 | 2048.00 | 138.75 |
| LDS | 12 | 4096.00 | 87.47 |
| LDS | 13 | 8192.00 | 11.73 |
| LDS | 14 | 16384.00 | 32.86 |
| LDS | 15 | 32768.00 | 2.30 |
| LDS | 16 | 65536.00 | 3.99 |
| LDS | 2 | 4.00 | 1890.18 |
| LDS | 3 | 8.00 | 1082.39 |
| LDS | 4 | 16.00 | 1272.59 |
| LDS | 5 | 32.00 | 1134.28 |
| LDS | 6 | 64.00 | 1342.21 |
| LDS | 7 | 128.00 | 834.97 |
| LDS | 8 | 256.00 | 987.24 |
| LDS | 9 | 512.00 | 325.31 |
| LDS2 | 0 | 1.00 | 3813.29 |

Table 6 (cont.)

| Site | Size class | Mass (ug) | Normalized biomass ($m^{-2}$) |
|---|---|---|---|
| LDS2 | 1 | 2.00 | 5710.47 |
| LDS2 | 10 | 1024.00 | 1207.78 |
| LDS2 | 11 | 2048.00 | 805.81 |
| LDS2 | 12 | 4096.00 | 10.86 |
| LDS2 | 13 | 8192.00 | 26.74 |
| LDS2 | 2 | 4.00 | 6060.23 |
| LDS2 | 3 | 8.00 | 4203.09 |
| LDS2 | 4 | 16.00 | 1820.76 |
| LDS2 | 5 | 32.00 | 3512.38 |
| LDS2 | 6 | 64.00 | 6307.79 |
| LDS2 | 7 | 128.00 | 7288.08 |
| LDS2 | 8 | 256.00 | 1370.10 |
| LDS2 | 9 | 512.00 | 1346.38 |
| LDS2 | -1 | 0.50 | 7257.46 |
| LDS2 | -2 | 0.25 | 7100.49 |
| LDS2 | -3 | 0.13 | 1914.09 |
| LDSb | 0 | 1.00 | 1103.01 |
| LDSb | 1 | 2.00 | 859.65 |
| LDSb | 10 | 1024.00 | 20.40 |
| LDSb | 11 | 2048.00 | 14.84 |
| LDSb | 12 | 4096.00 | 18.47 |
| LDSb | 13 | 8192.00 | 4.38 |
| LDSb | 2 | 4.00 | 660.80 |
| LDSb | 3 | 8.00 | 595.18 |
| LDSb | 4 | 16.00 | 220.12 |
| LDSb | 5 | 32.00 | 56.71 |
| LDSb | 6 | 64.00 | 104.28 |
| LDSb | 7 | 128.00 | 36.07 |
| LDSb | 8 | 256.00 | 7.23 |
| LDSb | 9 | 512.00 | 16.78 |
| LMS | 0 | 1.00 | 1081.80 |
| LMS | 1 | 2.00 | 5176.50 |
| LMS | 10 | 1024.00 | 1053.01 |
| LMS | 11 | 2048.00 | 424.82 |
| LMS | 12 | 4096.00 | 509.83 |
| LMS | 13 | 8192.00 | 137.20 |
| LMS | 2 | 4.00 | 3121.03 |
| LMS | 3 | 8.00 | 2380.81 |
| LMS | 4 | 16.00 | 2657.65 |
| LMS | 5 | 32.00 | 2193.89 |
| LMS | 6 | 64.00 | 4530.51 |
| LMS | 7 | 128.00 | 3446.90 |
| LMS | 8 | 256.00 | 1554.01 |
| LMS | 9 | 512.00 | 1545.67 |
| LMS | -1 | 0.50 | 2420.96 |
| RR2 | 0 | 1.00 | 23231.09 |
| RR2 | 1 | 2.00 | 42443.71 |
| RR2 | 10 | 1024.00 | 3915.84 |

Table 6 (cont.)

| Site | Size class | Mass (ug) | Normalized biomass ($m^{-2}$) |
|---|---|---|---|
| RR2 | 11 | 2048.00 | 3331.35 |
| RR2 | 12 | 4096.00 | 2666.25 |
| RR2 | 13 | 8192.00 | 921.85 |
| RR2 | 14 | 16384.00 | 221.86 |
| RR2 | 15 | 32768.00 | 182.14 |
| RR2 | 16 | 65536.00 | 23.14 |
| RR2 | 2 | 4.00 | 26787.75 |
| RR2 | 3 | 8.00 | 23581.39 |
| RR2 | 4 | 16.00 | 15794.41 |
| RR2 | 5 | 32.00 | 14607.47 |
| RR2 | 6 | 64.00 | 9717.89 |
| RR2 | 7 | 128.00 | 7172.86 |
| RR2 | 8 | 256.00 | 7049.35 |
| RR2 | 9 | 512.00 | 5572.72 |
| RR2 | -1 | 0.50 | 30631.71 |
| RR2 | -2 | 0.25 | 1386.79 |
| RR3 | 0 | 1.00 | 1539.65 |
| RR3 | 1 | 2.00 | 2027.84 |
| RR3 | 10 | 1024.00 | 365.26 |
| RR3 | 11 | 2048.00 | 101.82 |
| RR3 | 12 | 4096.00 | 104.66 |
| RR3 | 13 | 8192.00 | 25.91 |
| RR3 | 14 | 16384.00 | 4.82 |
| RR3 | 15 | 32768.00 | 133.44 |
| RR3 | 16 | 65536.00 | 20.21 |
| RR3 | 2 | 4.00 | 1710.48 |
| RR3 | 3 | 8.00 | 324.83 |
| RR3 | 4 | 16.00 | 764.00 |
| RR3 | 5 | 32.00 | 1354.86 |
| RR3 | 6 | 64.00 | 2950.10 |
| RR3 | 7 | 128.00 | 2427.55 |
| RR3 | 8 | 256.00 | 2387.70 |
| RR3 | 9 | 512.00 | 476.90 |
| RR3 | -1 | 0.50 | 539.73 |
| RR3 | -2 | 0.25 | 2222.88 |
| BRA1 | 10 | 1024.00 | 320.00 |
| BRA1 | 11 | 2048.00 | 353.34 |
| BRA1 | 12 | 4096.00 | 154.32 |
| BRA1 | 13 | 8192.00 | 71.30 |
| BRA1 | 14 | 16384.00 | 25.04 |
| BRA1 | 15 | 32768.00 | 21.71 |
| BRA1 | 16 | 65536.00 | 10.00 |
| BRA1 | 2 | 4.00 | 445.15 |
| BRA1 | 3 | 8.00 | 847.69 |
| BRA1 | 4 | 16.00 | 1915.73 |
| BRA1 | 5 | 32.00 | 399.27 |
| BRA1 | 6 | 64.00 | 710.74 |
| BRA1 | 7 | 128.00 | 170.19 |

Table 6 (cont.)

| Site | Size class | Mass (ug) | Normalized biomass ($m^{-2}$) |
|---|---|---|---|
| BRA1 | 8 | 256.00 | 162.90 |
| BRA1 | 9 | 512.00 | 550.88 |
| BRA2 | 10 | 1024.00 | 1171.64 |
| BRA2 | 11 | 2048.00 | 853.36 |
| BRA2 | 12 | 4096.00 | 572.95 |
| BRA2 | 13 | 8192.00 | 288.01 |
| BRA2 | 14 | 16384.00 | 41.46 |
| BRA2 | 15 | 32768.00 | 23.15 |
| BRA2 | 16 | 65536.00 | 51.02 |
| BRA2 | 5 | 32.00 | 917.99 |
| BRA2 | 6 | 64.00 | 1597.00 |
| BRA2 | 7 | 128.00 | 1502.11 |
| BRA2 | 8 | 256.00 | 655.88 |
| BRA2 | 9 | 512.00 | 1243.99 |
| C9a | 0 | 1.00 | 2245.24 |
| C9a | 1 | 2.00 | 1717.72 |
| C9a | 10 | 1024.00 | 434.61 |
| C9a | 11 | 2048.00 | 570.82 |
| C9a | 12 | 4096.00 | 706.80 |
| C9a | 13 | 8192.00 | 42.75 |
| C9a | 14 | 16384.00 | 72.74 |
| C9a | 15 | 32768.00 | 39.18 |
| C9a | 16 | 65536.00 | 5.29 |
| C9a | 2 | 4.00 | 2752.62 |
| C9a | 3 | 8.00 | 1332.10 |
| C9a | 4 | 16.00 | 2505.25 |
| C9a | 5 | 32.00 | 1115.31 |
| C9a | 6 | 64.00 | 464.89 |
| C9a | 7 | 128.00 | 703.89 |
| C9a | 8 | 256.00 | 1020.13 |
| C9a | 9 | 512.00 | 437.10 |
| C9b | 1 | 2.00 | 1615.76 |
| C9b | 10 | 1024.00 | 23.31 |
| C9b | 11 | 2048.00 | 8.17 |
| C9b | 12 | 4096.00 | 11.63 |
| C9b | 16 | 65536.00 | 2.79 |
| C9b | 2 | 4.00 | 750.16 |
| C9b | 3 | 8.00 | 208.17 |
| C9b | 4 | 16.00 | 644.01 |
| C9b | 5 | 32.00 | 468.12 |
| C9b | 6 | 64.00 | 233.91 |
| C9b | 7 | 128.00 | 226.53 |
| C9b | 8 | 256.00 | 153.59 |
| C9b | 9 | 512.00 | 145.47 |

Table 7 – Normalized biomass per size class for crayfish in each site.

| Station | Size class | Mass (ug) | Normalized biomass ($m^{-2}$) |
|---|---|---|---|
| BEC | 16 | 65536 | 0.03 |
| BEC | 17 | 131072 | 0.08 |
| BEC | 18 | 262144 | 0.05 |
| BEC | 19 | 524288 | 0.13 |
| BEC | 23 | 8388608 | 0.08 |
| BECb | 17 | 131072 | 0.08 |
| BECb | 18 | 262144 | 0.09 |
| BECb | 19 | 524288 | 0.08 |
| BECb | 20 | 1048576 | 0.02 |
| BECb | 21 | 2097152 | 0.01 |
| BRA1 | 16 | 65536 | 0.07 |
| BRA1 | 17 | 131072 | 0.04 |
| BRA1 | 18 | 262144 | 0.05 |
| BRA1 | 20 | 1048576 | 0.02 |
| BRA1 | 22 | 4194304 | 0.08 |
| BRA1 | 23 | 8388608 | 0.04 |
| BRA1 | 24 | 16777216 | 0.07 |
| BRA2 | 20 | 1048576 | 0.07 |
| BRA2 | 21 | 2097152 | 0.81 |
| BRA2 | 22 | 4194304 | 1.39 |
| BRA2 | 23 | 8388608 | 0.70 |
| BRA2 | 24 | 16777216 | 0.14 |
| C2 | 21 | 2097152 | 0.09 |
| C2 | 22 | 4194304 | 0.04 |
| C2 | 23 | 8388608 | 0.03 |
| C3 | 16 | 65536 | 0.03 |
| C3 | 24 | 16777216 | 0.03 |
| C9b | 17 | 131072 | 0.03 |
| C9b | 18 | 262144 | 0.03 |
| C9b | 19 | 524288 | 0.02 |
| C9b | 23 | 8388608 | 0.02 |
| DT1 | 12 | 4096 | 0.23 |
| DT1 | 16 | 65536 | 0.04 |
| DT1 | 19 | 524288 | 0.18 |
| DT1 | 20 | 1048576 | 0.47 |
| DT1 | 21 | 2097152 | 0.23 |
| DT1 | 22 | 4194304 | 0.11 |
| DT2 | 12 | 4096 | 0.23 |
| DT2 | 19 | 524288 | 0.07 |
| DT2 | 20 | 1048576 | 0.14 |
| DT2 | 21 | 2097152 | 0.13 |
| DT2 | 22 | 4194304 | 0.06 |
| DT2 | 23 | 8388608 | 0.04 |
| LDS | 12 | 4096 | 0.04 |
| LDS | 19 | 524288 | 0.07 |
| LDS | 21 | 2097152 | 0.06 |
| LDS | 23 | 8388608 | 0.09 |
| LDS | 24 | 16777216 | 0.04 |

Table 7 (cont.)

| Station | Size class | Mass (ug) | Normalized biomass ($m^{-2}$) |
|---|---|---|---|
| LDSb | 16 | 65536 | 0.15 |
| LDSb | 23 | 8388608 | 0.21 |
| LDSb | 24 | 16777216 | 0.17 |
| RR2 | 15 | 32768 | 0.02 |
| RR2 | 16 | 65536 | 0.37 |
| RR2 | 17 | 131072 | 1.84 |
| RR2 | 18 | 262144 | 0.85 |
| RR2 | 19 | 524288 | 0.11 |
| RR2 | 20 | 1048576 | 0.04 |
| RR2 | 21 | 2097152 | 0.88 |
| RR2 | 22 | 4194304 | 0.20 |
| RR3 | 15 | 32768 | 0.04 |
| RR3 | 16 | 65536 | 0.05 |
| RR3 | 21 | 2097152 | 0.24 |
| RR3 | 22 | 4194304 | 0.17 |
| RR3 | 23 | 8388608 | 0.03 |

Table 8 – Normalized biomass in each size class for fish at each site.

| Station | Size class | Mass (ug) | Normalized biomass ($m^{-2}$) |
|---|---|---|---|
| BEC | 16 | 65536 | 0.08 |
| BEC | 17 | 131072 | 0.35 |
| BEC | 18 | 262144 | 0.13 |
| BEC | 19 | 524288 | 0.98 |
| BEC | 20 | 1048576 | 0.82 |
| BEC | 21 | 2097152 | 1.56 |
| BEC | 22 | 4194304 | 0.42 |
| BEC | 23 | 8388608 | 0.10 |
| BEC | 24 | 16777216 | 0.08 |
| BEC | 25 | 33554432 | 0.03 |
| BECb | 16 | 65536 | 0.04 |
| BECb | 17 | 131072 | 0.20 |
| BECb | 18 | 262144 | 0.49 |
| BECb | 19 | 524288 | 1.48 |
| BECb | 20 | 1048576 | 0.95 |
| BECb | 21 | 2097152 | 0.36 |
| BECb | 22 | 4194304 | 0.21 |
| BECb | 23 | 8388608 | 0.03 |
| BECb | 24 | 16777216 | 0.06 |
| BECb | 25 | 33554432 | 0.02 |
| BRA1 | 18 | 262144 | 0.21 |
| BRA1 | 19 | 524288 | 1.58 |
| BRA1 | 20 | 1048576 | 0.25 |
| BRA1 | 21 | 2097152 | 0.43 |
| BRA1 | 22 | 4194304 | 0.13 |
| BRA1 | 23 | 8388608 | 0.05 |
| BRA1 | 24 | 16777216 | 0.02 |
| BRA2 | 17 | 131072 | 0.03 |
| BRA2 | 18 | 262144 | 0.96 |
| BRA2 | 19 | 524288 | 1.77 |
| BRA2 | 20 | 1048576 | 0.31 |
| BRA2 | 21 | 2097152 | 1.41 |
| BRA2 | 22 | 4194304 | 0.58 |
| BRA2 | 23 | 8388608 | 0.23 |
| BRA2 | 24 | 16777216 | 0.21 |
| C2 | 15 | 32768 | 0.43 |
| C2 | 16 | 65536 | 0.06 |
| C2 | 19 | 524288 | 0.05 |
| C2 | 20 | 1048576 | 0.26 |
| C2 | 21 | 2097152 | 0.44 |
| C2 | 22 | 4194304 | 0.04 |
| C3 | 15 | 32768 | 0.13 |
| C3 | 16 | 65536 | 0.09 |
| C3 | 17 | 131072 | 0.03 |
| C3 | 19 | 524288 | 0.16 |
| C3 | 20 | 1048576 | 0.51 |
| C3 | 21 | 2097152 | 0.22 |
| C3 | 22 | 4194304 | 0.06 |

Table 8 (cont.)

| Station | Size class | Mass (ug) | Normalized biomass ($m^{-2}$) |
|---|---|---|---|
| C3 | 23 | 8388608 | 0.02 |
| C6 | 20 | 1048576 | 0.22 |
| C6 | 23 | 8388608 | 0.07 |
| C6 | 24 | 16777216 | 0.07 |
| C9a | 19 | 524288 | 0.06 |
| C9a | 20 | 1048576 | 0.03 |
| C9a | 21 | 2097152 | 0.47 |
| C9a | 22 | 4194304 | 0.18 |
| C9b | 17 | 131072 | 0.04 |
| C9b | 18 | 262144 | 0.34 |
| C9b | 19 | 524288 | 1.57 |
| C9b | 20 | 1048576 | 0.90 |
| C9b | 21 | 2097152 | 0.62 |
| C9b | 22 | 4194304 | 0.29 |
| C9b | 23 | 8388608 | 0.07 |
| C9b | 24 | 16777216 | 0.02 |
| DT1 | 15 | 32768 | 0.06 |
| DT1 | 16 | 65536 | 0.02 |
| DT1 | 17 | 131072 | 0.05 |
| DT1 | 19 | 524288 | 0.17 |
| DT1 | 20 | 1048576 | 0.95 |
| DT1 | 21 | 2097152 | 1.26 |
| DT1 | 22 | 4194304 | 0.49 |
| DT1 | 23 | 8388608 | 0.08 |
| DT1 | 24 | 16777216 | 0.03 |
| DT2 | 14 | 16384 | 0.05 |
| DT2 | 15 | 32768 | 0.48 |
| DT2 | 16 | 65536 | 0.75 |
| DT2 | 17 | 131072 | 0.95 |
| DT2 | 19 | 524288 | 0.13 |
| DT2 | 20 | 1048576 | 0.40 |
| DT2 | 21 | 2097152 | 1.10 |
| DT2 | 22 | 4194304 | 0.63 |
| LDS | 21 | 2097152 | 0.27 |
| LDS | 22 | 4194304 | 0.09 |
| LDSb | 17 | 131072 | 0.50 |
| LDSb | 18 | 262144 | 1.04 |
| LDSb | 19 | 524288 | 0.70 |
| LDSb | 21 | 2097152 | 1.01 |
| LDSb | 22 | 4194304 | 0.11 |
| LMS | 17 | 131072 | 0.08 |
| LMS | 18 | 262144 | 0.67 |
| LMS | 19 | 524288 | 1.45 |
| LMS | 20 | 1048576 | 0.99 |
| LMS | 21 | 2097152 | 1.04 |
| RR2 | 14 | 16384 | 0.33 |
| RR2 | 15 | 32768 | 2.58 |
| RR2 | 16 | 65536 | 2.84 |
| RR2 | 17 | 131072 | 1.12 |

Table 8 (cont.)

| Station | Size class | Mass (ug) | Normalized biomass ($m^{-2}$) |
|---|---|---|---|
| RR2 | 18 | 262144 | 1.49 |
| RR2 | 19 | 524288 | 0.28 |
| RR2 | 20 | 1048576 | 0.20 |
| RR2 | 21 | 2097152 | 0.27 |
| RR2 | 22 | 4194304 | 0.03 |
| RR3 | 14 | 16384 | 0.04 |
| RR3 | 15 | 32768 | 0.28 |
| RR3 | 16 | 65536 | 0.37 |
| RR3 | 17 | 131072 | 0.27 |
| RR3 | 18 | 262144 | 0.44 |
| RR3 | 19 | 524288 | 0.40 |
| RR3 | 20 | 1048576 | 0.24 |
| RR3 | 21 | 2097152 | 0.50 |
| RR3 | 22 | 4194304 | 0.17 |
| RR3 | 23 | 8388608 | 0.04 |

Table 9 – Normalized biomass per size class for combined data for macroinvertebrates, crayfish, and fish for all sites.

| Site | Size class | Mass (ug) | Normalized biomass ($m^{-2}$) |
|---|---|---|---|
| BEC | -2 | 0.25 | 1068.66 |
| BEC | -1 | 0.5 | 617.31 |
| BEC | 0 | 1 | 9997.69 |
| BEC | 1 | 2 | 21318.68 |
| BEC | 2 | 4 | 9596.19 |
| BEC | 3 | 8 | 5465.12 |
| BEC | 4 | 16 | 6014.34 |
| BEC | 5 | 32 | 7195.86 |
| BEC | 6 | 64 | 8563.73 |
| BEC | 7 | 128 | 8157.68 |
| BEC | 8 | 256 | 5399.23 |
| BEC | 9 | 512 | 8943.22 |
| BEC | 10 | 1024 | 3458.84 |
| BEC | 11 | 2048 | 2133.87 |
| BEC | 12 | 4096 | 2830.70 |
| BEC | 13 | 8192 | 1286.22 |
| BEC | 14 | 16384 | 240.12 |
| BEC | 15 | 32768 | 7.41 |
| BEC | 16 | 65536 | 0.10 |
| BEC | 17 | 131072 | 0.43 |
| BEC | 18 | 262144 | 0.19 |
| BEC | 19 | 524288 | 1.12 |
| BEC | 20 | 1048576 | 0.82 |
| BEC | 21 | 2097152 | 1.56 |
| BEC | 22 | 4194304 | 0.42 |
| BEC | 23 | 8388608 | 0.19 |
| BEC | 24 | 16777216 | 0.08 |
| BEC | 25 | 33554432 | 0.03 |
| BECb | -1 | 0.5 | 1543.29 |
| BECb | 0 | 1 | 31321.07 |
| BECb | 1 | 2 | 54469.83 |
| BECb | 2 | 4 | 25295.50 |
| BECb | 3 | 8 | 21488.16 |
| BECb | 4 | 16 | 10421.67 |
| BECb | 5 | 32 | 8560.18 |
| BECb | 6 | 64 | 7991.51 |
| BECb | 7 | 128 | 4293.63 |
| BECb | 8 | 256 | 3613.69 |
| BECb | 9 | 512 | 2673.74 |
| BECb | 10 | 1024 | 723.86 |
| BECb | 11 | 2048 | 466.24 |
| BECb | 12 | 4096 | 254.00 |
| BECb | 13 | 8192 | 94.80 |
| BECb | 14 | 16384 | 7.36 |
| BECb | 15 | 32768 | 35.77 |
| BECb | 16 | 65536 | 0.04 |
| BECb | 17 | 131072 | 0.28 |
| BECb | 18 | 262144 | 0.58 |
| BECb | 19 | 524288 | 1.56 |
| BECb | 20 | 1048576 | 0.97 |
| BECb | 21 | 2097152 | 0.38 |
| BECb | 22 | 4194304 | 0.21 |
| BECb | 23 | 8388608 | 0.03 |
| BECb | 24 | 16777216 | 0.06 |
| BECb | 25 | 33554432 | 0.02 |
| BRA1 | 2 | 4 | 445.15 |
| BRA1 | 3 | 8 | 847.69 |
| BRA1 | 4 | 16 | 1915.73 |
| BRA1 | 5 | 32 | 399.27 |
| BRA1 | 6 | 64 | 710.74 |
| BRA1 | 7 | 128 | 170.19 |
| BRA1 | 8 | 256 | 162.90 |
| BRA1 | 9 | 512 | 550.88 |
| BRA1 | 10 | 1024 | 320.00 |
| BRA1 | 11 | 2048 | 353.34 |
| BRA1 | 12 | 4096 | 154.32 |
| BRA1 | 13 | 8192 | 71.30 |
| BRA1 | 14 | 16384 | 25.04 |
| BRA1 | 15 | 32768 | 21.71 |
| BRA1 | 16 | 65536 | 10.07 |
| BRA1 | 17 | 131072 | 0.04 |
| BRA1 | 18 | 262144 | 0.27 |
| BRA1 | 19 | 524288 | 1.58 |
| BRA1 | 20 | 1048576 | 0.27 |
| BRA1 | 21 | 2097152 | 0.43 |
| BRA1 | 22 | 4194304 | 0.20 |
| BRA1 | 23 | 8388608 | 0.08 |
| BRA1 | 24 | 16777216 | 0.08 |
| BRA2 | 5 | 32 | 917.99 |
| BRA2 | 6 | 64 | 1597.00 |
| BRA2 | 7 | 128 | 1502.11 |
| BRA2 | 8 | 256 | 655.88 |
| BRA2 | 9 | 512 | 1243.99 |
| BRA2 | 10 | 1024 | 1171.64 |
| BRA2 | 11 | 2048 | 853.36 |
| BRA2 | 12 | 4096 | 572.95 |
| BRA2 | 13 | 8192 | 288.01 |
| BRA2 | 14 | 16384 | 41.46 |
| BRA2 | 15 | 32768 | 23.15 |
| BRA2 | 16 | 65536 | 51.02 |
| BRA2 | 17 | 131072 | 0.03 |
| BRA2 | 18 | 262144 | 0.96 |

Table 9 (cont.)

| Site | Size class | Mass (ug) | Normalized biomass ($m^{-2}$) |
|---|---|---|---|
| BRA2 | 19 | 524288 | 1.77 |
| BRA2 | 20 | 1048576 | 0.37 |
| BRA2 | 21 | 2097152 | 2.23 |
| BRA2 | 22 | 4194304 | 1.97 |
| BRA2 | 23 | 8388608 | 0.93 |
| BRA2 | 24 | 16777216 | 0.34 |
| C2 | -3 | 0.125 | 1879.07 |
| C2 | -1 | 0.5 | 15208.04 |
| C2 | 0 | 1 | 15802.69 |
| C2 | 1 | 2 | 2583.49 |
| C2 | 2 | 4 | 2589.61 |
| C2 | 3 | 8 | 1764.11 |
| C2 | 4 | 16 | 975.49 |
| C2 | 5 | 32 | 721.48 |
| C2 | 6 | 64 | 361.91 |
| C2 | 7 | 128 | 411.49 |
| C2 | 8 | 256 | 294.01 |
| C2 | 9 | 512 | 339.52 |
| C2 | 10 | 1024 | 226.32 |
| C2 | 11 | 2048 | 202.14 |
| C2 | 12 | 4096 | 97.70 |
| C2 | 13 | 8192 | 43.22 |
| C2 | 14 | 16384 | 26.20 |
| C2 | 15 | 32768 | 12.87 |
| C2 | 16 | 65536 | 0.06 |
| C2 | 17 | 131072 | 1.94 |
| C2 | 18 | 262144 | 1.99 |
| C2 | 19 | 524288 | 0.05 |
| C2 | 20 | 1048576 | 0.26 |
| C2 | 21 | 2097152 | 0.53 |
| C2 | 22 | 4194304 | 0.08 |
| C2 | 23 | 8388608 | 0.03 |
| C3 | 0 | 1 | 468.03 |
| C3 | 1 | 2 | 1186.97 |
| C3 | 2 | 4 | 1000.42 |
| C3 | 3 | 8 | 404.96 |
| C3 | 4 | 16 | 30.56 |
| C3 | 5 | 32 | 634.69 |
| C3 | 6 | 64 | 1394.91 |
| C3 | 7 | 128 | 708.68 |
| C3 | 8 | 256 | 222.44 |
| C3 | 9 | 512 | 390.19 |
| C3 | 10 | 1024 | 220.66 |
| C3 | 11 | 2048 | 137.02 |
| C3 | 12 | 4096 | 40.55 |
| C3 | 13 | 8192 | 16.56 |
| C3 | 14 | 16384 | 8.76 |
| C3 | 15 | 32768 | 17.63 |
| C3 | 16 | 65536 | 2.41 |
| C3 | 17 | 131072 | 0.03 |
| C3 | 19 | 524288 | 0.16 |
| C3 | 20 | 1048576 | 0.51 |
| C3 | 21 | 2097152 | 0.22 |
| C3 | 22 | 4194304 | 0.06 |
| C3 | 23 | 8388608 | 0.02 |
| C3 | 24 | 16777216 | 0.03 |
| C6 | 1 | 2 | 137.62 |
| C6 | 2 | 4 | 334.12 |
| C6 | 3 | 8 | 84.16 |
| C6 | 4 | 16 | 669.19 |
| C6 | 5 | 32 | 235.31 |
| C6 | 6 | 64 | 398.03 |
| C6 | 7 | 128 | 320.99 |
| C6 | 8 | 256 | 407.37 |
| C6 | 9 | 512 | 388.94 |
| C6 | 10 | 1024 | 241.51 |
| C6 | 11 | 2048 | 80.95 |
| C6 | 12 | 4096 | 136.17 |
| C6 | 13 | 8192 | 145.15 |
| C6 | 14 | 16384 | 22.25 |
| C6 | 15 | 32768 | 22.54 |
| C6 | 16 | 65536 | 25.91 |
| C6 | 20 | 1048576 | 0.22 |
| C6 | 23 | 8388608 | 0.07 |
| C6 | 24 | 16777216 | 0.07 |
| C9a | 0 | 1 | 2245.24 |
| C9a | 1 | 2 | 1717.72 |
| C9a | 2 | 4 | 2752.62 |
| C9a | 3 | 8 | 1332.10 |
| C9a | 4 | 16 | 2505.25 |
| C9a | 5 | 32 | 1115.31 |
| C9a | 6 | 64 | 464.89 |
| C9a | 7 | 128 | 703.89 |
| C9a | 8 | 256 | 1020.13 |
| C9a | 9 | 512 | 437.10 |
| C9a | 10 | 1024 | 434.61 |
| C9a | 11 | 2048 | 570.82 |
| C9a | 12 | 4096 | 706.80 |
| C9a | 13 | 8192 | 42.75 |
| C9a | 14 | 16384 | 72.74 |
| C9a | 15 | 32768 | 39.18 |
| C9a | 16 | 65536 | 5.29 |
| C9a | 19 | 524288 | 0.06 |
| C9a | 20 | 1048576 | 0.03 |
| C9a | 21 | 2097152 | 0.47 |
| C9a | 22 | 4194304 | 0.18 |
| C9b | 1 | 2 | 1615.76 |
| C9b | 2 | 4 | 750.16 |

Table 9 (cont.)

| Site | Size class | Mass (ug) | Normalized biomass ($m^{-2}$) |
|---|---|---|---|
| C9b | 3 | 8 | 208.17 |
| C9b | 4 | 16 | 644.01 |
| C9b | 5 | 32 | 468.12 |
| C9b | 6 | 64 | 233.91 |
| C9b | 7 | 128 | 226.53 |
| C9b | 8 | 256 | 153.59 |
| C9b | 9 | 512 | 145.47 |
| C9b | 10 | 1024 | 23.31 |
| C9b | 11 | 2048 | 8.17 |
| C9b | 12 | 4096 | 11.63 |
| C9b | 16 | 65536 | 2.79 |
| C9b | 17 | 131072 | 0.07 |
| C9b | 18 | 262144 | 0.37 |
| C9b | 19 | 524288 | 1.59 |
| C9b | 20 | 1048576 | 0.90 |
| C9b | 21 | 2097152 | 0.62 |
| C9b | 22 | 4194304 | 0.29 |
| C9b | 23 | 8388608 | 0.09 |
| C9b | 24 | 16777216 | 0.02 |
| DT1 | -3 | 0.125 | 6607.27 |
| DT1 | 0 | 1 | 1309.24 |
| DT1 | 1 | 2 | 1441.03 |
| DT1 | 2 | 4 | 694.09 |
| DT1 | 3 | 8 | 217.58 |
| DT1 | 4 | 16 | 90.51 |
| DT1 | 5 | 32 | 304.64 |
| DT1 | 6 | 64 | 887.26 |
| DT1 | 7 | 128 | 829.71 |
| DT1 | 8 | 256 | 635.85 |
| DT1 | 9 | 512 | 482.92 |
| DT1 | 10 | 1024 | 95.75 |
| DT1 | 11 | 2048 | 219.32 |
| DT1 | 12 | 4096 | 180.29 |
| DT1 | 13 | 8192 | 84.36 |
| DT1 | 14 | 16384 | 162.96 |
| DT1 | 15 | 32768 | 24.99 |
| DT1 | 16 | 65536 | 3.69 |
| DT1 | 17 | 131072 | 0.05 |
| DT1 | 19 | 524288 | 0.35 |
| DT1 | 20 | 1048576 | 1.42 |
| DT1 | 21 | 2097152 | 1.50 |
| DT1 | 22 | 4194304 | 0.60 |
| DT1 | 23 | 8388608 | 0.08 |
| DT1 | 24 | 16777216 | 0.03 |
| DT2 | -3 | 0.125 | 1404.39 |
| DT2 | -2 | 0.25 | 763.90 |
| DT2 | -1 | 0.5 | 9700.82 |
| DT2 | 0 | 1 | 11326.49 |
| DT2 | 1 | 2 | 9713.37 |

| Site | Size class | Mass (ug) | Normalized biomass ($m^{-2}$) |
|---|---|---|---|
| DT2 | 2 | 4 | 10206.14 |
| DT2 | 3 | 8 | 4476.25 |
| DT2 | 4 | 16 | 2252.68 |
| DT2 | 5 | 32 | 2269.61 |
| DT2 | 6 | 64 | 2247.47 |
| DT2 | 7 | 128 | 1498.24 |
| DT2 | 8 | 256 | 2123.59 |
| DT2 | 9 | 512 | 847.73 |
| DT2 | 10 | 1024 | 444.31 |
| DT2 | 11 | 2048 | 360.48 |
| DT2 | 12 | 4096 | 76.75 |
| DT2 | 13 | 8192 | 112.64 |
| DT2 | 14 | 16384 | 60.62 |
| DT2 | 15 | 32768 | 71.05 |
| DT2 | 16 | 65536 | 0.75 |
| DT2 | 17 | 131072 | 0.95 |
| DT2 | 19 | 524288 | 0.20 |
| DT2 | 20 | 1048576 | 0.55 |
| DT2 | 21 | 2097152 | 1.23 |
| DT2 | 22 | 4194304 | 0.68 |
| DT2 | 23 | 8388608 | 0.04 |
| LDS | 0 | 1 | 1827.43 |
| LDS | 1 | 2 | 2645.99 |
| LDS | 2 | 4 | 1890.18 |
| LDS | 3 | 8 | 1082.39 |
| LDS | 4 | 16 | 1272.59 |
| LDS | 5 | 32 | 1134.28 |
| LDS | 6 | 64 | 1342.21 |
| LDS | 7 | 128 | 834.97 |
| LDS | 8 | 256 | 987.24 |
| LDS | 9 | 512 | 325.31 |
| LDS | 10 | 1024 | 27.24 |
| LDS | 11 | 2048 | 138.75 |
| LDS | 12 | 4096 | 87.51 |
| LDS | 13 | 8192 | 11.73 |
| LDS | 14 | 16384 | 32.86 |
| LDS | 15 | 32768 | 2.30 |
| LDS | 16 | 65536 | 3.99 |
| LDS | 19 | 524288 | 0.07 |
| LDS | 21 | 2097152 | 0.33 |
| LDS | 22 | 4194304 | 0.09 |
| LDS | 23 | 8388608 | 0.09 |
| LDS | 24 | 16777216 | 0.04 |
| LDS2 | -3 | 0.125 | 1914.09 |
| LDS2 | -2 | 0.25 | 7100.49 |
| LDS2 | -1 | 0.5 | 7257.46 |
| LDS2 | 0 | 1 | 3813.29 |
| LDS2 | 1 | 2 | 5710.47 |
| LDS2 | 2 | 4 | 6060.23 |

Table 9 (cont.)

| Site | Size class | Mass (ug) | Normalized biomass ($m^{-2}$) |
|---|---|---|---|
| LDS2 | 3 | 8 | 4203.09 |
| LDS2 | 4 | 16 | 1820.76 |
| LDS2 | 5 | 32 | 3512.38 |
| LDS2 | 6 | 64 | 6307.79 |
| LDS2 | 7 | 128 | 7288.08 |
| LDS2 | 8 | 256 | 1370.10 |
| LDS2 | 9 | 512 | 1346.38 |
| LDS2 | 10 | 1024 | 1207.78 |
| LDS2 | 11 | 2048 | 805.81 |
| LDS2 | 12 | 4096 | 10.86 |
| LDS2 | 13 | 8192 | 26.74 |
| LDSb | 0 | 1 | 1103.01 |
| LDSb | 1 | 2 | 859.65 |
| LDSb | 2 | 4 | 660.80 |
| LDSb | 3 | 8 | 595.18 |
| LDSb | 4 | 16 | 220.12 |
| LDSb | 5 | 32 | 56.71 |
| LDSb | 6 | 64 | 104.28 |
| LDSb | 7 | 128 | 36.07 |
| LDSb | 8 | 256 | 7.23 |
| LDSb | 9 | 512 | 16.78 |
| LDSb | 10 | 1024 | 20.40 |
| LDSb | 11 | 2048 | 14.84 |
| LDSb | 12 | 4096 | 18.47 |
| LDSb | 13 | 8192 | 4.38 |
| LDSb | 16 | 65536 | 0.15 |
| LDSb | 17 | 131072 | 0.50 |
| LDSb | 18 | 262144 | 1.04 |
| LDSb | 19 | 524288 | 0.70 |
| LDSb | 21 | 2097152 | 1.01 |
| LDSb | 22 | 4194304 | 0.11 |
| LDSb | 23 | 8388608 | 0.21 |
| LDSb | 24 | 16777216 | 0.17 |
| LMS | -1 | 0.5 | 2420.96 |
| LMS | 0 | 1 | 1081.80 |
| LMS | 1 | 2 | 5176.50 |
| LMS | 2 | 4 | 3121.03 |
| LMS | 3 | 8 | 2380.81 |
| LMS | 4 | 16 | 2657.65 |
| LMS | 5 | 32 | 2193.89 |
| LMS | 6 | 64 | 4530.51 |
| LMS | 7 | 128 | 3446.90 |
| LMS | 8 | 256 | 1554.01 |
| LMS | 9 | 512 | 1545.67 |
| LMS | 10 | 1024 | 1053.01 |
| LMS | 11 | 2048 | 424.82 |
| LMS | 12 | 4096 | 509.83 |
| LMS | 13 | 8192 | 137.20 |

| Site | Size class | Mass (ug) | Normalized biomass ($m^{-2}$) |
|---|---|---|---|
| LMS | 17 | 131072 | 0.08 |
| LMS | 18 | 262144 | 0.67 |
| LMS | 19 | 524288 | 1.45 |
| LMS | 20 | 1048576 | 0.99 |
| LMS | 21 | 2097152 | 1.04 |
| RR2 | -2 | 0.25 | 1386.79 |
| RR2 | -1 | 0.5 | 30631.71 |
| RR2 | 0 | 1 | 23231.09 |
| RR2 | 1 | 2 | 42443.71 |
| RR2 | 2 | 4 | 26787.75 |
| RR2 | 3 | 8 | 23581.39 |
| RR2 | 4 | 16 | 15794.41 |
| RR2 | 5 | 32 | 14607.47 |
| RR2 | 6 | 64 | 9717.89 |
| RR2 | 7 | 128 | 7172.86 |
| RR2 | 8 | 256 | 7049.35 |
| RR2 | 9 | 512 | 5572.72 |
| RR2 | 10 | 1024 | 3915.84 |
| RR2 | 11 | 2048 | 3331.35 |
| RR2 | 12 | 4096 | 2666.25 |
| RR2 | 13 | 8192 | 921.85 |
| RR2 | 14 | 16384 | 222.19 |
| RR2 | 15 | 32768 | 184.74 |
| RR2 | 16 | 65536 | 26.35 |
| RR2 | 17 | 131072 | 2.96 |
| RR2 | 18 | 262144 | 2.34 |
| RR2 | 19 | 524288 | 0.38 |
| RR2 | 20 | 1048576 | 0.24 |
| RR2 | 21 | 2097152 | 1.15 |
| RR2 | 22 | 4194304 | 0.23 |
| RR3 | -2 | 0.25 | 2222.88 |
| RR3 | -1 | 0.5 | 539.73 |
| RR3 | 0 | 1 | 1539.65 |
| RR3 | 1 | 2 | 2027.84 |
| RR3 | 2 | 4 | 1710.48 |
| RR3 | 3 | 8 | 324.83 |
| RR3 | 4 | 16 | 764.00 |
| RR3 | 5 | 32 | 1354.86 |
| RR3 | 6 | 64 | 2950.10 |
| RR3 | 7 | 128 | 2427.55 |
| RR3 | 8 | 256 | 2387.70 |
| RR3 | 9 | 512 | 476.90 |
| RR3 | 10 | 1024 | 365.26 |
| RR3 | 11 | 2048 | 101.82 |
| RR3 | 12 | 4096 | 104.66 |
| RR3 | 13 | 8192 | 25.91 |
| RR3 | 14 | 16384 | 4.86 |
| RR3 | 15 | 32768 | 133.76 |

Table 9 (cont.)

| Site | Size class | Mass (ug) | Normalized biomass ($m^{-2}$) |
|---|---|---|---|
| RR3 | 16 | 65536 | 20.63 |
| RR3 | 17 | 131072 | 0.27 |
| RR3 | 18 | 262144 | 0.44 |
| RR3 | 19 | 524288 | 0.40 |
| RR3 | 20 | 1048576 | 0.24 |
| RR3 | 21 | 2097152 | 0.75 |
| RR3 | 22 | 4194304 | 0.34 |
| RR3 | 23 | 8388608 | 0.06 |

# Appendix B – Substrate Program Code

The following is the code for the substrate analysis program described in Chapter 4. This code was used in Visual Basic 6.0. Please note that file locations have been replaced by names describing the input and output files. Several steps require input from the user on the Visual Basic form for the program.

## Declarations

```
Option Explicit

Dim sngLong!, sngLength!, sngZ!, strShape$, strBuried$, strDirection$, sngWidth!, sngCut!, sngX!,
sngLToMax!
'These are long axis, horiz. profile length, Z, shape, whether buried, and then direction for
'P and E (apex or no, lengthwise or no), width (base of P or short axis for E), and length from edge to
profile
'sngX is the x-value along the profile. sngLToMax is the length along the profile to the maximum Z
(because won't always be half)

Dim sngFirstHyp!, sngSecondHyp!, sngFirstTan!, sngSecondTan! 'these are hyp and cos theta for
beginning and end of pyramid (profile)

Dim sngNewZ!, sngXmax! 'This is the Z that is calculated for the profile, and the maximum X value for a
rock

Dim sngStart! 'The x value for the start of a rock (used for ellipse)

Dim sngSurface!, sngHalf! 'half is the length at which you're at the maximum z (to start decreasing z)

Public Function ArcCos(ByVal X As Double) As Double 'Function to calculate ArcCos because there is no
built-in code
  If X <> 1 Then
    ArcCos = Atn(-X / Sqr(-X * X + 1)) + 2 * Atn(1)
  Else
    ArcCos = 0
  End If
End Function
```

## Calculate z-values

```
Private Sub cmdCalculateZ_Click()

Dim strStream$, strSite$, strFilename$, strZOutput$

strStream = txtStream.Text 'Gets the stream code for Output
strSite = txtSite.Text  'Gets the profile code for Output file
strFilename = txtFilename.Text  'File to be read for analysis
strZOutput = Path for file location & strSite & "withZ.csv"
'Creates output file that will show Z values (with other data) that has profile name in
'file title

Open strFilename For Input As #1
```

```
  Open strZOutput For Append As #2

    Do

      sngZ = 0  'Reset to 0

      Input #1, sngLong, sngLength, strShape, strBuried, strDirection, sngLToMax, sngWidth, sngCut
        If strBuried = "Y" Then
          If strShape = "E" Then
            sngZ = sngLong * 0.511
            Call ellipseZ
          End If
          If strShape = "P" Then
            sngZ = sngLong * 0.626
            Call pyramidZ
          End If
          If strShape = "R" Then sngZ = 0.5 * (sngLong * 0.374)
          If strShape = "S" Then sngZ = 0.5 * (sngLong * 0.687)
          If strShape = "F" Then sngZ = 0
          'Calculated Z based on shape of rock. Multiplies length of long by
          'value for % of long that Z was on average for each shape, divided by half for buried
          'For ellipse and pyramid, calls subroutine to calculate Z for the cut scenario
        Else
          If strBuried = "N" Then
            If strShape = "E" Then
              sngZ = sngLong * 0.51
              Call ellipseZ
            End If
            If strShape = "P" Then
              sngZ = sngLong * 0.627
              Call pyramidZ
            End If
            If strShape = "R" Then sngZ = sngLong * 0.391
            If strShape = "S" Then sngZ = sngLong * 0.702
            If strShape = "F" Then sngZ = 0
            'Calculated Z based on shape of rock. Multiplies length of long by
            'value for % of long that Z was on average for each shape
            'For ellipse and pyramid, calls subroutine to calculate Z for the cut scenario (no buried)
          End If
        End If

      Write #2, sngLong, sngLength, sngZ, strShape, strBuried, strDirection, sngLToMax, sngWidth,
sngCut
      'Writes data for that rock to output file.
    Loop Until (EOF(1) = True)

  Close #2
Close #1

MsgBox ("Z values have been calculated.")

End Sub
```

*Ellipse sub-program for z-calculation*

```
Private Sub ellipseZ()
```

```
Const sngPi! = 3.14159265358979
Dim sngA!, sngB!, sngX2!, sngC!, sngE!, sngS!, sngR!, sngCos!, sngTheta!
'a and b are submajor and subminor axes. X2 is length from center to cut, c is length from center to focus.
'e is eccentricity, s is length of adjacent for new Z triangle, r is length of hypoteneuse.

'Set all to 0
sngA = 0
sngB = 0
sngX2 = 0
sngC = 0
sngE = 0
sngS = 0
sngR = 0
sngCos = 0
sngTheta = 0

sngA = sngLong / 2
sngB = sngZ / 2

If strDirection = "Y" Then

   sngZ = sngZ

Else
   If strDirection = "N" Then

      sngX2 = sngA - sngCut
      sngC = Sqr((sngA ^ 2) - (sngB ^ 2))
      sngE = sngC / sngA
      sngS = sngX2 - sngC

      sngR = sngA * (1 - sngE ^ 2) - sngE * (sngS)

      'No ArcCos, so using code found online (multiple places)
      sngCos = sngS / sngR
      If Abs(sngCos) <> 1 Then
         sngTheta = Atn(-sngCos / Sqr(-sngCos * sngCos + 1)) + 2 * Atn(1)
      Else
         sngTheta = IIf(sngCos = 1, 0, Atn(1) * 4)
      End If

      sngZ = sngR * Sin(sngTheta)

      sngZ = 2 * sngZ

   End If
End If


End Sub
```

*Pyramid sub-program for z-calculation*

```
Private Sub pyramidZ()
```

```
Dim sngHyp!, sngLong2!, sngTanAngle!, sngEdge!
'For non-apex. Long2 is length from apex to edge, Hyp is for Z and Long2 triangle. TanAngle is where Hyp
meets Long2.
'Edge is the edge length (calculated, no sqrt)

'Set all to 0 to start
sngHyp = 0
sngLong2 = 0
sngTanAngle = 0
sngEdge = 0

If strDirection = "Y" Then

   sngZ = sngZ

Else
   If strDirection = "N" Then

      sngEdge = (sngZ ^ 2) + ((1 / 3) * (sngWidth ^ 2))
      sngHyp = Sqr(sngEdge)

      sngLong2 = Sqr((sngHyp ^ 2) - (sngZ ^ 2))

      sngTanAngle = (sngZ) / sngLong2

      sngZ = sngTanAngle * sngCut

   End If
End If


End Sub
Public Function ArcCos(ByVal X As Double) As Double
   If X <> 1 Then
      ArcCos = Atn(-X / Sqr(-X * X + 1)) + 2 * Atn(1)
   Else
      ArcCos = 0
   End If
End Function
```

## Profile extraction

```
Private Sub cmdSurface_Click()

Dim strStream$, strSite$, strFilename$, strOutput$
Dim sngEnd! 'For pyramid calc, length between middle and Xmax

strStream = txtStream.Text 'Gets the stream code for Output
strSite = txtSite.Text  'Gets the profile code for Output file
strFilename = Path for file location & strSite & "withZ.csv"
'File to be read for analysis (file created in last step)
strOutput = Path for file location & strSite & "ProfileCoordinatesXZ.csv"
'Creates output file that will show the input data and the calculated surface length
'for each rock

Open strFilename For Input As #1
```

```
Open strOutput For Append As #2

  sngX = 0
  sngXmax = 0
  sngNewZ = 0

  Write #2, sngX, sngNewZ
  'Puts initial X and Z at (0,0)

  Do

    Input #1, sngLong, sngLength, sngZ, strShape, strBuried, strDirection, sngLToMax, sngWidth,
     sngCut

    sngX = sngX + 0.1 'Moves to next x value
    sngStart = sngX
    sngXmax = sngStart + Round(sngLength, 1)  'Sets value along X axis for end of rock
    sngHalf = sngStart + Round(sngLToMax, 1)  'Sets value along X axis for max height of rock
    'Sets beginning x, as well as half-way x and max x for rock

    If strShape = "R" Then sngNewZ = sngZ
    If strShape = "S" Then sngNewZ = sngZ
    If strShape = "F" Then sngNewZ = sngZ
    If strShape = "P" Then
      sngFirstTan = sngZ / (sngHalf - sngX)
      sngEnd = sngXmax - sngHalf
      sngSecondTan = sngZ / sngEnd
      'Determines tan theta for first and second half of pyramid for calculation of Z values
      sngNewZ = 0  'Initial Z value for pyramid is 0, starting at base
    End If
    If strShape = "E" Then
      If strDirection = "Y" Then
        sngNewZ = 0
      Else
        If strDirection = "N" Then
          sngNewZ = 0
        End If
      End If

    End If

    Write #2, sngX, sngNewZ

    For sngX = (sngStart + 0.1) To sngXmax Step 0.1

        If strShape = "R" Then
          If (sngXmax - sngX) < 0.1 Then
            sngNewZ = 0
          Else
            If (sngXmax - sngX) > 0.1 Then sngNewZ = sngNewZ
          End If
        End If  'Height will be Z for length, until end when it drops back to 0
        If strShape = "S" Then
          If (sngXmax - sngX) < 0.1 Then
            sngNewZ = 0
          Else
```

```
            If (sngXmax - sngX) > 0.1 Then sngNewZ = sngNewZ
          End If
        End If  'Height will be Z for length, until end when it drops back to 0
        If strShape = "E" Then Call ellipseprofile
        If strShape = "P" Then Call pyramidprofile
        If strShape = "F" Then sngZ = sngZ


      Write #2, sngX, sngNewZ

    Next sngX


  Loop Until (EOF(1) = True)

  sngX = sngX + 0.1
  sngNewZ = 0

  Write #2, sngX, sngNewZ

 Close #2
Close #1

MsgBox ("Profile has been calculated.")

End Sub
```

*Ellipse sub-program for profile extraction*

```
Private Sub ellipseprofile()

Dim sngA!, sngB!, sngX2!, sngC!, sngE!, sngS!, sngR!, sngT!, sngCos!, sngTheta!
'a and b are submajor and subminor axes. X2 is length from center to cut, c is length from center to focus.
'e is eccentricity, s is length of adjacent for new Z triangle, r is length of hypoteneuse. T is equiv. of "cut"

'Set all to 0
sngA = 0
sngB = 0
sngT = 0
sngX2 = 0
sngC = 0
sngE = 0
sngS = 0
sngR = 0
sngCos = 0
sngTheta = 0


sngB = sngZ / 2


 If sngX = sngHalf Then
   sngNewZ = sngB
 Else
   If sngX < sngHalf Then
     sngT = sngX - sngStart
```

```
    sngA = sngLToMax
    If sngA < sngB Then
      sngNewZ = sngB
    Else
      sngX2 = sngA - sngT
      sngC = Sqr(Abs((sngA ^ 2) - (sngB ^ 2)))
      sngE = sngC / sngA
      sngS = sngX2 - sngC

      sngR = sngA * (1 - sngE ^ 2) - sngE * (sngS)

      'No ArcCos, so using code found online (multiple places)
      sngCos = sngS / sngR

      If Abs(sngCos) <> 1 Then
      sngTheta = Atn(-sngCos / Sqr(-sngCos * sngCos + 1)) + 2 * Atn(1)
        Else
        sngTheta = IIf(sngCos = 1, 0, Atn(1) * 4)
      End If

      sngNewZ = sngR * Sin(sngTheta)
    End If

  Else
    If sngX > sngHalf Then
      sngT = sngXmax - sngX
      If sngT < 0.1 Then
        sngNewZ = 0
      Else

      sngA = sngLength - sngLToMax
      If sngA < sngB Then
        sngNewZ = sngB
      Else
        sngX2 = sngA - sngT
        sngC = Sqr(Abs((sngA ^ 2) - (sngB ^ 2)))
        sngE = sngC / sngA
        sngS = sngX2 - sngC

        sngR = sngA * (1 - sngE ^ 2) - sngE * (sngS)

        'No ArcCos, so using code found online (multiple places)
        sngCos = sngS / sngR

        If Abs(sngCos) <> 1 Then
          sngTheta = Atn(-sngCos / Sqr(-sngCos * sngCos + 1)) + 2 * Atn(1)
        Else
          sngTheta = IIf(sngCos = 1, 0, Atn(1) * 4)
        End If

        sngNewZ = sngR * Sin(sngTheta)
      End If
      End If

    End If
  End If
```

```
    End If

    If strBuried = "N" Then
      If sngNewZ > 0 Then
        sngNewZ = sngNewZ + (0.5 * sngZ)
      Else
        sngNewZ = 0
      End If
    End If

End Sub
```

*Pyramid sub-program for profile extraction*

```
Private Sub pyramidprofile()

Dim sngZIncrease!, sngZDecrease! 'The change in Z with increase in X
Dim sngHyp

If sngX = sngHalf Then

   sngNewZ = sngZ

Else
   If sngX < sngHalf Then

      sngZIncrease = sngFirstTan * 0.1
      sngNewZ = sngNewZ + sngZIncrease

   Else
      If sngX > sngHalf Then

         sngZDecrease = sngSecondTan * 0.1
         sngNewZ = sngNewZ - sngZDecrease

      End If
   End If
End If


End Sub
```

## Fitting macroinvertebrates to profiles

```
Private Sub cmdBugs_Click()

Dim strStream$, strSite$, strFilename$, strOutput$, strMaxLengthFile$, strHorizontalProfileFile$,
strTaxon$
Dim sngSC(1 To 50) As Single, sngMaxLength(1 To 50) As Single
Dim intB%, intEnd% 'The values for the length array
Dim intMinSC%, intMaxSC% 'Range of size classes input by user
Dim sngHorizontal!, sngProfile! 'The horizontal and 3D lengths of the profile, respectively
Dim sngNumber! 'The number of organisms that can fit on the profile
Dim sngCorrNumber! 'Number of organisms corrected for horizontal profile length
```

```
Dim sngX(1 To 10000) As Single, sngZ(1 To 10000) As Single, sngH(1 To 10000) As Single, sngA(1 To
10000) As Single
'Arrays for moving along profile - X, Z values, hypoteneuse value, angle value.
Dim sngHyp!, sngSumH!, intR%, intN%
'H is hypoteneuse length, SumH is profile length. R is array number, N is total number of rows in array.
Dim sngExtra!, intHInt% 'Values for non-flexible
Dim strSiteProfile$ 'The profile name to be read from Horizontal Profile File

strStream = txtStream.Text 'Gets the stream code for Output
strSite = txtSite.Text  'Gets the profile code for Output file
strTaxon = txtOrganism.Text 'Gets the taxon from the text box on the form
strFilename = Path for file location & strSite & "ProfileCoordinatesXZ.csv"
'File to be read for analysis (file created in last step)
strOutput = Path for file location & strSite & "SizeClassResults.csv"
'Creates output file that will show the results for each size class


  strMaxLengthFile = Path for file location & strStream & "MaxLength.csv"

  strHorizontalProfileFile = Path for file location strStream & "HorizontalProfiles.csv"

  Open strFilename For Input As #1
  Open strOutput For Append As #2
  Open strMaxLengthFile For Input As #3

  Open strHorizontalProfileFile For Input As #4

  sngHorizontal = 0

  Do
    Input #4, strSiteProfile, sngHorizontal

  Loop Until strSiteProfile = strSite

  intR = 0
  intB = 0

  Do Until (EOF(1) = True)
    intR = intR + 1
    Input #1, sngX(intR), sngZ(intR)
  Loop
  'Running through the data to count the number of rows (i.e., the number of x and z values)

  intN = intR
  'intN is now the number of rows


    Do Until (EOF(3) = True)
      intB = intB + 1
      Input #3, sngSC(intB), sngMaxLength(intB)
    Loop
    'Running through the data to count the number of rows (i.e., the number of SCs and lengths)

    intEnd = intB
    'intEnd is now the number of rows
```

```
sngSumH = 0

'Doing infinitely flexible first
  For intR = 2 To intN
    sngHyp = 0
    sngHyp = Sqr(((sngZ(intR) - sngZ(intR - 1)) ^ 2) + ((sngX(intR) - sngX(intR - 1)) ^ 2))
    'Calculating the hypotenuse of the triangle formed by the difference between x1 and 2 and z1 and 2
    sngSumH = sngSumH + sngHyp
    'Total sum of all the hypotenuses calculated.
  Next intR



  For intB = 1 To intEnd
    sngNumber = 0
    sngCorrNumber = 0
    'Resets both counts to 0

    sngNumber = Round((sngSumH / sngMaxLength(intB)) - 0.5, 0)
    sngCorrNumber = sngNumber / sngHorizontal

    Write #2, strSite, "Infinitely Flexible", sngSC(intB), sngCorrNumber, sngNumber,
     sngMaxLength(intB), sngHorizontal

  Next intB


'Now infinitely inflexible

  For intB = 1 To intEnd

    sngNumber = 0
    sngCorrNumber = 0
    sngSumH = 0
    'Resets all counts to 0

    intR = 2  'This does the initial calculation

      sngH(intR) = Sqr(((sngZ(intR) - sngZ(intR - 1)) ^ 2) + ((sngX(intR) - sngX(intR - 1)) ^ 2))
      'Calculating the hypotenuse of the triangle formed by the difference between x1 and 2 and z1 and
       2
      intHInt = CInt((sngH(intR) / sngMaxLength(intB)) - 0.49)  'determining how many bugs can fit
       on H and setting to integer (rounding down)
      sngExtra = sngH(intR) - (intHInt * sngMaxLength(intB))  'determining the extra length of H not
       filled by bugs (to add to next H)
      sngNumber = sngNumber + intHInt  'Total number of bugs fit on substrate

      If Abs(sngZ(intR) - sngZ(intR - 1)) = 0 Then
        sngA(intR) = 0
      Else
        sngA(intR) = sngH(intR) / Abs(sngZ(intR) - sngZ(intR - 1))  'Gives the sin of the angle formed
      End If

    For intR = 3 To intN  'loop for the rest of the calculations
      sngH(intR) = Sqr(((sngZ(intR) - sngZ(intR - 1)) ^ 2) + ((sngX(intR) - sngX(intR - 1)) ^ 2))
```

```
        If Abs(sngZ(intR) - sngZ(intR - 1)) = 0 Then
          sngA(intR) = 0
        Else
          sngA(intR) = sngH(intR) / Abs(sngZ(intR) - sngZ(intR - 1)) 'Gives the sin of the angle formed
        End If

        If sngA(intR - 1) = sngA(intR) Then 'If angles are the same
          sngH(intR) = sngH(intR) + sngExtra  'Add leftover to H, because bug can straddle adjacent
              blocks
          sngExtra = 0 'Reset Extra
          intHInt = CInt((sngH(intR) / sngMaxLength(intB)) - 0.49)  'determining how many bugs can
              fit on H and setting to integer (rounding down)
          sngExtra = sngH(intR) - (intHInt * sngMaxLength(intB))  'determining the extra length of H
              not filled by bugs (to add to next H)
          sngNumber = sngNumber + intHInt  'Total number of bugs fit on substrate
        Else
          sngExtra = 0
          intHInt = CInt((sngH(intR) / sngMaxLength(intB)) - 0.49)  'determining how many bugs can
              fit on H and setting to integer (rounding down)
          sngExtra = sngH(intR) - (intHInt * sngMaxLength(intB))  'determining the extra length of H
              not filled by bugs (to add to next H)
          sngNumber = sngNumber + intHInt  'Total number of bugs fit on substrate
        End If
      Next intR

      sngCorrNumber = sngNumber / sngHorizontal

      Write #2, strSite, "Infinitely Inflexible", sngSC(intB), sngCorrNumber, sngNumber,
        sngMaxLength(intB), sngHorizontal

    Next intB



'Now 10 Degrees Flexible

    For intB = 1 To intEnd

      sngNumber = 0
      sngCorrNumber = 0
      sngSumH = 0
      'Resets all counts to 0

      intR = 2  'This does the initial calculation

        sngH(intR) = Sqr(((sngZ(intR) - sngZ(intR - 1)) ^ 2) + ((sngX(intR) - sngX(intR - 1)) ^ 2))
        'Calculating the hypotenuse of the triangle formed by the difference between x1 and 2 and z1 and
            2
        intHInt = CInt((sngH(intR) / sngMaxLength(intB)) - 0.49)  'determining how many bugs can fit
            on H and setting to integer (rounding down)
        sngExtra = sngH(intR) - (intHInt * sngMaxLength(intB))  'determining the extra length of H not
            filled by bugs (to add to next H)
        sngNumber = sngNumber + intHInt  'Total number of bugs fit on substrate

        If Abs(sngZ(intR) - sngZ(intR - 1)) = 0 Then
```

```
            sngA(intR) = 0
          Else
            sngA(intR) = sngH(intR) / Abs(sngZ(intR) - sngZ(intR - 1)) 'Gives the sin of the angle formed
          End If

        For intR = 3 To intN  'loop for the rest of the calculations
          sngH(intR) = Sqr(((sngZ(intR) - sngZ(intR - 1)) ^ 2) + ((sngX(intR) - sngX(intR - 1)) ^ 2))

          If Abs(sngZ(intR) - sngZ(intR - 1)) = 0 Then
            sngA(intR) = 0
          Else
            sngA(intR) = sngH(intR) / Abs(sngZ(intR) - sngZ(intR - 1)) 'Gives the sin of the angle formed
          End If

          If Abs(sngA(intR - 1) - sngA(intR)) < 0.173649 Then 'If difference between angles is 10 degrees
           or less
            sngH(intR) = sngH(intR) + sngExtra  'Add leftover to H, because bug can straddle adjacent
               blocks
            sngExtra = 0 'Reset Extra
            intHInt = CInt((sngH(intR) / sngMaxLength(intB)) - 0.49)  'determining how many bugs can
               fit on H and setting to integer (rounding down)
            sngExtra = sngH(intR) - (intHInt * sngMaxLength(intB))  'determining the extra length of H
               not filled by bugs (to add to next H)
            sngNumber = sngNumber + intHInt  'Total number of bugs fit on substrate
          Else
            sngExtra = 0
            intHInt = CInt((sngH(intR) / sngMaxLength(intB)) - 0.49)  'determining how many bugs can
               fit on H and setting to integer (rounding down)
            sngExtra = sngH(intR) - (intHInt * sngMaxLength(intB))  'determining the extra length of H
               not filled by bugs (to add to next H)
            sngNumber = sngNumber + intHInt  'Total number of bugs fit on substrate
          End If
        Next intR

        sngCorrNumber = sngNumber / sngHorizontal

        Write #2, strSite, "10 Degrees Flexible", sngSC(intB), sngCorrNumber, sngNumber,
         sngMaxLength(intB), sngHorizontal

      Next intB


'Now 25 Degrees Flexible

      For intB = 1 To intEnd

        sngNumber = 0
        sngCorrNumber = 0
        sngSumH = 0
        'Resets all counts to 0

        intR = 2  'This does the initial calculation

          sngH(intR) = Sqr(((sngZ(intR) - sngZ(intR - 1)) ^ 2) + ((sngX(intR) - sngX(intR - 1)) ^ 2))
          'Calculating the hypotenuse of the triangle formed by the difference between x1 and 2 and z1 and
           2
```

```
        intHInt = CInt((sngH(intR) / sngMaxLength(intB)) - 0.49)  'determining how many bugs can fit
          on H and setting to integer (rounding down)
        sngExtra = sngH(intR) - (intHInt * sngMaxLength(intB))  'determining the extra length of H not
          filled by bugs (to add to next H)
        sngNumber = sngNumber + intHInt  'Total number of bugs fit on substrate

        If Abs(sngZ(intR) - sngZ(intR - 1)) = 0 Then
          sngA(intR) = 0
        Else
          sngA(intR) = sngH(intR) / Abs(sngZ(intR) - sngZ(intR - 1))  'Gives the sin of the angle formed
        End If

      For intR = 3 To intN  'loop for the rest of the calculations
        sngH(intR) = Sqr(((sngZ(intR) - sngZ(intR - 1)) ^ 2) + ((sngX(intR) - sngX(intR - 1)) ^ 2))

        If Abs(sngZ(intR) - sngZ(intR - 1)) = 0 Then
          sngA(intR) = 0
        Else
          sngA(intR) = sngH(intR) / Abs(sngZ(intR) - sngZ(intR - 1))  'Gives the sin of the angle formed
        End If

        If Abs(sngA(intR - 1) - sngA(intR)) < 0.422619 Then 'If difference between angles is 25 degrees
            or less
          sngH(intR) = sngH(intR) + sngExtra  'Add leftover to H, because bug can straddle adjacent
              blocks
          sngExtra = 0 'Reset Extra
          intHInt = CInt((sngH(intR) / sngMaxLength(intB)) - 0.49)  'determining how many bugs can
              fit on H and setting to integer (rounding down)
          sngExtra = sngH(intR) - (intHInt * sngMaxLength(intB))  'determining the extra length of H
              not filled by bugs (to add to next H)
          sngNumber = sngNumber + intHInt  'Total number of bugs fit on substrate
        Else
          sngExtra = 0
          intHInt = CInt((sngH(intR) / sngMaxLength(intB)) - 0.49)  'determining how many bugs can
              fit on H and setting to integer (rounding down)
          sngExtra = sngH(intR) - (intHInt * sngMaxLength(intB))  'determining the extra length of H
              not filled by bugs (to add to next H)
          sngNumber = sngNumber + intHInt  'Total number of bugs fit on substrate
        End If
      Next intR

      sngCorrNumber = sngNumber / sngHorizontal

      Write #2, strSite, "25 Degrees Flexible", sngSC(intB), sngCorrNumber, sngNumber,
          sngMaxLength(intB), sngHorizontal

    Next intB


  'Now 45 Degrees Flexible

    For intB = 1 To intEnd

      sngNumber = 0
      sngCorrNumber = 0
```

```
        sngSumH = 0
        'Resets all counts to 0

        intR = 2  'This does the initial calculation

          sngH(intR) = Sqr(((sngZ(intR) - sngZ(intR - 1)) ^ 2) + ((sngX(intR) - sngX(intR - 1)) ^ 2))
          'Calculating the hypotenuse of the triangle formed by the difference between x1 and 2 and z1 and
             2
          intHInt = CInt((sngH(intR) / sngMaxLength(intB)) - 0.49)  'determining how many bugs can fit
             on H and setting to integer (rounding down)
          sngExtra = sngH(intR) - (intHInt * sngMaxLength(intB))  'determining the extra length of H not
             filled by bugs (to add to next H)
          sngNumber = sngNumber + intHInt  'Total number of bugs fit on substrate

          If Abs(sngZ(intR) - sngZ(intR - 1)) = 0 Then
            sngA(intR) = 0
          Else
            sngA(intR) = sngH(intR) / Abs(sngZ(intR) - sngZ(intR - 1))  'Gives the sin of the angle formed
          End If

        For intR = 3 To intN  'loop for the rest of the calculations
          sngH(intR) = Sqr(((sngZ(intR) - sngZ(intR - 1)) ^ 2) + ((sngX(intR) - sngX(intR - 1)) ^ 2))

          If Abs(sngZ(intR) - sngZ(intR - 1)) = 0 Then
            sngA(intR) = 0
          Else
            sngA(intR) = sngH(intR) / Abs(sngZ(intR) - sngZ(intR - 1))  'Gives the sin of the angle formed
          End If

          If Abs(sngA(intR - 1) - sngA(intR)) < 0.707108 Then 'If difference between angles is 45 degrees
             or less
            sngH(intR) = sngH(intR) + sngExtra  'Add leftover to H, because bug can straddle adjacent
               blocks
            sngExtra = 0 'Reset Extra
            intHInt = CInt((sngH(intR) / sngMaxLength(intB)) - 0.49)  'determining how many bugs can
               fit on H and setting to integer (rounding down)
            sngExtra = sngH(intR) - (intHInt * sngMaxLength(intB))  'determining the extra length of H
               not filled by bugs (to add to next H)
            sngNumber = sngNumber + intHInt  'Total number of bugs fit on substrate
          Else
            sngExtra = 0
            intHInt = CInt((sngH(intR) / sngMaxLength(intB)) - 0.49)  'determining how many bugs can
               fit on H and setting to integer (rounding down)
            sngExtra = sngH(intR) - (intHInt * sngMaxLength(intB))  'determining the extra length of H
               not filled by bugs (to add to next H)
            sngNumber = sngNumber + intHInt  'Total number of bugs fit on substrate
          End If
        Next intR

        sngCorrNumber = sngNumber / sngHorizontal

        Write #2, strSite, "45 Degrees Flexible", sngSC(intB), sngCorrNumber, sngNumber,
sngMaxLength(intB), sngHorizontal

      Next intB
    Close #4
```

```
Close #3
Close #2
Close #1

MsgBox ("Number per profile has been calculated for each size class.")


End Sub
```

## Fitting crayfish to profiles

```
Private Sub cmdBugs_Click()

Dim strStream$, strSite$, strFilename$, strOutput$, strMaxLengthFile$, strHorizontalProfileFile$,
strTaxon$
Dim sngSC(1 To 50) As Single, sngMaxLength(1 To 50) As Single
Dim intB%, intEnd% 'The values for the length array
Dim intMinSC%, intMaxSC% 'Range of size classes input by user
Dim sngHorizontal!, sngProfile! 'The horizontal and 3D lengths of the profile, respectively
Dim sngNumber! 'The number of organisms that can fit on the profile
Dim sngCorrNumber! 'Number of organisms corrected for horizontal profile length
Dim sngX(1 To 10000) As Single, sngZ(1 To 10000) As Single, sngH(1 To 10000) As Single, sngA(1 To
10000) As Single
'Arrays for moving along profile - X, Z values, hypoteneuse value, angle value.
Dim sngHyp!, sngSumH!, intR%, intN%
'H is hypoteneuse length, SumH is profile length. R is array number, N is total number of rows in array.
Dim sngExtra!, intHInt% 'Values for non-flexible
Dim strSiteProfile$ 'The profile name to be read from Horizontal Profile File
Dim sngStartX!, sngZMin!, sngZMax!, sngXAtMin!, sngXAtMax!, sngLimit!
Dim sngDepth(1 To 50) As Single, sngCarapace(1 To 50) As Single

strStream = txtStream.Text 'Gets the stream code for Output
strSite = txtSite.Text  'Gets the profile code for Output file
strTaxon = txtOrganism.Text 'Gets the taxon from the text box on the form
strFilename = Path for file location & strSite & "ProfileCoordinatesXZ.csv"
'File to be read for analysis (file created in last step)
strOutput = Path for file location 'Creates output file that will show the results for each size class


If strTaxon = "Crayfish1" Then

   strMaxLengthFile = Path for file location & strStream & strTaxon & "MaxLength.csv"

   strHorizontalProfileFile = Path for file location & strStream & "HorizontalProfiles.csv"

   Open strFilename For Input As #1
   Open strOutput For Append As #2
   Open strMaxLengthFile For Input As #3

   Open strHorizontalProfileFile For Input As #4

   sngHorizontal = 0

   Do
      Input #4, strSiteProfile, sngHorizontal
```

```
Loop Until strSiteProfile = strSite

intR = 0
intB = 0

Do Until (EOF(1) = True)
   intR = intR + 1
   Input #1, sngX(intR), sngZ(intR)
Loop
'Running through the data to count the number of rows (i.e., the number of x and z values)

intN = intR
'intN is now the number of rows


   Do Until (EOF(3) = True)
      intB = intB + 1
      Input #3, sngSC(intB), sngMaxLength(intB)
   Loop
   'Running through the data to count the number of rows (i.e., the number of SCs and lengths)

   intEnd = intB
   'intEnd is now the number of rows

sngSumH = 0

'Now infinitely inflexible

   For intB = 1 To intEnd

      sngNumber = 0
      sngCorrNumber = 0
      sngSumH = 0
      'Resets all counts to 0

      intR = 2  'This does the initial calculation

         sngH(intR) = Sqr(((sngZ(intR) - sngZ(intR - 1)) ^ 2) + ((sngX(intR) - sngX(intR - 1)) ^ 2))
         'Calculating the hypotenuse of the triangle formed by the difference between x1 and 2 and z1 and
               2
         intHInt = CInt((sngH(intR) / sngMaxLength(intB)) - 0.49)  'determining how many bugs can fit
               on H and setting to integer (rounding down)
         sngExtra = sngH(intR) - (intHInt * sngMaxLength(intB))  'determining the extra length of H not
               filled by bugs (to add to next H)
         sngNumber = sngNumber + intHInt  'Total number of bugs fit on substrate

         If Abs(sngZ(intR) - sngZ(intR - 1)) = 0 Then
            sngA(intR) = 0
         Else
            sngA(intR) = sngH(intR) / Abs(sngZ(intR) - sngZ(intR - 1))  'Gives the sin of the angle formed
         End If

      For intR = 3 To intN  'loop for the rest of the calculations
         sngH(intR) = Sqr(((sngZ(intR) - sngZ(intR - 1)) ^ 2) + ((sngX(intR) - sngX(intR - 1)) ^ 2))
```

```
        If Abs(sngZ(intR) - sngZ(intR - 1)) = 0 Then
          sngA(intR) = 0
        Else
          sngA(intR) = sngH(intR) / Abs(sngZ(intR) - sngZ(intR - 1)) 'Gives the sin of the angle formed
        End If

        If sngA(intR - 1) = sngA(intR) Then 'If angles are the same
          sngH(intR) = sngH(intR) + sngExtra  'Add leftover to H, because bug can straddle adjacent
              blocks
          sngExtra = 0 'Reset Extra
          intHInt = CInt((sngH(intR) / sngMaxLength(intB)) - 0.49)  'determining how many bugs can
              fit on H and setting to integer (rounding down)
          sngExtra = sngH(intR) - (intHInt * sngMaxLength(intB))  'determining the extra length of H
              not filled by bugs (to add to next H)
          sngNumber = sngNumber + intHInt  'Total number of bugs fit on substrate
        Else
          sngExtra = 0
          intHInt = CInt((sngH(intR) / sngMaxLength(intB)) - 0.49)  'determining how many bugs can
              fit on H and setting to integer (rounding down)
          sngExtra = sngH(intR) - (intHInt * sngMaxLength(intB))  'determining the extra length of H
              not filled by bugs (to add to next H)
          sngNumber = sngNumber + intHInt  'Total number of bugs fit on substrate
        End If
      Next intR

      sngCorrNumber = sngNumber / sngHorizontal

      Write #2, strSite, strTaxon, "Infinitely Inflexible", sngSC(intB), sngCorrNumber, sngNumber,
sngMaxLength(intB), sngHorizontal

    Next intB


  'Now 45 Degrees Flexible

    For intB = 1 To intEnd

      sngNumber = 0
      sngCorrNumber = 0
      sngSumH = 0
      'Resets all counts to 0

      intR = 2  'This does the initial calculation

        sngH(intR) = Sqr(((sngZ(intR) - sngZ(intR - 1)) ^ 2) + ((sngX(intR) - sngX(intR - 1)) ^ 2))
        'Calculating the hypotenuse of the triangle formed by the difference between x1 and 2 and z1 and
            2
        intHInt = CInt((sngH(intR) / sngMaxLength(intB)) - 0.49)  'determining how many bugs can fit
            on H and setting to integer (rounding down)
        sngExtra = sngH(intR) - (intHInt * sngMaxLength(intB))  'determining the extra length of H not
            filled by bugs (to add to next H)
        sngNumber = sngNumber + intHInt  'Total number of bugs fit on substrate

        If Abs(sngZ(intR) - sngZ(intR - 1)) = 0 Then
          sngA(intR) = 0
        Else
```

```
            sngA(intR) = sngH(intR) / Abs(sngZ(intR) - sngZ(intR - 1)) 'Gives the sin of the angle formed
          End If

        For intR = 3 To intN  'loop for the rest of the calculations
          sngH(intR) = Sqr(((sngZ(intR) - sngZ(intR - 1)) ^ 2) + ((sngX(intR) - sngX(intR - 1)) ^ 2))

          If Abs(sngZ(intR) - sngZ(intR - 1)) = 0 Then
            sngA(intR) = 0
          Else
            sngA(intR) = sngH(intR) / Abs(sngZ(intR) - sngZ(intR - 1)) 'Gives the sin of the angle formed
          End If

          If Abs(sngA(intR - 1) - sngA(intR)) < 0.707108 Then 'If difference between angles is 45 degrees
                or less
            sngH(intR) = sngH(intR) + sngExtra  'Add leftover to H, because bug can straddle adjacent
                blocks
            sngExtra = 0 'Reset Extra
            intHInt = CInt((sngH(intR) / sngMaxLength(intB)) - 0.49)  'determining how many bugs can
                fit on H and setting to integer (rounding down)
            sngExtra = sngH(intR) - (intHInt * sngMaxLength(intB))  'determining the extra length of H
                not filled by bugs (to add to next H)
            sngNumber = sngNumber + intHInt  'Total number of bugs fit on substrate
          Else
            sngExtra = 0
            intHInt = CInt((sngH(intR) / sngMaxLength(intB)) - 0.49)  'determining how many bugs can
               fit on H and setting to integer (rounding down)
            sngExtra = sngH(intR) - (intHInt * sngMaxLength(intB))  'determining the extra length of H
               not filled by bugs (to add to next H)
            sngNumber = sngNumber + intHInt  'Total number of bugs fit on substrate
          End If
        Next intR

        sngCorrNumber = sngNumber / sngHorizontal

        Write #2, strSite, strTaxon, "45 Degrees Flexible", sngSC(intB), sngCorrNumber, sngNumber,
sngMaxLength(intB), sngHorizontal

    Next intB

ElseIf strTaxon = "Crayfish2" Then

    strMaxLengthFile = Path for file location & strStream & strTaxon & "MaxLength.csv"

    strHorizontalProfileFile = Path for file location & strStream & "HorizontalProfiles.csv"

    Open strFilename For Input As #1
    Open strOutput For Append As #2
    Open strMaxLengthFile For Input As #3

    Open strHorizontalProfileFile For Input As #4

    sngHorizontal = 0

    Do
      Input #4, strSiteProfile, sngHorizontal
```

```
  Loop Until strSiteProfile = strSite

  intR = 0
  intB = 0

  Do Until (EOF(1) = True)
    intR = intR + 1
    Input #1, sngX(intR), sngZ(intR)
  Loop
  'Running through the data to count the number of rows (i.e., the number of x and z values)

  intN = intR
  'intN is now the number of rows


  Do Until (EOF(3) = True)
    intB = intB + 1
    Input #3, sngSC(intB), sngMaxLength(intB), sngDepth(intB)
  Loop
  'Running through the data to count the number of rows (i.e., the number of SCs and lengths)

  intEnd = intB
  'intEnd is now the number of rows

sngSumH = 0


  For intB = 1 To intEnd

    sngNumber = 0
    sngCorrNumber = 0
    sngSumH = 0
    'Resets all counts to 0
    sngLimit = sngDepth(intB)

    intR = 1  'This does the initial calculation

      sngStartX = sngX(intR)
      sngZMin = sngZ(intR)
      sngXAtMin = sngX(intR)
      sngZMax = sngZ(intR)
      sngXAtMax = sngX(intR)

    intR = 2

      If Abs(sngZ(intR) - sngZ(intR - 1)) <= sngLimit Then
        If sngZ(intR) > sngZ(intR - 1) Then
          sngZMax = sngZ(intR)
          sngXAtMax = sngX(intR)
        Else
          If sngZ(intR) < sngZ(intR - 1) Then
            sngZMax = sngZ(intR - 1)
            sngXAtMax = sngX(intR - 1)
            sngZMin = sngZ(intR)
            sngXAtMax = sngX(intR)
          End If
```

```
    End If
  Else
    sngStartX = sngX(intR)
    sngZMin = sngZ(intR)
    sngZMax = sngZ(intR)
    sngXAtMin = sngX(intR)
    sngXAtMax = sngX(intR)
  End If


For intR = 3 To intN  'loop for the rest of the calculations

  If sngZ(intR) > sngZMax Then
    sngZMax = sngZ(intR)
    sngXAtMax = sngX(intR)
  Else
    If sngZ(intR) < sngZMin Then
      sngZMin = sngZ(intR)
      sngXAtMax = sngX(intR)
    End If
  End If

  If sngZMax = sngZMin Then

    sngH(intR) = sngX(intR) - sngStartX

    intHInt = CInt((sngH(intR) / sngMaxLength(intB)) - 0.49)  'determining how many crayfish
          can fit on H and setting to integer (rounding down)
    'Not doing extra because crayfish will always be longer than the hyp between 2 points, so only
          1 will be added at a time (unlike bugs)
    'So can start over without leaving much extra space

    If intHInt > 0 Then

      sngNumber = sngNumber + intHInt  'Total number of bugs fit on substrate

      sngStartX = sngX(intR)
      sngZMin = sngZ(intR)
      sngZMax = sngZ(intR)
      sngXAtMin = sngX(intR)
      sngXAtMax = sngX(intR)

    End If


  ElseIf sngZMax - sngZMin <= sngLimit Then

    If sngZ(intR) > sngZMin Then sngH(intR) = Sqr(((sngZ(intR) - sngZMin) ^ 2) + ((sngX(intR)
      - sngStartX) ^ 2))
    If sngZ(intR) < sngZMax Then sngH(intR) = Sqr(((sngZMax - sngZ(intR)) ^ 2) + ((sngX(intR)
      - sngStartX) ^ 2))

    intHInt = CInt((sngH(intR) / sngMaxLength(intB)) - 0.49)  'determining how many crayfish
      can fit on H and setting to integer (rounding down)
    'Not doing extra because crayfish will always be longer than the hyp between 2 points, so only
      1 will be added at a time (unlike bugs)
```

```
            'So can start over without leaving much extra space

            If intHInt > 0 Then

               sngNumber = sngNumber + intHInt  'Total number of bugs fit on substrate

               sngStartX = sngX(intR)
               sngZMin = sngZ(intR)
               sngZMax = sngZ(intR)
               sngXAtMin = sngX(intR)
               sngXAtMax = sngX(intR)
            End If

         ElseIf sngZMax - sngZMin > sngLimit Then

            sngStartX = sngX(intR)
            sngZMin = sngZ(intR)
            sngZMax = sngZ(intR)
            sngXAtMin = sngX(intR)
            sngXAtMax = sngX(intR)
         End If

      Next intR

      sngCorrNumber = sngNumber / sngHorizontal

      Write #2, strSite, strTaxon, sngSC(intB), sngCorrNumber, sngNumber, sngMaxLength(intB),
sngDepth(intB), sngHorizontal

   Next intB


ElseIf strTaxon = "Crayfish3" Then

   strMaxLengthFile = Path for file location & strStream & strTaxon & "MaxLength.csv"

   strHorizontalProfileFile = Path for file location & strStream & "HorizontalProfiles.csv"

   Open strFilename For Input As #1
   Open strOutput For Append As #2
   Open strMaxLengthFile For Input As #3

   Open strHorizontalProfileFile For Input As #4

   sngHorizontal = 0

   Do
      Input #4, strSiteProfile, sngHorizontal

   Loop Until strSiteProfile = strSite

   intR = 0
   intB = 0

   Do Until (EOF(1) = True)
      intR = intR + 1
```

```
    Input #1, sngX(intR), sngZ(intR)
  Loop
  'Running through the data to count the number of rows (i.e., the number of x and z values)

  intN = intR
  'intN is now the number of rows


  Do Until (EOF(3) = True)
    intB = intB + 1
    Input #3, sngSC(intB), sngMaxLength(intB), sngCarapace(intB)
  Loop
  'Running through the data to count the number of rows (i.e., the number of SCs and lengths)

  intEnd = intB
  'intEnd is now the number of rows

sngSumH = 0


  For intB = 1 To intEnd

    sngNumber = 0
    sngCorrNumber = 0
    sngSumH = 0
    'Resets all counts to 0
    sngLimit = sngCarapace(intB)

    intR = 1  'This does the initial calculation

      sngStartX = sngX(intR)
      sngZMin = sngZ(intR)
      sngXAtMin = sngX(intR)
      sngZMax = sngZ(intR)
      sngXAtMax = sngX(intR)

    intR = 2

      If Abs(sngZ(intR) - sngZ(intR - 1)) <= sngLimit Then
        If sngZ(intR) > sngZ(intR - 1) Then
          sngZMax = sngZ(intR)
          sngXAtMax = sngX(intR)
        Else
          If sngZ(intR) < sngZ(intR - 1) Then
            sngZMax = sngZ(intR - 1)
            sngXAtMax = sngX(intR - 1)
            sngZMin = sngZ(intR)
            sngXAtMax = sngX(intR)
          End If
        End If
      Else
        sngStartX = sngX(intR)
        sngZMin = sngZ(intR)
        sngZMax = sngZ(intR)
        sngXAtMin = sngX(intR)
        sngXAtMax = sngX(intR)
```

```
  End If

For intR = 3 To intN  'loop for the rest of the calculations


  If sngZ(intR) > sngZMax Then
    sngZMax = sngZ(intR)
    sngXAtMax = sngX(intR)
  Else
    If sngZ(intR) < sngZMin Then
      sngZMin = sngZ(intR)
      sngXAtMax = sngX(intR)
    End If
  End If

  If sngZMax = sngZMin Then

    sngH(intR) = sngX(intR) - sngStartX

    intHInt = CInt((sngH(intR) / sngMaxLength(intB)) - 0.49)  'determining how many crayfish
        can fit on H and setting to integer (rounding down)
    'Not doing extra because crayfish will always be longer than the hyp between 2 points, so only
        1 will be added at a time (unlike bugs)
    'So can start over without leaving much extra space

    If intHInt > 0 Then

      sngNumber = sngNumber + intHInt  'Total number of bugs fit on substrate

      sngStartX = sngX(intR)
      sngZMin = sngZ(intR)
      sngZMax = sngZ(intR)
      sngXAtMin = sngX(intR)
      sngXAtMax = sngX(intR)

    End If

  ElseIf sngZMax - sngZMin <= sngLimit Then

    If sngZ(intR) > sngZMin Then sngH(intR) = Sqr(((sngZ(intR) - sngZMin) ^ 2) + ((sngX(intR)
        - sngStartX) ^ 2))
    If sngZ(intR) < sngZMax Then sngH(intR) = Sqr(((sngZMax - sngZ(intR)) ^ 2) + ((sngX(intR)
        - sngStartX) ^ 2))

    intHInt = CInt((sngH(intR) / sngMaxLength(intB)) - 0.49)  'determining how many crayfish
        can fit on H and setting to integer (rounding down)
    'Not doing extra because crayfish will always be longer than the hyp between 2 points, so only
        1 will be added at a time (unlike bugs)
    'So can start over without leaving much extra space

    If intHInt > 0 Then

      sngNumber = sngNumber + intHInt  'Total number of bugs fit on substrate

      sngStartX = sngX(intR)
      sngZMin = sngZ(intR)
```

```
            sngZMax = sngZ(intR)
            sngXAtMin = sngX(intR)
            sngXAtMax = sngX(intR)
          End If

        ElseIf sngZMax - sngZMin > sngLimit Then

          sngStartX = sngX(intR)
          sngZMin = sngZ(intR)
          sngZMax = sngZ(intR)
          sngXAtMin = sngX(intR)
          sngXAtMax = sngX(intR)
        End If

      Next intR

      sngCorrNumber = sngNumber / sngHorizontal

      Write #2, strSite, strTaxon, sngSC(intB), sngCorrNumber, sngNumber, sngMaxLength(intB),
sngCarapace(intB), sngHorizontal

    Next intB

End If

  Close #4
  Close #3
  Close #2
  Close #1

  MsgBox ("Number per profile has been calculated for each size class.")

End Sub
```

## Fitting fish to profiles

```
Private Sub cmdBugs_Click()

Dim strStream$, strSite$, strFilename$, strOutput$, strMaxLengthFile$, strHorizontalProfileFile$,
strTaxon$
Dim sngSC(1 To 50) As Single, sngMaxLength(1 To 50) As Single
Dim intB%, intEnd% 'The values for the length array
Dim intMinSC%, intMaxSC% 'Range of size classes input by user
Dim sngHorizontal!, sngProfile! 'The horizontal and 3D lengths of the profile, respectively
Dim sngNumber! 'The number of organisms that can fit on the profile
Dim sngCorrNumber! 'Number of organisms corrected for horizontal profile length
Dim sngX(1 To 10000) As Single, sngZ(1 To 10000) As Single, sngH(1 To 10000) As Single, sngA(1 To
10000) As Single
'Arrays for moving along profile - X, Z values, hypoteneuse value, angle value.
Dim sngHyp!, sngSumH!, intR%, intN%
'H is hypoteneuse length, SumH is profile length. R is array number, N is total number of rows in array.
Dim sngExtra!, intHInt% 'Values for non-flexible
Dim strSiteProfile$ 'The profile name to be read from Horizontal Profile File
Dim sngStartX!, sngZMin!, sngZMax!, sngXAtMin!, sngXAtMax!, sngLimit!
Dim sngDepth(1 To 50) As Single, sngCarapace(1 To 50) As Single
```

```
strStream = txtStream.Text 'Gets the stream code for Output
strSite = txtSite.Text  'Gets the profile code for Output file
strTaxon = txtOrganism.Text 'Gets the taxon from the text box on the form
strFilename = Path for filename & strSite & "ProfileCoordinatesXZ.csv"
'File to be read for analysis (file created in last step)
strOutput = Path for filename
'Creates output file that will show the results for each size class

If strTaxon = "Fish1" Then

   strMaxLengthFile = Path for filename & strStream & strTaxon & "MaxLength.csv"

   strHorizontalProfileFile = Path for filename & strStream & "HorizontalProfiles.csv"

   Open strFilename For Input As #1
   Open strOutput For Append As #2
   Open strMaxLengthFile For Input As #3

   Open strHorizontalProfileFile For Input As #4

   sngHorizontal = 0

   Do
      Input #4, strSiteProfile, sngHorizontal

   Loop Until strSiteProfile = strSite

   intR = 0
   intB = 0

   Do Until (EOF(1) = True)
      intR = intR + 1
      Input #1, sngX(intR), sngZ(intR)
   Loop
   'Running through the data to count the number of rows (i.e., the number of x and z values)

   intN = intR
   'intN is now the number of rows

       Do Until (EOF(3) = True)
         intB = intB + 1
         Input #3, sngSC(intB), sngMaxLength(intB)
      Loop
      'Running through the data to count the number of rows (i.e., the number of SCs and lengths)

      intEnd = intB
      'intEnd is now the number of rows

   sngSumH = 0


      For intB = 1 To intEnd

         sngNumber = 0
         sngCorrNumber = 0
         sngSumH = 0
```

```
        'Resets all counts to 0

            intHInt = CInt((sngHorizontal / sngMaxLength(intB)) - 0.49)  'determining how many fish can
fit on the horizontal profile and setting to integer (rounding down)
            sngNumber = sngNumber + intHInt  'Total number of fish fit across substrate (floating above
substrate)

        sngCorrNumber = sngNumber / sngHorizontal

        Write #2, strSite, strTaxon, sngSC(intB), sngCorrNumber, sngNumber, sngMaxLength(intB),
sngHorizontal

    Next intB

ElseIf strTaxon = "Fish2" Then  'Instead of total length, uses body depth to fit fish

    strMaxLengthFile = Path for filename & strStream & strTaxon & "MaxLength.csv"

  strHorizontalProfileFile = Path for filename & strStream & "HorizontalProfiles.csv"

  Open strFilename For Input As #1
  Open strOutput For Append As #2
  Open strMaxLengthFile For Input As #3

  Open strHorizontalProfileFile For Input As #4

  sngHorizontal = 0

  Do
    Input #4, strSiteProfile, sngHorizontal

  Loop Until strSiteProfile = strSite

  intR = 0
  intB = 0

  Do Until (EOF(1) = True)
    intR = intR + 1
    Input #1, sngX(intR), sngZ(intR)
  Loop
  'Running through the data to count the number of rows (i.e., the number of x and z values)

  intN = intR
  'intN is now the number of rows


    Do Until (EOF(3) = True)
      intB = intB + 1
      Input #3, sngSC(intB), sngMaxLength(intB)
    Loop
    'Running through the data to count the number of rows (i.e., the number of SCs and lengths)

    intEnd = intB
    'intEnd is now the number of rows

  sngSumH = 0
```

```
    For intB = 1 To intEnd

        sngNumber = 0
        sngCorrNumber = 0
        sngSumH = 0
        'Resets all counts to 0

            intHInt = CInt((sngHorizontal / sngMaxLength(intB)) - 0.49)  'determining how many fish can
fit on the horizontal profile and setting to integer (rounding down)
            sngNumber = sngNumber + intHInt  'Total number of fish fit across substrate (floating above
substrate)

        sngCorrNumber = sngNumber / sngHorizontal

        Write #2, strSite, strTaxon, sngSC(intB), sngCorrNumber, sngNumber, sngMaxLength(intB),
sngHorizontal

    Next intB

ElseIf strTaxon = "Fish3" Then  'Again using depth instead of total length, but applying crayfish model

    strMaxLengthFile = Path for filename & strStream & strTaxon & "MaxLength.csv"

    strHorizontalProfileFile = Path for filename & strStream & "HorizontalProfiles.csv"

    Open strFilename For Input As #1
    Open strOutput For Append As #2
    Open strMaxLengthFile For Input As #3

    Open strHorizontalProfileFile For Input As #4

    sngHorizontal = 0

    Do
      Input #4, strSiteProfile, sngHorizontal

    Loop Until strSiteProfile = strSite

    intR = 0
    intB = 0

    Do Until (EOF(1) = True)
      intR = intR + 1
      Input #1, sngX(intR), sngZ(intR)
    Loop
    'Running through the data to count the number of rows (i.e., the number of x and z values)

    intN = intR
    'intN is now the number of rows


    Do Until (EOF(3) = True)
      intB = intB + 1
      Input #3, sngSC(intB), sngMaxLength(intB)
```

```
    Loop
    'Running through the data to count the number of rows (i.e., the number of SCs and lengths)

    intEnd = intB
    'intEnd is now the number of rows

sngSumH = 0


    For intB = 1 To intEnd

        sngNumber = 0
        sngCorrNumber = 0
        sngSumH = 0
        'Resets all counts to 0
        sngLimit = sngMaxLength(intB)

        intR = 1  'This does the initial calculation

            sngStartX = sngX(intR)
            sngZMin = sngZ(intR)
            sngXAtMin = sngX(intR)
            sngZMax = sngZ(intR)
            sngXAtMax = sngX(intR)

        intR = 2

            If Abs(sngZ(intR) - sngZ(intR - 1)) <= sngLimit Then
                If sngZ(intR) > sngZ(intR - 1) Then
                    sngZMax = sngZ(intR)
                    sngXAtMax = sngX(intR)
                Else
                    If sngZ(intR) < sngZ(intR - 1) Then
                        sngZMax = sngZ(intR - 1)
                        sngXAtMax = sngX(intR - 1)
                        sngZMin = sngZ(intR)
                        sngXAtMax = sngX(intR)
                    End If
                End If
            Else
                sngStartX = sngX(intR)
                sngZMin = sngZ(intR)
                sngZMax = sngZ(intR)
                sngXAtMin = sngX(intR)
                sngXAtMax = sngX(intR)
            End If


        For intR = 3 To intN  'loop for the rest of the calculations


            If sngZ(intR) > sngZMax Then
                sngZMax = sngZ(intR)
                sngXAtMax = sngX(intR)
            Else
                If sngZ(intR) < sngZMin Then
```

```
        sngZMin = sngZ(intR)
        sngXAtMax = sngX(intR)
    End If
End If

If sngZMax = sngZMin Then

    sngH(intR) = sngX(intR) - sngStartX

    intHInt = CInt((sngH(intR) / sngMaxLength(intB)) - 0.49)  'determining how many crayfish
        can fit on H and setting to integer (rounding down)
    'Not doing extra because crayfish will always be longer than the hyp between 2 points, so only
        1 will be added at a time (unlike bugs)
    'So can start over without leaving much extra space

    If intHInt > 0 Then

        sngNumber = sngNumber + intHInt  'Total number of bugs fit on substrate

        sngStartX = sngX(intR)
        sngZMin = sngZ(intR)
        sngZMax = sngZ(intR)
        sngXAtMin = sngX(intR)
        sngXAtMax = sngX(intR)

    End If

ElseIf sngZMax - sngZMin <= sngLimit Then

    sngH(intR) = sngX(intR) - sngStartX

    intHInt = CInt((sngH(intR) / sngMaxLength(intB)) - 0.49)  'determining how many crayfish
        can fit on H and setting to integer (rounding down)
    'Not doing extra because crayfish will always be longer than the hyp between 2 points, so only
        1 will be added at a time (unlike bugs)
    'So can start over without leaving much extra space

    If intHInt > 0 Then

        sngNumber = sngNumber + intHInt  'Total number of bugs fit on substrate

        sngStartX = sngX(intR)
        sngZMin = sngZ(intR)
        sngZMax = sngZ(intR)
        sngXAtMin = sngX(intR)
        sngXAtMax = sngX(intR)
    End If

ElseIf sngZMax - sngZMin > sngLimit Then

    sngStartX = sngX(intR)
    sngZMin = sngZ(intR)
    sngZMax = sngZ(intR)
    sngXAtMin = sngX(intR)
    sngXAtMax = sngX(intR)
End If
```

```
        Next intR

        sngCorrNumber = sngNumber / sngHorizontal

        Write #2, strSite, strTaxon, sngSC(intB), sngCorrNumber, sngNumber, sngMaxLength(intB),
sngHorizontal

    Next intB

End If

  Close #4
  Close #3
  Close #2
  Close #1

  MsgBox ("Number per profile has been calculated for each size class.")

End Sub
```